Molecular studies on plant glycerol-s-phosphate acyltransferases

Johannes Theodorus Maria Kroon

Molecular Studies on Plant Glycerol-3-Phosphate Acyltransferases

PhD 2000

Johannes Theodorus Maria Kroon

Abstract

The main objective of this research is to advance our understanding of the biochemical properties and the structure-function relationships of the chloroplast glycerol-3-phosphate acyltransferases in plants. *De novo* synthesised fatty acyl chains are diverted into the prokaryotic pathway of plant lipid biosynthesis by a soluble glycerol-3-phosphate acyltransferase (GPAT [EC. 2.3.1.15]) in the chloroplast. GPAT catalyses acylation at the *sn*-1 position of *sn*-glycerol-3-phosphate to form lysophosphatidic acid. Recombinant GPAT from squash and *Arabidopsis* were overproduced in *Escherichia coli,* purified to about 23-fold and 90% pure enzyme using a procedure developed in this study. Antibodies were raised in rabbits against these denatured recombinant GPAT preparations and four peptide antigens, and preliminary experiments were performed to test their suitability for use in Western blotting. In collaboration with the University of Sheffield, squash GPAT was successfully crystallised, isomorphous heavy metal derivatives prepared and the complete 3-dimensional structure of the protein at 2.3 Angstrom resolution determined. The cloning, functional expression and characterisation of a novel GPAT from oil palm, 'domainswap' chimeric recombinant proteins of *Arabidopsis* and squash GPAT, and spinach and squash GPAT respectively, and the influence of the N-terminal domain and amino acid substitutions in the C-terminal domain of the squash GPAT, was described. By determining the apparent kinetic constants for acyl-ACP substrates of most of the enzymes and by *in vitro* assays using mixtures of two acyl-ACP substrates under physiologically relevant conditions, it was found that their substrate selectivities could be dramatically altered. The development of ribozyme-technology as a molecular tool to down-regulate the gene expression of one out of multiple GPATs, was initiated. The strategy would allow for a phenotypic indication of ribozyme-efficacy *in vivo* and may help further contribute to the role of glycerol-3-phosphate acyltransferase in processes determining the phenomenon of chilling-sensitivity of plants.

Molecular Studies on Plant Glycerol-3-Phosphate Acyltransferases

by

Johannes Theodorus Maria Kroon

A thesis submitted to the Department of Biological Sciences

University of Durham

In accordance with the requirements for the degree of Doctor of Philosophy

April 2000

For

My Mum and Dad

Bettina and Kees

and

Rosie

Molecular Studies on Plant Glycerol-3-Phosphate Acyltransferases

Chapters

Table of contents

List of Figures

List of Tables

Abbreviations.

a (or α)	=	anti
AA (or aa)	=	amino acid
Amp	=	ampicillin
Ara (or ARA)	=	*Arabidopsis*
ATP	=	adenosine triphosphate
b	=	base(s)
bp	=	base pairs
BSA	=	bovine serum albumin (fraction V)
cDNA	=	complementary DNA
Cm	=	chloramphenicol
CoA	=	coenzyme A
cpm	=	counts per minute
CTP	=	cytidine triphosphate
d	=	deoxy
dd	=	double distilled
DAF	=	days after flowering
DGAT (or 3-AT)	=	diacylglycerol acyltransferase
DMF	=	N,N-dimethyl formamide
DMSO	=	dimethyl sulphoxide
DNA	=	deoxyribonucleic acid
DNase	=	deoxyribonuclease I
dNTPs	=	deoxyribonucleoside triphosphates
dpm	=	desintegrations per minute
ds	=	double stranded
DTT	=	dithiothreitol
EDTA	=	ethylenediaminetetraacetic acid
GPAT (or 1-AT)	=	glycerol-3-phosphate acyltransferase
GTP	=	guanidine triphosphate
HEPES	=	N-[2-Hydroxyethyl]piperazine-N'-[2-ethane-sulphonic acid]
hr	=	hours
IPTG	=	isopropyl-β-D-thiogalactopyranoside
Kan	=	kanamycin
kb	=	kilobases
kDa	=	kilodaltons
LPAT (or 2-AT)	=	lysophosphatidic acid acyltransferase

MES	=	2-[N-morpholino]ethane sulphonic acid
min	=	minutes
MOPS	=	3-[N-morpholino]propane sulphonic acid
mQ	=	milliQ (filtered)
mRNA	=	messenger RNA
nt	=	nucleotides
OD	=	optical density (absorbance)
ORF	=	open reading frame
PAGE	=	polyacrylamide gel electrophoresis
PBS	=	phosphate buffered saline
PCR	=	polymerase chain reaction
pfu	=	plaque forming units
pI	=	isoelectric point
polyA$^+$	=	poly adenylated
RNA	=	ribonucleic acid
RNase	=	ribonuclease
rpm	=	revolutions per minute
Rz	=	ribozyme
SDS	=	sodium dodecyl sulphate
snRNA	=	small nuclear RNA
ss	=	single stranded
TEMED	=	N,N,N',N'-tetramethylethylene diamine
Tet	=	tetracycline
Tm	=	melting (annealing) temperature
Tris	=	tris-(hydroxymethyl)-aminomethane
TTP	=	thymidine triphosphate
tRNA	=	transfer RNA
U (or u)	=	units of enzyme activity
UTP	=	uridine triphosphate
UV	=	ultraviolet
var.	=	variety
v/v	=	volume for volume
w/v	=	weight for volume
XGAL (or X-gal)	=	5-bromo-4-chloro-3-indolyl-b-D-galactopyranoside
5'	=	5' terminal end (phosphate) of (ribo-) nucleic acid molecule
3'	=	3' terminal end (hydroxyl) of (ribo-) nucleic acid molecule

Acknowledgements

I would like to thank my supervisor Prof. Toni (A. R.) Slabas for allowing me to study for this Ph.D as a Research Assistant in his laboratory. Who knows, maybe I might even get that excellent bottle of wine off your hands someday! I am also grateful to Nickerson Biocem for the funding and collaboration in the first period of the project.

Many thanks to Dr. Kieran Elborough, my current 'boss', for his trust, enthousiasm, patience and a degree of flexibility, allowing a major part of the writing-up of this work.

Thanks are also due to Bill "W.J." Simon and John "S.P." Gilroy for the down-to-earth scientific deliberations, sharing their wisdom and answering silly questions about proteins and protein sequencing.

I have enjoyed working with Dr. Ikuo Nishida in the first year of my study and like to say thanks for his friendship, his help and the 'teachings of GPAT'.

I would also like to thank Dr. Toon Stuitje for the help, support and chat over the years.

In the lab., I have worked with a large number of great people over the years. I hope that they understand that I can not mention everyone seperately but I like to thank them all for the good, the bad, the ugly (the singing) and the teamwork.

Thanks to Julia Bartley, Vicky Kelly and Gillian Storey for the excellent DNA sequencing work and Paul Sidney and David Hutchinson for the great service and brilliant photographic work. Paul, thanks for the Adobe Photoshop secrets and I still owe you money.

Acknowledged is the work of Dr. Ted Schierer, with whom I collaborated when he performed initial experiments with the acyl-ACP substrates and who kindly provided the acyl-ACP substrates.

A **big thankyou** to my family, particularly my mum Anne and dad Jaap, my sis Bettina and Zwaag Kees, for their love and encouragement throughout the years and without whom I would simply not have survived and achieved so much.

Also many thanks to Dorothy, Michael (J.), Lorraine and the rest of the family (including the cats), for their friendship and support.

Finally, my love and thanks to Rosie, who's been there for me, providing support and encouragement, love and friendship, even during the recent times of writing-up stress.

!

Declaration

I declare that no part of the work contained within this thesis has been previously submitted for any other degree in this or any other university, and that all work was performed by the author , except where otherwise stated.

Johan Kroon

Chapter I

∞∞∞∞∞

Membrane Lipids and Storage Triacylglycerol Biosynthesis in Plants; Unravelling and Genetic Engineering of a Primary Metabolic Pathway

Chapter I

1.1 General introduction

Plants have always been a resource for food, feeds, aesthetic and technical purposes. Mankind has adapted crop plants to their needs and end use, via breeding, for many centuries. In recent years, rapid progress has been made towards knowledge-acquisition and a fundamental understanding of plant biology and metabolic processes in plants. Revolutionary progress in scientific achievements has made plant- and agricultural biotechnology and its commercialisation gain momentum and are now in a blooming phase. Genetic engineering and the ability to create transgenic plants have made it reality that (part of -) a plants gene pool can consist of genes from any organism, or even synthetic genes. Transgenic plants can now be developed with new 'input' traits (influencing performance of the plant during growth on the field) and 'output' traits (new quantitative or qualitative traits with respect to (new -) products) (Willmitzer, L., 1999). Transgenic crops are being developed in roughly three major areas:
1] productivity enhancing 'input' traits towards crop protection, such as herbicide-, insect- and disease resistance.
2] qualitative or quantitative 'output' traits concerning food and (animal and industrial-) feed modifications or to improve harvest quality, based on altering the grain, fruits or seeds.
3] qualitative 'output' traits for expressing foreign proteins/products at high level in plants for industrial or pharmaceutical purposes (Briggs, S.P. and Koziel, M., 1998).
Rational engineering of transgenic plant crops towards the above mentioned traits will lead to a vast variety of new products in plants.

It is obvious that these plant biotechnological developments and the engineering of new plant strains has enormous potential to be of great benefit. It will have important consequences for an ecologically friendlier agriculture, 'enhanced economics' and has great commercial viability. One day it might even be a necessity to sustaining, a good and healthy standard of living in a world with a rapidly increasing population size along with potential climatic changes, dwindling genetic diversity and the depletion of global reserves of fossil-derived hydrocarbons (oil, coal and gas) (Kerr, R.A., 1998).
As with the development of any new technology there are fundamental (or technical) problems and limitations, as well as great potential for positive and also negative use. Society has different degrees of wariness for acceptance of such technology with regards to ethics, religion ('tampering' with nature/'God's creation'), scientific or social merits.

Therefore, the advancement of the fundamental knowledge, the technology and its commercialisation should go hand in hand with realistic and safe scientific/experimental evaluation. This will also require debate of merits and consensus opinion of an international regulatory process.

The plant kingdom has evolved the ability to produce an enormous diverse range of structures. Altering the level and spectrum of products in plants, via manipulation of metabolic pathways, represents an active area of research for plant physiologists, - biochemists and – molecular biologists. The biosynthetic pathways of plant products are complex and highly regulated networks through which metabolite flux (or metabolic partitioning) is directed according to developmental and environmental conditions. Directed and effective engineering of plant metabolism is dependent upon an understanding of such complex biochemical and genetic regulation, the orchestra between different pathways and the flux through the metabolic pathways. Certainly not the least important factor is knowledge about the function and overall influence of changes within a particular pathway on the overall phenotype.
Many of the vast arrays of chemical structures are only found in specialised cell types and are called **'secondary metabolites'** because they are not essential to cell growth.
Unravelling and rational engineering of **'primary metabolic'** pathways is also complicated because the metabolites are found in every cell of the plant and are essential to growth. Too much perturbation of these pathways will likely be lethal (Moore, T.S., Jr., 1993). The major constituents of plants are nucleic acids, proteins, carbohydrates and **lipids**. The most abundant type of lipids is derived from the fatty acid – and glycerolipid biosynthetic pathways.

1.2 Lipids

The word 'lipids' comes from the Greek word *lipos*, meaning fat, greasy to the touch. Lipids comprise one of the three large classes of food and along with carbohydrates and proteins, are essential components of all living cells. This extremely diverse heterogeneous class of compounds is defined on the basis of their overall physical properties, which are their insolubility in water and solubility in nonpolar organic solvents. Even when restricting ourselves to just look at plant lipids, different distinct biosynthetic pathways exist to produce several classes of lipid compounds, including over 25 000 different isoprenoid-derived metabolites (alkaloids, terpenoids, flavonoids), abscissic acid, gibberellins, the phytol side chain of chlorophyll (Moore, T.S., Jr., 1993; Bartley, G.E. and Scolnik, P.A., 1995; McGarvey, D.J. and Croteau, R., 1995), and more. Metabolic or catabolic products of such lipid compounds are precursors for the formation of essential molecules such as, for example,

prostaglandines and their derivatives (Stumpf, P.K., 1981) and the plant hormone jasmonic acid (Ohlrogge, J. and Browse, J., 1995; Vick, B.A. and Zimmermann, D.C., 1984). However, the predominant type of lipids is derived from the fatty acid and the glycerolipid biosynthetic pathway.

1.3 Fatty acids and glycerolipids in plants

1.3.1 Fatty acids

Fatty acids are a class of compounds containing a medium to long hydrocarbon chain and a terminal carboxylate group. The systematic name for a fatty acid is derived from the name of the hydrocarbon, determined by the number of carbon atoms (Gunstone, F.D. and Herslöf, B.G., 1992), by the substitution of *oic* for the final *e*. The chemical abbreviation of fatty acids is a **C** followed by the number of carbon atoms and the number of double bonds after a colon. Fatty acid carbon atoms are numbered starting at the carboxyl terminus with the C of the carboxyl group being the first. Carbon atoms 2 and 3 can also be referred to as α and β, respectively. The methyl carbon at the distal end of the chain is called the ω carbon. The position of double bonds is defined from the carboxyl end, represented by the symbol Δ followed by a superscript number indicating the carbon number, which is followed by the double bond position. Another nomenclature for the double bond position is defined by counting from the ω methyl carbon (as number 1) followed by the carbon number before the double bond. An example is shown in Figure 1.1.

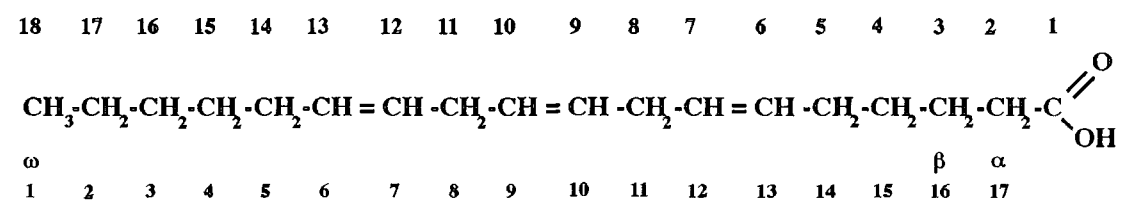

Chemical nomenclature	Systematic name	Trivial name
C 18:3 [$\Delta^{6,9,12\ cis}$]	***cis,cis,cis*-6,9,12 Octadecatrienoic acid**	**γ-linolenic acid**

Figure 1.1. Chemical structure and nomenclature of fatty acids.

The study of fatty acids has a long chemical history and many of them have trivial names. The most common and important fatty acids for food and non-food applications are presented in Table 1.1.

Table 1.1

Nomenclature for important fatty acids.

Chemical name	Trivial name	Systematic name
C 8:0	Caprylic acid	Octanoic acid
C 10:0	Capric acid	Decanoic acid
C 12:0	Lauric acid	Dodecanoic acid
C 14:0	Myristic acid	Tetradecanoic acid
C 16:0	Palmitic acid	Hexadecanoic acid
C 16:1 [Δ^{9cis}]	Palmitoleic acid	*cis*-9-Hexadecenoic acid
C 16:1 [Δ^{11cis}]	Palmitvaccenic acid	*cis*-11-Hexadecenoic acid
C 18:0	Stearic acid	Octadecanoic acid
C 18:1 [Δ^{6cis}]	Petroselenic acid	*cis*-6-Octadecenoic acid
C 18:1 [Δ^{9cis}]	Oleic acid	*cis*-9-Octadecenoic acid
C 18:1 [Δ^{11cis}]	Vaccenic acid	*cis*-11-Octadecenoic acid
C 18:1 [Δ^{9cis},12OH]	Ricinoleic acid	D-12-Hydroxyoctadec-cis-9-enoic acid
C 18:2 [$\Delta^{9,12cis}$]	Linoleic acid	*cis,cis*-9,12-Octadecadienoic acid
C 18:3 [$\Delta^{6,9,12cis}$]	γ-linolenic acid	*cis,cis,cis*-6,9,12-Octadecatrienoic acid
C 18:3 [$\Delta^{9,12,15cis}$]	α-linolenic acid	*cis,cis,cis*-9,12,15-Octadecatrienoic acid
C 20:0	Arachidic acid	Eicosanoic acid
C 20:1 [Δ^{11cis}]	Gondoic acid	*cis*-11- Eicosenoic acid
C 22:0	Behenic acid	Docosanoic acid
C 22:1 [Δ^{13cis}]	Erucic acid	*cis*-13- Docosenoic acid
C 24:0	Lignoceric acid	Tetracosanoic acid
C 24:1 [Δ^{15cis}]	Nervonic acid	*cis*-15-Tetracosenoic acid

In cells, fatty acids are almost always found with their carboxyl group esterified or otherwise modified. These modifications lead to a wide range of structures and account for multiple roles (of the different forms) of fatty acids in cellular properties and processes. In plants, and most other organisms, the major fatty acids are hydrocarbons with a chain length of 16 or 18 and containing from one to three double bonds.

Cuticular lipids

Many fatty acids are reduced to alcohols and aldehydes, esterified to fatty alcohols (wax esters) or polymerised (cross-linked) by esterification of carboxylgroups to hydroxyl groups on the other acyl chains (cutin), and are found in the epicuticular lipid matrix outside cells (Post-Beittenmiller, D., 1996; Von Wettstein-Knowles, P.M., 1993; Todd, J. et al., 1999). These cuticular lipids provide a crucial hydrophobic barrier against environmental stresses, such as pathogens and water loss.

1.3.2 Glycerolipids; the 'knows' and 'don't knows'

The most abundant lipid fraction of plants consists of ester-derivatives of glycerol and is termed glycerides, or glycerolipids.
Glycerolipids can basically be divided in two major groups:

1 **Structural membrane glycerolipids**
2 **Storage triacylglycerols** (TAG)

1.3.2.1 Structural membrane glycerolipids.

Membrane lipids have fatty acids attached to both the *sn*-1 and *sn*-2 position of a glycerol backbone and a polar headgroup attached to the *sn*-3 position. The amphipathic physical properties of glycerolipids, which are essential to formation of membrane bilayers, come from this combination of polar headgroups and nonpolar fatty acylchains.

Within a single membrane, each lipid class has a distinct fatty acid composition (Browse, J. et al., (1993) and each subcellular membrane has a distinct and characteristic complement of glycerolipid types. Various extrachloroplast membranes mainly consist of the characteristic **phospholipids**: phosphatidyl-choline (PC), phosphatidyl-ethanolamine (PE) and phosphatidyl-inositol (PI), in order of abundance (Harwood, J.L., 1988). In contrast to the phospholipid nature of extrachloroplast membranes, the plastid membranes have uniquely different compositions (Harwood, J.L., 1980). The major or only phospholipid in chloroplast thylakoid membranes is phosphatidyl-glycerol (PG). Three **glucosylglycerides** make up the complement of major plastid membrane lipids; monogalactosyldiacylglycerol (MGDG), digalactosyldiacylglycerol (DGDG) and sulphoquinovosyldiacylglycerol (SL) (Joyard, J. et al., 1993; Gounaris, K. et al., 1986). An exclusive lipid component of inner mitochondrial membranes is diphospatidylglycerol (DPG) (Bligny, R. and Douce, R., 1980).

The composition of each lipid class and membrane is largely conserved throughout evolution in the plant kingdom and is defined by its structure-function relationship. The structural membrane glycerolipids, by forming a phospolipid bilayer, are essential for the functioning of every plant cell. They define the permeability barrier of cells and organelles, and serve as a matrix or active support for a vast array of proteins involved in important functions of the cell, for example, signal transduction (Martin, T.F.J., 1998), energy transduction, solute transport, protein targetting and trafficking, DNA replication, secretion, cell-cell recognition.

1.3.2.2 Storage triacylglycerols (TAG)

Triacylglycerol (TAG) molecules have all three position of the glycerol backbone esterified with fatty acids and are as such not suitable for formation of membranes. TAG serves primarily as a storage form of carbon in seeds. The amount and types of oil in different species may vary widely and TAG is stored in densely packed lipid (or oil-) bodies (Huang, A.H.C, 1992; Murphy, D.J., 1993; Herman, E.M., 1994).

Nature shows that an enormous variety of storage lipids is possible. Over 500 different kinds of fatty acids have been observed in the oils of plant species (Schmid, R.D., 1988). Several plant species produce storage lipids, with an enormous variation in chain length, degree of saturation or modification of fatty acids. These can constitute up to 60% of their dry seed weight (Gunstone, F.D. et al., 1994). Also it has been shown that major changes in the types of fatty acids in the TAG can be made without affecting seed germination or viability of the crop plant (for example: Kinney, A.J. and Knowlton, S., 1997). This analogy to being 'secondary metabolites' has made TAG synthesis an attractive target for genetic modification. It has already proven to be possible to produce plant oils with new functionality by expressing one or a number of heterologous genes (Kinney, A.J., 1997).

In the last two decades the need for specific and detailed knowledge of the mechanisms regulating plant glycerolipid metabolism, the biosynthetic pathways, the metabolic partitioning and the enzymes involved in it, has led to major advances in this area. Combined biochemical-, molecular-, genetic- (mutational analysis) and transgenic approaches have enriched our current understanding of the basic metabolic pathways and regulation of both membrane synthesis and seed TAG synthesis in plants. However, our endeavours to solubilise and purify/clone membrane bound proteins involved in the pathways, still present challenging difficulties. We know relatively little about metabolic partitioning (flux through the pathways)(Kinney, A.J., 1998; Herbers, K. and Sonnewald, U., 1996), pleiotropic effects of single genes, *in vivo* interaction between different metabolic pathways and upper hierarchy level regulatory components (transcription factors). Alternative strategies such as gene-tagging, map-based cloning, mutant complementation and formation and analysis of rapidly growing (computerised-) databases (DNA sequencing projects, Proteomics and protein structural data) are being employed in overcoming this problem.
Overall, the current status of our understanding of the pathways and their regulation is a developing area but leaves plant lipid scientists still with a lot of important questions to answer.

Excellent and comprehensive reviews of plant fatty acid metabolism (Harwood, J., 1996), regulation of fatty acid synthesis (Ohlrogge, J. and Jaworski, J.G., 1997) and plant lipid metabolism (Ohlrogge, J. and Browse, J., 1995), genetics, molecular biology and biotechnological aspects (Browse, J. and Somerville, C.R., 1994; Kinney, A.J., 1994; Murphy, D.J., 1999; Slabas, A.R. and Fawcett, T., 1992; Töpfer, R. et al., 1995), have been published in recent years. Within the scope of this thesis a relatively simple overview of fatty acid and lipid biosynthesis is presented, partly with reference to the above publications.

1.4 Fatty acid and lipid synthesis in plants

Fatty acid biosynthesis is a conserved primary metabolic pathway. It is found in all living cells of the plant and is essential to growth. Mutations that block fatty acid biosynthesis have not been isolated and inhibition of the pathway is lethal. Overall, fatty acid and lipid biosynthesis in plants and its regulation seems fundamentally different from that in animals, fungi and some bacteria, in a number of respects:

I) **Structural organisation of the fatty acid synthetase (FAS)**

II) **Compartmentalisation of lipid metabolism**

III) **Prokaryotic/eukaryotic model; plants posses two distinct pathways for glycerolipid synthesis**

1.4.1 Structural organisation and biochemistry of the FAS complex

The *de novo* biosynthesis pathway, to produce 16- or 18- carbon fatty acids from acetyl-CoA and malonyl-CoA, consists of two enzyme systems: acetyl-CoA carboxylase (ACCase) and the fatty acid synthetase (FAS) complex of reactions. At least 30 enzymatic reactions are required.

ACCase catalyses the formation of malonyl-CoA from acetyl-CoA (reaction 1 in Figure 1.2) and FAS catalyses the transacylation of a protein cofactor (acyl carrier protein (ACP)), with the malonyl moiety and further extension of the growing acyl chain with malonyl-ACP. ACP is a small acidic protein that contains a phosphopanthotein prosthetic group to which the growing acyl chain is attached as a thioester.

It is not within the scope of this chapter to give an enormously detailed description of the individual reactions and their regulation, as this has been done elsewhere (Harwood, J., 1996; Ohlrogge, J. and Browse, J., 1995; Ohlrogge, J.B. and Jaworski, J.G., 1997).

In animals (vertebrates), fungi and some bacteria all of the reactions are catalysed by domains of one or two high molecular weight, multifunctional polypeptides, located in the cytosol, the **FAS I** complex (Bloch, K. and Vance, D., 1977; Battey, J.F. and Ohlrogge, J.B., 1990).
A **type II fatty acid synthetase (FAS II) complex** occurs in the stroma of plastids in **plants** and is structurally and functionally very similar to the FAS system in most bacteria (Stumpf, P.K., 1981; Verwoert, I., (1994). This FAS II system consists of an easy dissociable multisubunit form of the enzyme system and has now been thoroughly studied in *Escherichia coli* (Volpe, J.J. and Vagelos, P.R., 1973) and several plants. Most of the FAS components/genes from *E. coli* and plants have been isolated (Magnuson, K. et al., 1993; Töpfer, R. and Martini, N., 1994; Slabas, A.R. et al., 1995; Wilmer, J.A., 1997) and it has been shown by "heterologous gene approaches" that these enzymes have a conserved, similar function in general mode of regulation between species (Verwoert, I., 1994; Kater, M.M., 1994). However, intriguing questions remain about the regulatory mechanisms, the stoichiometry, metabolic partitioning and whether or not FAS II enzymes are organised *in vivo* in a metabolon or supramolecular complex (Roughan, P.G. and Ohlrogge, J.B., 1996).

All the carbon atoms found in fatty acids are derived from **acetyl-coenzyme A** (CoA) in the plastid. The carbon source for the generation of this acetyl-CoA pool and thus for *de novo* fatty acid synthesis has been the topic of considerable debate (Ohlrogge, J. and Browse, J., 1995; Ohlrogge, J.B. and Jaworski, J.G., 1997). A relatively constant, large pool of acetyl-CoA is present during development and different pathways might act under different demands; for instance, the plastidial pyruvate dehydrogenase complex to generate acetyl-CoA or, the generation of free acetate, by the mitochondrial pyruvate dehydrogenase complex coupled to acetyl-CoA hydrolase, which can be converted to acetyl-CoA in the chloroplast stroma (Harwood, J.L., 1988; Roughan, P.G. and Ohlrogge, J.B., 1994).

The final products of the FAS complex are fully saturated 16- and 18- carbon fatty acids (palmitate and stearate respectively) attached to ACP. However, some species accumulate shorter fatty acids (caprylic (8:0), capric (10:0), lauric (12:0) or myristic (14:0)) as a result of the action of other enzymes (thioesterases) that cleave the growing fatty acid from ACP and as such prevent further elongation (reaction 7 in Figure 1.2).
After the malonyl moiety is transferred to ACP by malonyl-CoA: ACP transacylase (MCAT) (reaction 2 in Figure 1.2), the subsequent FAS reactions involve a series of condensation reactions with acyl-ACP (or acetyl-CoA) as acceptors. Three separate condensing enzymes act in formation of a 18-carbon saturated fatty acid. The initial FAS reaction is a condensation of acetyl-CoA and malonyl-ACP, catalysed by 3-ketoacyl-ACP III (KAS III) to form a 4-carbon product (Jaworski, J.G. et al., 1993; Tsay, J.T. et al., 1992). Kas I catalyses the condensations

from 4- to 16- carbon chain lengths and KAS II the final elongation from palmitoyl-ACP (16:0-ACP) to stearoyl-ACP (18:0-ACP). After each subsequent cycle of condensation to 3-ketoacyl-ACP, three reactions take place to form the next saturated fatty acid. These three reactions are sequentially catalysed by 3-ketoacyl-ACP reductase, 3-hydroxyacyl-ACP dehydrase and enoyl-ACP reductase (reactions 3,4, 5 and 6 in Figure 1.2).
For a clear schematic representation of the reactions of saturated fatty acid biosynthesis the reader is referred to Figure 3 in the paper by Ohlrogge, J. and Browse, J. (Ohlrogge, J. and Browse, J., 1995).

1.4.2 Compartmentalisation of lipid metabolism and intermixing of lipid intermediates

In plants, in contrast to other organisms, *de novo* fatty acid biosynthesis doesn't occur within the cytosol but is localised in an organelle, the chloroplast. The final products of FAS now undergo different fates as a portion is used for lipid synthesis within the plastid and a major portion is exported into the cytosol for glycerolipid formation at the endoplasmic reticulum (ER) or other sites (Figure 1.2). Intermixing between plastid and ER lipid pools occurs because some extraplastidial lipids return to the plastid (Kunst, L. et al., 1988). This compartmentalisation requires specific regulatory mechanisms for the major pathways of plant lipid metabolism both in and outside the plastid. The exact nature of control of overall levels and composition of distinct lipids, the regulation of the metabolic flux under different conditions, and interorganelle communication is not known at present (Ohlrogge, J.B. and Jaworski, J.G., 1997).

1.4.3 The Prokaryotic/Eukaryotic Model; Higher plants posses two distinct pathways for glycerolipid synthesis

The two major products at the termination phase of the plastidial FAS system, 16:0-ACP and 18:0-ACP, are key substrates for further metabolism. The final fatty acid composition of the plant cell (structural membranes and storage TAG) is in large part determined by the relative activities of several different enzyme classes that further use these acyl-ACPs.
The prokaryotic/eukaryotic model for lipid assembly in the plant cell has been constructed from a large number of studies, including leaf and chloroplast labelling experiments, compositional analysis of cytosolic and chloroplastic lipids, substrate specificity studies, enzyme localisation and the characterisation of *Arabidopsis* mutants (Roughan, P.G. and Slack, C.R., 1982; Somerville, C. and Browse, J. 1991; Pollard, M. and Ohlrogge, J., 1999).

Figure 1.2. The main aspects of glycerolipid biosynthesis in plant tissues.

(I) The acetyl-CoA carboxylase (ACCase) and fatty acid synthetase (FAS) reaction complex convert acetyl-CoA into C 8 – C18 saturated acyl-ACPs, with the final chain length regulated by 3-ketoacyl-ACP synthetases (KAS) and thioesterases (TE) (reactions 1 –7). In different plant species, C14 – C18 saturates may be desaturated by specific soluble acyl-ACP desaturases (A-DES) (reaction 8). The acyl-ACPs may then be used in two ways: 1) they serve as substrates for the prokaryotic pathway in the plastid which esterifies predominantly palmitate (16:0) at the *sn*-2 position of glycerol (reactions 9 –12), or 2) they are converted to acyl-CoAs (reaction 13) and exported to the cytoplasmic endoplasmic reticulum (ER) via relatively uncertain mechanisms (possibly with involvement of an acyl-CoA binding protein (ACBP)).
(II) Depending on the plant species, in the ER, oleate (18:1 Δ^9), as a central metabolite, may be subject to fatty acid modifications (reactions 14a –18c).
(III) All these acyl-CoAs may serve as substrates for the eukaryotic pathway which primarly esterifies 18- carbon atoms at the *sn*-2 position of glycerol-3-phosphate (G3P) (reactions 19 + 20). With phosphatidic acid (PA) as a branchpoint lipid intermediate, some PA is channelled to signalling or membrane lipid formation (reactions 21 +22) and another portion of PA is used for the synthesis of storage triacylglycerols (TAG) via reaction 23 catalysed by diacylglycerol acyltransferase (DAGAT). The TAG is stored in oil bodies but may still be available for further metabolism. This representation of a plant cell is not to scale, but is drawn to emphasise the compartmentalisation of the pathways. **Reaction steps** are depicted by numbers: **1)** acetyl-CoA carboxylase (ACCase), **2)** malonyl-CoA: ACP transacylase (MCAT), **3)** 3-ketoacyl-ACP synthase (KAS), **4)** 3-ketoacyl-ACP reductase (3-KR), **5)** 3-hydroxyacyl-ACP dehydrase (3-HAD), **6)** enoyl-ACP reductase (ER), **7)** thioesterases (TE), **8)** acyl-ACP desaturases (A-DES), **9)** chloroplastic glycerol-3-phosphate acyltransferase (c-G3PAT; c-1AT), **10)** chloroplastic lysophosphatidic acid acyltransferase (c-LPAAT; c-2AT), **11)** phosphatidate cytidyl transferase (PCT), **12)** chloroplastic phosphatidic acid phosphatase (c-PAP), **13)** acetyl-CoA synthetase (ACS), **14a-c)** 3-ketoacyl-ACP synthase dependent elongases (EL), **15)** epoxydases (EP), **16)** hydrolases (HYD), **17)** acetylinases (AC), **18a)** ω3 desaturase (ω3 DES), **18b)** Δ^6 desaturase (Δ^6 DES), **18c)** ω3 desaturase (ω3 DES), **19)** endoplasmic glycerol-3-phosphate acyltransferase (e-G3PAT; e-1AT), **20)** endoplasmic lysophosphatidic acid acyltransferase (e-LPAAT; e-2AT), **21)** endoplasmic PCT, **22)** endoplasmic PAP, **23)** diacylglycerol acyltransferase (DGAT; 3-AT) Glycerol-3-phosphate (G3P), lysophosphatidic acid (LPA), diacylglycerol (DAG), phoshatidic acid (PA), triacylglycerol (TAG), cytidine diphosphate-diacylglycerol (CDP-DG), phosphatidyl glycerol (PG), monogalactosyldiacylglycerol (MGDG), digalactosyldiacylglycerol (DGDG), sulphoquinovosyldiacylglycerol (SL), phosphatidyl choline (PC), phosphatidyl ethanolamine (PE), phosphatidyl inositol (PI).

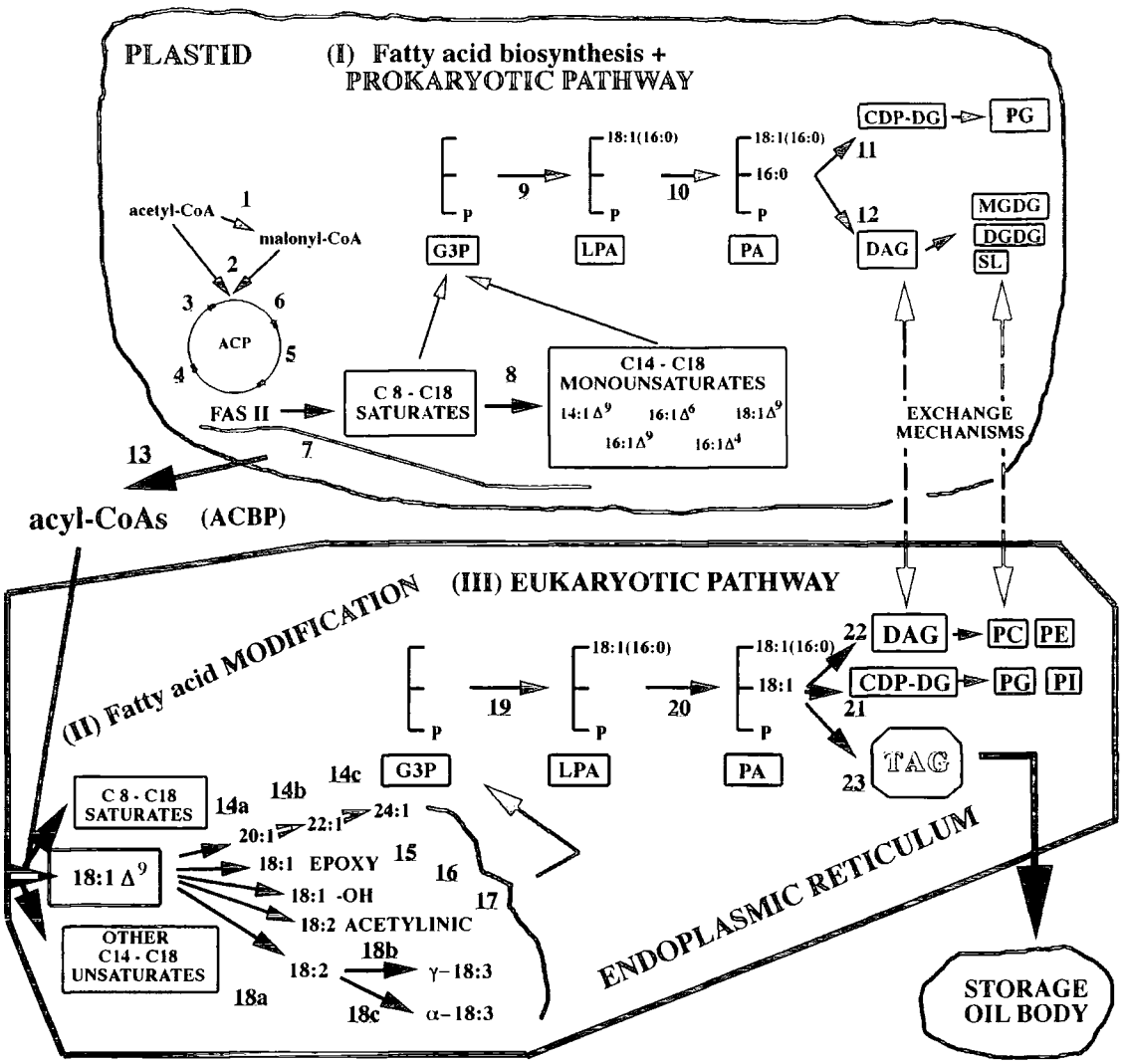
PLASTID
(I) Fatty acid biosynthesis +
PROKARYOTIC PATHWAY
acetyl-CoA
malonyl-CoA
ACP
FAS II
C 8 - C18
SATURATES
G3P
LPA
PA
18:1(16:0)
16:0
18:1
CDP-DG
PG
DAG
MGDG
DGDG
SL
C14 - C18
MONOUNSATURATES
14:1 Δ9
16:1 Δ6
18:1 Δ9
16:1 Δ9
16:1 Δ4
EXCHANGE
MECHANISMS
acyl-CoAs
(ACBP)
(II) Fatty acid MODIFICATION
(III) EUKARYOTIC PATHWAY
PC
PE
PG
PI
TAG
C 8 - C18
SATURATES
18:1 Δ9
OTHER
C14 - C18
UNSATURATES
20:1
22:1
24:1
18:1 EPOXY
18:1 -OH
18:2 ACETYLINIC
18:2
γ-18:3
α-18:3
ENDOPLASMIC RETICULUM
STORAGE
OIL BODY

In this model, *de novo* produced fatty acyl-ACPs can be used directly by plastid-localised acyltransferases for the synthesis of intermediates for the "prokaryotic" plastid lipids that are assembled totally within the chloroplast, such as phosphatidyl glycerol (PG), and in 16:3 plants, (mono- or di-) galactosyldiacylglycerol (GDG) and sulphoquinovosyldiacylglycerol (SL) (Joyard, J. et al., 1993; Ohlrogge, J. and Browse, J., 1995). Alternatively, the acyl-ACPs provide acyl groups for export from the plastid for subsequent modification, activation and assembly of lipids in the endoplasmic reticulum by an other set of acyltransferases constituting the "eukaryotic" pathway. The eukaryotic pathway leads to the synthesis of the major structural phospholipids of the endomembrane system and, up to a certain step (phosphatidic acid intermediate), of storage triacylglycerol.

The activity and substrate specificity of mainly three classes of plastidial enzymes seem to determine the products of fatty acid synthesis

1) Desaturases

Depending on the plant species, C14-C18 saturated acyl-ACPs can be desaturated by a variety of soluble chloroplast acyl-ACP desaturases: Δ^9 myristoyl-ACP desaturase (Schultz, D.J. et al., 1996), Δ^9 palmitoyl-ACP desaturase (Cahoon, E.B. et al., 1997), Δ^6 palmitoyl-ACP desaturase (Cahoon, E.B. et al., 1994), Δ^4 palmitoyl-ACP desaturase (Cahoon, E.B. et al., 1992), Δ^9 stearoyl-ACP desaturase (Thompson, G.A. et al. 1991; Shanklin, J. and Somerville, C. 1991).

The best characterised is the soluble stearoyl-ACP desaturase which inserts a *cis* double bond at the Δ^9-position of the C18:0-ACP. A crystal structure for the castor bean Δ^9 stearoyl-ACP desaturase (Lindqvist, Y. et al., 1996) has allowed a detailed structure-function analysis and has now offered the rational engineering of the chain length specificity, the double bond formation as well as the position of hydrogen abstraction (Cahoon, E.B., et al., 1997; Cahoon, E.B. et al., 1998).

The 16- carbon fatty acids, after incorporation in chloroplast membranes, are desaturated by the sequential action of a family of lipid-linked desaturases (Somerville, C.R. and Browse, J., 1996). Further desaturation into polyunsaturated fatty acids (PUFAs) (Napier, J. et al., 1999) is catalysed by integral membrane acyl-lipid desaturases once the fatty acids have been esterified to CoA or on glycerolipids. A comprehensive overview of all aspects of desaturation is recently published by Shanklin, J. and Cahoon, E.B. (Shanklin, J., and Cahoon, E.B., 1998).

2) Thioesterases

Two distinct but related types of acyl-ACP thioesterases catalyse chain termination by hydrolysis of the acyl chain from ACP and are essential for channelling of carbon flux between the two lipid biosynthesis pathways in plants.

One thioesterase has greater specificity for 18:1-ACP and another type of thioesterase is more specific for saturated acyl-ACPs ('long chain' thioesterases) (Dörmann, P. et al., 1995; Jones, A. et al., 1995). In some plants, 'medium chain' thioesterases with specificity for shorter chain length acyl-ACP (C 8, C10, C12) can prematurely terminate fatty acid synthesis with consequences for the chain length of products incorporated into lipids (Davies, H.M., 1993; Dörmann, P. et al., 1993; Pollard, M.R. et al., 1991).

3) Acyltransferases

Key enzymes for defining the prokaryotic pathway of the chloroplast inner envelope and the eukaryotic pathway are acyltransferases. Plant cells contain three separate sets of acyltransferases, in the chloroplasts, in the endoplasmic reticulum (ER) and in mitochondria. Acyltransferases transesterify acyl moieties from acyl-ACPs or acyl-CoAs to glycerol in a biochemical process generally known as the Kennedy pathway (Kennedy, E., 1961; Vogel, G. and Browse., J., 1996).

sn-Glycerol-3-phosphate acyltransferase (**GPAT** [EC 2.3.1.15]) and 1-acyl-glycerol-3-phosphate (LPA) acyltransferase (**LPAAT** [EC 2.1.1.51]) catalyse sequential acylation at the *sn*-1 and *sn*-2 position of glycerol-3-phosphate (G3P) respectively. The phosphatidic acid (PA) produced is a precursor in a branchpoint for the formation of triglycerides and for the synthesis of complex cellular glycerolipids in plastids or cytosol.

The glycerol-3-phosphate acyltransferase (GPAT) from chloroplasts is a soluble protein localised in the stroma (Joyard, D. and Douce, R., 1977). The GPAT in the cytoplasm is bound to the ER (Frentzen, M., 1990a) and the GPAT in mitochondria is bound to the outer membrane (Frentzen, M. et al., 1990b).

The LPAAT in the chloroplast, cytoplasm and mitochondria are all bound to membranes (Joyard, D. and Douce, R., 1977; Ichihara, K. et al., 1987; Frentzen, M. et al., 1990b). DAGAT is a membrane bound enzyme that is thought to be located in the ER (Settlage, S.B. et al., 1996; Lacey, D.J. and Hills, M.J., 1996).

The **PA** made via the prokaryotic pathway have 16:0 at the *sn*-2 position and, in most cases, 18:1 at the *sn*-1 position due to the substrate specificities of the plastid localised acyl-ACP acyltransferases (Frentzen, M., 1993). The PA can subsequently be converted either to diacylglycerol (DAG) by phosphatidic acid phosphatase (**PAP** [EC 3.1.3.4]), located in the inner plastid envelope, or to cytidine diphosphate-DAG (CDP-DG) by phosphatidate cytidyltransferase (**PCT** [EC 2.7.7.41])

The eukaryotic pathway occurs primarily at the ER and the microsomal acyltransferases use acyl-CoA substrates to produce PA with a different positional distribution of fatty acids at the *sn*-positions of the glycerol backbone. This PA is highly enriched in C18 fatty acids at the *sn*-2 position and gives rise to phospholipids characteristic of extrachloroplast membranes (PC, PI and PE).

However, a reversible lipid exchange between the ER and chloroplast is possible by return of the DAG moiety of PC to the chloroplast, contributing to the synthesis of plastid lipids (Miquel, M. and Browse, J., 1992; Browse, J. et al., 1993).

It is assumed that the only difference between '18:3 plants', in which extraplastidial membranes are exclusively synthesised by the eukaryotic pathway, and '16:3 plants', is the absence or presence of plastidial PAP activity (Mongrand, S. et al., 1998).

DAG is a common precursor to membrane PC and storage TAG. The enzymatic reaction exclusively committed to TAG biosynthesis is catalysed by diacylglycerol acyltransferase (**DAGAT** [EC 2.3.1.20]) (Stymne, S. and Stobart, A.K., 1987; Katavic, V. et al., 1995; Zou, J. et al., 1999; Hobs, D.H. et al., 1999). An hypothesis to be tested fully, is that DAGAT may be one of the rate limiting steps in plant storage lipid accumulation and thus a potential target for genetic modification (Ichihara, K. et al., 1988; Perry, H.J. and Harwood, J.L., 1993).

Acyl-ACPs produced and perhaps modified in the plastid, which have not entered the plastidial prokaryotic pathway are converted to acyl-CoAs (Fulda, M. et al., 1997) and exported to the ER. There is indication that this export requires a free fatty acid (Pollard, M. and Ohlrogge, J., 1999). However, the mechanism for acyl export from the chloroplast may be complex, possibly involving acyl binding proteins from the cytosol (Chye, M.-L., 1998; Brown, A.P. et al., 1998; Chye, M.-L. et al., 1999).

The acyl-CoA pool of the ER consists not only of the plastid-derived C 8 – C18 saturates and C14 – C18 monounsaturates, but also of polyunsaturated fatty acids (PUFAs) and a variety of 'unusual' fatty acids. Oleate (18:1 Δ^9) on the ER membrane is a central metabolite and can be subject to a variety of modifications and elongations as follows:

- elongations with two to six additional carbons by poorly characterised 3-ketoacyl-ACP synthase dependent elongases (Leonard, J.M. et al., 1998),
- epoxydation (Broun, P. et al., 1998),
- hydroxylation (Cahoon, E.B. et al., 1998; Broun, P. and Somerville, C., 1997),
- acetylination (Broun, P. et al., 1998),
- desaturation (Schneider, G. and Schmidt, H. 1997; Fukuchi-Mizutani, M. et al., 1998).

This acyl-CoA pool can be channelled to signalling, membrane glycerolipid formation and storage triacylglycerols formation(Millar, A.A. and Kunst, L., 1997; Zou, J. et al., 1997).

1.5 Storage TAG metabolism in plants

The fatty acid composition of storage oils in oil seeds is much more varied than that of membrane glycerolipids. The exact reasons for this great diversity in storage oils and concomitant exclusion of the majority of 'unusual' fatty acids from membranes (PC) is as yet unknown. If they would be incorporated as a major membrane component they could disrupt the important physical properties of membranes. The regulatory control of metabolic selection steps for restriction of fatty acids to membranes or channelling to TAG, and, if or not, there is spatial distinction of TAG and membrane synthesis, is not clear. Part of the explanation could be the substrate specificities/selectivities of the acyltransferases (specifically DAGAT) and CDP-choline:choline phosphotransferase (CDP-choline CPT; responsible for synthesis of PC from DAG or reverse) (Vogel, G. and Browse, J., 1996) or spatial- or subcellular separation of key reactions within the ER (Lacey, D.J. and Hills, M.J., 1996; Lacey, D.J. et al., 1999).

Storage TAG biosynthesis can take place via basically two ways. The most straightforward pathway is the Kennedy pathway with the central metabolite PA being dephosphorylised by PAP to diacylglycerol (DAG) which is subsequently acylated at the *sn*-3 position by DAGAT. However, in many oil seeds, most fatty acids do not immediately enter TAG biosynthesis but instead are incorporated mainly via phosphatidyl choline (PC) and become desaturated, elongated or otherwise modified. Fatty acids from PC may then become available for TAG synthesis via an acyl exchange or an exchange of the DAG moiety of PC (Stymne, S. and Stobart, A.K., 1987).

In developing oil seeds of most plant species the storage TAGs are stored in densely packed **oil bodies** until germination, at which time they are catabolised as an energy source. These organelles, which bud off from the ER, comprise 90 to 95 % TAG surrounded by a phospholipid monolayer and characteristic proteins termed oleosins (Napier, J. et al., 1996). During seed development accumulation of oil is accompanied by an increase in the number of oil bodies. Several studies indicate that TAG produced in storage tissues, such as oil seeds, is not necessarily a metabolically inert end product of metabolism. Desaturases (Sarmiento, C. et al., 1998), transacylases (Mancha, M. and Stymne, S., 1997) and acyltransferases may play a role in further TAG remodelling (Murphy, D.J., 1999).

In each plant species, regulatory mechanisms for catabolic pathways of exotic fatty acids, such as β-oxidation and the glyoxylate cycle (Eccleston, V.S. and Ohlrogge, J., 1998) seem to exist. This could be a mechanism for segregating or channelling 'unusual fatty acids' away from membrane lipids (a less flexible composition) to protect their integrity and function. The whole concept of metabolic channelling is underexplained.

1.6 The importance of genetic engineering of plant lipids

Genetic engineering of plant lipid metabolism is important for two, inextricably linked, main reasons; firstly, the use of transgenic biotechnology to fundamentally understand the complex biochemical and regulatory inter-relationships of lipid metabolism and secondly, to use the technologies to rationally direct the lipid metabolic pathways towards the production of novel oils or altered physiological properties (for example, stress- or chilling resistance).
Several recent publications provide a comprehensive overview on the status to date of the genetic engineering of plant lipids, the production of novel industrial and edible oils, the biotechnological aspects and what we have learned about the regulatory-, biochemical, aspects of lipid metabolism so far (Browse, J. and Somerville, C.R., 1994; Kinney, A.J., 1994; Murphy, D.J., 1999; Slabas, A.R. and Fawcett, T., 1992; Töpfer, R. et al., 1995; Broun, P. et al., 1999; Shewry, P.A. et al. (eds.), 1998).

1.6.1 Designing storage lipids

With the growing scientific knowledge about the different aspects of lipid biosynthesis, more potential targets for genetic manipulation of storage oils and even membrane lipids (chilling sensitivity) are being identified.
Plant oils are a commodity. Vegetable oils account for about 85 % of the globally traded seed oils used as **edible fat and oil**. Refined fats and oils enter the human diet as a major component mainly via processed food, salad and cooking oils, baking and frying fats, margarines and butter (Murphy, D.J., 1996). The major crops responsible for the world production of edible oils are soybean, oil palm, oilseed rape, sunflower, olive, coconut, peanut and cottonseed. The species used to produce mesocarp-derived lipids, such as oil palm and olive, are currently not as yet amenable to practical genetic manipulation and therefore the research and technology development has mainly been focussed on manipulating seed oils of the temperate crops.
A mixture of TAGs form the predominant constituent of all refined edible oils but these vegetable oils could contain varying amounts of undesirable lipid species formed during extraction, processing or depending on the status of the seed (or fruit). This points in the direction of one opportunity for plant modification, to reduce or eliminate oxidative and hydrolytic enzymes, such as lipoxygenases and lipases, which play a role in formation of these byproducts.

The manipulation of oilseed crops with improved nutritional qualities for human consumption has a number of other attractions and the main ones are:

1) manipulation of relative amounts of saturated to polyunsaturated faty acids in order to eliminate the need for industrial hydrogenation to form (semi-) solid fats, a process that produces undesirable *trans*-isomers of unsaturated fatty acids. This can be accomplished using very high-oleic (sunflower) oil or manipulating oil seeds towards high stearate and low palmitate content (Fitch Haumann, B., 1997; Knutzon, D.S. et al., 1992).

2) regulated reduction of saturates (principally palmitate and stearate) by, for instance, regulating the ratio of 16:0-ACP thioesterase, KAS II activities, stearoyl-ACP thioesterase and stearoyl-ACP reductase.

3) improving oxidative stability of the oil, by decreasing the levels of PUFA (linoleic acid (18:2)) and increasing the content of medium chain fatty acids (MUFAs) in oilcrops (such as soybean or rapeseed).

4) production of essential long-chain PUFAs with nutritional benefits as precursors for prostaglandins and as cholesterol-lowering agents (Newton, I.S., 1998).

5) production of 'designer TAG' with selected fatty acids at the *sn*-2 position. In principle this requires genetic manipulation to desired ratios of fatty acids and of acyltransferases with specific substrate selectivities to esterify them to the selected *sn*-positions of the glycerol backbone in TAG.

The contribution of thioesterases to oil quality in this respect has been shown by the accumulation of ~20% 18:0 (stearic) acid in transgenic rapeseed with a thioesterase gene from mangosteen (Hawkins, D.J. and Kridl, J.C., 1998) and the accumulation of 40 mol % 12:0 (lauric) acid in transgenic rapeseed TAG with a California bay acyl-ACP thioesterase (Voelker, T.A. et al., 1996). This oil is being used to produce filling fats, whipped toppings, coffee whiteners and confectionary coatings.

Recent progress relates to the isolation and manipulation of the acyltransferases, prompted by the moderate capacity or inability of rapeseed LPA AT to use unusual fatty acids (Slabas, A.R. and Brough, C.L., 1997a; Voelker, T.A. et al., 1996). The importance of addressing the strict specificity of the LPA AT in manipulation of oil composition has been demonstrated by, for instance, work in our laboratory (Brough, C.L. et al, 1996) and by Lassner and co-workers (Lassner, M. et al., 1995) on the modification of rape to accumulate higher levels of erucic acid (22:1) in the *sn*-2 position of seed TAG.

Global production of plant oils for **industrial use** (i.e. oleochemicals) are, at present, undercompetitive with petrochemicals but can succeed at the moment as high-value niche products for very specific applications (Murphy, D.J., 1999). However, this is possibly to change in the coming decades because the vast variety of unusual fatty acids in plants have

valuable chemical or physical properties that give them potential as industrial commodities, such as soaps, detergents and other surfactants (Ohlrogge, J., 1994; Töpfer, R. et al., 1995; Slabas, A.R. et al., 1997; Murphy, D.J., 1992).

Erucic acid (22:1 Δ^{13}), a monoene fatty acid which naturally occurred in high erucic acid rapeseed (HEAR) varieties and other *Cruciferae*, has recently gained considerable interest in this respect. Its long chain length makes it a valuable component of biodegradable lubricants and solvents, waxes, polishes and hydraulic fluids. The Δ^{13} position allowes oxidative cleavage resulting in a dicarboxilic 13-carbon brassylic acid which can be used in the perfume industry and as a precursor to nylon 13,13, a high-temperature thermoplastic. If the level of erucic acid in seeds could increase to high levels (~90%), the cost of purification could fall, making it competitive with petrochemicals.

1.6.2 Engineering membrane lipids

The characteristic composition of each membrane and lipid class is largely conserved throughout the plant kingdom. Differences in the distinct complement of different lipid structures in different membranes are important for their respective functions. The use of biotechnology and genetic engineering is important for gaining greater understanding of its structure-function relationship and of the effects of changes in lipid composition on the physiology and cell biology of plant cells. Isolating mutants, cloning the genes and manipulation of the pathways via transgenic technologies is not only important for elucidating metabolic pathways of complex membrane lipids but also helps us to learn about the mechanisms involved in channelling fatty acids to membrane lipids or storage lipids, its regulation and the influence of the genotype on overall plant physiology.

Major changes in membrane lipid composition might well be lethal, but subtle changes, specifically in the degree of unsaturation of membrane lipids, seem to be tolerated. This flexibility is a naturally occurring phenomenon in certain plants and micro-organisms in response to environmental temperature (Murata, N. and Nishida, I., 1990). Polyunsaturated lipids in membranes are essential for cellular function and plant viability at low temperatures. Biochemical characterisation of several *Arabidopsis* mutants (Somerville, C. and Browse, J., 1991) in combination with practical (rapid, high-throughput) analysis of fatty acid composition has been very powerful in elucidating parts of the metabolic pathways and isolation of difficult-to-clone genes.

The *fab1* and *fab2* mutants of *Arabidopsis* have increased levels of 16:0 and 18:0, respectively, in seed and leaf tissues (James, J., Jr. and Dooner, H.K., 1990; Wu, J. et al., 1994; Lightner, J. et al., 1994). In the *fab1* mutant, the mutation leads to a reduction in the

activity of the condensing enzyme catalysing elongation of the 16:0 to 18:0. In *fab2*, the 18:0-ACP desaturase activity is reduced. Both mutants appear to be leaky but, despite changes in overall fatty acid composition being small, there is a profound effect on the biology of the plants. The *fab2* mutant has an extreme dwarf growth phenotype. An increased 16:0 content in leaves of *fab1* plants also influences synthesis of chloroplast PG that contain only so called high-melting-point (HMP) molecular species (16:0, 16:1-trans and 18:0), accounting for up to 42% of the PG in leaves of the mutant. These HMP-PGs have been correlated with a major role in determining plant chilling sensitivity (Nishida, I. and Murata, M., 1996). Five mutants have been isolated which are affected in chloroplast lipid desaturation: *fad4*, *fad5*, *fad6*, *fad7* and *fad8* (Browse, J. et al., 1985; Kunst, L. et al., 1989a; Browse, J. et al., 1989;Browse, J. et al., 1986; McConn, M. et al., 1994). Two mutants primarily affect desaturation of the extrachloroplast lipids (PC): *fad2* and *fad3* (Miquel, M. and Browse, J. 1992; Browse, J. et al., 1993).

FAD2 was cloned using a T-DNA tagging approach (Okuley, J. et al., 1994) and *fad2* mutants are deficient in the activity of the ER 18:1 desaturase involved in production of polyunsaturated lipids via the eukaryotic pathway. The mutation at the *fad2* locus is largely irrelevant to growth and survival of the plants at normal temperatures (22 °C) but has a dramatic chilling sensitive phenotype when plants are transferred to 6 °C (Miquel, M. et al., 1993).

Transgenic plants manipulated with specific desaturase cDNAs have provided valuable and interesting pieces of knowledge. Antisense experiments using Δ^9-stearoyl-ACP desaturase cDNA from *Brassica campestris* resulted in high amounts of stearic acid in transgenic *Brassica campestris* and *Brassica napus* seeds (Knutzon, D.S. et al., 1992). Introduction of a desaturase cDNA from coriander endosperm, which accumulates petroselenic acid (C18:1 Δ^6), proved the desaturase to be a Δ^4-palmitoyl-ACP desaturase and not a Δ^6-stearoyl-ACP desaturase (Cahoon, E.B. and Ohlrogge, J.B., 1993).

1.6.2.1 Chilling resistance

Many economically important crops such as, soybean, maize, rice and cotton, and many tropical and subtropical fruits, are classified as chilling sensitive. Chilling resistant plants such as *Arabidopsis* and spinach, are able to develop at chilling temperatures (0 °C – 15 °C). The ability of plants to tolerate chilling temperatures seems closely correlated with the degree of unsaturation of fatty acids in the phosphatidyl glycerol (PG) of chloroplast membranes (Nishida, I. and Murata, M., 1996). Disaturated phosphatidyl glycerol can only be obtained via the prokaryotic pathway (Figure 1.2) and therefore the substrate preference of the soluble chloroplast GPAT has been implicated as a major determinant of plant chilling sensitivity.

Murata and co-workers (Murata, M. et al., 1992) demonstrated that the degree of chilling sensitivity of *Nicotiana tabacum* could be altered by transformation with cDNAs from *Arabidopsis*, a chilling resistant plant, or from squash, a chilling sensitive plant. The content of *cis*-unsaturates of chloroplastic PG was increased in plants with the *Arabidopsis* transgene and plant chilling sensitivity was decreased, whereas the introduction of the squash transgene increased the chilling sensitivity. In a similar approach Wolter and co-workers (Wolter, F.P. et al., 1992) transformed *Arabidopsis* with a modified *E.coli* glycerol-3-phosphate acyltransferase (*plsB*), resulting in increase in the level of HMP-PG and increased chilling sensitivity. Recently, also the importance of the unsaturation of membrane lipids in protecting the photosynthetic machinery from photo-inhibition under cold conditions has been emphasised (Nishida, I. and Murata, M., 1996).
Freezing damage is thought to occur by a different mechanism than chilling injury but it has been postulated that lipid composition plays a role in increased freezing tolerance induced by low-temperature acclimation of certain species (Steponkus, P.L. et al., 1990).

1.7 Requirements for genetic manipulation of plant lipid synthesis

Overall, the above studies show that in order to understand the regulation of de *novo* fatty acid biosynthesis, molecular techniques are indispensable tools and rely on the availability of respective cDNAs or genes. Although a majority of representative genes encoding enzymes of lipid metabolism have now been cloned, the characterisation and cloning of variants or isozymes with different substrate preference or other properties might be important. For some proteins involved in the metabolic pathways, multiple isoforms exist, which differ in expression in tissue types, developmental stages and environment. An illustrative example is the existence of individual ACP isoforms specifically involved in the biosynthesis of unusual fatty acids and suggestions that expression of a specific set of such isoforms participates in determination and division of the products of fatty acid biosynthesis (Suh, M.C. et al., 1999). Some isoforms are constitutively expressed, others are developmentally and tissue-specifically regulated. The same seems to be true for other lipid metabolism enzymes such as the acyltransferases.
The expression of other lipid gene-products, also when encoded by single copies in the genome, might be subject to strict *cis*- and/or *trans*- (and even post-translational), tissue- and developmental regulatory control (possibly even depending on environmental conditions). Characterisation and analysis of these specific regulatory elements (promoters and/or trans-acting factors) is important for in depth understanding of the metabolism and genetic manipulation.

Besides 'classical' molecular approaches such as biochemical purification of the proteins, antibody (immuno-) based cloning, heterologous or oligo-nucleotide library screening, or PCR based approaches, other powerful methods such as gene-tagging (T-DNA or transposon insertions) (Feldmann, K.A. et al., 1989), chromosome-walking (Arondel, V. et al., 1992) and complementation cloning (Brown, A.P. et al., 1995; Hanke, C. et al., 1995;Bourgis, F. et al., 1999) have been employed to isolate a variety of genes/cDNAs. Other approaches may be differential- or substraction based screening/cloning methods, maybe in combination with mapping techniques (for example AFLP) (Wan, J.S. et al., 1996).
The generation of the rapid growing complement of information, as consequence of sequencing projects (EST databases and genome sequencing), proteomics (Persidis, A., 1998; Abbot, A., 1999), with tools such as MALDI-TOF (Fu, D.-J. et al., 1998) and a structural database, in combination with biochemical and functional information of these different sequences, is without doubt enormously powerful to identify desired or novel macromolecules by comparison.

Other essential requirements for genetic engineering of plant metabolism are:

- the availability of a suitable gene transfer/transformation system (such as *Agrobacterium tumefaciens*, electroporation or chemical treatment, particle gun, micro-injection) and regeneration protocols for the desired crops.
- alteration of enzymatic activity through overexpression, gene-silencing, antisense- and other technologies (Chapter VI and VII).
- Last, but not least, in combination with the power of bacterial- (and other) protein-overproducing and purification methods (for example the pET systems), using X-ray crystallography to elucidate the complete 3-dimensional (3-D) structure of proteins, can provide an unparalleled understanding of molecular catalysis and the basis of substrate preference. Recent advances in the structure determination of at least two enzymes of plant lipid biosynthesis; enoyl-ACP reductase (Rafferty, J.B. et al., 1994a; Rafferty, J.B. et al., 1995) and Δ^9 stearoyl-ACP desaturase (Lindqvist, Y. et al., 1996) prove the power of these studies.

It is very likely that analysis of the 3-D structure in combination with appropriate biochemical information may make it possible to rationally engineer the functionality, specifically substrate preference, of certain enzymes.

Part of the aim of the research presented in this thesis was to start and build a basis for examining the structure-function relationship of the soluble chloroplast glycerol-3-phosphate acyltransferases (GPAT).

1.8 Glycerol-3-phosphate acyltransferases in plants

De novo biosynthesis of glycerolipids in plants occurs via the glycerol-3-phosphate pathway in different subcellular localisations in plant cells, namely plastids, mitochondria and endoplasmic reticulum (ER). Glycerol-3-phosphate acyltransferase (GPAT [EC 2.3.1.15]) catalyses acylation at the *sn*-1 position of *sn*-glycerol-3-phosphate to form *sn*-1-acylglycerol-3-phosphate (lysophosphatidic acid; LPA). The isozymes, which are probably all nuclear encoded, differ appreciable in their ability to use CoA and ACP thioesters and have different specificities and selectivities for defined acyl groups of the substrates.
The intraorganelle localisation and general properties of GPAT are shown in Table 1.2

Table 1.2. Comparison of general properties of GPAT from different subcellular compartments of vegetative organs of plants*.

GPAT	PLASTIDS	MITOCHONDRIA	MICROSOMES
Localisation:	Stroma, envelope	Intermembrane space, OM, IM**	ER, Golgi
pH optimum:	7 – 8	7 – 8	7 – 8
Acyl acceptor:	G3P	G3P	G3P
Acyl donor:	acyl-ACP	acyl-CoA	acyl-CoA
FA selectivity:	18:1 ≥ 16:0	16:0 > 18:1	16:0 > 18:1

*Adapted from Frentzen, M., 1993.

**OM, outer membrane; IM, inner membrane.

1.8.1 Microsomal GPAT

In the cytoplasmic part of plant cells, the ER is the primary site of the eukaryotic pathway. Cytoplasmic GPAT is hydrophobic and is bound to the ER (Frentzen, M., 1990a). The specific activities of the microsomal GPAT vary significantly with respect to the plant tissue (for example leaf and oil seeds) and species. The microsomal GPAT specifically uses acyl-CoA thioesters, is inactive with the respective ACP thioesters and has a slight preference for palmitoyl groups (Frentzen, M., 1993).

1.8.2 Mitochondrial GPAT

The contribution of mitochondria to plant cell glycerolipid production is relatively low, for example, about 10% of total cellular GPAT activity, in castor bean endosperm (Vick, B. and Beevers, H., 1977) and Euglena (Boehler, B.A. et al., 1976). In these plants, the ratio of GPAT activities in preparations of chloroplasts, microsomes and mitochondria is about 6:3:1. In contrast to the plastidial soluble GPAT, there are only a few publications concerning GPAT in purified mitochondrial fractions of plants. The mitochondrial GPAT in pea leaves is a soluble protein of the intermembrane space but in potato tubers (outer membrane) and castor bean endosperm (both outer and inner membrane) the enzyme is membrane bound (Frentzen, M. et al., 1990b). Mitochondrial GPAT displays higher activities with acyl-CoA than with corresponding ACP thioesters, with a slight preference for saturated fatty acids (Frentzen, M., 1993).

1.8.3 Chloroplastic GPAT

The chloroplast GPAT of various plant species is a soluble stromal protein and has been studied in detail (Cronan, J.E., Jr. and Roughan, P.G., 1987; Nishida, I. et al., 1987; Joyard, D. and Douce, R., 1977; Alban, C. et al., 1988; Bertrams, M. and Heinz, E., 1981).
The protein has been partially purified from several sources; spinach (Frentzen, M. et al., 1983), squash (Nishida, I. et al., 1987) and pea (Douady, D. and Dubacq, J.-P., 1987; Weber, S. et al., 1991). Studies on homogeneous enzymes have only been performed on two isomeric GPAT forms from squash and one from pea. Depending on the plant species, isofunctional GPAT occur in one to three isoforms (Nishida, I. et al., 1987; Bertrams, M. and Heinz, E., 1981). The two isoforms from pea show the same catalytic properties whilst one of the three isomeric forms from squash chloroplasts , AT1, is significantly different from AT2 and AT3 with regard to molecular mass (30 kDa instead of 40 kDa), isoelectric point (6.6 instead of 5.6 or 5.5 respectively) and kinetic properties (Nishida, I. et al., 1987).
The cDNAs for the soluble GPAT of squash (Ishizaki, O. et al., 1988), pea (Weber, S. et al., 1991), cucumber (Johnson, T.C. et al., 1992), *Arabidopsis* (Nishida, I. et al., 1993), *Carthamus* (Bhella, R.S. and MacKenzie, S.L., 1994), kidney bean (Fritz, M. et al., 1995), spinach (Ishizaki-Nishizawa, O. et al., 1995), oil palm (this thesis) and the gene for chloroplast GPAT (ATS1) from *Arabidopsis* (Nishida, I. et al., 1993) have been characterised. Genetic analysis indicates that chloroplastic GPAT is encoded by a single gene in *A. thaliana* (Kunst, L. et al., 1988).
The DNA sequence data suggests that the plastidial GPAT is synthesised as a preprotein of about 450-475 amino acids with a transit peptide of about 90 amino acids. The precise

processing site has not been determined but N-terminally truncated mature enzymes are catalytically active. The mature forms of GPAT from *A. thaliana,* cucumber and squash were predicted on the basis of molecular mass of the mature protein and consensus sequences for protein processing sites in chloroplasts (Murata, N. and Tasaka, Y., 1997). The recombinant, putatively mature-, GPAT enzymes from *Arabidopsis* and squash have been overproduced in *Escherichia coli* (Nishida, I. et al., 1993; Nishida, I., personal communication; this thesis). Maybe surprisingly, there is hardly any overall sequence homology between the sequences of plastidial GPAT and the GPAT of *Escherichia coli* (*plsB*) (Lightner, V.A. et al., 1983).
In spite of a high degree of sequence homologies between the plastidial GPATs of various plant species (up to 80%), the fatty acid selectivities can vary significantly from plant to plant. The chloroplast GPAT of higher plants can use both acyl-CoA and acyl-ACP thioesters but when the enzyme is presented with a mixture of CoA and ACP thioesters, they show a pronounced preference for acyl-ACPs (Frentzen, M. et al., 1983).
The substrate specificities, selectivities and kinetics of the enzyme from different sources have been studied *in vitro*. Selectivities are determined by incubating enzyme fractions with mixtures of , for instance, various acyl-labeled acyl-ACP and/or acyl-CoA thioesters and analysing the fatty acid composition of the reaction products via chemical extraction or chromatography. The chloroplast GPAT from pea and spinach uses 18:1-ACP in preference to 16:0-ACP (Bertrams, M. and Heinz, E., 1981). The substrate selectivity of the enzyme from squash is different; AT1 prefers 18:1-ACP at pH 7.4 (chloroplast pH in the dark), but under physiologically relevant conditions (pH8, chloroplast pH in the light) there is not much difference in substrate specificity among the three isoforms and they hardly show any discrimination between 18:1, 16:0 and 18:0 (Frentzen, M. et al., 1987). The abundance and kinetic parameters (Km and Vmax) of the isoforms differ considerably, most distinctively for AT1 compared to AT2 and AT3 (introduction to Chapter III (3.1); Frentzen, M. et al., 1987; Frentzen, M. et al., 1983; Nishida, I. et al., 1987).

1.8.3.1 GPAT and chilling resistance

Overall, the fatty acid composition of plant glycerolipids may be determined by :
1) the pool size and composition of acyl donors available to the enzymes, which could be altered by metabolic channelling, and
2) the substrate specificities and selectivities of the acyltransferases, determined by the physical and kinetic parameters of the enzymes.

To determine whether the fatty acid composition at the *sn*-1 position of glycerolipids synthesised in the chloroplasts, in particular PG, corresponded to the substrate specificity of

the plastidial GPAT, tobacco (*N. tabacum* var. Samsun) was transformed with transgenic constructs expressing squash and *Arabidopsis* GPAT (Murata, M. et al., 1992). Analysis of the transgenic plants revealed a significantly altered acyl composition of PG, but not of the relative composition of other glycerolipid classes. The tobacco plants transformed with the squash GPAT cDNA had increased levels of 16:0 at the *sn*-1 position of PG, from 16 % to 31 % and a decreased level of total *cis*-unsaturation of PG molecules from 64% down to 24%. In transgenic plants with the *Arabidopsis* GPAT cDNA, 16:0 at *sn*-1 of PG decreased from 16% to 12%, with an increase in total *cis*-unsaturation of PG from 64% to 72%.
Recently a similar effect was shown to occur in rice (*Oryza sativa*) which was transformed with the oleate-(18:1) selective GPAT of *Arabidopsis*. The levels of unsaturated fatty acids in leaf PG were found to be 28% higher than that of untransformed controls (Yokoi, S. et al., 1998).
Arabidopsis transformed with a modified version of the *E. coli plsB* gene, with a relative preference for saturated thioesters (mainly 16:0-), showed an increase of 16:0 in all the membrane lipids. In particular, the fraction of HMP-molecular species of PG was elevated (Wolter, F.P. et al., 1992).

The chilling sensitivity of plant species has considerable agricultural significance. It has been shown to be closely correlated with their proportion of non-fluid, prokaryotic PG species, in particular when both the *sn*-1 and *sn*-2 position are esterified with a saturated-(16:0 or 18:0) or *trans* unsaturated (*trans*-16:1) fatty acid (Murata, N. et al., 1982;Murata, N., 1983).
The formation of a critical proportion of non fluid lipid species is postulated to be determined by the substrate preference of the plastidial GPAT for 2 reasons:

1) *cis* double bonds cannot be introduced into saturated acyl groups esterified to PG by plant desaturases, and
2) the plastidial LPA AT invariantly directs palmitoyl (16:0) fatty acids to the *sn*-2 position of the glycerol-3-phosphate backbone.

Direct evidence for a major role of the plastidial GPAT with regard to chilling sensitivity was provided by the above mentioned transgenic studies. In accordance with the changes in fatty acid composition, the sensitivity of transformed plants to chilling treatments increased after transformation with squash GPAT cDNA (non-selective) or *E. coli plsB* DNA (16:0 selective) and decreased after transformation with 18:1 selective *Arabidopsis* GPAT cDNA.
Studies of an *Arabidopsis* mutant that lacks activity (< 5%) for the plastidial glycerol-3-phosphate acyltransferase, due to a single nuclear mutation at the *act1* locus, also demonstrated the importance of plastidial GPAT for the biosynthesis of glycerolipids via the prokaryotic pathway (Kunst, L. et al., 1988). In this mutant, the amounts of the individual lipids are hardly altered but the chloroplast membranes have an altered lipid composition and

the mutation seems to effectively convert the 16:3-plant into a 18:3-plant (Kunst, L. et al., 1989b).

The existence of a *fab1 Arabidopsis* mutant (single recessive nuclear mutation), with leaf PG containing an higher percentage (43%) of HMP-molecular species, suggests that HMP-PGs cannot alone account for chilling sensitivity in all plants (Wu, J. and Browse, J., 1995). *Fab1* may encode plastidial 3-ketoacyl-acyl carrier protein synthase II involved in elongation of palmitic acid (16:0) (Wu, J. et al., 1994). The *fab1* mutant does not show classic chilling sensitivity, despite its increased 16:0 content, but under more severe chilling treatment (prolonged growth at 2 °C) the *fab1* plants eventually show injury damage.
Other factors such as the importance of the unsaturation of membrane lipids in protecting the photosynthetic machinery from photoinhibition under cold conditions may also have physiological significance (Nishida, I. and Murata, M., 1996).

1.9 Objectives and outline of the thesis

The recent years have seen rapid advances in research to understanding principle reactions and aspects of plant lipid biosynthesis. A major driving force behind this is the goal of rationally modifying the lipid composition of plants towards commercial production of unusual and valuable fatty acids in oilseeds.
The first objective of this study was to initiate the detailed biochemical and molecular structural analysis of recombinant chloroplast glycerol-3-phosphate acyltransferase (GPAT) from plants (Chapter III, IV and V). A second aim within the scope of this thesis was to start evaluation and development of a molecular tool for specific gene-downregulation. This involved designing a strategy to use ribozyme-technology and the strong correlation between substrate preference of chloroplast GPAT and chilling tolerance as a phenotypic identification of specific gene-downregulation by the ribozymes *in vivo* (Chapter VI and VII).
In Chapter III, recombinant mature squash and *Arabidopsis* GPAT were overproduced in *Escherichia coli* and a method was developed for purification and obtaining relatively large amounts of the active enzymes. This did not only allow for detailed *in vitro* studies of the catalytic enzyme activities and substrate selectivities, the production of polyclonal antibodies for use in Western blotting experiments, but also for the elucidation of the crystal structure of the enzyme. This will provide a greater understanding of the catalytic mechanism and the structural requirements determining substrate preferences of this type of acyltransferases.
In order to establish the closest possible correlation with *in vivo* substrate selectivity of the GPAT enzymes as found in transgenic- and other studies, *in vitro* assay conditions were investigated using their natural substrates (acyl-ACPs) under physiologically relevant pH and

substrate concentrations (the 'Standard Selectivity Assay'). These assay conditions were used in Chapter IV and V to start evaluation of addressing the influence of the amino- (N-) terminus and specific regions of the enzymes in determining the substrate selectivity. In Chapter IV, the cloning of a novel GPAT cDNA and gene from oil palm (*Elaeis guineensis*) is reported. The isolation and characterisation of another variant of GPAT enzymes with different substrate selectivities and kinetic parameters is valuable for greater understanding of the structure-function relationships of these enzymes. The fatty acid selectivities of the GPAT enzymes can vary significantly from plant to plant but due to a high degree of sequence conservation, even careful examination cannot reveal structural elements that might be related to the preference for 18:1-ACP or 16:0-ACP. Chapter V describes the (re-) cloning of spinach GPAT and the construction of chimeric genes of *Arabidopsis* and squash GPAT to determine the importance of domains on overall substrate selectivity under physiologically relevant conditions. Also the effect of the N-terminus and two amino-acid substitutions in the carboxyl- (C-) terminus of the squash GPAT was examined. In this study, it has been found that, although the central region of the enzyme is important, one single amino acid substitution in the C-terminus can dramatically modify the substrate preference of the squash GPAT. Kinetic parameters for 16:0-ACP and 18:1-ACP were determined using crude cell-free enzyme preparations of a range of overproduced recombinant GPATs and 'domain swap' chimeras. In Chapter VI, a strategy was initiated to test the concept of specifically downregulating the expression of one out of multiple and sequence-similar acyltransferase genes. A series of experiments was designed to develop an *Arabidopsis* plant transformed with a squash GPAT cDNA and to subsequently evaluate the use of ribozyme technology, to specifically downregulate the endogenous *Arabidopsis* chloroplast GPAT activity. This strategy would potentially allow for a phenotypic indication for specific ribozyme-efficacy in *vivo* by examining the chilling sensitivity of the transgenic plants. The *in vitro* activity and specificity of essentially two endonucleolytic ribozymes, based on the hammerhead structure and directed against two different GUC codons in the *Arabidopsis* GPAT mRNA, was tested in Chapter VII.

Chapter II

∞∞∞∞∞∞

General Materials and Methods

Chapter II General Materials and Methods

2.1 Materials

Unless otherwise specified, all materials used throughout this study were obtained from either Sigma Chemical Company Ltd., Fancy Road, Poole, Dorset, BH17 7NH, or BDH Chemicals Ltd., Merck Ltd., Merck House, Poole, Dorset, BH15 1 TD. All reagents were of Molecular Biology or Ultrapure standard.

For DNA-labeling: [α-^{32}P]dCTP (10 mCi/ml; 3000 Ci/mmol; PB10205), for 5'-end-labeling of DNA: [γ-^{32}P]ATP (10 mCi/ml; 3000 Ci/mmol; PB10168), for RNA-labeling: [α-^{32}P]UTP (10 mCi/ml; 400 mCi/mmol; PB10163), for acyl-CoA and acyl-ACP synthesis: [1-^{14}C]16:0 (200 µCi/ml; 55 Ci/mol; CFA23) and [9,10(n)-^{3}H]18:1 (5 mCi/ml; 10.3 Ci/mmol; TRK140), for the standard GPAT assay: L-[U-^{14}C] glycerol-3-phosphate (50 µCi/ml; 151 Ci/mol; CFB171) and donkey-anti-rabbit Ig (whole Ab) [^{125}I] (750-3000 Ci/mmol; IM134) were purchased from Amersham International Plc., Little Chalfont, Amersham, Buckinghamshire, HP7 9NA.

Agar, Bacto-Tryptone, Bacto-yeast extract and casamino acids were obtained from DIFCO Laboratories, PO Box 14B, Central Avenue, West Molesey, Surrey, KT8 2SE or from Oxoid Ltd., Basingstoke, Hants., U.K.

Agarose MP (multi purpose agarose) was from Boehringer Mannheim Biochemica UK Ltd., Bell Lane, Lewes, East Sussex, BN7 1LG, UK.

Altered Sites® II *in vitro* Mutagenesis System and the *E. coli* strains ES1301 and JM109, were purchased from Promega Ltd., Delta House, Enterprise Road, Chilworth Research Centre, Southampton, SO16 7NS.

Ampicillin and Tetracycline were from NBL Gene Sciences Ltd., South Nelson Industrial Estate, Cramlington, Northumberland, NE23 9HL.

AquaPhenol™ was from Appligene, Pinetree Centre, Durham Road, Birtley, Chester-le-Street, Co. Durham, DH3 2TD, UK.

Bio-Spin 6 Chromatography Columns were purchased from from BioRad Laboratories Ltd., BioRad, Maylands Avenue, Hemel Hempstead, Hertfordshire, HP2 7TD.

BIOTAQ™ DNA Polymerase was obtained from BIOLINE, 16 The Edge Business Centre, Humber Road, London, NW2 6EW, UK.

Chromatography media (Hiload™ Q Sepharose (HP) [Q Sepharose High Performance are strong anion exchangers based on a rigid highly cross-linked beaded agarose with a mean particle size of 34 μm], Superose-12 HR 10/30) were from Pharmacia LKB Biotec, 23 Crosvenor Road, St. Albans, Hertfordshire, AL1 3AW, and used as indicated in the text.

Colony/Plaque Screen™ Hybridisation Transfer Membrane were obtained from NEN® Research Products, Du Pont (UK) Ltd., Diagnostics & Biotechnology Systems, Wedgewood Way, Stevenage, Hertfordshire, SG1 4QN.

Computers and computer software were of the MacIntosh family of computers. For most primary computing purposes the Microsoft Office (Word, Excell and Powerpoint), DNAStar and DNAStrider, and Adobe Photoshop (for pictures and figures) software packages were used. When deemed necessary, a Storage Phosphor Imaging System (a Model GS-525 Molecular Imager ®, BioRad) and an Imaging Densitometer (Model GS-690; BioRad) was used in combination with MacIntosh software for BioRad's Image Analysis System : MultiAnalyst version 1.0.2

Developing (Ilford Phenisol) and fixation solutions (Kodak Unifix)) were purchased from H.A. West [X-Ray] Ltd., 41 Watson Crescent, Edinburgh, EH11 1ES.

DTT, IPTG and X-Gal were obtained from Melford Laboratories Ltd., Chelsworth, Ipswich, Suffolk, IP7 7LE.

Ecoscint A scintillation fluid was purchased from National Diagnostics, and used in conjunction with 5 ml scintillation vials and a 1600TR Liquid Scintillation Counter that were manufactured by Canberra Packard Ltd., Brook House, 14 Station Road, Pangbourne, Berks, RG8 7DT.

ElectroMAX DH10B™ Cells were from Gibco BRL, Life Technologies, 3 Fountain Drive Inchinnan Business Park, Paisley, PA4 9RF.

Electrophoresis-pure Acrylamide , Ammonium persulphate (aps), Bis-acrylamide, glycine, SDS, Tris base, TEMED and Coomassie R-250 were from BioRad Laboratories Ltd., BioRad, Maylands Avenue, Hemel Hempstead, Hertfordshire, HP2 7TD.

Filter paper (3MM) and laboratory sealing film were from Whatmann International Ltd., Maidstone, UK.

GeneAMP™ Thin Walled Reaction Tubes were from Perkin Elmer Ltd., Post Office Lane, Beaconsfield, Buckinghamshire, HP9 1QA.

GFX™ PCR DNA and Gel Band Purification Kit was purchased from Amersham Pharmacia biotech, Amersham Life Science Ltd., Amersham Place, Little Chalfont, Amersham, Buckinghamshire, HP7 9NA.

Glass centrifuge tubes (13 ml) with Teflon-lined screw caps were purchased from Fisons, and the bottom of each subsequently tapered into a point by the Glass Blowing Department, University of Durham. The customised tubes were used for containment of large scale biochemical assays of GPAT or to contain the master-mixtures or during the synthesis of radiolabeled acyl-CoAs.

Hybond-N, Hybond-N^+ and Hybond-C were purchased from Amersham International Plc., Amersham Place, Little Chalfont, Amersham, Buckinghamshire, HP7 9NA.

Lambda (λ) BlueSTAR *Bam*HI Arms Kit (including the *E. coli* host strains: ER1647 and BM25.8) was purchased from Novagen, CN Biosciences Inc., (an affiliate of Merck KgaA, Darmstadt, Germany), Boulevard Industrial Park, Padge Road, Beeston, Nottingham, NG9 2JR.

Lambda (λ) ZAP ® II/*Eco*RI/CIAP Cloning Kit (including the *E. coli* strains: XL-Blue MRF' and SOLR™ Strain) and Gigapack ® II Packaging Extracts were obtained from Stratagene, La Jolla, CA 92037, USA.

Maleimide Activated Keyhole Limpet Hemocyanin and Ellman's Reagent were obtained from Pierce Chemical Company, Pierce Warriner (UK) Ltd., 44 Upper Northgate Street, Chester, CH1 4EF.

Minisart 0.2 μm sterile filters were from Sartorius GmbH, Postfach 3243, D-3400, Göttingen, Germany.

Oil Palm (*Elaeis guineensis* var. *Tenera*) fruit and spear-leaves were obtained from Pamol Plantations SDN. BHD., PO BOX 1, 86007 Kluang, Johor, Malaysia via Unifield T.C. Ltd., Unilever Plantations & Plant Science Group, Maris Lane, Trumpington, Cambridge, CB2 2LQ, UK.

Oligonucleotides for use in sequencing and PCR procedures were from MWG-Biotech, Germany and PE-Applied Biosystems UK, Cheshire, UK. Oligonuclotides used for cloning of ribozymes were purchased from Cruachem Ltd., Todd Campus, West of Scotland Science Park, Acre Road, Glasgow G20 0UA, UK.

pET System (specifically the vectors pET 17b, pET 24a and pET11d), developed for the cloning and overexpression of recombinant proteins in *Escherichia coli*, and the pET System Host Strains BL21 (DE3) and BL21 (DE3) pLysS, were obtained from Novagen, CN Biosciences Inc., (an affiliate of Merck KgaA, Darmstadt, Germany), Boulevard Industrial Park, Padge Road, Beeston, Nottingham, NG9 2JR.

pGEM-T easy Vector System (for cloning of *Taq* polymerase-amplified PCR products) was obtained from Promega Ltd., Delta House, Enterprise Road, Chilworth Research Centre, Southampton, SO16 7NS.

QIAEX® II Gel Extraction Kit was from Qiagen Ltd., Unit 1, Tillingbourne Court, Dorking Business Park, Dorking, Surrey, RH4 1HJ, UK.

*redi*prime DNA labelling system was from Amersham Life Science Ltd., Amersham Place, Little Chalfont, Amersham, Buckinghamshire, HP7 9NA.

Restriction endonucleases, Klenow enzyme, yeast tRNA, glycogen and *Taq* DNA polymerase and accompanying buffers were obtained from Boehringer Mannheim UK, (Diagnostics and Biochemicals) Ltd., Bell Lane, Lewes, East Sussex, BN7 1LG, UK.

Riboprobe Gemini II Core System for RNA transcription *in vitro*, was purchased from Promega Ltd., Delta House, Enterprise Road, Chilworth Research Centre, Southampton, SO16 7NS.

Shrimp Alkaline Phosphatase was purchased from United States Biochemical, P.O. Box 22400, Cleveland, Ohio 44122, USA.

Silica gel G TLC plates were from Whatmann International Ltd., St. Leonard's Road, Maidstone, Kent, ME16 0LS, UK.

T4 DNA Ligase, T4 DNA Polymerase and T4 Polynucleotide Kinase with reaction buffers were purchased from Promega Ltd., Delta House, Enterprise Road, Chilworth Research Centre, Southampton, SO16 7NS.

Thermal cyclers for polymerase chain reaction (PCR) experiments, used in these studies, were Perkin-Elmer Thermal Cycler model PE 9600 or the Robocycler Gradient 96 Temperature Cycler, Stratagene Ltd., Cambridge, Cambridge Innovation Centre, Cambridge Science Park, Milton Road, Cambridge, CB4 4GF, UK.

TimeSaver™ cDNA Synthesis Kit was obtained from Pharmacia LKB Biotec, 23 Crosvenor Road, St. Albans, Hertfordshire, AL1 3AW.

TOPO TA Cloning Kit (for cloning of *Taq* polymerase-amplified PCR products) with *E.coli* TOP10F' competent cells were purchased from Invitrogen, Invitrogen BV, PO Box 2312, 9704 CH Groningen, The Netherlands.

TrackerTape™ was obtained from Amersham Life Science Ltd., Amersham Place, Little Chalfont, Amersham, Buckinghamshire, HP7 9NA.

TRIzol Reagent (a ready-to-use reagent for the isolation of total RNA from cells and tissues) was purchased from Gibco BRL, Life Technologies, 3 Fountain Drive, Inchinnan Business Park, Paisley, PA4 9RF.

UltraPure Solution dNTPs were from Pharmacia LKB Biotec, 23 Crosvenor Road, St. Albans, Hertfordshire, AL1 3AW.

UV Stratalinker 2400 (for UV crosslinking nucleic acids to membranes); at auto crosslink settings) was from Stratagene Ltd., Cambridge, Cambridge Innovation Centre, Cambridge Science Park, Milton Road, Cambridge, CB4 4GF, UK.

$Vent_R$ ® DNA Polymerase was purchased from New England Biolabs (NEB) UK Ltd., 67 Knowl Piece, Wilbury Way, Hitchin, Hertfordshire, SG4 OTY, UK.

Wizard ® *Plus* SV Minipreps DNA Purification System was obtained from Promega Ltd., Delta House, Enterprise Road, Chilworth Research Centre, Southampton, SO16 7NS.

X-Ray film (RX-100) was from Fuji Photo Film (UK) Ltd., Fuji Film House, 125 Finchley Road, Swiss Cottage, London, NW3 6JH.

2.1.1 Bacterial growth media, antibiotic- and other stock solutions

Generally solutions and growth media were prepared according to Sambrook, J. et al. (1989) and were sterilised by autoclaving at 121 °C, 15 p.s.i. for 20 minutes. Otherwise solutions were filter-sterilised through a 0.22 µm nitrocellulose filter into a sterile container. All glassware, plasticware and other equipment were sterilised by autoclaving, as above, if possible.
The following media and stock solutions were routinely used in this work:

the growth media could be used as liquid media, or could be solidified by the addition of 1.5% agar or 0.7% agarose.

LB (Luria-Bertani):
10 g Bacto-Tryptone, 5 g Bacto-Yeast extract, 10 g NaCl made up to 1 l with ddH_2O. The pH was adjusted to 7.5 with NaOH.

2xYT Broth:
16 g Bacto-Tryptone, 10 g Bacto-Yeast extract, 10 g NaCl made up to 1 l with ddH_2O. The pH was adjusted to 7.5 with NaOH

NZY Broth:
5 g Bacto-Yeast extract, 5 g NaCl, 2 g $MgSO_4.7H_2O$, 10 g NZ amine (casein hydrolysate) made up to 1 l with ddH_2O. The pH was adjusted to 7.5 with NaOH

Lambda Top Agarose:
NZY Broth or LB with 0.7% agarose

SM Buffer:
5.8 g NaCl, 2 g $MgSO_4.7H_2O$, 50 ml of 1 M Tris-HCl (pH 7.5), 5 ml of 2% gelatin made up to 1 l with ddH_2O.

TE Buffer:
10 mM Tris-HCl (pH 7.5), 1 mM EDTA

20xSSC Buffer:
175.3 g of NaCl, 88.2 g sodium citrate made up to 1 l with ddH_2O. The pH was adjusted to 7.0 with NaOH (10.0 N).

10 x SDS running buffer:
10 g SDS, 144 g glycine, 30.3 g Tris base made up to 1 l with ddH_2O. The pH of 1 x running buffer should be 8.3.

5 x Laemmli SDS sample buffer:
2.5 g SDS, 1.25 g DTT, 0.95 g Tris base, 0.0125 g bromophenol blue, 12.5 ml glycerol made up to 25 ml with ddH_2O. The pH was adjusted to 6.8 and, after aliquoting (1 ml), stored at –20 °C.

50 x Denhardt's solution:
1 g BSA, 1 g Ficoll 400, 1 g Polyvinylpyrrolidone made up to 100 ml with ddH_2O, filter sterilised and stored at –20 °C.

6 x nucleic acid loading dye:
0.25% (w/v) bromophenol blue, 0.25% (w/v) xylene cyanol, 15% Ficoll 400, 60 mM EDTA in ddH_2O.

50 x TAE (DNA electrophoresis buffer):
242 g Tris base, 18.6 g EDTA-sodium salt made up to 800 ml with ddH_2O. The pH was then adjusted to 8 with glacial acetic acid (57 ml/l) and then made up to a final volume of 1 l with ddH_2O.

Depurination solution (for Southern blotting of large DNA molecules, such as genomic DNA):
0.25 N HCl (11 ml HCl and 989 ml ddH_2O.

Denaturation solution (for plaque-or colony lifting):
87.66 g NaCl and 20 g NaOH made up to 1 l with ddH_2O.

Neutralisation solution (for plaque-or colony lifting):
87.66 g NaCl and 60.5 g Tris base made up to 1 l with ddH_2O and the pH was adjusted to 7.5 with concentrated HCl.

10 x MOPS buffer (for RNA gel analysis):
41.2 g MOPS, 10.9 g sodium acetate 3-hydrate, 3.7 g EDTA made up to 1 l with ddH_2O and the pH was adjusted to 7 with NaOH (prepared in nuclease-free water). Usually this was autoclaved as above and turned light-yellow. Stored at room temperature protected from light. Recommendations in other protocols are to filter sterilise the buffer and not to use the solution when it appears yellow in color. However, during the course of this study, no adverse influence of the solution prepared in the described way was experienced.

Phosphate Buffered Saline (PBS) (for immuno-screening of proteins):
8 g NaCl, 0.2 g KCl, 1.44 g Na_2HPO_4, 0.24 g KH_2PO_4 made up to 1 l with ddH_2O (pH 7.4).

Hybridisation buffers (for nucleic acid hybridisations):
A variety of hybridisation buffers, specifically for particular experiments, were used, however the following hybridisation buffers were used routinely:
Standard: 5 x SSC, 5 x Denhardt's solution, 0.5 % SDS.
Formamide: 50% formamide, 5 x SSPE, 2 x Denhardt's solution, 0.1% SDS, 100 µg/ml denatured, fragmented DNA (herring sperm DNA).
'JODEX': 1 M NaCl, 10% Dextrane-sulphate, 1% SDS.

Antibiotics

Antibiotics (stored at –20 °C) were added to growth media after autoclaving and before use.
Ampicillin (Amp): stock solution was made in ddH_2O at a concentration of 50 mg/ml and working concentration for selection of *E. coli* clones was routinely at 100 µg/ml. Ampicillin is a derivative of penicillin that kills growing cells by affecting bacterial cell wall synthesis. The resistance gene (*bla*) encodes a periplasmic β-lactamase enzyme and cleaves the β-lactam ring of the antibiotic.
Kanamycin (Kan): stock solution was made in ddH_2O at a concentration of 25 mg/ml and working concentration for selection of *E. coli* clones was routinely at 25 µg/ml. Kanamycin is an aminoglycoside compound that binds to 70S ribosomes and inhibits protein synthesis by causing misreading of the mRNA. The resistance gene (*kan*) encodes an aminoglycoside

phosphotransferase that phosphorylates the antibiotic and inhibits its binding to the ribosomes and transport of the antibiotic into the cell (Sambrook, J. et al., 1989).
Tetracycline (Tet): stock solution was made in 96% ethanol at a concentration of 12.5 mg/ml and working concentration for selection of *E. coli* clones was routinely at 12.5 μg/ml. Tetracycline is a bacteriostatic compound that binds to the 30S subunit of ribosomes and prevents bacterial protein synthesis by inhibiting binding of the tRNA-amino acid complexes. The resistance gene (tet) encodes a membrane associated protein that modifies the bacterial membrane and prevents transport of the antibiotic into the cell (Sambrook, J. et al., 1989).
Chloramphenicol (Cm): stock solution was made in 96% ethanol at a concentration of 34 mg/ml and working concentration for selection of *E. coli* clones was routinely at 68 μg/ml. Chloramphenicol is a bacteriostatic compound that binds to the 50S subunit of ribosomes and interferes with protein synthesis by preventing peptide bond formation. The resistance gene (cat) encodes chloramphenicol acetyltransferase that modifies the antibiotic and prevents its binding to the ribosome.

2.2 Methods

2.2.1 Bacteriological and genetic procedures - Nucleic acid manipulations and other molecular biology procedures

A sterile working practice and aseptic technique was used throughout. Examination gloves were worn when handling RNA, radioisotopes and material involved in RNA manipulation. Appropriate radiological safety techniques were employed during this study.

Liquid bacterial cultures were inoculated with a flamed loop or a sterile cocktail stick. Solutions and bacteria were spread onto solidified growth media using a glass spreader, which had been sterilised in 70% ethanol and flamed.
Liquid bacterial (*E. coli*) cultures were incubated on an orbital shaker at 100-200 rpm at 37 °C (or at required temperature). Short term (1 month) stocks of cultures were kept at 4 °C on solid (selective) agar plates. Long term stock cultures were maintained as 15% glycerol stocks at –80 °C. Phage stocks were maintained for long term storage at –80 °C after addition of 7% DMSO. For short term storage, phage particles were stored at 4 °C in SM buffer and 4% chloroform.
For blue-white color selection of clones, by α-complementation with appropriate plasmid or phage vectors, 40 μl of 0.1 M IPTG (in ddH_2O) (when appropriate) and 40 μl of 20 mg/ml X-Gal (in DMF) was added to 20 ml molten (< 60 °C) growth medium, containing agar, prior to

pouring in 90 mm petri-dishes. Alternatively the same amounts were spread over the surface of solidified agar plates. For the lambda ZAPII vector (plaques) higher amounts of IPTG-X-Gal were required for the generation of the blue color. 15 µl of 0.5 M IPTG (in ddH_2O) and 50 µl of 250 mg/ml X-Gal (in DMF) was added to 2-3 ml lambda top agarose prior to pouring the toplayers. Selection is based on insertional inactivation of the N-terminal portion of the *lac*Z gene fragment, interrupted by a multiple cloning site (polylinker), present in many vectors currently employed. These vectors are used in conjunction with bacterial strains carrying the lacZΔM15 gene on a F' episome and vectors having no inserts in the polylinker are capable of α-complementation of the lacZΔM15 mutation. These cells produce a functional β-galactosidase enzyme, which is capable of metabolising the X-Gal leading to blue colonies.

Standard molecular cloning techniques, cell transformation and electrophoresis procedures were routinely according to the following protocols:
procedures as described in Sambrook, J. et al., 1989; Protocols and Applications Guide, Promega Corporation, 1996; in manuals and instructions of the manufacturer, accompanying vectors, enzymes, competent (bacterial) cells, hybridisation membranes and molecular biology kits, compounds or reagents (see section 2.1).

Procedures with modifications or particularly relevant in certain parts of this study are described below or in the relevant sections of the specific Chapters.

2.2.1.-1

Growth, measurement of growth, plating of bacterial host strains for plasmid vectors or phage, amplification and maintenance of phage suspensions (cDNA or genomic libraries and clones), were as described in Sambrook, J. et al., 1989, or as in the manuals with the lambda (λ) ZAP ® II/*Eco*RI/CIAP Cloning Kit (including the *E. coli* strains: XL-Blue MRF' and SOLR™ Strain) and Gigapack ® II Packaging Extracts (Stratagene, La Jolla, CA 92037, USA) and lambda (λ) BlueSTAR *Bam*HI Arms Kit, including the *E. coli* host strains: ER1647 and BM25.8 (Novagen, CN Biosciences Inc., Boulevard Industrial Park, Padge Road, Beeston, Nottingham, NG9 2JR, UK).
Subcloning of inserts contained within the lambda (λ) ZAP II or lambda (λ) BlueSTAR vectors was by *in vivo* excision of the pBluescript SK(-) phagemid (from λ ZAP II) using the ExAssist/SOLR system or by automatic subcloning by Cre-mediated excision of a plasmid (from λ BlueSTAR) respectively.

2.2.1.-2

The synthesis and screening of an oil palm cDNA library and an oil palm genomic DNA library is described in sections 4.2.5 and 4.2.6 respectively.

2.2.1.-3

Plant genomic DNA isolation was according to a modified method based on the CTAB isolation procedure and is described in section 4.2.1.

2.2.1.-4

RNA isolation of oil palm tissue was according to the method described in section 4.2.3. Total RNA from tissues of other plant species was usually by using TRIzol Reagent (Gibco BRL, Life Technologies) according instructions with the reagent. The reagent was a mono-phasic solution of phenol and guanidine isothiocyanate, a chaotropic agent. 100-200 µg tissue samples were homogenised and lysed in 1 ml TRIzol reagent. During incubation of the homogenised samples for 5 minutes at room temperature, the reagent maintains the integrity of the RNA, while disrupting cells and dissolving cell components. Addition of 200 µl chloroform followed by centrifugation at no more than 12000 x g for 15 minutes at 2 to 8 °C, separates the solution into an aqueous phase and an organic (lower) phase. After transfer of the aqueous phase, the RNA was recovered by precipitation with a mixture of 250 µl isopropyl alcohol and 250 µl 0.8 M sodium citrate/1.2 N NaCl at room temperature for 10 minutes, followed by centrifugation at no more than 12000 x g for 15 minutes at 2 to 8 °C. The gel-like RNA pellet was washed with 1 ml 75% ethanol and after centrifugation at no more than 7500 x g for 5 minutes at 2 to 8 °C redissolved in an appropriate volume of nuclease-free water. RNA was quantified by spectrophotometry (A_{260}) and the RNA integrity was monitored via formaldehyde-agarose gel electrophoresis as described for Northern analysis.

2.2.1.-5

Plasmid DNA was prepared by the alkaline lysis method. Single or multiple minipreps were performed using bacterial cultures of at least 10 ml. For all applications, including automated fluorescent sequencing, subcloning, *in vitro* transcription and PCR, plasmid DNA was purified using the Wizard ® *Plus* SV Minipreps DNA Purification System (Promega Ltd.) according to the recommendations and instructions of the supplier (Technical Bulletin No. 225). Basically the system uses alkaline lysis of bacterial cells (harboring the plasmids of interest) and, after removal of aggregated and precipitated cellular debris, chromosomal DNA and proteins, binding and washing the plasmid DNA on a resin. High quality and pure DNA is recovered in a concentrated form by elution with a low ionic strength buffer (10 mM Tris-HCl pH8, TE or water).

2.2.1.-6

Restriction enzyme digestions of DNA were carried out by incubation with the buffer at recommended temperature according to the enzyme manufacturer's recommendations. Generally plasmid DNA (0.2 – 5 µg) was digested in a total volume of 10-40 µl, with 1-5 units restriction enzyme, 0.1 volume of the appropriate 10 x concentrated enzyme buffer and sterile ddH_2O. Usually, genomic DNA was digested in a total volume of 500µl, with the equivalent of 2 units restriction enzyme per 1 µg. Reactions were incubated at the recommended temperatures (usually 37 °C) for 1-3 hrs (genomic DNA incubations were left overnight). When multiple digests were required, restriction enzyme buffer compatibility and star activity was taken into account and the buffer which gave maximum activity for all enzymes was chosen. The reaction times or units of enzyme may be increased.

2.2.1.-7

DNA molecular weight markers were prepared by digestion of lambda DNA (Pharmacia) with *Hin*DIII, *Hin*DIII and *Eco*RI, or P*st*I. 50 µg of DNA was incubated with 50 units of the respective restriction enzymes and the appropriate 1 x restriction enzyme buffer in a total volume of 250 µl and left overnight at 37 °C. After digestion, 50 µl of 6 x nucleic acid dye was added with 200 µl of sterile ddH_2O and mixed. The mix was aliquoted and was stored at –20 °C. An equivalent of 0.25, 0.5 or 1 µg was loaded onto agarose gels as size standards and the intensity of the ethidium bromide stained fragmented DNA bands were also used as a rough indication of approximate DNA quantity by comparison.

2.2.1.-8

Separation of DNA fragments by agarose gel electrophoresis was routinely performed in Scotlab electrophoresis tanks and was according to standard procedures (Sambrook, J. et al., 1989). Gels were made of the appropriate agarose concentration depending on the size of the DNA to be separated. Usually 0.7%-1% (w/v) agarose gels were used, which efficiently separated linear DNA between 0.5 – 10 kb. The required amounts of agarose and 1 x TAE buffer were mixed and the agarose dissolved by microwaving the mixture. The solution was cooled to about 60 °C, ethidium bromide (intercalating dye) was added to 0.5 µg/ml and the agarose mixture was poured and allowed to set in a gel mould with a well comb in place. Medium gels were 15 cm long x 11 cm wide, smaller gels were 6 cm long x 11 cm wide. Running buffer consisted of 1 x TAE. DNA samples were prepared by the addition of 1/6 volume of 6 x nucleic acid dye, loaded into the wells and submerged gels were usually run at 100 V until the bromophenol blue had migrated about 2/3 distance along the gel. DNA was viewed by illumination with UV light and a permanent record made using a gel documentation system (BioRad).

2.2.1.-9

The isolation of DNA fragments from agarose gels was routinely performed by using the GFX™ PCR DNA and Gel Band Purification Kit (Amersham Pharmacia biotech.) or the QIAEX® II Gel Extraction Kit (Qiagen Ltd.) according the instructions of the supplier. Basically, both methods make use of the principle that the DNA of interest is specifically bound to a glass fiber or silica matrix using a chaotropic agent that denatures protein and dissolves agarose. DNA bound to the matrix is washed with a low ionic strength buffer in ethanol and DNA is eluted in a low strength ionic buffer.

2.2.1.-10

Purification of nucleic acids in solutions was by making use of the different partitioning properties of nucleic acids and contaminants such as proteins, in aqueous and organic phases. AquaPhenol™ (Appligene) was processed according to the manufacturer's instructions to buffer the phenol at pH 8.0. For the phenol:chloroform extraction of nucleic acids to remove proteins, an equal volume of a 25:24:1 (v/v/v) mixture of phenol: chloroform:isoamyl alcohol was added to the nucleic acid solution. The 1:1 mixture was usually emulsified by multiple inversions (genomic DNA) or by vortexing for 30-60 seconds (smaller nucleic acid molecules) and the phases were separated by centrifigation at 12000 x g for 2 –5 minutes in a centrifuge. The (upper) aqueous phase was then transferred to a fresh tube and subsequently extracted with a 24:1 (v/v) mixture of chloroform: isoamyl alcohol in a 1:1 ratio (v/v) and

treated as for the phenol: chloroform extraction. To remove traces of phenol or chloroform from the purified nucleic acid solution and, if necessary, to concentrate the nucleic acids, a nucleic acid precipitation was performed.

2.2.1.-11

Precipitation of nucleic acids from aqueous solutions was with ethanol or isopropanol in the presence of monovalent anions. For a standard ethanol precipitation of nucleic acids, 1/5th volume of 10 M NH4Ac or 1/10th volume of 3 M sodium actetate (pH 5.2) was added to the nucleic acid solution and, after mixing and subsequent addition of 2 volumes of room temperature ethanol (95%), the mixtures were incubated at room temperature for 1 – 2hrs or at –20 °C for 30 minutes – overnight or at –70 °C for 15 minutes, depending on the amount and size of the nucleic acids, the desired level of recovery and the presence of potential contaminants. The nucleic acids were recovered by centrifugation at maximum speed (usually 12000 x g in a microfuge), the pellets were washed with 200 – 500 µl cold 70% ethanol and, after centrifugation as above, the pellets were air dried and resuspended in an appropriate amount of (nuclease-free) water or buffer. To keep the total precipitation volume down and to have efficient precipitation of nucleic acids at room temperature, 0.7 volume of isopropanol was added to the nucleic acid solution. The mixture was then centrifuged immediately or after a short incubation (< 20 min) at room temperature and further treated as described for the ethanol precipitation.

2.2.1.-12

Radiolabeling of DNA fragments, for use as radioactive probes in nucleic acid blot-hybridisation experiments, was routinely by using the *redi*prime DNA labelling system (Amersham Life Science Ltd.) according to the manufacturer's instructions. The system is based on the use of random sequence hexonucleotides to prime DNA synthesis on denatured template DNA at numerous sites along its length. The primer-template complex is a substrate for the Klenow fragment of DNA polymerase I. Substitution of a radiolabeled nucleotide for a non-radioactive equivalent in the reaction mixture leads to newly synthesised and radioactive DNA. Hybridisation of radiolabeled probes to blots, washing of the blots and detection of radioactivity on the solid supports was according to standard procedures as described by Sambrook, J. et al. (1989), according to instructions and recommendations with the Hybond-N membrane (Amersham International Plc.) and specific details are described in the text or in the legends with the figures.

2.2.1.-13

DNA gel blot analysis (Southern analysis) was performed according to standard procedures as described by Sambrook, J. et al. (1989), in section 4.2.3, and according to instructions and recommendations with the Hybond-N membrane (Amersham International Plc.).

2.2.1.-14

RNA gel blot analysis (Northern analysis) was as described in section 4.2.4.

2.2.1.-15

RNA transcription *in vitro* was as described in section 7.2.4.

2.2.1.-16

Polymerase Chain Reaction (PCR) experiments were carried out using thermostable DNA polymerases based upon the method described by Saiki, R.K. et al. (1988).
When PCR reactions were performed in a Perkin-Elmer Thermal Cycler model 9600, thin-walled 0.5 ml PCR tubes were used. When the Robocycler Gradient 96 Temperature Cycler was employed, PCR reactions were carried out in 200 µl GeneAmp Thin-walled reaction Tubes. Reactions were usually carried out in a total volume of 50 µl.
$Vent_R$ ® DNA Polymerase (New England Biolabs) was used when a high level of fidelity was desired (for example in the creation of complex constructs or in cloning DNA fragments for bacterial protein overproduction). $Vent_R$ ® DNA Polymerase possesses a strong 3'-5' proofreading exonuclease responsible for a level of fidelity that is 5 – 15 fold higher than that of Taq DNA polymerase (~1 mismatch in 17000 bp). Unless otherwise stated, PCR reactions contained 1 x ThermoPol reaction Buffer (20 mM Tris-HCl pH 8.8 @ 24 °C, 10 mM KCl, 10 mM $(NH_4)_2SO_4$, 2 mM $MgCl_2$, 0.1% Triton X-100), 400 µM dNTPs, 0.4 µM each primer, 1 ng – 25 ng plasmid DNA template or 50 – 500 ng genomic DNA, 1 unit of $Vent_R$ ® DNA Polymerase.
BIOTAQ™ DNA Polymerase (BIOLINE) was used in all routine PCR applications (for instance in DNA insert-size determinations and PCR analysis of newly created DNA constructs). Unless otherwise stated, PCR reactions contained 1 x $(NH_4)_2SO_4$ Buffer (10 x= 160 mM $(NH_4)_2SO_4$, 670 mM Tris-HCl (pH 8.8 @ 25 °C), 0.1% Tween-20), 1.5 mM $MgCl_2$, 200 µM dNTPs, 0.4 - 1 µM each primer, 1 ng – 200 ng plasmid DNA template or 50– 500 ng genomic DNA, 1-5 units of BIOTAQ™ DNA Polymerase. To prevent evaporation of the reaction during the amplification procedure, the sample was carefully overlayed with mineral oil (Sigma). Occasionally "hot start" PCR was performed, by addition of the enzyme through the oil layer to the other reaction components at 94 °C, or by compartmentalisation of

the contents of the reaction tubes until the denaturing temperature was reached. The latter procedure involved the use of AmpliWax™ PCR Gems (Perkin-Elmer) according instructions with the product. Basically, half the volume of the reaction (consisting of the reaction buffer, dNTPs, Mg^{2+}, primer 1 and ddH_2O) was placed in a reaction tube and after a wax bead was added, the tube was heated for 1 – 5 minutes at 60 °C to melt the wax. After cooling to room temperature to allow the wax to seal off the bottom half of the tube, the second half of the reaction volume (consisting of the enzyme, template DNA, primer 2 and ddH_2O) was added and thermal cycling was started as normal. Hot start generally reduces the level of non-specific binding of the primers to each other or the template DNA. Thermal cycling protocols differed with regards to the respective times of the individual incubations but were according to the same basic pattern: 1 cycle at 94 °C for 5 minutes, 25 – 30 cycles of denaturation (94 °C for 30 – 60 seconds), annealing (50 – 68 °C; depending on the Tm of the primers, for 30 –60 seconds) and extension (72 –74 °C; allowing 1 minute per kilobase of expected extension product), 1 cycle at 72 –74 °C for 5 – 10 minutes.
Primers used were generally (if possible) designed so as to contain at least 20 nt., containing an equal number of G+C's and A+T's preferably well distributed throughout the primer, ending with 2 G+C's at the 3'-end and low chance for self-annealing or hairpin formation. The approximate Tm for each primer was calculated by the supplier or was roughly estimated on basis of the equation: Tm = {[no. of G + C) x 4] + [(no. of A + T) x 2]} – 5 °C.

2.2.1.-17

DNA sequencing was carried out by automatic fluorescent sequencing using an applied Biosystems 373A DNA Stretch Sequencer and a 377 DNA Sequencer, using double stranded DNA templates and dye-dideoxy terminator chemistries. Automated sequencing was performed by the DNA Sequence Laboratory of the Department of Biological Sciences, University of Durham.

2.2.1.-18

Sequence analysis was performed by using a number of up-to-date computer software packages. Primary DNA sequence analysis was with the DNA Strider (Marck, C., 1988) and DNAStar (Clewley, J.P., 1995) software. Sequence homology searches were carried out against the Genbank, Swiss-Prot and EMBL databases by using BLAST (Altschul, S.F. et al., 1990, 1997) or by using the Fasta programme at the Daresbury BBSRC SEQNET facility. Multiple sequence alignments and phylogenetic trees were constructed using Clustal V (Higgins, D.G. and Sharp, P.M., 1989) as part of the DNAStar software or the GCG Software package of the University of Wisconsin (Devereux, J. et al., 1984).

2.2.2 Biochemical methods

A number of biochemical procedures most relevant in particular parts of this study are described in the Materials and Methods sections of the Chapters. These procedures include: bacterial overproduction of recombinant protein (section 3.2.1), the standard GPAT assay (section 3.3.2.), ACP preparation, Acyl-ACP synthesis, Acyl-ACP purification and Acyl-CoA synthesis (sections 3.3.3 to 3.3.6), preparation of anti denatured GPAT rabbit polyclonal antibodies (section 3.3.7), the synthesis of peptides, coupling of peptides to keyhole limpet hemocyanin and preparation of rabbit anti-peptide polyclonal antibodies (sections 3.3.7 to 3.3.10), SDS-PAGE and Western blotting, Ponceau staining and Western blotting for preparation of a protein for N-terminal amino-acid sequencing (sections 3.3.11. to 3.3.13). Also the preparation of a bacterial crude cell-free extract (section 5.2.2) and the preparation of an analytical denaturing polyacrylamide sequence gel (section 7.3.5) is described.

2.2.2.-1

For **preparation of dialysis tubing**, the tubing was cut into convenient length and, to remove chemical contaminants, was then boiled in 20% (w/v) sodium bicarbonate, 1 mM EDTA (pH 8.0) for 10 minutes. The tubing was rinsed thoroughly in distilled water and boiled again in 1 mM EDTA (pH 8.0) for 10 minutes. After cooling and rinsing with sterile distilled water, it was stored submerged in 25% ethanol and 1 mM EDTA (pH 8.0) at 4 °C. Prior to use, tubing was washed thoroughly in ddH2O and handled with gloves. The protein samples to be dialysed, were retained within the tubing with the combined use of plastic clamps and a knot tied at each end of the tube.

2.2.2.-2

Concentration of protein was usually determined using **the Bradford protein assay** (Bradford, M.M., 1976). The reagents were purchased from BioRad in a ready to use solution for the rapid and simple BioRad protein assay. The BioRad protein assay is a dye-binding assay based on the differential change of the absorbance maximum for an acidic solution of Coomassie Brilliant Blue G-250 from 465 nm to 595 nm when binding to protein occurs. The assay was performed according to the manufacturer's recommendations for the micro-assay procedure.

Usually bovine serum albumin (BSA) or ovalbumin (OA) was used as a standard and protein solutions, in the range of 1 – 20 µg, were made up in 800 µl with sterile ddH_2O. 200 µl of undiluted dye reagent concentrate was added and after mixing the OD595 was measured after 5 minutes to one hour. The OD595 versus concentration of the standards was plotted and the

protein concentration of the samples was calculated from a point in the graph where the correlation between OD595 and protein concentration was linear.

2.2.2.-3

Preparation of crude total protein extract from plant tissues for SDS-PAGE was by a simple procedure involving resuspension of powdered (ground in liquid nitrogen) tissue in 1 x Laemmli SDS sample buffer (ratio of 1 gr powder in 5 ml buffer). The mixture was boiled for two minutes followed by centrifugation at 12000 x g for 5 minutes in a microfuge. Protein recovery and quality was determined by the Bradford assay and SDS-PAGE analysis.

2.2.2.-4

Coomassie Brilliant Blue R-250 staining of SDS-PAGE gels was routinely performed to visualise protein bands in the gels. The gels were removed from the Protean II apparatus and immersed in hot Coomassie staining solution (25% (v/v) propan-2-ol, 10% (v/v) glacial acetic acid, 0.04% (w/v) Coomassie R-250) in a microwave-safe container. The gels were agitated gently for 20 minutes, whereupon the loosely covered container was placed in a microwave and reheated at a medium setting for 1 – 2 minutes. The gels were agitated gently as before, and allowed to cool. After cooling to room temperature, the Coomassie staining solution was removed, the gels rinsed in ddH_2O, and agitated gently in hot de-staining solution (10% (v/v) acetic acid, 1% (v/v) glycerol). A small piece of sponge was included in the container to soak up Coomassie Blue until the background stain was completely removed. The gels were dried using an Easy Breeze Gel Drier (Hoefer Scientific Instruments).

2.2.2.-5

Immuno-screening of protein was routinely performed by detection with I^{125}-labeled secondary antibody. Following protein transfer to a membrane (usually Hybond-C from Amersham International Plc.) in a Western blot procedure, the membranes were incubated in blocking solution (1% (w/v) haemoglobin in 1 x PBS buffer containing 0.1% (v/v) Tween-20 and 0.02% (w/v) sodium azide), to block non-specific antibody binding sites, for 1 hour at room temperature or at 4 °C overnight. The membrane was removed from the blocking solution and washed three times with aliquots of 1 x PBS buffer before being incubated for 2 hrs in a dilution (usually in the range 1:500 – 1:10000) of primary antibody in blocking solution (5 – 10 ml) with gentle agitation or in a rolling tube. Non-bound primary antibody was removed by extensive washing: 3 quick washes with 50 ml PBS + 0.1% Tween-20, followed by three washes of 10 minutes with fresh aliquots of the same buffer. (Tween-20 prevents non-specific hydrophobic interactions). After incubation, the antibody solution was stored at 4 °C for repeated use. Subsequently, the membrane was incubated with a 1:1000 dilution of the secondary donkey-anti-rabbit Ig (whole Ab) [^{125}I] (Amersham International

Plc.) in blocking solution without Tween-20 for 60 - 90 minutes at room temperature. The labeled membrane was again washed extensively as above and carefully wrapped in SaranWrap followed by exposure to X-Ray film at –80 °C overnight – 4 days.

Chapter III

Overproduction and Purification of Recombinant Plastidial Glycerol-3-Phosphate Acyltransferases for Substrate Selectivity Studies, Antibody Production and Elucidation of Structure – Function Relationships

3.1 Introduction

De novo synthesised faty acyl chains are diverted into the prokaryotic pathway of plant lipid biosynthesis by a soluble glycerol-3-phosphate acyltransferase (GPAT [EC 2.3.1.15]) in the chloroplast. At least in certain plants, it appears to be a rate-limiting step of glycerolipid synthesis (Joyard, J. and Douce, R., 1987). GPAT transfers mainly 16:0 and 18:1 acyl chains to the *sn*-1 position of glycerol-3-phosphate (G3P). Despite the fact that these proteins have a high degree of similarity in primary structure, their fatty acyl preferences can vary from plant to plant. The unsaturation level of phosphatidyl glycerol (PG) of chloroplasts appears to be a major determinant of a plant's chilling tolerance (Murata, N. et al., 1982; Murata, N., 1983). Disaturated PG can only be obtained via the chloroplastic prokaryotic pathway and the substrate preference of the soluble GPAT for 16:0-ACP or 18:1-ACP has been implicated to be a critical determinant for chilling sensitivity in plants (Murata, N., 1983; Nishida, I. and Murata, N., 1996). Transgenic studies with tobacco (Murata, N. et al., 1992), rice (Yokoi, S. et al., 1998) and *Arabidopsis* (Wolter, F.P. et al., 1992) have proven this concept. However, the existence of an *Arabidopsis fab1* mutant illustrates that chilling sensitivity is a more complex phenomenon and GPAT substrate preference may not be the sole factor involved in determining this property (Wu, J. and Browse, J., 1995; Nishida, I. and Murata, N., 1996).

The protein has been purified from various plant species such as: pea (Weber, S. et al., 1991), spinach (Frentzen, M. et al., 1983) and squash (Nishida, I. et al., 1987) and depending on the source, it has been found to occur in one to three isomeric forms with different molecular masses, isoelectric points and substrate preferences (Nishida, I. et al., 1987; Bertrams, M. and Heinz, E., 1981). Substrate preference studies on homogenous enzyme preparations have only been performed on one isomeric form of pea (Douady, D. and Dubacq, J.-P., 1987; Weber, S. et al., 1991) and two of squash chloroplasts (AT2 and AT3) (Nishida, I. et al., 1987; Frentzen, M. et al., 1987).
Plastidial acyltransferases of higher plants have the ability to use both acyl-CoA and acyl-ACP thioesters as substrates. However, it is now accepted that acyl-ACP thioesters are the physiological acyl donors for these enzymes for two main reasons:
1) ACP thioesters are formed in the chloroplast stroma and CoA thioesters at the outer envelope membrane (Frentzen, M., 1981) , and
2) when mixtures of acyl-CoAs and acyl-ACPs are offered, the plastidial GPAT shows a pronounced preference for the acyl-ACP thioesters.

With only a few exceptions, often for ease researchers have not systematically used the natural acyl-ACP substrates but tended to use acyl-CoAs as these are commercially available and because of the relative difficulty in obtaining large quantities of pure acyl-ACP substrates for use in *in vitro* assays.

Based on limited sets of reaction conditions it appeared that using the substrate-analogue acyl-CoA would reflect substrate preferences and catalytic properties similar to using acyl-ACPs. However, this has not been rigorously tested. There are a number of possible arguments against the use of acyl-CoA as the substrate for soluble GPAT:

1) acyl-ACP is the physiological substrate
2) in plant cells of different species, different ACP isoforms may be specifically involved in determining the products of fatty acid biosynthesis (Suh, M.C. et al., 1999)
3) there are differences in critical micelle size of acyl-ACPs and acyl-CoAs
   The critical micelle size for acyl-CoA concentrations is thought to be in the range of 2 to 6 μM (Bertrams, M. and Heinz, E., 1981) with more acyl groups per weight unit. Therefore, *in vitro*, these substrates are likely to be provided at very high, non-physiological concentrations
4) in plant cells there may be an influence of the possible interaction of particular proteins with acyl-ACP on the availability of the substrate.

The substrate selectivities of some of the enzymes have been determined by analysing the fatty acid composition of the reaction products, after incubation with mixtures of various acyl-labeled acyl-ACP and acyl-CoA thioesters.

Obtaining meaningful kinetic parameters of the GPAT enzymes in *in vitro* studies has been less straightforward. The apparent kinetic data (apparent Km and Vmax) for G3P can be relatively easy determined due to commercial availability of the substrate and an easily modified and controlled concentration in the reaction mixture. However, when using the substrate analogue acyl-CoA, proper kinetic studies are difficult and could be meaningless with respect to the *in vivo*, physiological environment. Besides the undesirable micelle properties, in combination with poor solubility of long-chain acyl-CoA thioesters, in most *in vitro* assays there is a requirement for bovine serum albumin (BSA) in the reaction mixture (Bertrams, M. and Heinz, E., 1981). Therefore, especially when acyl-CoA substrates are used, the precise amount of substrate in solution and availability to the enzyme is not known and is likely non-physiological. A more accurate appraisal of kinetic parameters of any GPAT *in vitro*, more relevant to physiological conditions, would come from using acyl-ACPs. With two exceptions (Frentzen, M. et al., 1983; Frentzen, M. et al., 1987), this has not been systematically done.

The substrate selectivities of pea and spinach GPAT has been investigated using mixtures of acyl-ACPs and acyl-CoAs (Bertrams, M. and Heinz, E., 1981; Frentzen, M. et al., 1983). Mainly equimolar mixtures of acyl-CoAs (up to 20 μM) or acyl-ACPs (up to 5 μM) were used. It was found that the pea and spinach GPAT had a strong preference for oleoyl (18:1) over stearoyl (18:0) or palmitoyl (16:0) but the preference was more marked in the 16:3 plant spinach (*Spinacia oleracea*) than in the 18:3 plant pea (*Pisum sativum*). Both isoforms of pea show the same catalytic properties with regard to the apparent Km for G3P being close to 0.7 mM and substrate preference as the ratio 18:1/16:0 of about 5.5. Spinach GPAT was determined to select 18:1 over 16:0 with a factor of about 9. Apparent kinetic constants have been reported for **spinach GPAT** (with 16:0-ACP as acyl donor: Km (16:0-ACP) = 3.2 μM; Km (G3P) = 3.15 mM; V = 5.3 nkat/mg protein/ with 18:1-ACP: Km (18:1-ACP) = 0.3 μM; Km (G3P) = 0.031 mM; V = 1.5 nkat/mg protein) and for **pea GPAT** (with 16:0-ACP: Km (16:0-ACP) = 5.6 μM; V = 6.5 nkat/mg protein/ with 18:1-ACP: Km (18:1-ACP) = 0.7 μM; V = 0.6 nkat/mg protein) (Frentzen, M. et al., 1983).

The most detailed study using homogenous enzyme preparations and determination of substrate preference and kinetic constants, is that for the **three isoforms of squash GPAT** (Frentzen, M. et al., 1987). The AT2 and AT3 isoforms, as well as the GPAT of *Amaranthus* (*Amaranthus lividus*) chloroplasts (Cronan, J.E., Jr. and Roughan, P.G., 1987), catalyse an unselective *sn*-1 acylation of G3P. The apparent kinetic constants for these isoforms are in a similar range:

for **AT2 and AT3** respectively: with 16:0-ACP: Km (16:0-ACP) = 1.7/1.3 μM; Km (G3P) = 0.13/0.16 mM; Vmax = 27/31 mU/mg protein/ with 18:1-ACP: Km (18:1-ACP) = 1.1/1.3 μM; Km (G3P) = 0.017/0.016 mM; Vmax = 13/16 mU/mg protein.

The AT1 isoform differs considerably, as it seems to preferentially use 18:1-ACP as a substrate but under physiological conditions (pH 8), this selectivity is less distinct and certainly less than spinach (18:1/16:0 usage by AT1 and spinach is <2.5 and 9 respectively).

The higher abundance of **AT1** and the different kinetic parameters (with 16:0-ACP: Km (16:0-ACP) = 0.72 μM; Km (G3P) = 0.3 mM; Vmax = 3800 mU/mg protein with 18:1-ACP: Km (18:1-ACP) = 0.36 μM; Km (G3P) = 0.004 mM/ V = 2300 mU/mg protein) might suggest major incorporation of unsaturated fatty acids on the *sn*-1 position of G3P *in vivo*. However, it seems that more complex kinetic parameters are involved in plant cells because squash is a chilling sensitive plant with a relatively high percentage of saturated fatty acids at the *sn*-1 position of PG. Also, the transgenic studies using the AT3 isoform, squash GPAT cDNA, resulted in significantly increased levels of 16:0 at the *sn*-1 position of PG in tobacco, points in this direction.

The *Arabidopsis* (*Ara*) and squash GPAT cDNAs have been cloned (Nishida, I. et al., 1993; Ishizaki, O. et al., 1988) and used in transgenic studies with tobacco (Murata, N. et al., 1992). *Arabidopsis* is a chilling resistant 16:3 plant and its GPAT cDNA seems to compete effectively with the endogenous GPAT to confer this property onto tobacco. The squash non-selective GPAT AT3 cDNA made tobacco more chilling sensitive. This suggests that plastidial Ara GPAT would preferentially use unsaturated fatty acids. Despite its use in transgenic studies, substrate selectivity analysis of *Ara* GPAT *in vitro* has not been reported.

Mature proteins of *Arabidopsis* and squash GPAT enzymes, similar to the ones used in the transgenic studies, have been overproduced in *E.coli*, purified and shown to be catalytically active (Nishida, I. et al., 1993; Nishida, I., personal communication; this study). The recombinant overproduced *Arabidopsis* and squash GPAT enzymes were investigated for their substrate selectivities in this study (this chapter) and the purified protein subjected to crystallisation trials in collaboration with the group of Professor D. Rice at the University of Sheffield. In combination with physiologically relevant determination of the functional properties of the enzymes, the X-ray crystallography may well reveal the structural basis of the catalytical mechanism and substrate selectivity. The structure for the recombinant squash GPAT was elucidated to atomic resolution.
For use in Western blotting experiments to evaluate protein expression levels in plant tissues in later experiments, polyclonal immunosera were raised against the purified denatured *Ara* and squash recombinant GPAT proteins. In order to obtain specific antibodies against the respective proteins, peptide antigens were used in an immunisation strategy resulting in one anti-*Ara* GPAT polyclonal antiserum specifically recognising denatured *Arabidopsis* GPAT.
Unfortunately, it was found that the polyclonal antisera also recognised other components in crude plant protein extracts and such experimentation will need further optimisation, possibly involving purification and concentration of the antibodies.

Throughout this study it was the intention to establish and use *in vitro* assay conditions for GPAT, reflecting physiologically relevant conditions as closely as possible. With the benefit of knowledge resulting from transgenic studies, reflecting the *in vivo* selectivities of the squash and *Ara* GPAT, a standard was set for these assay conditions (this chapter). This is of particular importance to appraise structure – function relationships of these acyltransferases and the effect of modification of the protein structure on its catalytic properties and substrate selectivities (Chapter IV, V).
As a guide and criteria for the GPAT assay strategy, the following considerations were taken into account:

1) the importance of the pH: the chloroplast stromal pH is 8.0 in the light,
2) the level of G3P has been measured in the range of 0.15 – 0.7 mM in cell compartments of illuminated leaves (in spinach leaf: 0.15 mM in chloroplasts and 0.7 mM within the cytoplasm, in chloroplasts of other species: 0.3 – 0.6 mM (Frentzen, M., 1993; Cronan, J.E. and Roughan, P.G., 1987),
3) GPAT mainly transfers 16:0 and 18:1 acyl chains to the *sn*-1 position of G3P (Frentzen, M., 1993),
1) acyl-ACPs are the physiological acyl donors and can reach a total concentration from 0.6 to up to about 3 or 4 µM *in vivo* (Roughan, G. and Nishida, I., 1990; Soll, J. and Roughan, G., 1982),
5) assay conditions in which the enzymes have to compete for substrates within a physiological range of concentration, would reflect the *in vivo* preferences of the enzymes. Selectivity assays using mixtures of 16:0-ACP and 18:1-ACP therefore seemed the most appropriate,
6) cell-free enzyme preparations had to be free of significant hydrolytic activities and selectivities were based on basis of initial enzyme velocities using enzyme amounts resulting in linear rates for at least 2 minutes in a timeseries.

The effect of changing single reaction parameters on *in vitro* selectivity for 16:0 or 18:1 acyl thioesters, and how the results corresponded to the *in vivo* behaviour of the enzymes, was examined.

3.2 Materials and methods

3.2.1 Plasmids and overproduction of fusion proteins of mature regions of *Arabidopsis* and squash GPAT in *Escherichia coli*

The plasmids pET-AR1 (in this study further referred to as pAR1) and pNA4 were kindly provided by Dr. I. Nishida. The pET-AR1 (pAR1) was constructed as described by Nishida, I. et al. (1993): a 1.2 kb *Hga*I-*Eco*RI DNA fragment of *Arabidopsis* GPAT cDNA was blunt ended (5'-3' fill-in) and subcloned in pET-3c x *Bam*HI blunt (5' – 3' fill in). In this way a fusion protein encoding 14 N-terminal amino acids (AA) originating from the T7 bacteriophage leader sequence and the cloning junction, and 369 AA residues encoding *Arabidopsis* GPAT starting from residue E91 (Genbank Accession Nr.: Q43307) was produced. The pNA4 construction has not been published: a 1.22 kb *Nae*I-*Eco*RI fragment of squash GPAT cDNA (clone AT03 (Ishizaki, O. et al., 1988)) was blunt ended (5' –3' fill in) and subcloned in pET-3a x *Bam*HI blunt (5' – 3' fill in). This plasmid encodes a fusion protein of 14 N-terminal amino acids (AA) originating from the T7 bacteriophage leader sequence and the cloning junction, and 366 AA residues encoding squash GPAT starting from residue E70 (Genbank Accession Nr.: Y00771). Schematic diagrams of the proteins are depicted in Figure 3.1.

Overproduction of the recombinant GPAT proteins in *E.coli* BL21 (DE3) or BL21 (DE3) pLysS after transformation with the respective plasmids, was achieved on mini-scale (50 ml culture) and large scale for bulk amount production (up to 1 litre) by the following procedure: fresh starter cultures (3 hrs. growth at 37 °C after inoculating from selective plates) of BL21 (DE3) (pLysS)/ pAR1 or pNA4 in 3 – 50 ml 2xYT/ 0.4% glucose/ 200 $mg.l^{-1}$ ampicillin, were used to inoculate prewarmed (37 °C) induction cultures (50 – 1000 ml 2xYT/ 0.4% glucose/ 200 $mg.l^{-1}$ ampicillin). Cultures were grown with aeration (200 rpm shaking platform) at 37 °C and the OD. 600 nm. was monitored at regular intervals. Overproduction was induced when the culture OD. 600 nm. reached about 0.5, at timepoint (T=0 hrs) by adding 0.4 – 0.6 mM IPTG to the culture. Starting from T = 0 hrs., 1 ml. culture samples were taken every one hour up to T = 3 hrs. for later evaluation of the progression and amounts of the overproduction of the GPAT protein via SDS-PAGE. Usually the culture OD 600 nm. could reach from 1 to up to 1.5.

For routine analysis of the GPAT overproduction, 1 ml. samples were centrifuged for 20 seconds at 15.000 rpm. in a microcentrifuge and resuspended in 200 µl. 1 x SDS sample loading buffer. Before SDS-PAGE analysis the samples were boiled for 5 – 10 minutes and 6 – 20 µl. was applied to 10 or 12 % SDS-polyacrylamide gels.

3.2.2 The standard GPAT assay

During the course of this study, the standard GPAT assay as described by Bertrams, M. and Heinz, E. (1981) was modified to accommodate our practical aims to work on a mini scale using 1.5 ml. eppendof tubes, for higher throughput and to standarise assay conditions towards working with acyl-ACPs in selectivity studies. It was found that when working with acyl-ACPs in the reaction mixtures higher centrifugal speeds (13 000 rpm in a microcentrifuge) were necessary to effectively separate reaction products (*sn*-1 acyl-glycerol-3-phosphate (1-LPA) in the lower organic phase away from unincorporated free acyl-ACPs in the upper aqueous phase.

The principle of the standard enzymatic activity determination was identical: a reaction to synthesise ^{14}C-labeled 1-LPA from 16:0-CoA and L-[U-^{14}C] glycerol-3-phosphate.This assay is not optimal (Nishida, I. et al. (1987). Although 16:0-CoA is a non-physiological substrate of the enzymes and very inefficient as an acyl carrier in this reaction, it was satisfactory to detect enzyme activity for example during purification procedures or for identification of GPAT activity during other procedures. However, when working with GPAT enzymes with very low affinity for 16:0 acyl chains, other acyl donors could, and should, be used.

The standard assay contained in a total volume of 80 µl: 0.25 M HEPES buffer (pH7.4 or pH8), 5 mg/ml BSA, 0.4 mM palmitoyl-CoA, and 2 mM L-[U-^{14}C] glycerol-3-phosphate (2000 dpm/nmol). After pre-incubation of the mastermix at 25 °C for at least 5 minutes, the reaction was started with appropriate amounts of enzyme. Incubations were carried out at 25 °C for at least 1 min. (standard = 5 min.) or depending on the purpose of the experiment (timeseries). The reaction was stopped by addition of chloroform-methanol (1:1 v/v. 710 µl) and 280 µl of acidic salt solution (1 M KCl in 0.2 M H_3PO_4). After mixing and phase separation by high speed centrifugation in a microcentrifuge (13 000 rpm), reaction products were recovered from the lower organic phase (250 µl, using a 250 µl Hamilton syringe) and dried down in a 5 ml scintillation vial in a Jouan vacuum centrifuge, with moderate heating (50 °C) for 15 min. The dried reaction products were resuspended in 280 µl methanol and quantified by liquid scintillation counting (Packard 100 TR LSC). Assays with radioactively labeled (^3H or ^{14}C) acyl-CoA contained thioesters in concentrations of up to 20 µM (standard 10 µM) and with radioactively labeled (^3H or ^{14}C) acyl-ACP up to 4 µM (standard 2 µM) depending on the experiment.

***Escherichia coli* ACP isolation, Acyl-ACP synthesis and Acyl-ACP purification**

These three procedures were carried out by and in collaboration with another member of the lab, Dr. T. Schierer.

3.2.3 ACP preparation

E. coli acyl carrier protein was purified according to a modified procedure devised by Majerus et al. (1969) with all steps performed at 0-4 °C. 250 g of frozen *E. coli* cells were suspended in 10 mM potassium phosphate buffer pH 6.2, 0.1% β-mercaptoethanol and left to defrost overnight at 4 °C. Cells were treated with DNAse I (Sigma, 0.5 mg/100 ml of cell suspension for 30 minutes) and broken by two passages through a Constant Systems cell disrupter set a 25,000 psi. Cell lysates were centrifuged at 40,000 x g for 30 min. to remove excess cell debris. Ammonium sulphate precipitations and acid precipitations were carried out as in Majerus et al. (1969). The DEAE-cellulose step in Majerus et al. (1969) was replaced by High Load mono-Q chromatography (Pharmacia) but all other procedures were as described. Fractions containing ACP were identified by 15% SDS-PAGE and the purest fractions were pooled, aliquoted, and stored at -80 °C.

3.2.4 Acyl-ACP synthesis

Radiolabeled fatty acid solutions ([1-^{14}C]16:0 and [9,10(n)-^{3}H]18:1; Amersham) were dried with 2 molar equivalents of NaOH in a vacuum centrifuge and resuspended in 5% Triton X-100 at a final concentration of 460 μM and 600 μM respectively with a specific activity of 55 Ci/mol. [1-^{14}C]Palmitoyl-ACP (55 Ci/mol.) and [9,10(n)-^{3}H]Oleoyl-ACP (55 Ci/mol.) were made using the procedure of Rock and Cronan (1979) with minor modifications.

Acyl-ACP synthetase was obtained via overproduction procedures with a construct kindly provided by John Shanklin (Brookhaven National Laboratory) and the enzyme was partially purified via blue sepharose chromatography as described in Rock and Cronan (1979).

The synthesis reaction, in a final volume of 22 ml, contained: 100 mM Tris-HCl pH 8.0, 400 mM LiCl, 10 mM $MgCl_2$, 2 mM DTT, 5 mM ATP, 1% Triton X-100, 33 μM ACP (~10 mg), 25 μM radiolabeled fatty acid and 6-20 units of acyl-ACP synthetase. After incubation at 30 °C for 36-48 hrs, the reaction was stopped by freezing in liquid N_2 and went to about 50% completion as judged by the recovery after purification.

3.2.5 Acyl-ACP purification

[^{14}C]16:0-ACP and [^{3}H]18:1-ACP were separated from free fatty acid and free ACP via Q-Sepharose and octyl sepharose column chromatography based on the procedure of Rock and Garwin (1979). Synthesis reactions (frozen) were thawed and diluted with 3 volumes of Milli-Q water in order to reduce the LiCl concentration to less than 100 mM. The mixture was loaded onto a 16 ml Q-Sepharose Fast Flow (Pharmacia) column (equilibrated with 10 column volumes of 20 mM HEPES pH 6.8) at 2 ml/min. In order to remove free fatty acids, the column was washed with 2.5 column volumes of 80% isopropanol, 20 mM HEPES pH 6.8. Isopropanol was removed by washing the column

with 8 column volumes of 20 mM HEPES pH 6.8. ACP and acyl-ACP was eluted with 450 mM LiCl, 20 mM HEPES pH 6.8 and fractions containing peak counts were pooled and stored at 4 °C.

A 17 ml octyl-Sepharose column (Pharmacia) was equilibrated with 5 column volumes of 20 mM N-ethylmorpholine acetate pH 6.5. Pooled fractions from the Q-Sepharose column were loaded onto the octyl-Sepharose column at 1.5 ml/min. followed by 5 column volumes of 20 mM N-ethylmorpholine acetate pH 6.5 to remove free ACP. Purified acyl-ACP was eluted using 20 mM N-ethylmorpholine acetate, 30% isopropanol. N-ethylmorpholine acetate was removed by vacuum centrifugation and the acyl-ACP was resuspended in 20 mM HEPES pH 6.8. The purity of the acyl-ACP was determined by 8-20% Phast gel analysis and free ACP was estimated to represent less than 10% of the total sample. Samples were then pooled, aliquoted and stored at -80 °C

3.2.6 Acyl-CoA synthesis

[9,10(n)-^{3}H]Oleoyl-CoA (55 Ci/mol) and [1-^{14}C]Palmitoyl-CoA (55 Ci/mol) were prepared enzymatically with a *Pseudomonas* acyl-CoA synthetase purchased from Sigma. A 750 µl mixture containing 75 mM Tris-HCl buffer pH 7.8, 10 mM CoASH, 10 mM ATP, 10 mM $MgCl_2$, 20 mM phosphoenoylpyruvate, 7 units pyruvate kinase, 4 units myokinase and 0.5 units of lyophilized acyl-CoA synthetase, was added to 250 µl 50 µCi [1-^{14}C]Palmitic acid (55 Ci/mol) or 33 µCi [9,10(n)-^{3}H]Oleic acid (55 Ci/mol) in 100 mM Tris-HCl pH 7.8 containing 0.5% Triton X-100. The total reaction mixture (1 ml) was incubated at 37 °C for 2.5 hours. Free fatty acids were extracted by 3 x 2 ml of petroleum ether (60-80 °C bp) after acidifying the reaction mixture with 100 µl concentrated HCl. The labeled acyl-CoA was extracted from the remaining layer with n-butanol. Further water soluble contaminants were removed from the n-butanol extracts by 2 water washes. The resulting [9,10(n)-^{3}H]acyl-CoA sample contained less then 5% of free fatty acids and the [1-^{14}C]acyl-CoA less then 1% as judged via TLC analysis (Silica gel G; developing solution: butanol/acetic acid/water; 5:4:1). Before being used in assays, the n-butanol extracts were taken to dryness by centrifugal evaporation and redissolved in 10 mM sodium acetate pH 6.0 to a concentration of 400 µM with a specific activity of 55 Ci/mol. Biochemicals and auxiliary enzymes were obtained from Sigma, and radiochemicals were obtained from Amersham unless otherwise stated.

3.2.7 Preparation of anti-denatured GPAT antibodies

A polyclonal antiserum to denatured *Arabidopsis* GPAT (AR1) and squash GPAT (NA4) was raised in rabbits using the following protocol.

An approximate equivalent of 15 µg of GPAT protein, from purified preparations or present in total soluble extract *of E. coli* in which the respective GPAT proteins were overproduced, was layered onto a preparative 10% SDS-PAGE gel with a 5% stacking gel without sample wells. After electrophoresis under standard conditions the proteins were transferred to Hybond-C (Amersham) using a standard Western blotting procedure. Proteins on the membrane were visualised and identified by Ponceau staining. The bands containing GPAT protein were cut out of the membrane and ground in liquid nitrogen. The powder was transferred to a sterile 2 ml. micro centrifuge tube and 300 µl of sterile 0.9% NaCl was added. The tube was vortexed moderately and complete Freund's adjuvant (1:1) was added drop wise from a Hamilton syringe (300 µl). Two rabbits were immunised intramuscular and subcutaneously on day 0 as follows: one rabbit (rabbit 9) with 150 µl of the squash GPAT (NA4) preparation and one other rabbit (rabbit 10) immunised with 150 µl of the *Arabidopsis* GPAT (AR1) preparation. Starting on and following 25 days after day 0, boosts were given at 2-3 weeks interval with a similar amount and preparation of protein but without adjuvant. This resulted in 3 bleeds: day 0, 4 ml pre-immune serum, day 30, 10 ml test-bleed 1; day 46, 9 ml rabbit 9 (α-NA4) and 6 ml rabbit 10 (α-AR1); day 60, about 3 ml α-NA4 and 6 ml α-AR1, no terminal bleeds were performed. Blood was placed at 37 °C for two hours before centrifugation at 4.500 rpm at 4 °C. Serum was aliquoted and stored at 4 °C with 0.04% Na-azide to prevent bacterial growth.

3.2.8 Synthesis of peptides

For this study, peptides were synthesised by J. Gilroy, who used the solid-phase methods developed by Merrifield and co-workers (Marglin, A. and Merrifield, R.B., 1970). One of the four synthetic peptides was not acetylated and sequenced directly on the resin to confirm the amino acid composition and overall integrity of the procedure. Peptides were synthesised according to the amino acid sequence predicted from the nucleotide sequences as described in the text. An additional cysteine (for the purpose of coupling to the protein carrier) was added to the C-terminus of all four synthetic peptides. After completion of synthesis the peptides were chemically cleaved (trifluoroacetic acid (TFA) off the resin and away from side-chain protective groups. After incubation with DTT (to keep the cysteine residues reduced) the peptides were purified via µBore HPLC and after collection subjected to solvent extraction to remove TFA and dried down under ether. After confirmation of the sequence, the non-acetylated peptide was taken through deprotection, washed with tetrahydrofuran (THF) and acetylated via incubation with 300 µl dimethylformamide (DMF) and 7 µl acetic anhydrate for 20 min. at room temperature. After a wash with THF the peptides were dried and stored at 4 °C.

3.2.9 Coupling of synthetic peptides to carrier protein

Small molecules (haptens) such as peptides are incomplete immunogens but can be made fully immunogenic by coupling them to a suitable carrier molecule. Peptides were coupled to the carrier protein keyhole lympet hemocyanin (KLH) through the cysteine of the peptides, using Maleimide Activated Keyhole Limpet Hemocyanin obtained from Pierce Chemical Company (Nr. 77105) and according to instructions with the product. The peptides were dissolved in phosphate buffered saline, pH 7.2 (PBS 7.2) with 10% DMSO. The pH for the solution was chosen to optimise peptide solubility and to prevent hydrolysis of the maleimide groups during conjugation. The content of free cysteine for soluble peptides (before and after coupling) was determined by Ellman's method (Ellman, G.L., 1959).

For each 2 mg of peptide, 2 mg of activated carrier (KLH in 83 mM NaPi, pH 7.2, 0.9 M NaCl, 0.1 M EDTA) was added in a total volume of 2 ml, mixed and reacted for 2 hrs at room temperature (RT). To remove EDTA, carried over from the activated KLH, the conjugate was dialysed against 2 l. PBS 7.2, filter sterilised, aliquoted and stored at - 20 °C. It was assumed that 80 % of the peptides were conjugated after failing to detect any free sulphydryl groups using Ellman's Reagent (Pierce Nr. 22582).

3.2.10 Preparation of anti-peptide antibodies

After obtaining about 4 ml pre-immuno bleeds rabbits were immunised, with the help of Dr. R. Croy (Department of Biological Sciences), according to the following schedule: first, 100 μg peptide-coupled KLH in complete Freund's adjuvant (1:1) intramuscular and subcutaneously on day 0; second, 100 μg in incomplete Freund's adjuvant subcutaneously on day 14; and finally, again 100 μg in incomplete Freund's adjuvant intraperitoneally on day 23. After this initial course of injections, the rabbits were boosted with 100 μg peptide-coupled KLH in incomplete Freund's adjuvant at average 3-4 week intervals and bled 1 and 2 weeks following the injection. Bleeds of between 4 – 7 ml were taken on days: 0, 60, 81, 97, 118, 139, 167 and a terminal bleed (TB) of about 20 – 45 ml on day 227. Blood was placed at 37 °C for two hours before centrifugation at 4.500 rpm at 4 °C. Serum was aliquoted and stored at 4 °C with 0.04% Na-azide to prevent bacterial growth.

3.2.11 SDS-polyacrylamide gel electrophoresis (PAGE) and Western blotting

BioRad mini ProteanII gel kits were used for all one dimension electrophoresis experiments and electrophoresis was carried out at 100 Volts through the stacking gel and 200 Volts through the resolving gel. Samples were loaded in a modified Laemmli sample buffer consisting of 2% SDS, 1% DTT, 0.01% Bromophenol Blue, 10% glycerol, made up in 62.3 mM Tris-HCl pH 6.8. This buffer was either used directly to solubilise samples or added as a 5 x stock to liquid samples. Samples were boiled for 3 min. and centrifuged for 10 sec. In a Hettich Mikrolitre bench top centrifuge prior to loading gels. A continuous buffer system consisting of 0.1% SDS, 192 mM glycine and 25 mM Tris-HCl pH 8.3 was used for all protein electrophoresis experiments. After electrophoresis, protein bands were visualised in the gel by staining with Coomassie Blue.
SDS-PAGE was performed by the method of Laemmli (Laemmli, U.K., 1970) with a 5% stacking gel and a 10 – 12% resolving gel (ratio of acrylamide to bis-acrylamide was 37.5: 1 for all experiments). BioRad mini ProteanII gel kits were used for wet electroblotting to Hybond-C (Amersham) for antibody experiments. For protein transfer to the membrane a continuous buffer system containing 25 mM Tris-HCl, 192 mM glycine, 0.05% SDS and 20% methanol at a constant voltage of 30 V was used overnight at 4 °C. Protein bands on the membrane were visualised via Ponceau S staining.

3.2.12 Ponceau S staining for Western blots

After Western blotting, proteins were detected on the membrane by gentle shaking in a solution of 0.2% Ponceau S (Sigma P3504) in 1% glacial acetic acid for 1 – 5 min. Membranes were destained with several changes of 1% glacial acetic acid followed by washes with water (milliQ). Protein bands appear as red on a white background.

3.2.13 Western blotting for preparation of a protein for sequencing

Standard SDS-PAGE gels were prepared but Sequencing grade (BioRad) chemicals were used to prepare all components/reagents. The gels were pre-run for 20 min. at 50 Volts in the presence of 200 μM thioglycolic acid in the cathodic (middle) buffer compartment. This was to eliminate free radicals , which can block the protein to be sequenced, before the sample was applied. BioRad mini ProteanII gel kits were used for wet electroblotting to ProBlott (Applied Biosystems) for protein sequencing experiments. Protein transfer to the membrane (pre-wetted with methanol for 5 min and equillibrated in blotting buffer) was in a continuous buffer system containing 1 x CAPS and 10% methanol in sterile water (milliQ) (10 x CAPS consists of 100 mM 3-[cyclohexylamino]-1-propanesulfonic acid, pH 11) at a constant voltage of 30 V overnight at 4 °C. Protein bands on the membrane were visualised via a modified Coomassie Blue staining, cut out with a clean razor blade and N-terminally sequenced via Edman chemistry by J. Gilroy in a protein sequencing laboratory (Department of Biological Sciences, University of Durham).

3.2.14 Coomassie Blue staining for Western blots with samples for protein sequencing

After Western blotting, proteins were detected on the membrane by the following procedure: ProBlott membranes were rinsed with water (milliQ) and saturated with 100% methanol for 15 sec. Followed by gentle shaking in a solution of 0.1% Coomassie Blue R-250 (Sigma) in 40% methanol and 1% acetic acid for 1 – 5 min. Membranes were destained with several changes of 50% methanol acid followed by washes with water (milliQ). Protein bands appear as blue on a white background

3.3 Results

3.3.1 Overproduction and purification of fusion proteins of mature regions of *Arabidopsis* and squash GPAT in *Escherichia coli*

The regions of the mature *Arabidopsis* and squash GPAT enzymes encoded by the plasmids pET-AR1 (pAR1) and pNA4 respectively, were overproduced in the *Escherichia coli* strains BL21 (DE3) or BL21 (DE3) pLysS. A schematic diagram of the proteins in figure 3.1 illustrates the amino acid (AA) residues on the N-terminal part of the protein to distinguish between the residues encoded by the vectors and the cloning junction (14 AAs in bold) and the true GPAT protein.

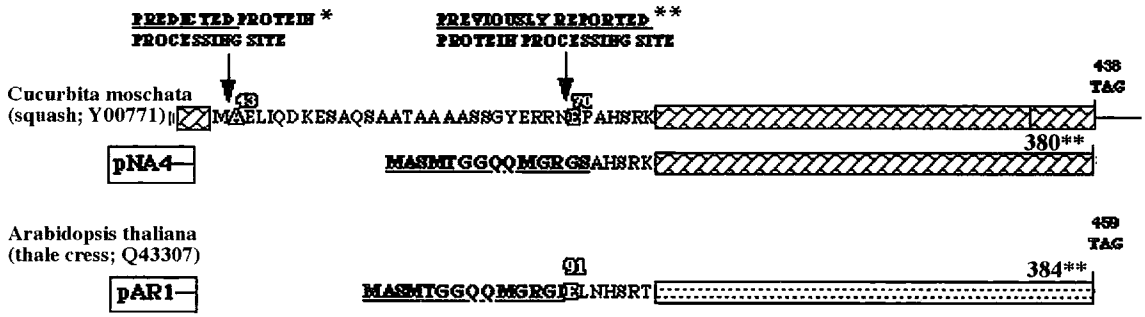

Figure 3.1 Comparison of the N-terminal amino acid sequences of the proteins encoded by the plasmids pNA4 and pAR1

The upper diagram depicts the squash GPAT amino acid sequence as present in the computer database (Accession P10349). The residue numbers are designated on basis of the protein sequence encoded by the cDNA sequence under Genbank Accession Number Y00771. This was originally thought to be the pre-protein and, after N-terminal sequencing of the mature protein from plants, it was concluded that the mature protein was encoded from the residue E70 (previously reported processing site**; Nishida, I. et al., 1987). The protein was possibly N-terminal truncated during purification procedures and the protein processing site was newly predicted to be at residue A43 on the basis of the molecular mass of the mature protein in plants in combination with evaluation of consensus sequences for protein processing sites in chloroplasts (predicted protein processing site*; Murata, N. and Tasaka, Y., 1997). The start of the mature protein of *Arabidopsis* GPAT was derived by comparison with squash GPAT under the original assumptions. The truncated enzymes are catalytically active and similar constructs have been used in transgenic studies with tobacco. Amino acid residues on the N-terminus of the proteins, encoded by the plasmids pNA4 and pAR1, which are encoded by the respective pET vecor leader sequences and the cloning junction, are depicted in bold. pNA4 encodes a protein of 380 AA and 41 kDa, pAR1 encodes a 42 kDA protein of 383 AAs.

Figures 3.2 and 3.3 show representative results of SDS-PAGE of proteins from BL21 (DE3) cells transformed with pAR1 or pNA4 respectively. Upon addition of isopropyl-β-thiogalactopyranoside (IPTG), a 42 kDa (pAR1) or 41 kDa (pNA4) GPAT fusion protein was synthesised, accounting for up to at least 10 - 30% of the total soluble *E. coli* proteins after 3 hrs induction.

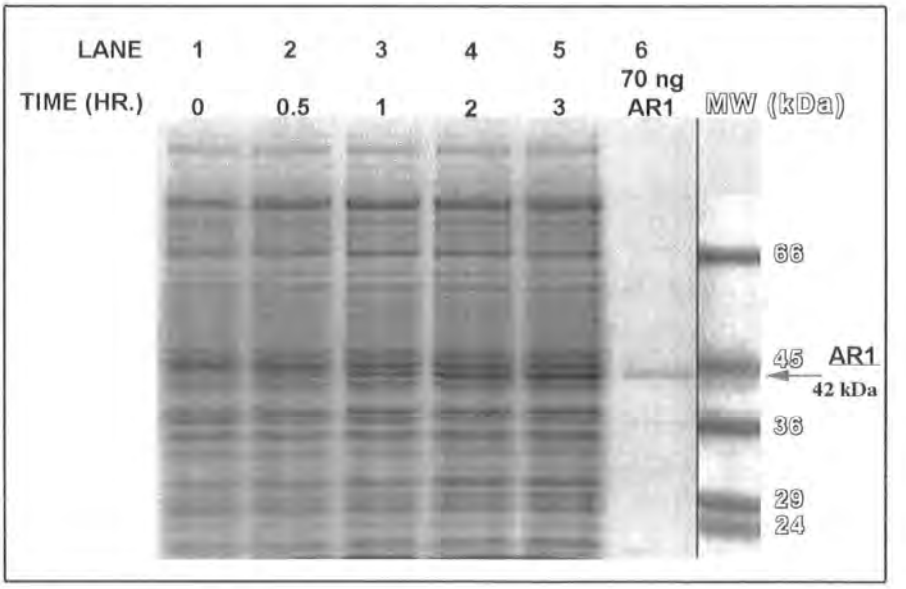

Figure 3.2 Progression of overproduction of GPAT in *E. coli*

Coomassie stained 10% SDS PAGE gel of total proteins from cells showing a typical induction for overproduction of GPAT encoded by pAR1 and pNA4, using an experiment with pAR1 as an illustration. Lane numbers are indicated in the top part of the figure. The time after addition of IPTG at T = 0 is indicated under the lane numbers. Lane 6 contains purified protein from a later experiment and was used as a standard for quantitation of amounts of GPAT produced. Molecular weight markers are depicted on the right.

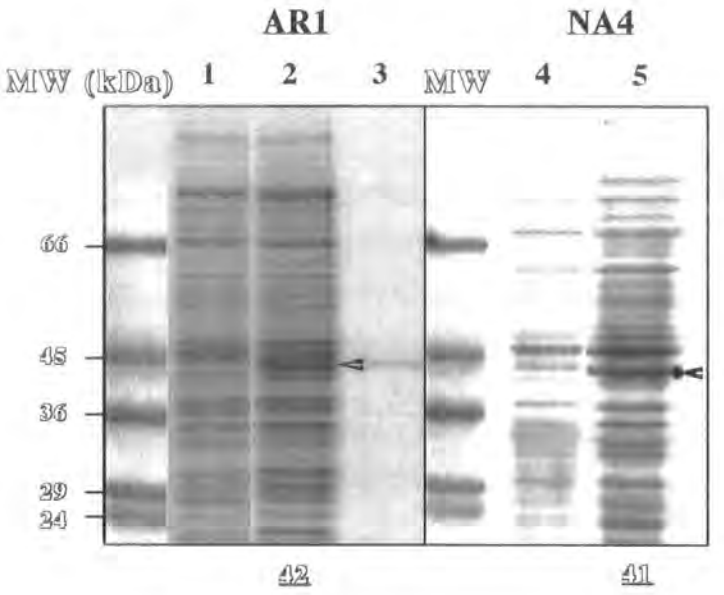

Figure 3.3 The bacterial overproduction of *Arabidopsis* and squash GPAT fusion proteins encoded by pAR1 and pNA4 respectively

Coomassie stained 10% SDS PAGE gel of total proteins from cells showing a typical induction for overproduction of GPAT encoded by pAR1 and pNA4. Lanes 1 and 2 show total *E.coli* protein fractions at T = 0 and 3 hrs after IPTG addition for pAR1 overproduction, and lanes 4 and 5 for pNA4. Lane 3 contains purified *Arabidopsis* GPAT protein from a later experiment and was used as a standard for quantitation of amounts of GPAT produced. Molecular weight markers are depicted in outlined numbers on the left. The arrows indicate the overproduced GPAT fusion protein bands and the outlined/underlined numbers below lanes 2 and 5 denote their size.

The purification protocol was standarised for the purification of both the overproduced squash GPAT (pNA4) and *Arabidopsis* GPAT (pAR1) fusion proteins. The final purified enzyme preparations for the overproduced proteins will be referred to as AR1 and NA4 throughout the course of this study.

Batch cultures of the transformed bacteria of 500 ml or 1 litre (up to 4 litre total volume) were grown to OD_{600} of 0.5, induced with 0.4 – 0.6 mM IPTG (as described) and cells were harvested by centrifugation. The following steps in the purification were all performed at 0–4 °C to maintain maximum enzymatic activity and protein integrity. Cells were washed in 50 mM Tris-HCl pH 7.4, 150 mM NaCl and collected via centrifugation at 10,000 x g. The cell pellets were resuspended in minimal volumes of 50 mM Tris-HCl pH 7.4, frozen in liquid N_2 and stored at -80 °C.

Frozen cell suspensions were thawed and lysed by 3 passages through a Constant Systems cell disrupter at 25,000 psi setting. DNAse I (Sigma 100 mg DNAse/50 ml of lysate) and 10 mM $MgCl_2$ was added to reduce viscosity by removing the nucleic acid macromolecules released during lysis. Cell debris (DNA, membranes and other water-insoluble components) was removed by centrifugation at 40,000 x g. The isoelectric points of all known GPAT enzymes, as well as the predicted pI of AR1 and NA4 on basis of the cDNA sequence are below 7 (mostly between pI 5 and 6.5). Anion chromatography with buffering systems at pH 7.4 at 0 °C, was chosen for the following purification steps.

The pH of the water soluble fraction of the enzyme lysates (sample) was adjusted to 7.4 and the conductivity was adjusted to between 1 and 2 (20 mS setting) using Milli-Q water. The sample was filtered through a 0.2 μm sterile filter and loaded onto an activated (1M NaCl) and equillibrated 50 ml High Load mono-Q column (Pharmacia). The mono-Q column was washed with 25 mM Tris-HCl pH 7.4, 1 mM DTT (Buffer A) until the $A_{280\ nm}$ of the flow through was returned to base line level (~0.01). A 0-100% Buffer B (Buffer B = Buffer A + 0.6 M NaCl) 10 column volume continuous NaCl gradient was applied (500 ml.) and eluted fractions were analysed for the presence of GPAT on 10 % SDS-PAGE gels stained with Coomassie Blue as shown in figure 3.4.

Fractions containing relatively high amounts of partially purified GPAT were pooled and dialysed with 3 changes of 2 litre of Buffer A overnight at 4 °C (fractions 23 – 27 in a total volume of 32.5 ml). The sample pH was re-adjusted to 7.4 and the conductivity adjusted to less than 2 mS (when necessary).

Figure 3.4 First anion exchange chromatography purification step of recombinant *Arabidopsis* GPAT (AR1) from *E.coli* BL21 (DE3)

(A) shows a typical elution profile for recombinant GPAT using a linear gradient of 0 – 0.6 M NaCl. The linear gradient is illustrated by the continuous line with [NaCl] on the right. Fractions of 6.5 ml were collected and indicated fractions, containing partially purified GPAT, were pooled for the next purification steps.

(B) a 10% SDS-PAGE gel stained with Coomassie Blue containing 8 µl samples from the enzyme fractions 21 –27. In the lane on the left, a fraction of the original protein preparation loaded onto the anion exchange column is separated to evaluate the partial purification of the overproduced GPAT (indicated by the arrow). Molecular weight markers are depicted on the right (outlined).
Fractions 23 – 27 (total volume = 32.5 ml) were pooled.

A

Anion Exchange Chromatography Purification; High Load monoQ Elution Profile I

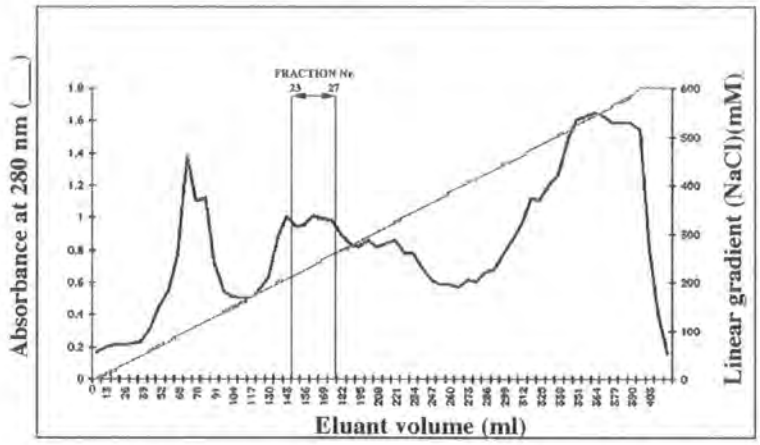

Column: **High Load monoQ 50 ml (Pharmacia)** *System:* **Pharmacia LKB GradiFrac System with LKB Uvicord SII to monitor Absorbance at 280 nm**

Sample: **Crude cell-free soluble protein extract of E. coli overproducing Arabidopsis GPAT (AR1) Conductivity is 1-2 mS and the pH is 7.4**

Buffer A: **25 mM Tris-HCl pH 7.4/ 1 mM DTT** *Buffer B:* **Buffer A + 0.6 M NaCl**

Gradient: **0 - 100% Buffer B in 500 ml** *Flow rate:* **5 ml/min** *Fraction size:* **6.5 ml**

B

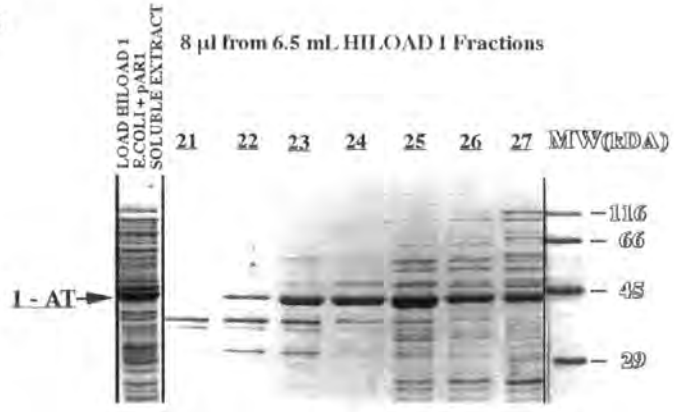

Pooled and dialysed fractions from High Load step I were subjected to a second anion exchange chromatography by loading another 50 ml Hiload mono-Q column and washing with Buffer A until the flow through peak was collected and A280 nm was returned to base line level. To elute the proteins bound to the column, a stepwise NaCl gradient was applied according to the following protocol: 0-75 ml, 0-15% Buffer B; 75-135 ml, 15% Buffer B; 135-155 ml, 15-19% Buffer B; 155-215 ml, 19% Buffer B; 215-250 ml 19-24% Buffer B; 250-310 ml, 24% Buffer B; 310-600 ml, 24-100% Buffer B; 600-650 ml, 100% Buffer B; 650-700 ml 100-0% Buffer B. Eluted 6.5 ml fractions were analysed by 10% SDS-PAGE and standard GPAT activity determination as shown in figure 3.5. The fractions of highest purity and containing high GPAT catalytic activities were pooled (fractions 19 – 23), quantified, aliquoted and stored at -80 °C. Samples of the pooled preparations of NA4 and AR1 were electrophoretically separated on a 10% SDS-PAGE gel and are shown in figure 3.6. Specific activities of indicated enzyme preparations before the two anion exchange purification steps and after the final chromatography step were determined using labeled acyl-ACP substrates (table 3.1).

Table 3.1 Purification of NA4 and AR1

Enzyme preparation	Specific activity (U/μg)**		Purification (fold)	
	[^{3}H]18:1-ACP	/ [^{14}C]16:0-ACP	[^{3}H]18:1-ACP	/ [^{14}C]16:0-ACP
NA4 (total soluble cell extract)	**10**	**8**		
NA4 (90% pure)	**187**	**166**	**18.7**	**20.8**
AR1 (total soluble cell extract)	**3.5**	**0.9**		
AR1 (90% pure)	**68**	**21**	**19.4**	**23**

*Data obtained in collaboration with Dr. T. Schierer

** Units are defined as the amount of enzyme transferring 1 pmol fatty acid to G3P per minute.

The overproduced *Arabidopsis* GPAT (pAR1) and squash GPAT (pNA4) were typically purified 23 fold and at least 90% purity after the final chromatography step.

A

Anion Exchange Chromatography Purification; High Load monoQ Elution Profile II

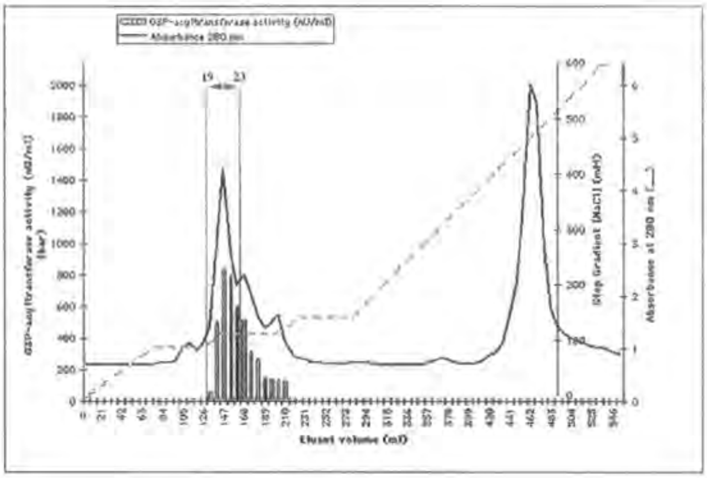

Column:	High Load monoQ 50 mL. (Pharmacia)
Sample:	Pooled 5 (6.5 ml) fractions (23 - 27) from High Load monoQ Chromatography in the first main purification step. The pooled fractions were dialysed against Buffer A, the conductivity was adjusted to 1 - 2 mS and the pH to 7.4
Buffer A:	25 mM Tris-HCl pH 7.4/1 mM DTT
Buffer B:	Buffer A + 0.6 M NaCl
Flow rate:	5 ml/min.
Gradient:	Step Gradient: 0 - 75 ml; 0 - 15%/ 75 - 135 ml; 15%/ 135 - 155 ml; 15 - 19%/ 155 - 215 ml; 19%/ 215 - 250 ml; 19 - 24%/ 250 - 310 ml; 24%/ 310 - 600 ml; 24 - 100% Buffer B
Fraction size:	6.5 ml
System:	Pharmacia LKB GradiFrac System with LKB Uvicord SII to monitor Absorbance at 280 nm

B

C

Standard 1-AT activity Assay on 2µl per 6.5 ml fractions from HILOAD II

Sample Nr. S#	TIME	CPMA	A:2SX	DPM1	%IN	LSIE / Fraction Nr.:
1	1.00	217.00	13.67	315.32	16.150	456. Blank
2	1.00	822.00	6.97	1218.80	13.050	443.18
3	1.00	6772.00	2.43	10061.3	12.380	481.19*
4	1.00	11367.0	1.87	16831.4	12.370	484.20*
5	1.00	11041.0	1.90	15842.0	12.690	465.21*
6	1.00	8117.00	2.21	11936.1	12.500	449.22*
7	1.00	7027.00	2.38	10374.5	12.390	446.23*
8	1.00	4317.00	3.08	6350.62	12.560	453.24
9	1.00	3675.00	3.29	5372.49	12.410	452.25
10	1.00	2107.00	4.35	3107.47	12.430	447.26
11	1.00	1923.00	4.56	2818.71	12.370	451.27
12	1.00	2019.00	4.45	2915.00	12.430	460.28
13	1.00	1819.00	4.68	2662.65	12.340	447.29
14	1.00	9622.00	2.03	14170.1	12.510	448. Pooled Fractions 23-27 from HILOAD I
15	1.00	9557.00	2.04	14055.1	12.320	449. Crude soluble extract (Load for HILOAD I)
16	1.00	303.00	11.49	449.42	12.340	445. Blank

Figure 3.5 The second anion exchange chromatography purification of recombinant *Arabidopsis* GPAT (AR1) from *E.coli* BL21 (DE3)

(A) Typical elution profile for GPAT in a stepwise gradient of 0 – 0.6 M NaCl. The step-gradient is illustrated by dashed line with [NaCl] on the right. Fractions of 6.5 ml were collected and indicated fractions containing purified GPAT were pooled. Standard GPAT activity of 2 µl samples per fraction (left y-axis and panel C) was determined and is depicted by vertical bars.

(B) A 10% SDS-PAGE gel stained with Coomassie Blue containing 10 µl samples from the enzyme fractions 18 – 26. In the lane on the left, a fraction of the original protein preparation loaded onto the anion exchange column is separated to evaluate the purification of the GPAT (indicated by the arrow). Molecular weight markers are depicted on the right. Fractions 19 -23 (eluent volume: 32.5 ml) were pooled.

(C) A result from a standard GPAT enzyme activity determination. Numbers of the fractions assayed are indicated on the right and the arrow indicates the dpm values used in calculations of the enzyme activities. The fractions 19 to 23, each accentuated with an asterisks, contain the highest concentrations of GPAT proteins and enzyme activities.

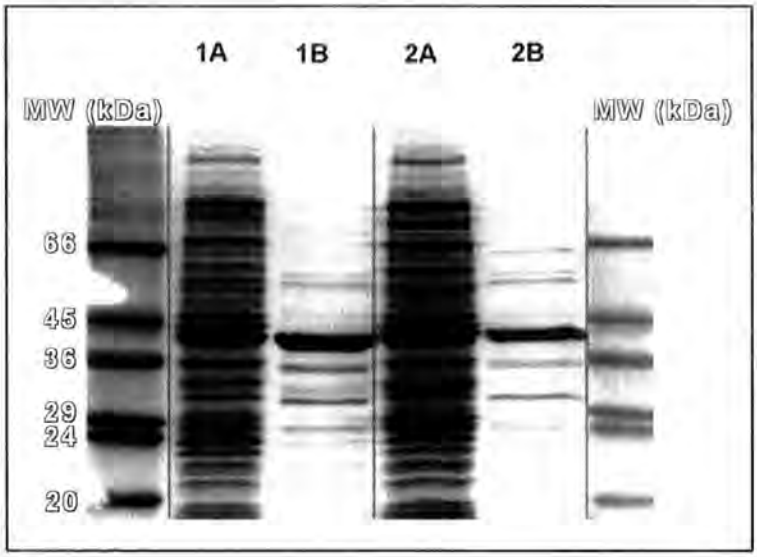

Figure 3.6 Typical NA4 and AR1 purity

The pooled fractions (fractions 19 – 23) of the highest purity and containing high GPAT catalytic activities after the final anion exchange column were analysed on a 10% SDS-PAGE gel stained with Coomassie Blue. GPAT amounts were quantified by means of comparing band intensities with known standards on the same gels and standard GPAT enzyme assays. Lanes 1A and 2A contain total soluble cell protein (loading equivalent to 50 µl original culture volume) after 3 hr. induction of BL 21 (DE3) transformed with pNA4 and pAR1 respectively. Lane 1B shows a loading of a purified NA4 preparation (the NA4 GPAT quantified at 0.320 ng/ µl) and lane 2B contains a purified AR1 preparation (the AR1 GPAT quantified at 0.055 ng/ µl). Molecular weight standards are in the flanking lanes.

Following a purification procedure of recombinant *Arabidopsis* GPAT (pAR1), it was found that the preparation had an aberrant SDS-PAGE gel profile. A doublet of two protein bands around 43 kDA and of about the same band intensity, after staining gels with Coomassie Blue, were seen. It was important to have a reasonably accurate quantification for the actual GPAT band, for later selectivity and kinetic studies. The band representing GPAT could be identified via N-terminal protein sequencing or via gel filtration chromatography in combination with the biological activity assay. The latter would have the added advantage of allowing for investigating whether or not the protein would be associated with other components after overproduction in *E. coli*.

3.3.2 Gel filtration chromatography of recombinant squash GPAT (NA4) and *Arabidopsis* GPAT (AR1) fusion proteins

To examine the molecular weight of the purified recombinant GPAT enzymes and to identify which of the two main bands in the AR1 preparation contained GPAT enzymatic activity, a sample of the enzyme preparations was subjected to gel filtration chromatography
(Figure 3.7).
A SMART Superose 12 PC 3.2/30 (Pharmacia) micro column was used on a Pharmacia SMART Chromatography System. Molecular weight (MW) standards used for the calibration of the gel filtration chromatography (monitoring the retention time of each against absorbance at 280 nm) were made at 1 mg/ml in 50 mM sodium phosphate buffer and were bovine serum albumin (67 kDa), ovalbumin (43 kDa) and RNAse (13.7 kDa). The molecular weight (MW) of the recombinant GPAT fusion proteins was 42 kDa, corresponding to a monomeric, fully enzymatically active protein.
It was concluded that the lower band of the doublet bands of equal Coomassie staining intensity in the AR1 preparation corresponded to *Arabidopsis* AR1 GPAT. The enzyme preparations purified via the anion exchange chromatography procedures could be purified further with a gelfiltration chromatography step but for the purpose of the experiments in this study (enzymatic studies and crystallography) that proved not to be necessary.

Figure 3.7 SMART Superose 12 micro gelfiltration chromatography of purified recombinant squash GPAT (NA4) and *Arabidopsis* GPAT (AR1) fusion proteins

(A) Calibration curve of the SMART Superose 12 PC 3.2/30 (Pharmacia) micro column used on a Pharmacia SMART Chromatography System. Retention time (recalculated as eluant volume) was depicted versus log MW.

(B) and **(C)** show elution profiles of NA4 (squash GPAT or –1-AT) and AR1 (*Arabidopsis* GPAT or 1-AT) respectively. Fraction numbers are depicted against the absorbance at 280 nm and fractions containing the majority of GPAT enzyme activity are outlined. The numbers above the peaks indicate retention volumes and were used to estimate the MW of the GPATs on basis of the calibration curve.

(D) 10% SDS-PAGE gel stained with Coomassie Blue and selected protein samples are indicated above the lanes. The arrows on the right identify the 42 kDa monomeric GPAT containing band and the upper unknown band.

A

SMART Superose 12 Gelfiltration
CALIBRATION

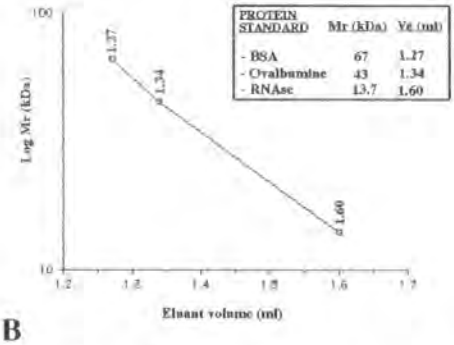

PROTEIN STANDARD	Mr (kDa)	Ve (ml)
- BSA	67	1.27
- Ovalbumine	43	1.34
- RNAse	13.7	1.60

Column:	Superose 12 PC 3.2/30 (2.4 ml)
Sample volume:	20 µl
Buffer:	25 mM Tris (pH 7.4)/150 mM NaCl/1 mM DTT
Flow rate:	40 µl/min (total run volume; 3.0 ml)
Fraction size:	50 µl
System/Instrumentation:	Pharmacia SMART System

B

SMART Superose 12 Gel Filtration
Elution Profile of purified recombinant Squash 1-AT (pNA4)

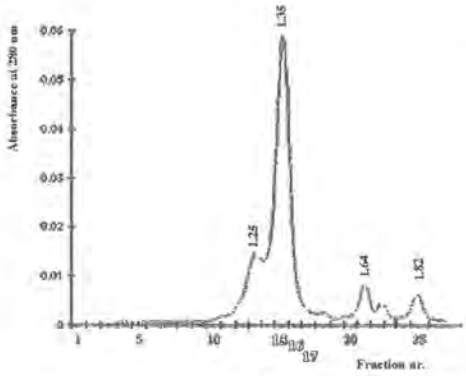

Sample: HighLoad pure Squash 1 - AT (pNA4)
Sample concentration: 0.3 mg/ml

C

SMART Superose 12 Gel Filtration
Elution Profile of purified recombinant Ara 1-AT (pAR1)

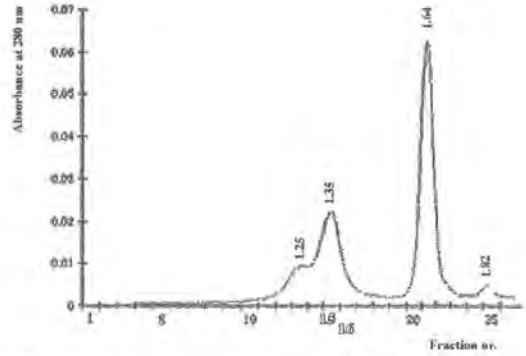

Sample: HighLoad pure Ara 1 - AT (pAR1)
Sample concentration: 0.1 mg/ml

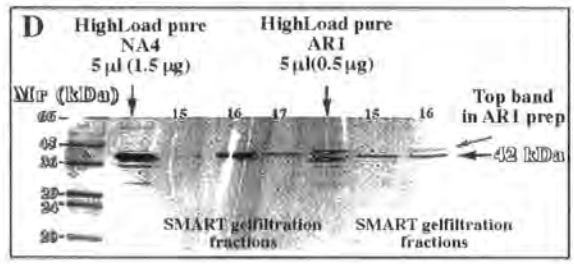

3.3.3 Substrate selectivity assays of soluble glycerol-3-phosphate acyltransferases

In order to appraise structure – function relationships of this type of acyltransferases and the effect of modification of the protein structure on its catalytic properties and substrate selectivities, it is of particular importance to have a practical but physiologically relevant *in vitro* assay. With the resulting data from transgenic studies, providing indications for the *in vivo* selectivities of the squash (similar to NA4) and *Arabidopsis* GPAT (similar to AR1), a standard was set for assay conditions, reflecting the physiological conditions and properties of these enzymes as close as practically possible.

A **standard selectivity assay for GPAT (SSA GPAT)** for soluble GPAT was evaluated by using equimolar mixtures of two acyl donors and investigating the effect of changing single reaction parameters on *in vitro* selectivity for 16:0 or 18:1 acyl thioesters. The following reaction parameters were examined and the results compared with the *in vivo* behaviour of the enzymes in the transgenic studies and previously reported *in vitro* data: acyl-CoA or acyl-ACP, pH at 7.4 or at 8.0, [G3P] at 7.5 μM, 300 μM or 30 mM and [BSA] at 0.5 or 5 mg/ml.

Selectivities of the enzymes in the **SSA GPAT** were determined on basis of initial enzyme velocities using enzyme amounts resulting in linear rates with both types of acyl donors for at least 2 minutes in a timeseries (Figure 3.8).

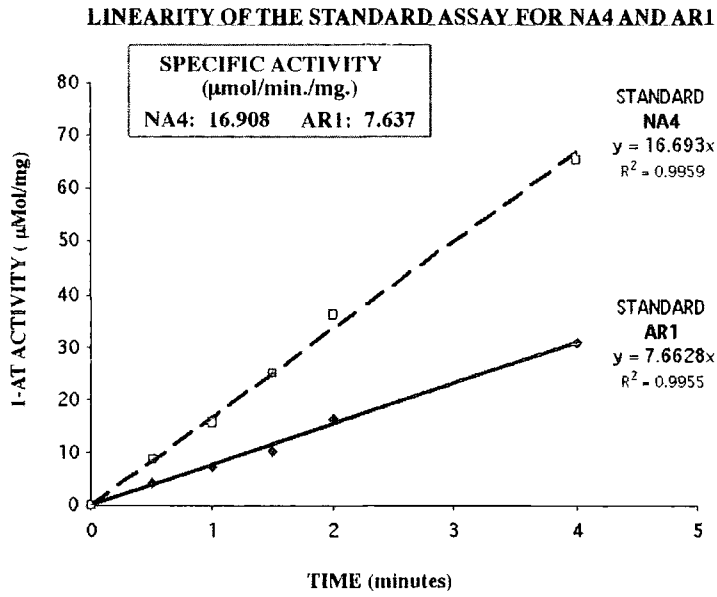

Figure 3.8 Specific activity and linearity of the standard GPAT (1-AT) assay for purified preparations of recombinant squash GPAT (NA4) and *Arabidopsis* GPAT (AR1)

The activity of the purified preparations of recombinant squash 1-AT (NA4) and recombinant *Arabidopsis* 1-AT (AR1) was tested in the standard GPAT enzyme assay (2mM [U-^{14}C] G3P (2000 dpm/nmol), 0.4 mM 16:0-CoA, 5 mg/ml BSA, pH 7.5 in a reaction volume of 80 µl at 25 °C). The reaction was followed over 30 minutes using 0.5 µl (160 ng.) NA4 and 2.5 µl (137.5 ng) AR1. Under these conditions the assay is linear for at least four minutes. The solid line illustrates the reaction velocity for AR1 and the interrupted line shows the reaction velocity for NA4. The specific activity for the respective enzyme preparations under these conditions is depicted in the box.

Apparent kinetic constants for NA4 and AR1 were determined for glycerol-3-phosphate when using acyl-CoA thioesters (0.4 mM) as the acyl donors. The rates of acylation of [U-^{14}C]G3P were measured over a suitable range of concentrations (0.30, 0.44, 0.76 and 2.2 mM) and at a fixed concentration of 16:0-CoA or 18:1-CoA. Lineweaver-Burke plots for both sets of data are shown in figure 3.9.

For the recombinant squash GPAT (NA4) it was found that the apparent Km for G3P with 16:0-CoA is 0.23 mM and with 18:1-CoA 0.082 mM. These data are close to the ones published by Ferri, S.R. and Toguri, T. (Ferri, S.R. and Toguri. T., 1997) for the recombinant squash GPAT (in the publication referred to as QQQ). Using a standard GPAT assay they found apparent Km values for G3P with 16:0-CoA and 18:1-CoA of 0.14 mM and 0.083 mM respectively.

Kinetic data for *Arabidopsis* GPAT have not been reported previously. For the AR1 enzyme, the apparent Km for G3P with 16:0-CoA is 0.548 mM and with 18:1-CoA 0.088mM. This is within physiological concentrations for G3P in chloroplasts of plant

cells, but the Km (G3P) value of 0.548 mM of AR1 with 16:0-CoA, is relatively high. This might be one of the indications for the lower preference of the *Arabidopsis* GPAT for 16:0 acyl chains. However, this is just an indication because acyl-CoAs are not the physiological acyl donors and other factors may play a role in determining the substrate selectivities. In combination with the apparent Vmax values (Figure 3.9), it could be implied from these data that the AR1 GPAT would prefer to select 18:1 over 16:0 acyl chains in a direct competition.

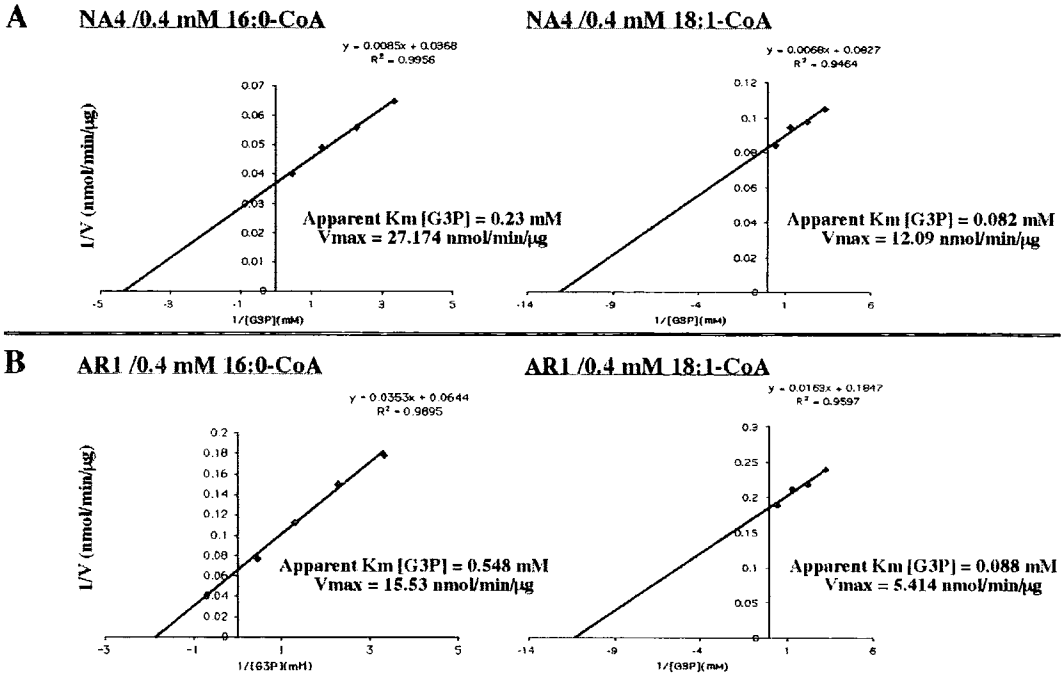

Figure 3.9 Lineweaver – Burke plots of initial velocity with 16:0-CoA and 18:1-CoA, versus glycerol-3-phosphate concentration using purified recombinant (A) **squash GPAT (NA4) and** (B) ***Arabidopsis*** **GPAT (AR1)**

Standard assay conditions were used (Materials and Methods) with 0.30, 0.44, 0.76 and 2.2 mM [U-^{14}C]G3P (3000 dpm/nmol) using a fixed concentration of 16:0-CoA or 18:1-CoA (0.4 mM). Initial velocity was measured over a 4 minute timeseries for purified recombinant squash 1-AT (NA4 ; 0.5 µl. = 0.160 µg) and *Arabidopsis* 1-AT (AR1 ; 3 µl. = 0.165 µg). The Vmax values were calculated in nmol.min $^{-1}$ per microgram of pure protein and the apparent Km values are calculated in mM for G3P with either 16:0-CoA or 18:1-CoA

Throughout the rest of this study, the **enzyme selectivities** as determined in the SSA GPAT (standard selectivity assay for GPAT) are described as

selectivity factor (SF): the ratio of the rate of 18:1 to 16:0 utilisation (**initial rate 18:1/ initial rate 16:0**).

Others have reported that pH has an influence on the soluble GPAT enzyme specificity and selectivity (Frentzen, et al., 1987). At pH 7.4 there is a higher preference for 18:1 acyl-chain utilisation whilst at pH 8.0 (the physiological pH of the chloroplast in the light) there is an increased preference for 16:0 concomitant with a relatively decreased preference for 18:1.

The main intention of the presented experiments was to evaluate conditions for the assay as close as possible to physiological conditions and to obtain a representable reflection of the *in vivo* behaviour of the GPATs

Acyl-CoAs ([9,10(n)-^{3}H]Oleoyl-CoA (55 Ci/mol) and [1-^{14}C]Palmitoyl-CoA (55 Ci/mol)) were used in equimolar mixtures of 10 μM each (20 μM total) and acyl-ACPs [1-^{14}C]Palmitoyl-ACP (55 Ci/mol.) and [9,10(n)-^{3}H]Oleoyl-ACP (55 Ci/mol.) were used in equimolar mixtures of 1 μM each (2 μM total). Acknowledged is the work of Dr. T. Schierer who provided the radiolabeled acyl-ACP substrates for this study (Materials and Methods) and performed initial experiments with the acyl-ACP substrates. The concentration of G3P substrate for the experimental determinations in figure 3.10 are within the physiological range, namely 300 μM. The resulting data of the effect with low [G3P] (7.5 μM) or high [G3P] (30 mM) might be published elsewhere.

The most significant results of the standard selectivity assay (SSA GPAT) for NA4 and AR1 in this study, with respect to the influence of the [BSA] and the use of the substrate analogue acyl-CoA compared to the physiological substrate acyl-ACP, are shown in figure 3.10.

Figure 3.10 The influence of the BSA concentration and the use of the substrate analogue acyl-CoA or the physiological substrate acyl-ACP on the selectivity factor of glycerol-3-phosphate acyltransferases

Results from standard selectivity assays (SSA) for squash GPAT (NA4) and *Arabidopsis* GPAT (AR1). The amount of reaction product (pmol LPA) formed in a timeseries is depicted against the time points in minutes. Solid lines represent the reactions for AR1 and the dashed lines illustrate the reactions for NA4. In all standard selectivity assay (SSA GPAT) experiments shown, 300 μM G3P and a pH 8.0 was used. The selectivity factors (SF) of the enzymes are depicted in the boxes.

(A) SSA GPAT with the substrate analogues (acyl-CoA) and a low [BSA] (0.5 mg/ml).

(B) as (A) except that [BSA] was 5 mg/ml.

(C) and **(D)** SSA GPAT with acyl-ACP substrates under low and high [BSA] respectively.

The lines represent a regression calculation of the increasing amounts of radio-active reaction products formed over time and illustrate the linearity of the initial rates of the reactions with the respective enzymes and substrates

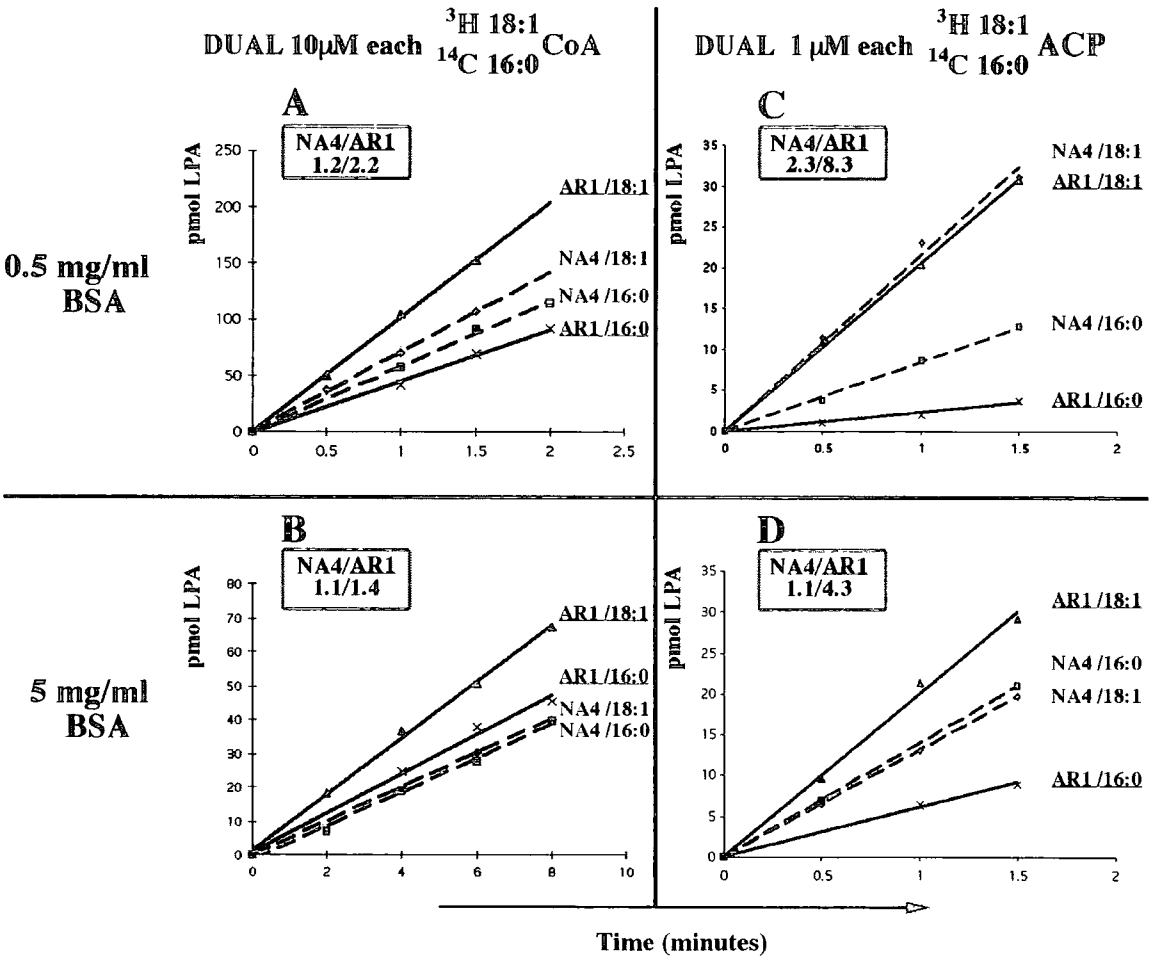
DUAL 10μM each ^{3}H 18:1 ^{14}C 16:0 CoA
DUAL 1 μM each ^{3}H 18:1 ^{14}C 16:0 ACP
0.5 mg/ml BSA
5 mg/ml BSA
A
B
C
D
NA4/AR1 1.2/2.2
NA4/AR1 1.1/1.4
NA4/AR1 2.3/8.3
NA4/AR1 1.1/4.3
pmol LPA
AR1/18:1
NA4/18:1
NA4/16:0
AR1/16:0
Time (minutes)

From these and previously published experimental determinations of enzyme kinetics and fatty acyl selectivities, it seems clear that the squash GPAT NA4 is a non-selective GPAT. This property is usually well reflected in the selectivity assays performed.

One exception is worth noting in the use of low amounts of BSA (0.5 mg/ml) in combination with the acyl-ACP substrates. The selectivity factor (SF) of the squash GPAT (NA4) is then around 2 (figure 3.10 (C) instead of around 1. Therefore these particular *in vitro* reaction conditions do not seem suitable as they do not give the same "apparent selectivity" as seen *in vivo*.

The effects of the [BSA] and the use of the different acyl thioesters was more pronounced for the *Arabidopsis* GPAT AR1. It is known that the *Arabidopsis* enzyme effectively competes with the endogenous tobacco GPAT for unsaturated (18:1-ACP) substrates *in planta* (Murata, N. et al., 1992). In combination with the fact that *Arabidopsis* is a chilling resistant plant, it is obvious that under the correct *in vitro* conditions the enzyme would prefer to use 18:1 acyl chains in a selectivity assay.
It is clearly shown in figure 3.10 that this property is not reflected when using the substrate-analogues (acyl-CoAs) under the reaction conditions tested. However, under the reaction conditions used in the experiments depicted in figure 3.10 (D), the selectivity of both the squash and the *Arabidopsis* GPAT closely resemble those seen *in vivo* (SF NA4 1.1, SF AR1 4.3).

It was decided to use these reaction conditions in future assays of soluble GPAT, namely: 300 μM G3P, pH 8.0, [BSA] 5 mg/ml, and an equimolar mixture of [1-^{14}C] 16:0-ACP and [9,10(n)-^{3}H] 18:1-ACP at 1 μM each.

3.3.4 Polyclonal immunosera recognising soluble denatured GPAT proteins

Polyclonal immunosera were raised against denatured *Arabidopsis* (AR1) and squash (NA4) proteins, with the intention to evaluate protein expression levels in plant tissues in later experiments and for use in other Western blotting experiments. One rabbit (rabbit 9) was immunised with the squash GPAT (NA4) protein preparation and the other (rabbit 10) with the *Arabidopsis* (AR1) enzyme. The polyclonal antibodies extracted from all the individual bleeds, were evaluated for their specificity of recognising the respective proteins as pure preparations and in total soluble extract *of E. coli* in which the respective GPAT proteins were overproduced.
The crude titre of the antibodies was determined by probing standard amounts of AR1 or NA4 with serial dilutions of the antibodies and it was found that the titres were moderate, but that a 1:1000 – 1:2500 dilution was more than sufficient to detect less than 100 ng of denatured antigen (results not shown). In further analysis if was found that the anti-sera did not cross-react with any denatured, soluble *E. coli* proteins. The overall primary structure (amino acid sequences) of these enzymes has a high degree of similarity (66.9% in 369 AA overlap) (Figure 3.12) and, as expected, the immunosera cross-recognised both denatured GPAT proteins. These findings are illustrated in figure 3.11, lanes 1 and 2 in (A) and (B).

The suitability of the use of the antisera to detect GPAT in denatured preparations of crude plant leaf extracts of *Arabidopsis* and squash was tested in preliminary experiments. It was observed that both the antisera recognised denatured proteins in these plant extracts a-specifically. This is shown in figure 3.11, lanes 3 and 4 in (A) and (B), illustrating that it is not clear whether GPAT is being detected in 25 µg total soluble plant protein extracts.
It is known that GPAT makes up only approximately 0.01% of total soluble proteins of leaves (Murata, N. et al., 1992) and might be hard to detect with an antiserum with a moderate titre of GPAT-specific antibody. There is a possibility that other proteins of similar size, present in this crude, total leaf protein preparation, could mask the GPAT band on the blot. Using a SDS-PAGE gel system with higher resolution could be used to try and circumvent this potential problem. The recognition of non specific plant proteins by the polyclonal antisera, could be caused by immunisation of the rabbits with components in their feed, which might have entered the bloodstream during the immunisation.

Figure 3.11 Western blot with rabbit polyclonal antisera against squash GPAT (NA4), *Arabidopsis* GPAT (AR1) and an *Arabidopsis* GPAT peptide

(I): Coomassie Brilliant Blue staining of a 10% SDS-polyacrylamide gel; **lane1**, partially purified squash GPAT (NA4) (580 ng); **lane 2**, partially purified *Arabidopsis* GPAT (AR1) (120 ng); **lane 3**, crude extract from squash leaf (25 μg); **lane 4**, crude extract from *Arabidopsis* leaf (25 μg).

(II): Immunoblotting of the samples in (I), using a 1 : 1000 dilution (v/v) of rabbit antisera in PBS buffer/1 % hemoglobin/0.02% Na-Azide and after secondary incubation with ^{125}I-donkey anti-rabbit Ig (Amersham Pharmacia biotech; IM 134) exposed to film for 2 days.

The antisera used are indicated as (**A**); α- squash 1-AT (rabbit 9: anti- denatured NA4, equal volume ratio of bleed 1 and 3), (**B**); α-*Arabidopsis* 1-AT (rabbit 10: anti- denatured AR1, equal volume ratio of bleed 1,2 and 3), (**C**) α- ARA-PEP2 (rabbit 13: anti *Arabidopsis* GPAT peptide 2, terminal bleed). Molecular weight markers are indicated on the left.

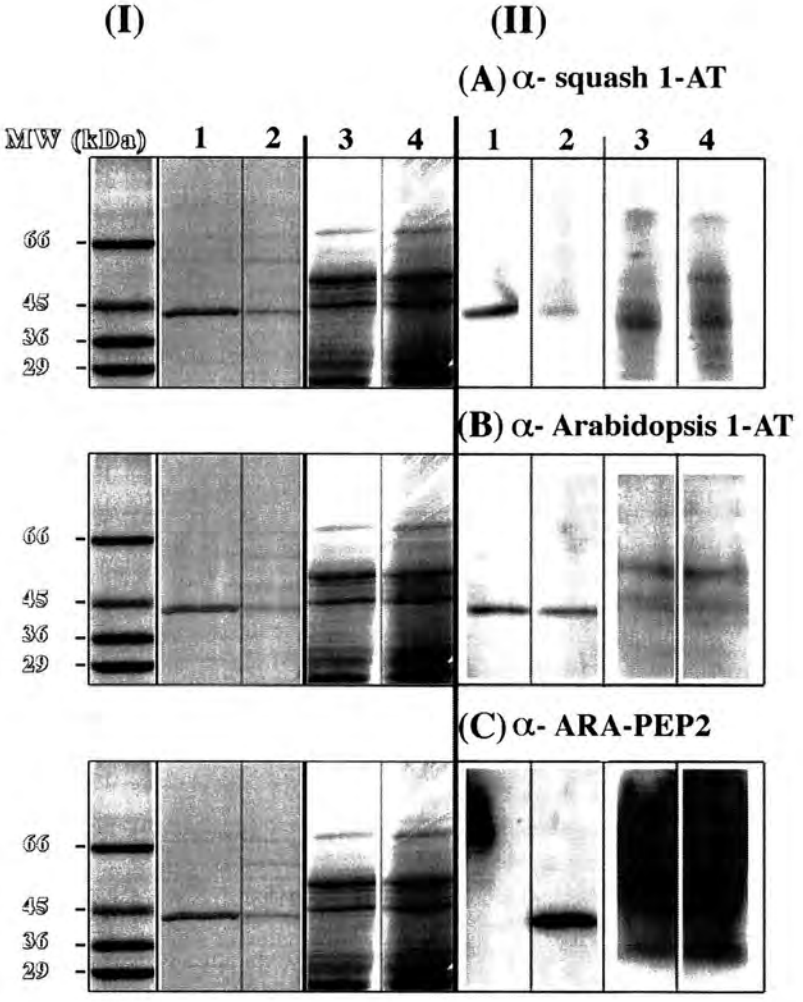
(I)
(II)
(A) α- squash 1-AT
MW (kDa)
1
2
3
4
1
2
3
4
66
45
36
29
(B) α- Arabidopsis 1-AT
66
45
36
29
(C) α- ARA-PEP2
66
45
36
29

In order to obtain specific polyclonal antibodies which would distinguish between *Arabidopsis* and squash GPAT, four peptide haptens were designed and used for immunisations of rabbits.

The full pre-protein amino acid sequences of *Arabidopsis* GPAT (Acc. Nr. Q 43307) and of squash GPAT (derived from the cDNA sequence under Acc. Nr. Y00771) were pairwise aligned according to the Martinez method (using the DNA Strider 1.3f software package) and the alignment is shown in figure 3.12.

Figure 3.12 Martinez pairwise protein alignment of *Arabidopsis* GPAT and squash GPAT

The full pre-protein sequences of *Arabidopsis* GPAT (top) and squash GPAT (bottom), were aligned according to the method and parameters above the alignment result. ARA-PEP 1 and ARA-PEP 2 depict the peptides derived from the *Arabidopsis* mature protein region and SQ-PEP 1 and SQ-PEP 2 for squash, which show the least similarity between the proteins.

Generating an antipeptide antibody to distinguish between two similar proteins is difficult. Usually, the use of synthetic peptides of 10 to 12 AA residues as antigens, is a compromise between the ease of synthesis and sufficient length for structural information. The following peptides were synthesised:

ARA-PEP1: NVDPELVDMKRK-C
ARA-PEP2: SDVTADCESP-C
SQ-PEP1: FDIPELTETKRK-C
SQ-PEP2: EEIAATHKNP-C.

For conjugation purposes, the C-terminal residue of each peptide was synthesised with a cysteine (C), providing a thiol group for use in conjugation to keyhole lympet hemocyanin (to elicit an immune response).
The antipeptide antibodies are used to recognise sequences within a protein. Therefore side chain structures will be the distinguishing properties. The N- and C-terminal amino and carboxyl groups were made neutrally charged to mimic the protein backbone. During peptide synthesis, a resin was used which generates a peptide amide and an acetylation procedure was performed to cap the N-terminus with an acetyl moiety.

Antisera were generated against all four peptides: Rabbit 11 (ARA-PEP1), Rabbit 12 (SQ-PEP1), Rabbit 13 (ARA-PEP2) and Rabbit 14 (SQ-PEP2). The titre and specificity of the antisera were tested against the denatured proteins (figure 3.13).
The Western blots shown in figure 3.13, were incubated with a 1 : 1000 dilution (v/v) of anti-peptide antisera in PBS buffer/1 % hemoglobin/0.02% Na-Azide and after secondary incubation with ^{125}I-donkey anti-rabbit Ig (Amersham Pharmacia biotech; IM 134) exposed to film for 2 days.
As the most important result, it was found that one of the polyclonal immunosera, raised against Ara PEP2 (figure 3.13 (C), specifically recognised the denatured *Arabidopsis* GPAT enzyme in *E. coli* extracts in which the protein was overproduced.

However, as illustrated in figure 3.11 (C), a persistent high non-specific background occurred in the analysis of crude plant leaf extracts and it was not possible to distinguish if denatured soluble *Arabidopsis* GPAT could be detected in these extract preparations. Therefore, affinity purification was performed to try purifying the Rabbit 13; ARA-PEP2 antiserum. In figure 3.14, the outline of the affinity purification procedure and analysis, involving the generation of an affinity column on basis of SulfoLink Coupling Gel (Pierce: 20401), the affinity purification procedure of anti-ARA-PEP2 polyclonal antiserum and the evaluation via Western blotting of the extent of the purification and influence on the titre, is illustrated.

Figure 3.13 Cross-reactivity of anti-GPAT (1-AT)-peptide polyclonal rabbit antisera

(I): Coomassie Brilliant Blue staining of a 10% SDS-polyacrylamide gel; **lane1**, soluble extract of *E.coli* BL21 (DE3), overproducing squash GPAT (NA4) (± 500 ng); **lane 2**, soluble extract of *E.coli* BL21 (DE3), overproducing *Arabidopsis* GPAT (AR1) (± 500 ng); **lane 3**, partially purified squash GPAT (NA4) (± 580 ng); **lane 4**, partially purified *Arabidopsis* GPAT (AR1) (± 120 ng)

(II): Immunoblotting of *E.coli* soluble extract as in **(I); lanes 1 and 2**, using anti -GPAT peptide antisera from different bleeds of rabbits 11 to 14.

The figure shows the western blot results for evaluation of the bleeds indicated by: **PI** (pre-immune), **B1** (bleed 1), **B3** (bleed 3), **B 2 – 6** (pool of bleeds 2 – 6 in equal volume ratio) and **TB** (terminal bleed).

The antisera used are indicated as **(A)**; α ARA-PEP1 (rabbit 11: anti *Arabidopsis* GPAT peptide 1, **(B)**; α SQ-PEP1 (rabbit 12: anti squash GPAT peptide 1), **(C)** α ARA-PEP2 (rabbit 13: anti *Arabidopsis* GPAT peptide 2 and **(D)**; α SQ-PEP2 (rabbit 14: anti squash GPAT peptide 2)

(III): Immunoblotting of partially purified, overproduced squash GPAT (NA4) and *Arabidopsis* GPAT (AR1) as in **(I); lanes 3 and 4**.

Molecular weight markers (outlined) are indicated on the left (in kDa).

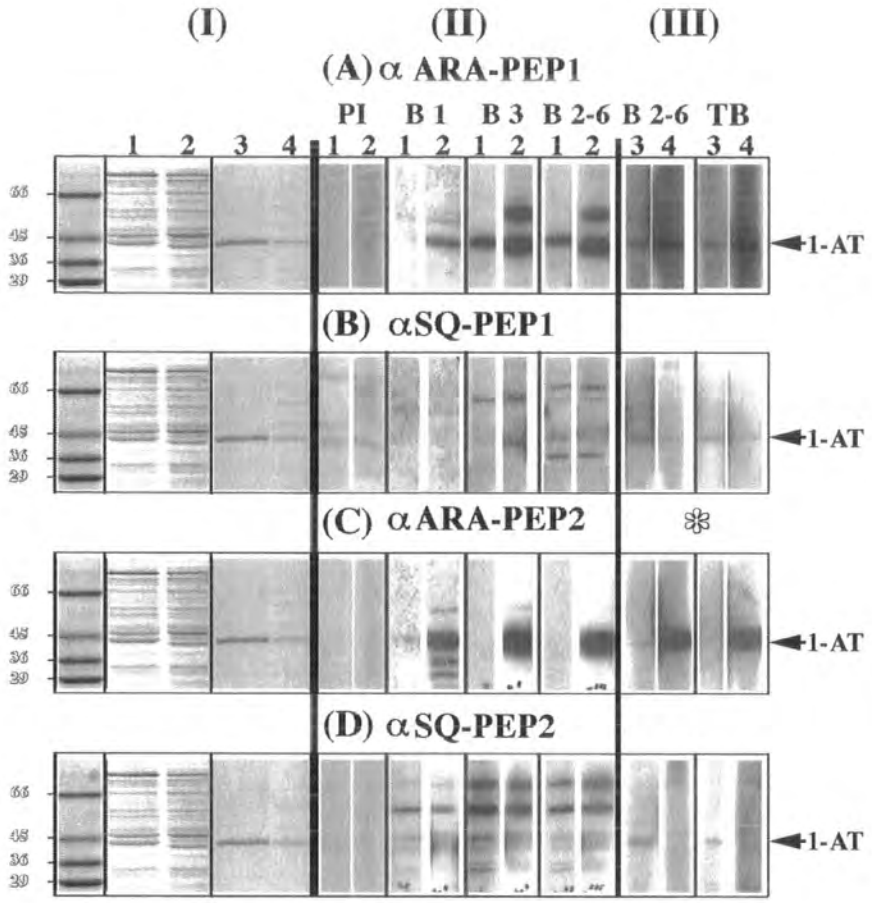
(I)
(II)
(III)
(A) α ARA-PEP1
PI
B 1
B 3
B 2-6
B 2-6
TB
1 2 3 4 1 2 1 2 1 2 1 2 3 4 3 4
66
45
36
29
1-AT
(B) αSQ-PEP1
66
45
36
29
1-AT
(C) αARA-PEP2
66
45
36
29
1-AT
(D) αSQ-PEP2
66
45
36
29
1-AT

Figure 3.14 Affinity purification of Rabbit 13; anti-ARA-PEP2 polyclonal antiserum attempting to improve specificity for GPAT in crude plant leaf extract

(A): Coupling of peptide antigen to SulfoLink Coupling Gel.

The principle of the coupling to SulfoLink Coupling Gel (Pierce: 20401) and the amino acid sequence of the peptide derived from *Arabidopsis* GPAT (ARA-PEP2) is illustrated on the left of the column cartoon. The procedural steps are summarised on the right. Ellman's Reagent was used to quantitate the number of available sulfhydryl groups before- and after immobilisation of the peptide to the column support.

(B): Affinity purification of α-ARA-PEP2 rabbit polyclonal antiserum.

25 ml. of Rabbit 13 antiserum from a terminal bleed (TB) was subjected to the procedures described. Extensive column washing and vigorous elution resulted in affinity purified antiserum proteins coming of the column in the early fractions. The elution profile of total eluted antiserum protein is shown. The fractions 3 – 8 were pooled and dialysed against Tris-Buffered Saline (TBS) and stored with 0.04% NaAzide at 4 °C.

(C): Cross-reactivity of affinity purified Rabbit 13; α-ARA-PEP2 polyclonal antiserum.

(I): Coomassie Brilliant Blue staining of a 10% SDS-polyacrylamide gel; **lane 1**, purified squash 1-AT (NA4) (580 ng); **lane 2**, purified *Arabidopsis* GPAT (AR1), (120 ng); **lane 3**, crude extract from squash leaf (25 μg. total protein); **lane 4**, crude extract from *Arabidopsis* leaf (25 μg. total protein). **(II)**: Immunoblotting of the samples in **(I)**; using a 1:500 dilution (v/v) of **PI** (pre-immune), a 1 : 1000/1:500 and 1: 100 dilution (v/v) of affinity purified Rabbit 13; α-ARA-PEP2 polyclonal antiserum (**COLUMN ELUENT**) and a 1:500 dilution (v/v) of the non-purified antiserum which didn't bind to the column (**PASS**). Antisera were diluted in PBS buffer/1 % hemoglobin/0.02% Na-Azide and Western blots were exposed to film for 2 days after secondary incubation with ^{125}I-donkey anti-rabbit Ig (Amersham Pharmacia biotech; IM 134). Molecular weight markers are indicated on the left .

(A) **Immobilization/Coupling of Peptide (ARA-PEP2) to SulfoLink Coupling Gel**

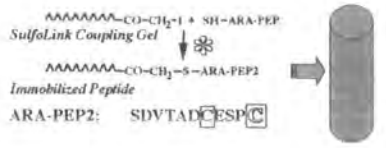

COUPLING TO GEL
- COLUMN + 2.5 ml. SULFOLINK COUPLING GEL
- EQUILIBRATE X 6 VOL. (15 mL) 50 mM TRIS/5 mM EDTA-Na/ pH 8.5
- MIX FOR 15' AT RT WITH 2 mg. ARA-PEP2 IN SAME BUFFER
- WASH X 3 VOL. (7.5 mL) WITH SAME BUFFER
- DETERMINE PEPTIDE CONTENT BEFORE - AND AFTER COUPLING USING ELLMAN'S REAGENT

BLOCKING NONSPECIFIC BINDING SITES ON GEL
- APPLY 3 ML. (1 ML/ML GEL) 50 mM CYSTEINE IN 50 mM TRIS/5 mM EDTA-Na/pH8.5
- MIX FOR 15' + INCUBATE FOR 30' AT RT
- WASH X 16 VOL. (40 mL) 1 M NACL/16 VOL. 0.05% NaN3/ 4 VOL. (10 mL) 50 mM TRIS/5 mM EDTA-Na (pH 8.5)/0.05% NaN3

(B) **Affinity Purification of Rabbit 13; anti-ARA-PEP2 (α-ARA-PEP2) Antiserum**

COLUMN: 2.5 ml SULFOLINK COUPLING GEL + 2 mg ARA-PEP2
SAMPLE: 25 ml α-ARA-PEP2 (RABBIT 13: POLYCLONAL ANTISERUM/TERMINAL BLEED (TB)

COLUMN EQUILIBRATION: 10 VOL (25 ml) WITH 50 mM TRIS pH 7.5 at FLOW RATE: 2 ml/min
SAMPLE LOADING: 25 ML AT FLOW RATE: 0.3 ML/MIN// REPEATED 2 X
PASS: VOLUME = 26 ML
COLUMN WASHING: 60 VOL (150 ml) WITH 50 mM TRIS pH 7.5 AT FOLLOWING FLOW RATES:
- 5 FRACTIONS (10 ml EACH) at 1 ml/min
- REST IN BULK (100 ml) at 2 ml/min

COLUMN ELUTION: 4 M MgCl2/20 mM TRIS pH 6.8 at FLOW RATE: 0.3 ml/min
FRACTION SIZE: 1 ml

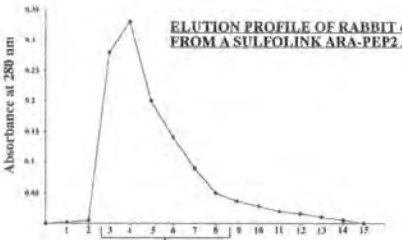

ELUTION PROFILE OF RABBIT αARA-PEP2 ANTISERUM FROM A SULFOLINK ARA-PEP2 AFFINITY COLUMN

POOL Fraction number (1 ml./fraction)
6 ml (3 - 8) → O/N DIALYSIS AGAINST 3 CHANGES OF TBS
→ AFFINITY COLUMN ELUENT
11.3 ml with [PROTEIN] = 0.385 mg/ml
= AFFINITY PURIFIED α-ARA-PEP2 ANTISERUM

(C)

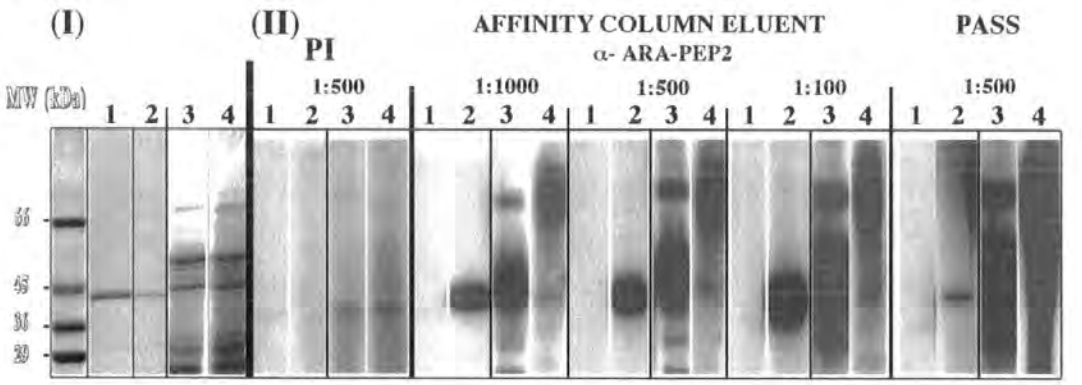

3.3.5 Crystallisation and X-ray analysis of purified squash GPAT (NA4)

Using X-ray crystallography to elucidate the complete 3-dimensional (3-D) structure of proteins, can provide an unparalleled understanding of molecular catalysis and the basis of substrate preference.
Recently, the structure determination of at least two enzymes of plant lipid biosynthesis; enoyl-ACP reductase (Rafferty, J.B. et al., 1994a; Rafferty, J.B. et al., 1995) and Δ^9 18:0-ACP desaturase (Lindqvist, Y. et al., 1996) proved the power of this type of studies. The crystals, X-ray diffraction patterns down to 1.9 Å resolution and further studies on enoyl-ACP reductase have implication for designing inhibitors of the enzyme aimed at the treatment of tuberculosis (Baldock, C. et al., 1996a/b). The high-resolution crystal structure of the soluble castor bean Δ^9 desaturase allowed a detailed structure-function analysis and the rational design of novel positional and chain-length specificities. It has been possible to convert a Δ^6-16:0 ACP desaturase into a Δ^9 18:0-ACP desaturase activity on the basis of only five amino acid changes (Cahoon, E.B. et al., 1997) and the conversion of a Δ^9 18:0-ACP desaturase into a Δ^9 -16:0 activity (Cahoon, E.B. et al., 1998).

In general however, one of the major obstacles is the ability to produce suitable crystals (Ollis, D. and White, S., 1990). The ability to produce large amounts of purified recombinant GPAT protein, in conjunction with a method developed to create an isomorphous heavy metal (selenium) derivative, enabled several crystallisation trials to be set up at the University of Sheffield (Professor D. Rice, Dr. J. Rafferty and Dr. Andy Turnbull). As a result, the squash GPAT mature recombinant protein (NA4) was crystallised and the crystal structure resolved to 2.3 Å resolution.

A reference protocol for the overproduction of the squash (NA4) enzyme, with a heavy metal (selenium) incorporated, was developed and described below. This is an invaluable tool in X-ray Crystallography structure determination in obtaining sufficient phase information for a readily interpretable map.
The standard overproduction procedure was modified to force an *E. coli* methionine-auxotrophic strain (BL21 (DE3) metC::Tn10 (tet^R) , developed by Dr. A.R. Stuitje (Genetics Department of the Free University of Amsterdam), to use selenium-methionine in the overproduction of NA4. The following protocol was designed to mimmick fermenter conditions as much as possible (based on Zeneca Ohr-and Harvest Fermenter protocol).

The *E. coli* methionine-auxotrophic strain (BL21 (DE3) metC::Tn10 (tet^R) was transformed with the pET based overexpression vector pNA4 according to a standard method ($CaCl_2$) and after verification of the transformed colonies (plasmid isolation and restriction analysis) stored as 200 µl 'seed' glycerol stocks in appropriate selective (150 mg/ml AMP/ 12.5 mg/ml TET) LB media at - 80°C or on selective LBagar plates at 4 °C.

FSM (Fermenter Selenomethionine Medium), recipe and preparation:
The protocol is for 1 litre culture induction in batch. A baffled 2 litre conical flask (Erlenmeyer) was cleaned and the following was added

FM (Fermenter Medium = FSM – Amino Acids/Selenomethionine/thiamine/antibiotic):
1 gr $(NH_4)_2SO_4$, 4.5 gr KH_2PO_4, 10.5 gr K_2HPO_4, 0.5 gr Sodium Citrate.$2H_2O$,
5 gr (= 4 ml) Glycerol, 1 ml. 1 M $MgSO_4.7H_2O$, 0.5 gr each guanosine, adenine, thymine and uracil (Sigma), made up to 917.8 ml with water (milliQ) and autoclaved.

After autoclaving and cooling down to 37 °C, the following components (filter sterilised) were added to the FM before use in the induction procedure:
76 ml **AA mix** (Amino Acid **mix** made up of 4 ml of each of the 19 **amino acids stock preparations** below), 4 ml of SELENO-L-METHIONINE stock (10 mg/ml) (SIGMA: cat. no.: S-3132), 200 µl (±200 mg.) thiamine stock (10 mg/ml) and antibiotics (4 ml ampicillin (AMP) stock at 50 mg/ml).

Amino Acid stock preparations: all AA stocks were made at 10 mg/ml
(**F**=filter 0.22 mm/**A**=autoclaving possible./*=could dilute in 0.1M HCl)

L-Valine (A/F), L-Lysine (A/F), L-Leucine (A/F), L-Histidine-HCl (A/F), L-Argenine-HCl (A/F), L-Threonine (A/F), Proline (A/F), L-Isoleucine (A/F), Alanine (A/F), L-Phenylalanine (A/F), Serine (A/F), Glycine (A/F), L-Glutamine (A/F), Tyrosine (F//in 0.1N NaOH), Tryptophan (F/*), Cysteine (F/*), Glutamate (A/F), Asparagine (F/*), Aspartate (F/*/heat).

SELENOMETHIONINE INCORPORATION:

protocol and growth induction regime used for protein overproduction with seleno-L-methionine for *E. coli* strain (BL21 (DE3) metC::Tn10 (tet^R) transformed with pNA4:

Starter culture: 50 ml. 2 X YT //BL21 (DE3) metC::Tn10//pNA4 (200 mg/l AMP) grown overnight at 30 °C

(could pellet the cells and wash away the rich 2x YT media but in this case this is not recommended. The cells grow very slow in FSM (Minimal Medium and also the selenomethionine is TOXIC)

After addition of all the supplements to the FM medium, growth was started by inoculation with 9 ml of starter culture to 1 litre FSM (<1:100) with vigorous shaking (200 rpm).

The following growth and induction regime was observed in a typical experiment:

TIME	**OD600**	
Start: 11.30 AM		
1 15.30 PM	0.062	
2 21.30 PM	0.4	**T=0/INDUCE:** ADD: -6 ml 0.1M IPTG extra -0.5 ml. AMP50
LEAVE OVERNIGHT **INDUCTION 37 °C**		
3 12.50 PM	1	HARVEST

Cells were harvested by centrifugation at 4000 x g for 20 min and washed to remove the growth medium components. Cell pellets were washed in 50 mM Tris-HCl pH 8.0/ 150 mM NaCl at 0 °C. The culture medium components have to be discarded safely as they contain toxic heavy metals. After centrifugation at 3000 x g, cells were frozen in liquid nitrogen before confirmation of the success of the incorporation of the heavy metal atoms. To evaluate if the incorporation of selenium, to create an isomorphon of NA4, was successful, a sample of total soluble protein of cells generated in the above procedure, together with a control sample (NA4 not grown with selenium), was subjected to electrophoresis and the recombinant protein band submitted for N-terminal protein sequencing (figures 3.15 and 3.16). It was thought that during the protein sequencing procedure, a selenium derivative of methionine would not be recorded. The samples were shipped to the University of Sheffield where they were purified and immediately subjected to crystallisation trials.

Figure 3.15 Protein sequencing confirms the incorporation of Seleno-L-Methionine in overproduced recombinant squash GPAT (NA4)

The amino terminus of a control sample and a heavy metal derivative of NA4, was sequenced via HPLC analysis of PTH coupled amino acids on a protein sequencer (Applied Biosystems Model 477A). A selenium derivative of methionine is not recorded by the protein sequencer.

(A) On the left is a calibration chromatogram of the protein sequencer and on the right a tabulation of the peak ID (identity) and retention time (in minutes) of all amino acids. Methionine (M, MET) is outlined. DPT (N,N'-diphenylthiourea) is a chemical side product of the sequencing procedure.

(B) Tabulation of the sequencing results of overproduced squash GPAT (NA4) grown under standard conditions (top) and under non-standard conditions in the presence of seleno-L-methionine (bottom).
Values which are boxed for clarification, provide a quantitative indication of the level of detection of amino acids. The arrows indicate the values for methionine.

A

CALIBRATION PROTEIN SEQUENCER

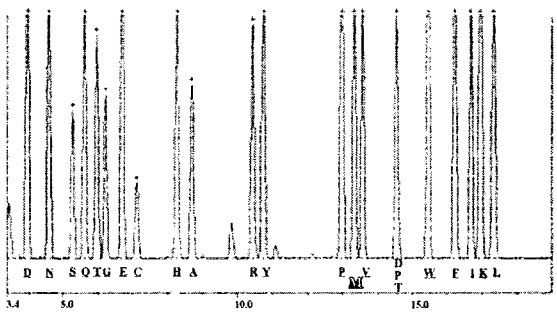

Retention time (minutes)

PEAK TABULATION

Peak ID		Retention Time (min.)	Height (uAU)
		3.42	6818
D	ASP	3.97	40932
N	ASN	4.58	38834
S	SER	5.32	15892
Q	GLN	5.65	33267
T	THR	5.98	24192
G	GLY	6.23	17748
E	GLU	6.78	43746
C	CYS	7.12	8265
H	HIS	8.20	28299
A	ALA	8.70	18825
		9.85	3948
R	ARG	10.47	25201
Y	TYR	10.77	32493
P	PRO	12.93	41499
M	MET	13.33	30246
V	VAL	13.67	31131
**	OPT	14.55	26220
W	TRP	15.45	45317
F	PHE	16.20	33741
I	ILE	16.68	28239
K	LYS	16.95	43519
L	LEU	17.32	31210

B

APPLIED BIOSYSTEMS 477A PROTEIN SEQUENCE REPORTS

Squash 1-AT (pNA4) overproduced in BL21 (DE3) in Standard Growth Medium

AAcid #	AAcid ID	R.Time (min)	C.Time (min)	Pmol (raw)	Pmol (-bkgd)	Pmol (+lag)	Pmol Ratio	AAcid ID	
1	A	8.75	8.77	44.84	44.77	46.46	95.00	ALA	
2	S	5.33	5.40	28.02	25.17	25.51	77.81	SER	
3	M	13.40	13.33	31.00	28.19	28.22	31.78	MET	<- +
4	T	6.05	6.07	20.39	18.86	19.58	55.59	THR	
5	G	6.32	6.32	47.85	38.05	39.53	22.51	GLY	
6	G	6.27	6.32	44.73	33.58	33.35	18.99	GLY	
7	Q	5.72	5.73	38.35	32.74	34.45	212.32	GLN	
8	Q	5.75	5.73	45.94	39.47	39.74	244.88	GLN	
9	M	13.40	13.33	38.20	26.71	28.59	32.22	MET	<- +

Squash 1-AT (pNA4) overproduced in BL21 (DE3) metC::Tn10 in Minimal Media supplemented with AA - Met (M) + Seleno-L-Methionine

AAcid #	AAcid ID	R.Time (min)	C.Time (min)	Pmol (raw)	Pmol (-bkgd)	Pmol (+lag)	Pmol Ratio	AAcid ID	
1	A	8.75	8.70	77.68	67.35	67.62	81.24	ALA	
2	S	5.35	5.32	37.81	27.29	27.21	26.94	SER	
3	M	13.37	13.33	4.78	3.47	3.49	14.03	MET	<- -
4	T	6.02	5.98	35.20	31.25	35.18	66.53	THR	
5	G	6.27	6.23	78.90	56.29	67.69	13.00	GLY	
6	X G	6.03	5.98	11.37	6.64	6.70	12.68	THR X GLY	
7	Q	5.68	5.65	42.55	33.36	40.03	47.15	GLN	
8	Q	5.70	5.65	48.68	38.40	38.22	45.02	GLN	
9	M	13.32	13.33	3.65	3.05	3.61	14.52	MET	<- -

Applied Biosystems 477A Protein Sequencer Chromatogram Report

Protein Sequencing of Amino Terminus of Overproduced Squash 1-AT (pNA4) in Absence (NO SELMET) or In presence (+ SELMET) of Seleno-L-Methionine

Amino Terminus of Overproduced Recombinant Squash 1-AT (pNA4):
M*-A-S-M-T-G-G-Q-Q-M-G-R-S-AHSRK--//

AMINO ACID 1 2 3 4 5 6 7 8 9

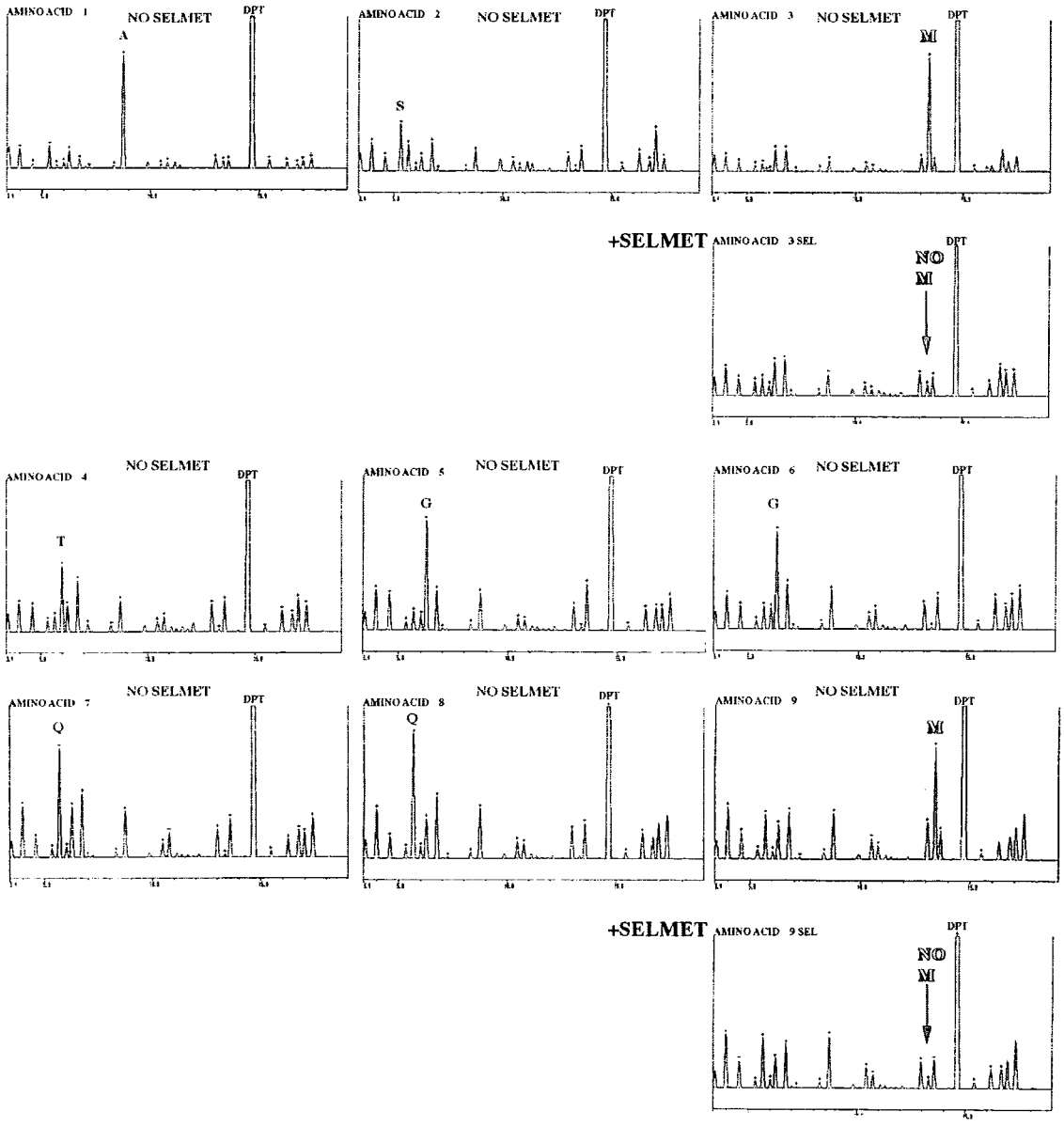

The crystallography and analysis was carried out by researchers in the team of Professor David Rice and Dr. John Rafferty, and especially involved were Dr. Andy Turnbull and Dr. Svetlana Sedelnikova at the University of Sheffield. For routine purification of GPAT for crystallisation trials they used another method involving DEAE-Sepharose Fast Flow chromatography, an ammonium sulphate precipitation (1.7 M), a Phenyl-Toyopearl 650S column equillibrated and eluted with ammonium sulphate solutions and a Superdex-200 gel filtration chromatography. Details of the crystallisation procedures will be reported elsewhere.

The squash GPAT isomorphous crystals have a needle-like morphology as is shown in figure 3.17 (A).

Crystals proved stable during X-ray analyses and a representative X-ray diffraction image with a maximum resolution of 2.3 Å is shown in figure 3.17 (B).

The phase angle and subsequently the X-ray structure of squash GPAT was solved using multiple isomorphous replacement techniques (such as with isomorphons containing mercury or selenium) and figure 3.17 (C) and (D) shows stereoview models of the squash GPAT.

It should be noted that overproduced recombinant GPAT protein samples, from a number of plant species (including *Arabidopsis* and spinach), were used in crystallisation trials and that only the NA4 protein crystallised.

In a separate study, a chemical modification of the cysteine (Cys) residues of overproduced NA4 with iodoacetamide was investigated. It appeared that potential modification of one of the Cys residues on position 191 (C191), was influencing the substrate preference of the enzyme and thus seemed accessible to the iodoacetamide. Catalytic regions of many types of enzymes include one or more Cys residues and it was thought that this cysteine C191 could potentially play a role in the catalytic mechanism. This formed the basis of performing site directed *in vitro* mutagenesis of NA4 (figure 3.18). It subsequently proved essential to mutagenise all the Cys residues individually, to start a systematic solving of the protein structure.

Figure 3.17 The crystalstructure of soluble glycerol-3-phosphate acyltransferase

(A) Squash GPAT (NA4) crystals.

The squash GPAT crystallises to needle-like crystals in the space group $P2_12_12$ or $P2_12_12_1$, with approximate dimensions 0.15 x 0.1 x 0.7 mm^3 and belong to the orthorhombic system point group 222 with unit cell dimensions of a = 61.4 Å, b = 66.9 Å, c = 104.1 Å and $\alpha = \beta = \gamma = 90°$.

(B) X-ray diffraction image of squash GPAT (NA4).

A representative X-ray diffraction image was taken at The University of Sheffield, recorded on a MAR Research imaging plate detection system. The diffraction limit (maximum resolution) at the edge of the plate is 2.3 Å.

(C) A stereo representation of squash GPAT.

14 α helices and 9 β strands are shown as coiled ribbons and flattened arrows, respectively.

(D) A space filled model of squash GPAT

The GPAT monomeric protein and a modelling of the substrates (G3P and 16:0-acyl chain) are shown with all atoms having full Van der Waals surfaces. The residues of the squash GPAT are depicted in light blue and the substrates in purple (16:0-acyl chain) and red (G3P). Produced using the program MIDAS in the Sheffield laboratory (The Krebs Institute)

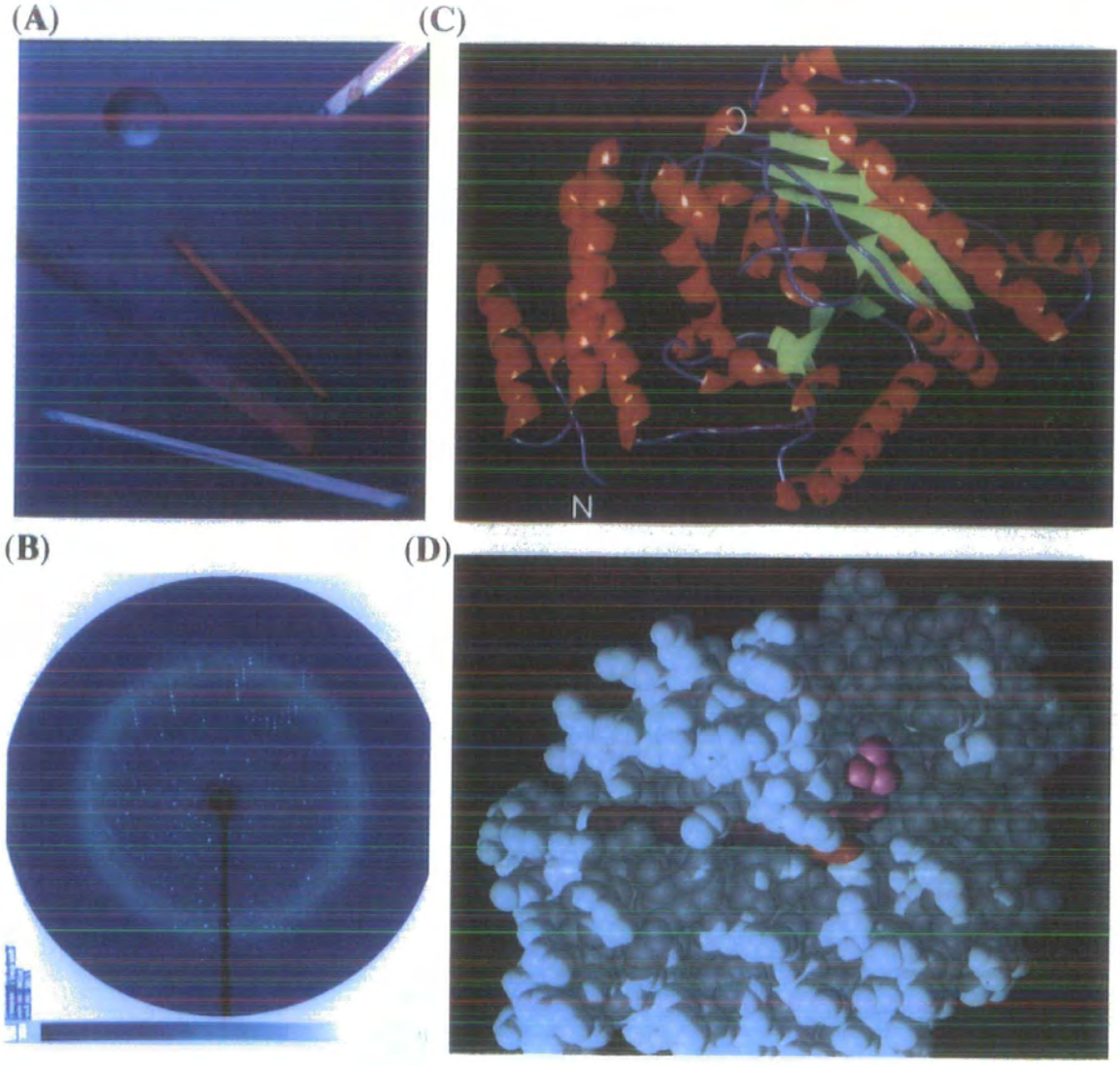
(A)
(C)
C
N
(B)
(D)

Figure 3.18 Site directed mutagenesis of Cysteine 191 to Serine 191 in a squash recombinant GPAT

(A) Flow diagram of the procedure for the site directed mutagenesis of squash GPAT. The pAlter-Ex2 System (Promega) was chosen for this type of experiments in first instance. After this period, in all recent experiments of this kind, it was proven to be more practical to use the QuickChange Site Directed Mutagenesis system of Stratagene (William Simon, personal communication). In this experiment, pNA4 was recloned in the pAlter-Ex2 vector replacing the original first methionine N-terminal amino acid by the three residues MHL. The C 191 was mutagenised to S 191 according to instructions with the system. The mutant cDNA insert was verified by DNA sequencing and sub-cloned to the pET 17b overexpression vector (Novagen). Overproduction and substrate selectivity analyses were performed as described.

(B) The principles of the site directed mutagenesis procedure with the pAlter-Ex2 System (Promega).

(C) A 10% SDS-PAGE gel stained with Coomassie Brilliant Blue showing the result of an overproduction of the mutant squash GPAT enzyme in *E. coli* BL21 (DE3). Lanes 1 and 2, samples of crude *E.coli* total protein, before and after induction with IPTG, respectively. MW markers are shown on the left.

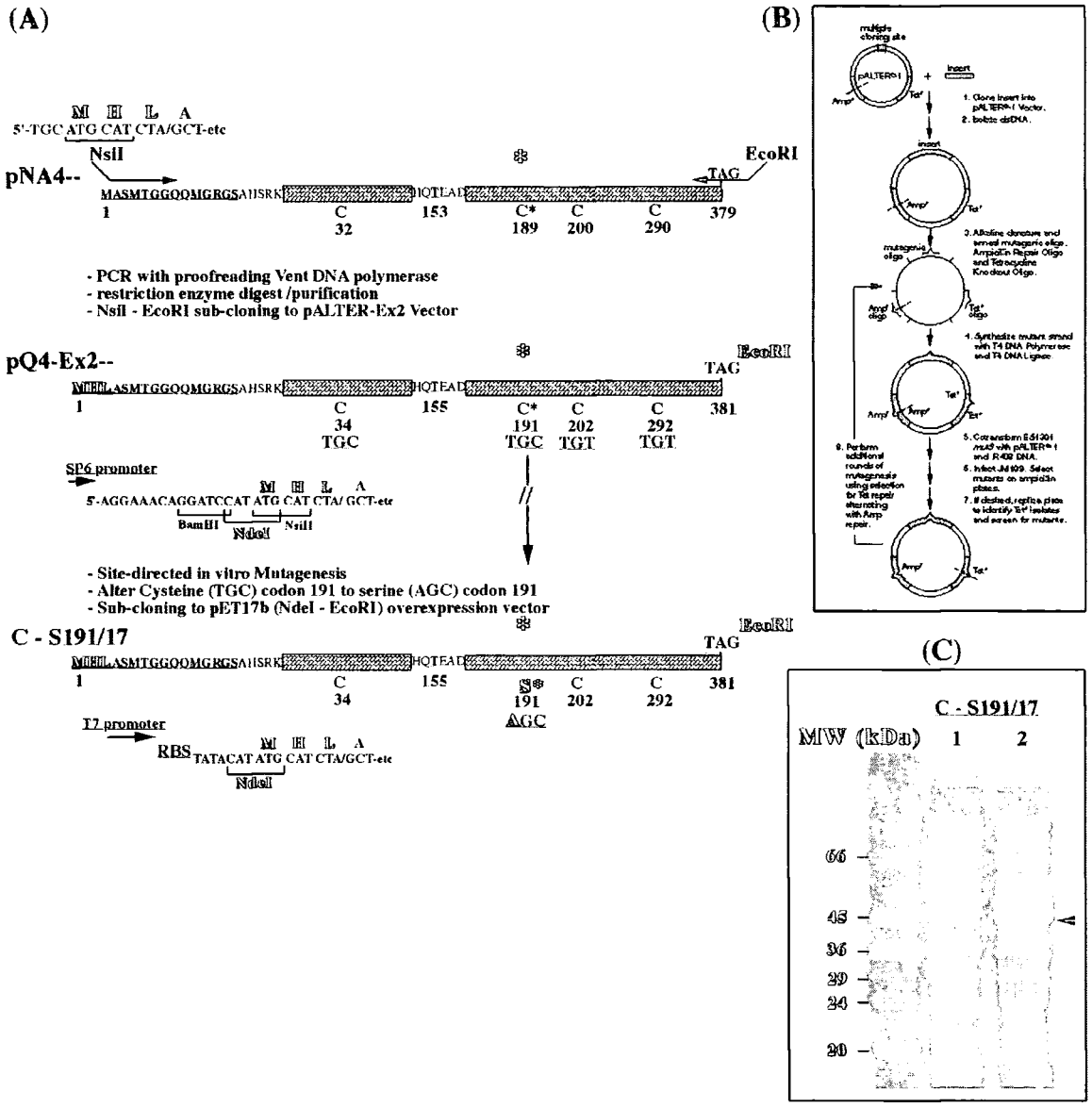
(A)
(B)
(C)
M H L A
5'-TGC ATG CAT CTA/GCT-etc
NsiI
pNA4--
EcoRI
TAG
MASMTGGQQMGRGSAHSRK
HQTEAD
1
C 32
153
C* 189
C 200
C 290
379
- PCR with proofreading Vent DNA polymerase
- restriction enzyme digest /purification
- NsiI - EcoRI sub-cloning to pALTER-Ex2 Vector
pQ4-Ex2--
MHHLASMTGGQQMGRGSAHSRK
1
C 34 TGC
155
C* 191 TGC
C 202 TGT
C 292 TGT
381
SP6 promoter
5'-AGGAAACAGGATCCAT ATG CAT CTA/ GCT-etc
BamHI
NdeI
NsiI
- Site-directed in vitro Mutagenesis
- Alter Cysteine (TGC) codon 191 to serine (AGC) codon 191
- Sub-cloning to pET17b (NdeI - EcoRI) overexpression vector
C - S191/17
T7 promoter
RBS
TATACAT ATG CAT CTA/GCT-etc
S* 191 AGC
C - S191/17
MW (kDa)
1
2
66
45
36
29
24
20
A

3.4 Conclusion

The crystal structure of a mature protein region of squash (*Cucurbita moschata*) glycerol-3-phosphate acyltransferase (GPAT), the first known structure of this type of acyltransferases, was elucidated at near atomic resolution in collaboration with the University of Sheffield.

For further refinement of a prediction of primary function, the importance of knowing the structure is most obvious. If the 3D- protein structure is known, the finer details of function may be defined. The interpretation of structure-function relationships becomes possible at a molecular level, such as the significance of the active-site structure for catalysis or molecular details of protein-substrate interactions. Structural studies of GPATs, able to use varying substrates, are expected to reveal these structure-function relationships. These GPATs could be natural enzyme variants from other plant sources (Chapter IV) or recombinant GPATs with subtle variations in secondary and tertiary structure (domainswaps in Chapter V or single/multiple amino acid changes via site directed mutagenesis, currently in progress).

This may enable the use of this fundamental knowledge of the workings of the enzyme and its sub-cellular localisation, to redesign functional properties, such as substrate selectivity, and to rationally design the end products of the relevant lipid synthesis pathways in desired crop plants.

Determinants of the selectivity of a soluble GPAT could be a combination of the affinity for the G3P and acyl chain substrates. It is hard to say precisely what the major determinant for selectivity is without meaningful kinetic data for all physiological substrates of the enzymes or even for the better, with a molecular crystal structure, allowing the elucidation of the catalytic mechanism. On basis of single substrate assays at pH 7.4, with acyl-CoA substrates in excess (all factors which are non-physiological), Ferri and Toguri (Ferri, S.R. and Toguri. T., 1997) can only explain their results on basis of affinity of the GPAT enzymes for G3P. From their findings they conclude that the relative affinities of the investigated recombinant GPAT enzymes for the acyl chains is not a major direct influence on substrate preference. On the basis of the apparent kinetic data for G3P under their non-physiological conditions, they speculate that the influence of the type of acyl chain (16:0 or 18:1) on the enzyme's affinity for G3P suggests a reaction mechanism in which the acyl chain binds to the enzyme first. Such an acylated enzyme would then interact with G3P, however, such an enzyme intermediate could not be detected. They suggested that enzyme could be non-covalently interacting with the fatty acid. Until relevant kinetic and selectivity data for all physiological substrates of the GPAT enzymes are determined, one can only make assumptions in this sort of direction. In Chapter V first determinations of this sort of data are reported.

The overall primary structure (amino acid sequences) of GPAT enzymes has a high degree of similarity and polyclonal rabbit-antisera against mature squash GPAT and mature *Arabidopsis* GPAT enzymes, cross-recognised both denatured GPAT proteins. The antisera were specific for GPAT in soluble extracts of *E. coli* proteins, but unfortunately recognised denatured proteins in *Arabidopsis* or squash leaf extracts a-specifically and, in preliminary experiments, it was not clear if they were detecting GPAT in such plant protein extracts.

Antisera against four specific peptides were generated and it was found Rabbit 13 anti-ARA- PEP2, was specific for the denatured purified- and *Arabidopsis* GPAT enzyme in *E. coli* extracts. However, even after an affinity purification procedure and analysis of Rabbit 13; ARA-PEP2 antiserum, a high level of non-specific background remained. Besides this high background in Western blotting procedures of denatured plant proteins, the native soluble GPAT protein may be hard to detect with an antiserum of moderate titre, because in plants, the enzyme amount seems to be low, making up only 0.04% of stromal protein of chloroplasts (Douady, D. et al., 1990). In tobacco the level of GPAT protein was estimated as only < 0.01% of the total soluble protein from leaves (Murata, N. et al., 1992).

There may be necessity for further purification and concentration of this antiserum or even consider implementing a new immunisation strategy in which immunised animals are kept on a particular diet to try to prevent a-specific immunisation against plant feed components. This might be hard to achieve, as raising anti-peptide antibodies requires an added factor of luck in immunisation.

The first site-directed mutagenesis experiment, namely, the conversion of a cysteine (Cys) residue (C 191) to a serine residue (S 191), was not based on knowledge of the structure (the structure was not solved at the time) but on a chemical modification of squash GPAT (NA4) with iodoacetamide. There were indications that the modification was influencing the substrate recognition properties of GPAT and that therefore the particular cysteine residue could be involved in the catalytic mechanism. However, substitution of that particular cysteine residue did not have a major influence on the function of the enzyme. The enzyme was still catalytically active and its substrate specificity as determined via the standard selectivity assay (SSA) did not seem significantly altered. It seemed obvious that the cysteine (C191) residue in the native structure was accessible to iodoacetamide and in later consideration of the crystalstructure this was confirmed as the particular residue was exposed on the outside of the protein structure. Possibly, binding of the enzyme to such a large molecule as iodoacetamide in these experiments, influenced the accessibility of substrates for the enzyme in some way.

Currently, other researchers in the laboratory are systematically targeting specific amino acid positions via site-directed mutagenesis, on basis of the elucidated squash GPAT crystal structure, derived model predictions for important amino acid residues and on basis of residues discussed in Chapter V.

The molecular activity and mechanism of action do not only define the entire function of a protein. Its function is also determined by the expression characteristics and the biological role and significance within the organism. Knowledge of the regulation of expression of the gene encoding the protein, or information on its biological significance, can not be deducted from its structural features. These aspects of the function of a protein is an important limitation in, for instance, the area of drug target identification.
The molecular information defining the regulation of a protein-coding gene (regulatory elements of transcription control) is mainly located in noncoding regions. If the entire gene of a protein of interest has not been cloned and its expression properties characterised, current computational prediction tools are (not yet) reliable enough to predict gene regulation (Bucher, P., 1999). In this era of genome projects, with the ultimate goal of determining the function and biological role for all of the genes in the genome, there is still a gap between the wealth of sequence information and functional information (X-ray crystal structures and functions of proteins in the proteome). Nevertheless, with the advent of microarray technology (micro-array based high-throughput mRNA quantification) (Schena, M. et al., 1995; Lockhart, D.J. et al., 1996) and high-throughput proteomics (Persidis, A., 1998), able to cope with genome-wide application, this gap may also be bridged in the future.

Chapter IV

∞∞∞∞∞

Molecular Cloning, Characterisation and Functional Expression of a Novel Glycerol-3-Phosphate Acyltransferase from Oil Palm (*Elaeis guineensis*)

4.1 Introduction

In recent years, cDNAs for soluble (plastid) glycerol-3-phosphate acyltransferase (GPAT) enzymes of 5 chilling-sensitive and 4 chilling-resistant plants have been isolated and the substrate specificity and selectivity of some of these proteins has been studied (see Chapter I and Figure 5.8). As described in Chapter I and III, the chloroplast GPAT of chilling-sensitive plants such as squash (*Cucurbita moschata*), tend to be non-selective for their main acyl-thioester substrates 18:1-ACP and 16:0-ACP (Frentzen, M. et al., 1987), whilst the enzymes from chilling resistant-plants such as pea (*Pisum sativum*), spinach (*Spinacia oleracea*) and *Arabidopsis* (*Arabidopsis thaliana*), use 18:1-ACP in preference to 16:0-ACP (Bertrams, M. and Heinz, E., 1981; Chapter III, this study).

Although the fatty acid selectivity of these soluble GPAT enzymes varies from plant to plant, there is an overall high degree of sequence conservation, as judged by multiple sequence comparisons. Therefore, even after careful examination, it is difficult to identify single amino acid residues, associated with the preference for 18:1-ACP or 16:0-ACP, according to the homology alone.

However, the evolutionary conservation of 'domains' of amino acid sequences within the proteins, could provide valuable indications for a vital role in the catalytic mechanism of GPAT enzymes. For example, Nishida, I. et al. (1993) defined at least seven conserved regions between the soluble GPAT from *Arabidopsis*, pea and squash, but the significance of these domains was not yet examined. In Chapter V (this study) and from work by Ferri, S.R. and Toguri, T. (1997), it became obvious that the central third part of the soluble GPAT protein, which has the highest degree of primary structure conservation, contains major structural determinants for GPAT functions.

Heath, R.J. and Rock, C.O. (1998) identified one domain sequence similarity between a range of different membrane-bound and soluble acyltransferases via multiple sequence alignment using the PILEUP program. This conserved H4XD motif contained an invariant histidine (H) and aspartic acid residue (D). Via site-directed mutagenesis of the *Escherichia coli* (*plsB*) GPAT and the bifunctional 2-acyl-glycerophosphoethanolamine acyltransferase/ acyl-ACP synthetase (*Aas*), they proved a vital role of the conserved histidine residue in acyltransferase catalysis.

Such identification of functionally and structurally similar domains between membrane-bound and soluble acyltransferases may allow for a few interesting speculations.
It is quite obvious that the overall sequence divergence between the two types of enzymes with different sub-cellular localisation, for instance between membrane-bound versus soluble GPAT, extends beyond the degree necessary to for cross-hybridisation on the DNA level. However, there appears to be the possibility that certain domains of both types of proteins, could potentially be common to both. Unfortunately, a plant membrane-bound GPAT has not been isolated to date. If such domains exist, they may be essential for a common type of catalytic reaction mechanism or accommodation of the glycerol-3-phosphate based substrate-structure.
A complementation approach, which has proven to be successful for membrane-bound *sn*-1-acyl-LPA acyltransferases (LPAT) cDNA isolation (Brown, A.P. et al., 1995; Hanke, C. et al., 1995;Bourgis, F. et al., 1999), could be employed towards cloning of these membrane bound GPATs.
It will be extremely interesting to compare the differences and similarities in structure of both the soluble and membrane-bound GPAT enzymes. The soluble plastid GPAT enzymes are more involved in prokaryotic synthesis of chloroplast membrane glycerolipids whilst microsomal (membrane-bound) GPAT enzymes act in the eukaryotic pathway and are therefore not only involved in membrane glycerolipid synthesis but also storage triacylglycerol (TAG) synthesis. The main substrates for both types of GPAT appear to be 18:1- and 16:0- acyl thioesters but from analysis of fatty acid compositions and studies of acyl-thioester (CoA) preference of membrane-bound acyltransferases of several oil seeds (for example: maize (*Zea mays*), rapeseed (*Brassica napus*) and palm seed (*Butia capitata*), come indications that shorter or longer fatty acyl chains can be used (Sun, C. et al., 1988).
An intriguing question is if therefore the membrane-bound GPAT could allow more flexibility in the usage of different types of acyl-chains than the soluble GPAT, and if and how this property is being reflected in the protein structure.
The solving of the crystal structure of the squash soluble GPAT enzyme will allow the modelling of the 3D-structure so predictions can be made which regions of the protein could be involved in, for instance, substrate binding. In combination with site-directed mutagenesis, specific amino acid residues may be identified which are involved with different aspects of the functioning of the enzymes.

At the moment, only one uncertainty about the primary structure of GPAT proteins remains. The soluble GPAT is a nuclear encoded protein, which has to be targeted to the chloroplast by means of a transit peptide and until now, the exact protein processing site of any plant GPAT has not been determined experimentally.

As outlined in Chapter I and in the legend of Figure 3.1, the predicted squash GPAT pre-protein processing site (predicted protein processing site*) is currently thought to be before amino acid residue A43. It has been shown that, even N-terminally truncated, mature enzymes are catalytically active (Chapter III).
However, there have been suggestions that composition, and maybe even the length, of the N-terminal sequence of the mature GPAT enzyme could have an influence on the substrate preference. These suggestions were inspired by the observation that there was a coincidence of a functional differentiation between two types of GPAT isozymes from squash and distinct amino (N-) terminal differences of the protein (Nishida, I. and Murata, N., unpublished study; Murata, N. and Tasaka, Y., 1997).

Here, the molecular isolation, characterisation and functional expression of a novel, natural variant, of a glycerol-3-phosphate acyltransferase (GPAT) from African oil palm (*Elaeis guineensis*) fruit mesocarp is described. Also, genomic clones from oil palm, cross-hybridising with cDNA for the soluble *Arabidopsis* GPAT, were isolated and genetic characterisation via Southern blot analysis shown. However, due to more urgent priorities on examining the cDNA clones, the genomic clones were not further characterised. A Northern blot analysis of total RNA from a variety of tissues from different species, using the *Arabidopsis* plastid GPAT cDNA as a probe, suggested that the steady-state mRNA level of the putative oil palm GPAT is very low in mesocarp, kernel and even leaf.
To confirm the identity of the gene product encoded by the largest open reading frame within the cDNA, and to examine the influence of the amino (N-) terminal region on the absolute activity and selectivity for acyl-ACP thioesters, three different versions of the protein were overproduced in *Escherichia coli* and the enzymatic activity tested.

4.2 Materials and methods

4.2.1 Plant genomic DNA isolation

Plant nuclear DNA was isolated from, preferably young, leaf tissue according to a modified method based on the CTAB (cetyltrimethylammonium bromide) isolation procedure used by Murray, M.G. and Thompson, W.F. (1980). The use of the nonionic detergent CTAB within the extraction step of this protocol is mainly intended for removal of polysaccharides, in combination with the subsequent chloroform extraction. The most critical parameter, besides the CTAB concentration, is the salt (NaCl) concentration. When the NaCl concentration is lower than 0.5 M, CTAB forms an insoluble complex with nucleic acids and can be precipitated. When it is the intention, as it is in this protocol, to keep the nucleic acid-CTAB complex in a soluble state, the NaCl concentration is kept high (>0.7 M). Under such high salt concentrations, CTAB complexes with polysaccharides and proteins and are removed to the interface upon organic solvent (chloroform) extraction.

Leaf tissue was ground to a very fine powder using a pre-cooled mortar and pestle in liquid N_2(l). The method is described for 300-400 mg. of powder, but can be scaled up or down at least ten times. The powder was added to 9 ml of CTAB extraction buffer (100 mM Tris-HCl pH 7.5, 0.7 M NaCl, 10 mM EDTA, 1% (w/v) CTAB, 0.14 M β-mercapto-ethanol) in a 16 ml polypropylene tube. The tube and contents were incubated at 65 °C for 60 – 90 minutes with occasional mixing by inversion. After extraction the tube was cooled to room temperature before addition of 4.5 ml chloroform/iso-amyl alchohol (v/v, 24:1). After gentle inversion for 5 minutes the tubes were centrifuged for 5 minutes at 2000 –2400 rpm to resolve the lower organic and upper aqueous phases. The aqueous phase was transferred to to a new, sterile 16 ml. polypropylene tube and after addition of 50 µl RNAse A (10 mg/ml, pre-boiled for 15 min.) with mixing, incubated at room temperature for 30 min. 6.0 ml of isopropanol was added and the contents gently mixed by inversion. Depending on the amount of polysaccharides and other co-precipitating components present in the original tissue (empirical), the tube was left at room temperature or ice for 10 minutes. The precipitated high-molecular weight genomic DNA was removed from the tube by means of a sterile mini glass hook (for mini preparations the precipitate was collected by centrifugation at 3000 rpm. for 5 min.) and washed in an abundant amount of 70% ethanol/0.2 N NaOAc. The DNA was resuspended in 500 µl of sterile water (milliQ) or TE pH 8.0 and stored at 4°C. The concentration of the DNA was estimated by absorption at OD260 nm and the concentration and integrity confirmed by gel electrophoresis in a 0.8% (w/v) agarose gel.

4.2.2 Genomic Southern analysis

For Southern analysis, usually 10 µg of total nuclear DNA was digested with restriction endonucleases overnight at 37 °C in the appropriate salt mixes, supplied with the enzymes (Boehringer Mannheim). Following electrophoresis in a 0.8% (w/v) (Tris,acetate, EDTA (TAE)) agarose gel containing 0.5 µg ml^{-1} ethidium bromide (4-6 V cm^{-1} for 4 hr. – overnight) the gels were viewed and photographed on a UV transilluminator. Fractionated DNA was denatured and transferred to a Hybond-N membrane according to instructions by the supplier (Amersham; Southern, E.M., 1975). After prehybridisation (minimum 3 hr) a ^{32}P-radiolabeled probe was added and hybridisation was carried out in a Hybaid rotisserie oven for 12 – 24 hr. at 60 °C in 10% (w/v) Dextran sulphate, 1M NaCl, 1% (w/v) SDS and 0.1 mg ml^{-1} denatured herring sperm DNA. After hybridisation, the membranes were washed at 65 °C in decreasing concentrations of SSC (4x, 2x, 1x, 0.1x) with 0.1% (w/v) SDS and then exposed to autoradiography film overnight (or longer if necessary).

4.2.3 RNA isolation of mesocarp (and kernel) tissue from yellow African oil palm fruit.

Total RNA purification

The isolation and purification of nucleic acids from plant tissues in general, and storage tissues especially, is made difficult by the content of carbohydrate polymers and polyphenols. A protocol was developed empirically, specifically for total RNA isolation from mesocarp (and kernel) tissue of yellow oil palm fruit. The method described by Manning, K. (1991), based on differential solvent precipitation in a procedure using 2-butoxyethanol (2-BE) was also successfully used, but the yields were very low for total RNA from these tissues. Mesocarp (or kernel) tissue was ground to a very fine powder using a pre-cooled mortar and pestle in liquid $N_2(l)$. The method is described for 7.5 gr. of frozen powder. This powder was added to 20 ml of HB (Homogenisation Buffer) (0.2 MTris-HCl pH 9, 0.4 M NaCl, 25 mM EDTA, 1% (w/v) SDS) in a 50 ml polypropylene tube. The tube and contents were mixed by inversion at room temperature until all the powder was well defrosted and suspended. An equal volume of phenol/ chloroform/iso-amyl alchohol (v/v, 24:24:1) was added and the contents were frequently mixed while the tube was left on ice for at least 30 minutes. The tubes were then centrifuged for 25 minutes at 2500 rpm to separate the lower organic and upper aqueous phases and to pellet the crude tissue. The aqueous phase was transferred to a new, sterile 50 ml. polypropylene tube and the phenol/ chloroform/iso-amyl alchohol (v/v, 24:24:1) extraction was repeated. Aqueous phases were now clear but coloured (green/yellowish for mesocarp and light yellowish for kernel). In the next manipulations, a two stage (differential) isopropanol precipitation was employed. The aqueous phase was diluted with 0.6 volume of sterile water (milliQ) and isopropanol was added to a final concentration of 20% (v/v). After

mixing carefully and incubation on ice for at least 30 minutes, the tube was centrifuged for 15 minutes at 2500 rpm (RT) to pellet a majority of the contaminating carbohydrate polymers (a clear jelly like pellet). The supernatant was transferred to a new sterile 50 ml Corex tube and isopropanol was added to 50% (v/v). After mixing the contents, the tube was centrifuged for 25 minutes at 3000 rpm. The nucleic acid pellet was gently resuspended in 5 ml. sterile water (milliQ) and the RNA was precipitated by addition of a half volume of 6 M LiCl (final 3 M LiCl). Following overnight precipitation on ice, the RNA was pelleted by centrifugation for 20 minutes at 10 000 rpm at 4 °C. Pellets were washed by crude rinsing with 2 M LiCl solution. After removal of all the LiCl from the tube (using a fine, drawn Pasteur pipette), the RNA pellet was resuspended in 2 ml of sterile, RNAse free, water and extracted with chloroform/iso-amylalchohol (v/v, 24:1) as described. The RNA in the aqueous phase was precipitated by addition of 1/10 volume 3 M NaOAc (pH5) and 2.5 volumes of ethanol and incubation at –20 °C for at least 1 hr. – overnight. Total RNA was pelleted for 20 minutes at 10 000 rpm and after removal of the supernatant, the pellet was washed by rinsing with 70% ethanol solution. The pellet was air dried for
10 minutes at room temperature (RT). Total RNA was carefully respuspended in an appropriate volume of sterile water. The concentration of the RNA was estimated by absorption at OD260 nm and the concentration and integrity confirmed by Northern gel electrophoresis in a 1.2% (w/v) agarose gel.

polyA$^+$ mRNA purification

For the purpose of cDNA library construction, mRNA (polyA$^+$ mRNA) was purified as previously described (Kroon, J. et al., 1994). PolyA$^+$ mRNA was prepared by two passages over a 1 ml affinity oligo-dT cellulose column (Boehringer Mannheim). A sterile 2 ml syringe, was used as a column and packed with 1 ml (packed bed volume) oligo-dT cellulose (with the outlet protected by siliconised glass-wool). The column was run under gravity and equillibrated with at least three volumes of Buffer A (0.5 M LiCl, 20 mM Tris-HCl pH 7.2, and 0.2 % (w/v) SDS). In the meantime, the total RNA sample (usually 500 – 1000 µg in not more then 500 µl volume) was denatured at 65 °C for 15 min. and immediately placed on ice.
The total RNA sample was made to 0.5 M LiCl, 20 mM Tris-HCl pH 7.2, 0.1 % (w/v) SDS in a maximum of 1 column volume (1 ml). The denatured total RNA sample was passed through the column twice and the final eluate stored on ice. Subsequently the column was washed with 10 ml of Buffer B (0.375 M LiCl, 15 mM Tris-HCl pH 7.2, and 0.15 % (w/v) SDS) followed by 4 ml of Buffer C (0.2 M LiCl, 20 mM Tris-HCl pH 7.2). PolyA$^+$ mRNA was eluted from the column using sterile water at 70 °C.
1 ml fractions were collected and 1/10 volume of 3 M NaOAc (pH5) and 2.5 volumes of ethanol were added and mRNA precipitated overnight at –20 °C. PolyA$^+$ mRNA was pelleted for 20 minutes at 13 000 rpm and the pellet washed by rinsing with 70% ethanol

solution. The pellet was air dried for 5 minutes at room temperature (RT) and respuspended in an appropriate volume of sterile water. The concentration of the polyA$^+$ mRNA was estimated by absorption at OD260 nm and the concentration and integrity confirmed by Northern gel electrophoresis in a 1.2% (w/v) agarose gel.

4.2.4 Northern blot analysis

In most analyses, either 10 µg total RNA or 1 µg polyA+ mRNA was denatured at 65 °C for 15 min., after addition of three volumes of Denaturing Buffer (26 mM MOPS pH 7, 6.5 mM Sodium acetate, 0.13 mM EDTA, 8.35% (v/v) formaldehyde, 65% (v/v) deionised formamide). Samples were placed on ice and 0.1 volume of 10 x Loading Buffer (10 x: 50% (v/v) glycerol, 1 mM EDTA, 0.4% Bromophenol blue and 0.4% Xylene cyanol) was added before size-fractionation by electrophoresis in a 1.2% (w/v) agarose gel. Agarose gels were prepared with 1.2% (w/v) agarose, 6.3% formaldehyde and 1 x RNA Running Buffer (10 x stock: 0.2 M MOPS pH 7.0, 50 mM Sodium acetate, 1 mM EDTA) and the electrophoresis was performed in 1 x RNA Running Buffer at 5 V cm^{-1} for 5 hr. Visualisation of the samples and markers (BRL RNA ladder, 0.24-9.5 kb), for ensuring equal loading and integrity of the RNA, was achieved by briefly staining the gels in 0.05 M NaOH, 10 mM NaCl with 5 µg/ml ethidium bromide (Sigma). Formaldehyde and ethidium bromide were removed from the gels by washes in 0.1 M Tris-HCl, pH 7.4 and sterile water for at least 2 hr. (Kroon, J. et al., 1994). After a wash with 10 x SSC for 15 min., the gel was capillary blotted in 10 x SSC on to a Hybond-N membrane and further manipulated according to the instructions by the supplier (Amersham). Hybridisation to radiolabeled probes was as described for Southern blots.

4.2.5 Synthesis and screening of an oil palm fruit mesocarp cDNA library and subcloning procedures

A 111 days post anthesis oil palm (*Elaeis guineensis* var. *tenera*) mesocarp cDNA library was constructed in the cloning vector λZAPII (Stratagene), using the TimeSaver cDNA Synthesis Kit (Pharmacia) for preparation of *EcoRI*- flanked double stranded cDNA. 1 µg polyA$^+$ mRNA was used as template for cDNA synthesis according to the instructions of the supplier (Pharmacia). The first strand cDNA synthesis, catalysed by Moloney Murine Leukemia Virus (MMLV) reverse transcriptase, was primed with 0.5 µg oligo(dT)$_{12\text{-}18}$ and both the first and second strand synthesis were initiated in predispensed reaction mixtures (principle reactions were based on the protocol by Gübler, U. and Hoffman, B.J., 1983). cDNA product was extracted with phenol/choroform (v/v, 1:1) and purified and equilibrated in ligation buffer (66 mM Tris-HCl pH 7.6, 0.1 mM spermidine, 6.6 mM $MgCl_2$, 10 mM dithiothreitol (DTT), 150 mM NaCl) on a Sepharose CL-4B spun column. An *EcoRI/NotI* adaptor was ligated to each end and after denaturation of the T4 DNA ligase (Promega) and phosphorylation by T4 polynucleotide kinase, purified and size-

fractionated on a new a Sepharose CL-4B spun column. 2 μg λZAPII vector (with dephosphorylated *Eco*RI overhangs) and column effluent (15, 10 and 5 μl respectively) were co-precipitated and three 'test' ligations were performed. Ligated DNA was packaged using Gigapack II packaging extracts (Stratagene) and the resulting libraries were titered on *E. coli* XL 1-Blue MRF' according to standard protocol. The three testlibraries were combined (the pooled library was designated OPMT2) and the titre was estimated approximately 6. 10^5 pfu., with at least 90% recombinants (as judged on basis of a color assay by IPTG-Xgal) and an average insert-size of between 500 – 1000 basepairs with ~10% pfu with insert size of > 1.5 kb. The insert –size was estimated via a PCR-amplification of the inserts of 15 independent pfu, using the primers complementary to the flanking DNA sequences in the pBS SK(-) plasmid within the λZAPII vector (the Reverse Primer and the M13 –20 Primer). 4 – 5 x 10^5 pfu from the original cDNA library was plate-amplified according to standard protocols and stored with 7% DMSO at –80 °C.

For cloning of the oil palm mesocarp, putative soluble glycerol-3-phosphate acyltransferase (GPAT) cDNA, at least 2. 10^5 pfu of the amplified cDNA library were screened by hybridisation with ^{32}P-labeled 1445 bp. *Eco*RI cDNA fragment of *Arabidopsis* GPAT (from plasmid p2-6; kindly provided by Nishida, I., University of Tokyo) according to standard procedures and instructions with Hybond-N membranes (Amersham). Conditions for hybridisation was as described for the genomic Southern analysis (section 4.2.2).

Cross-hybridising pfu's were purified in three rounds of re-plating and re-screening with the radioactive probe and subcloned according to instructions by Stratagene. The subcloning protocol was based on *in vivo* excision of the pBluescript SK(-) phagemid from the λZAPII phage containing the cDNA of interest, using the ExAssist/SOLR system. The ExAssist helper phage contains an amber mutation that prevents replication of its phage genome in the nonsuppressing *E. coli* SOLR strain, and therefore only the excised phagemid replicates in the host.
SOLR bacterial colonies containing pBS SK vector with the cDNA insert of interest, were plated in dilutions on LB plates with 150 μg/ml ampicillin (AMP). Plasmids were isolated according to standard protocol and analysed by restriction digest with *EcoRI* and by nucleotide sequencing of the cDNA insert.

4.2.6 Preparation and screening of an oil palm genomic DNA library

A genomic DNA library was constructed in the λBluestar vector (Novagen) according to the following methods. Nuclear DNA (from frozen spear leaves of oil palm) was prepared for cloning via partial digestion with *Sau3A I* to obtain the desired size range of DNA fragments ('partials', @ 15-20 kb)). After small scale test digestions with increasing dilutions of enzyme under standard reaction conditions, the large scale ('bulk') digestions were set up as follows:

10 separate digestions in 1.5 ml. Eppendorf micro-centrifuge tubes with each 500 µl total volume containing 35 µg nuclear DNA and 1:2800 dilution of *Sau3A I* (Boehringer Mannheim) in 1 x of the appropriate salt mix (A) for 30 minutes at 37 °C. Reactions were stopped by a phenol/chloroform (v/v, 1:1) extraction and concentrated by a standard ethanol precipitation. After resuspension of the pellets in 30 µl sterile water (milliQ), a sample (1/20) was analysed via gel electrophoresis (section 4.2.2). Eight of the partial digests were pooled (280 µg DNA in 240 µl water) and size-fractionated by centrifugation on a 10% – 40 % continuous sucrose density gradient. DNA solution was layered on top of a 34 ml sucrose gradient (in a 38 ml Beckmann polyallomer tube) and centrifuged at 22 000 rpm for 22 hr. at 20 °C (in a Beckmann SW 28 swing-out rotor). Following centrifugation, 400 µl fractions were collected, starting from the bottom of the tube, and 15 µl samples were analysed as before. Fractions containing DNA size fragments of about 15 – 20 kb. were pooled, precipitated with 10 µg glycogen as a carrier in a standard ethanol precipitation and ligated in (2 µl = 0.5 µg = 0.017 pmol) *Bam*HI-digested arms of the phage vector λBluestar (Novagen). Ligations were in 10 µl total volume according to instructions with T4 DNA ligase (Promega). Ligated DNA was packaged using Gigapack II packaging extracts (Stratagene) and the resulting libraries were titered on *E. coli* ER1647 according to standard protocol. This resulted in two separate genomic libraries of at least 8 x 10^5 pfu. each.

At least 2 x 10^5 pfu from each of the original genomic library was plate-amplified according to standard protocols and stored with 7% DMSO at –80 °C.

For cloning of the oil palm mesocarp, putative soluble glycerol-3-phosphate acyltransferase (GPAT) gene(s), at least 2. 10^5 pfu of the original genomic library were screened by hybridisation with ^{32}P-labeled 1445 bp. *EcoRI* cDNA fragment of *Arabidopsis* GPAT , as described for the cDNA cloning procedures.

Cross-hybridising pfu's were purified in three rounds of re-plating and re-screening with the radioactive probe and stored in 500 µl SM buffer (per liter: 5.8 gr. NaCl, 2 gr. $MgSO_4$-$7H_2O$, 50 ml 1 M Tris-HCl pH 7.5, 5 ml 2% gelatin) at 4 °C. with 20 µl chloroform.

4.2.7 Construction of plasmids encoding three separate versions of a GPAT from oil palm mesocarp

The pre-protein GPAT sequence, encoded by a 2043 bp. cDNA isolated from an oil palm fruit mesocarp cDNA library, was aligned to all known plant soluble GPAT protein sequences, using the Clustal W algorithm. The multiple sequence alignment with the *Arabidopsis*, squash and cucumber GPAT proteins, was given the greatest consideration. The reason for this was that a putative processing site for these proteins has been predicted on basis of molecular mass and consensus sequences for chloroplast transit peptide processing sites (Murata, M. and Tasaka, Y., 1997).

Three cDNA constructs were designed to encode:

-the entire oil palm GPAT pre-protein sequence (leader + mature protein; designated OA5N/1.9),

-a protein (designated p2/OA5N/2.2) starting with amino acid residue E66 (close to the position of alignment with A43 in the squash GPAT protein sequence; the 'predicted processing site *' as is depicted in figure 3.1) and

-a protein (designated p3/OA5N/3.4) which starts with AA residue E92 (in exact alignment with the 'previously reported processing site**', namely residue E70 in the squash GPAT protein).

For cloning purposes and to insert the GPAT DNA sequences in the *Nhe*I and *Eco*RI sites of pET24a (Novagen), the following oligonucleotides were designed for employment in a PCR based subcloning procedure using Vent DNA Polymerase (NEB), and the full-length 2043 bp. cDNA fragment in pBS KS (Stratagene) was used as a template.

-to create **OA5N/1.9**: primer OA5N(S); 5'- CAT CGCTAGC CCT TCG GCT CTG CCG CGT G-3' and primer OA3E (AS); CCG GAATTC CTTGCTGGAATACTCAGATTGC-3', -to create **p2/OA5N/2.2**: primer p2/OA5N; CAT CGCTAGC GAG AGC AAG GCT TCG GCG AGG-3' and primer OA3E (AS)

- to create **p3/OA5N/3.4**: primer p3/OA5N; CAT CGCTAGC GAG GTC GGG CAT TCC CGG TC-3' and primer OA3E (AS).

All PCR DNA fragments were analysed and purified via 1% (w/v) agarose gel electrophoresis, using the GFX PCR DNA and Gel Band Purification Kit (Amersham Pharmacia), digested with *Nhe*I and *Eco*RI in the appropriate salt mix (Boehringer Mannheim) at 37 °C overnight, purified as above and inserted into the *Nhe*I and *Eco*RI sites of pET24a. All clones were analysed and confirmed by nucleotide sequencing of the entire cDNA insert sequence using a series of oligonucleotides specifically designed for this purpose.

The construct **OA5N/1.9**, encodes a protein in which the first three amino acid residues on the amino (N-) terminus of the pre-protein, namely **MLV**, are replaced by the first three residues encoded by the ϕ10 fragment of the pET vector (**MAS**).

The constructs **p2/OA5N/2.2** and **p3/OA5N/3.4**, encode putatively mature regions of oil palm GPAT starting with amino acid residue E66 and E92 respectively. The recombinant proteins are N-terminally fused to the three amino acid residues encoded by the ϕ10 fragment of the pET vector (**MAS**).

Constructs were transformed to and overproduced in *E. coli* BL21 (DE3) pLysS. Crude cell-free extract (CCE) of total bacterial soluble protein fraction was prepared, analysed and quantitated. These procedures are described in sections 5.2.2. and 5.2.3..

4.3 Results

4.3.1 Southern and Northern analysis; The African oil palm (*Elaeis guineensis*) soluble glycerol-3-phosphate acyltransferase (GPAT) appears to be encoded by one, but possibly two genes

Southern analysis

In first instance, the main purpose of this experiment was to investigate the presence of cross-hybridising DNA sequences in the oil palm genome and to evaluate if the *Arabidopsis* GPAT cDNA could be used as a molecular probe in cloning procedures of an oil palm homologue. The investigation was extended to analyse the genetic organisation of the soluble GPAT genes in a number of other plant species because until now, no other such Southern analysis seems to have been reported.

An earlier study describes the cloning of one gene (ATS1) from *Arabidopsis thaliana* for the plastid-located GPAT but no Southern blots were shown (Nishida, I. et al., 1993). However, together with this study, from genetic analysis of an *Arabidopsis* lipid biosynthesis mutant (*act1*), deficient in chloroplast GPAT activity, it seems apparent that in the enzyme is encoded by a single nuclear gene (Kunst, L. et al., 1988).
This is confirmed by Southern blot analysis presented in Figure 4.1 and 4.2.

As is shown in Figure 4.1 and 4.2, Southern analysis of a distant other member of the Cruciferaceae revealed that the soluble plastid-located GPAT in these species may be encoded by at least two genes. It has been demonstrated that *Brassica napus* (rape) is an allo-tetraploid species originating from a spontaneous crossing between *Brassica oleracea* and *Brassica campestris* (Olsson, G., 1960; U, N., 1990). The number of gene copies in the genome of *Brassica napus* (rape) and its ancestors was estimated by Southern analysis. As can be deducted from this experiment, both *Brassica oleracea* and *Brassica campestris* have at least two gene copies per haploid genome encoding homologues of soluble GPAT. *Brassica napus* (var. Jet neuf), an allo-tetraploid, contains all the genes of both its parental species. In another rape variety (High Erucic Acid Rape) the hybridisation profile appears to be the same.

From Southern analysis of nuclear DNA of *Limnanthes douglassii* (Figure 4.2; LD) it could be deducted that no genomic sequences cross-hybridised to the radiolabeled probe under low stringency conditions. This suggested that in the genome of this species, DNA sequences homologous to the soluble *Arabidopsis* GPAT cDNA, were not present. It could be that that the level of DNA similarity between the soluble GPAT nucleic acids is too low for heterologous hybridisation.

In African oil palm (*Elaeis guineensis*, var. Tenera) total nuclear DNA on the same Southern blot (Figure 4.2), genomic sequences cross-hybridising with the *Arabidopsis* soluble GPAT cDNA probe were detected. This suggested that at least one, and maybe two, gene copies for an oil palm soluble GPAT could be present in the genome and that the *Arabidopsis* GPAT cDNA could be used as a tool to isolate oil palm GPAT DNA sequences.

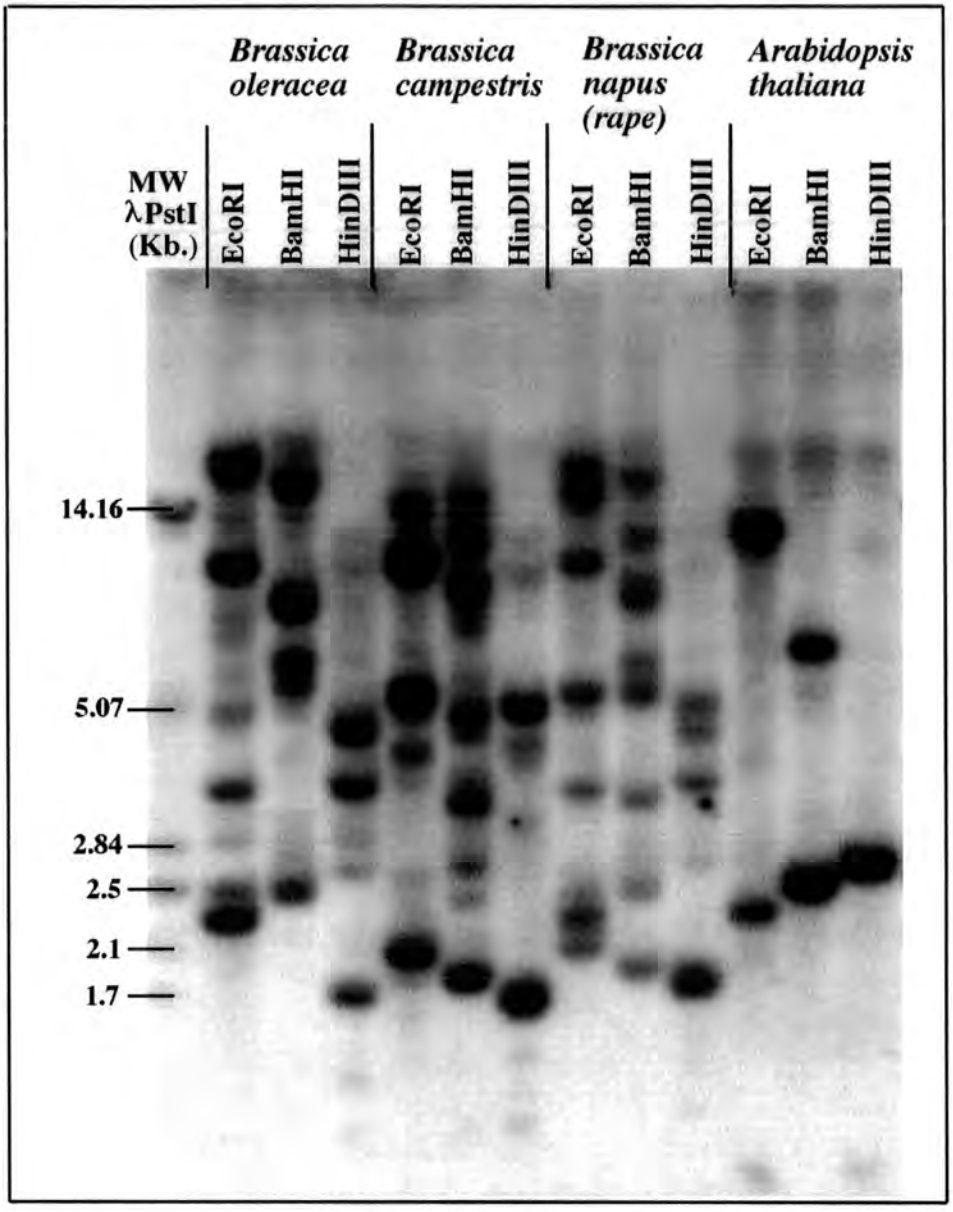

Figure 4.1 **Southern analysis of plastid-located soluble glycerol-3-phosphate acyltransferase (GPAT) genes in different Cruciferaceae**

10 µg nuclear DNA, extracted from *Brassica oleracea*, *Brassica campestris*, *Brassica napus* and *Arabidopsis thaliana*, was digested with 60 units of the restriction endonucleases (*Eco*RI, *Bam*HI, *Hin*DIII) in 500 µl total volume , overnight at 37 °C. After phenol-chloroform (v/v, 1:1) extraction and ethanol precipitation, resuspended DNA was size fractionated via electrophoresis on a 0.8% (w/v) agarose gel and Southern blotted to Hybond-N. After hybridisation with a ^{32}P-labeled 1445 bp. *Eco*RI cDNA fragment of *Arabidopsis* GPAT at 60 °C, the membrane was washed under low stringency conditions (2 x SSC/0.1% SDS) as described. Exposure to autoradiography film with intensifying screens was at –80 °C for 72 hr. DNA size markers are indicated on the left.

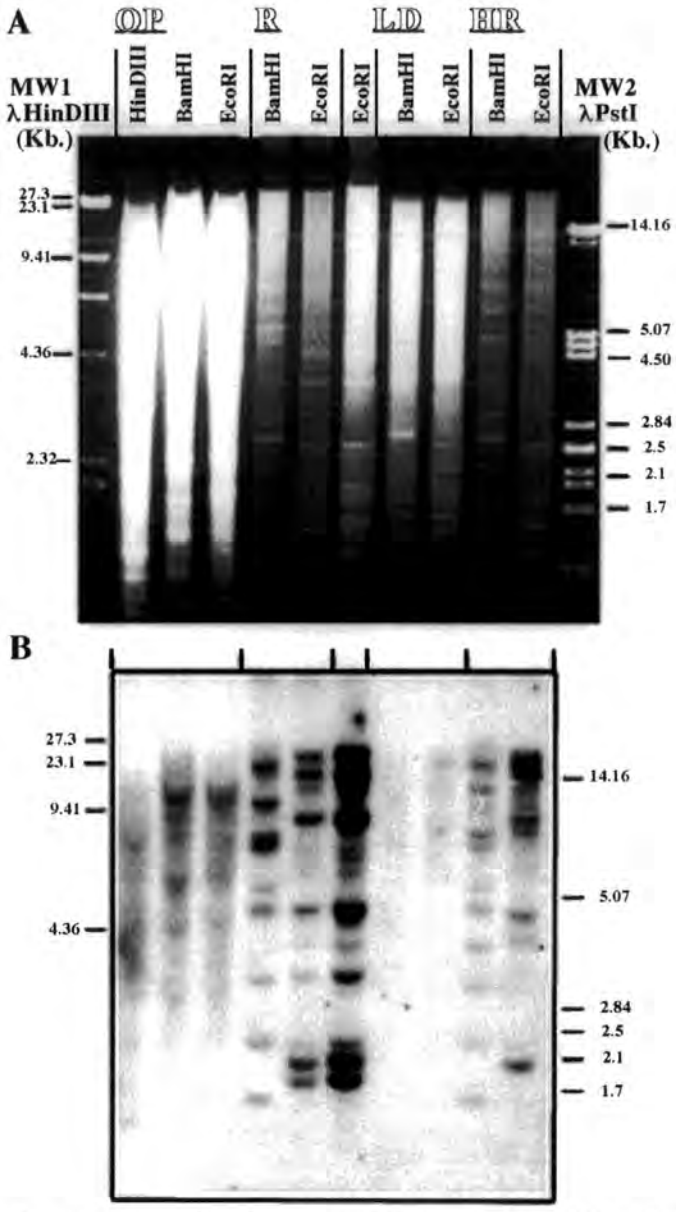

Figure 4.2 Southern analysis of plastid-located soluble glycerol-3-phosphate acyltransferase (GPAT) genes in oil palm, *Limnanthes* and rape

(A) Nuclear DNA from oil palm (O: *Elaeis guineensis*, var. Tenera, 15 µg), rape (*Brassica napus* var. Jet Neuf (R)and High Erucic Acid Rape (HR), 10 µg) and *Limnanthes douglassii*(LD, (10 µg)) was digested with *Hin*DIII, *Bam*HI or *Eco*RI, fractionated in a 0.8 % (w/v) agarose gel and transferred to an Hybond-N membrane (Amersham) according to the instructions.

(B) The membrane was hybridised at 60 °C with a ^{32}P-labeled 1445 bp. *Eco*RI cDNA fragment of *Arabidopsis* GPAT cDNA (p 2-6), washed with 2 x SSC/0.1% SDS up to 60 °C (low stringency conditions) and exposed to autoradiography film with intensifying screens for 90 hr. with intensifying screens at –70 °C. DNA markers are indicated MW1 (λ*Hin*DIII) and MW2 (λ*Pst*I).

Northern analysis

The steady state mRNA levels of the plastid-located soluble glycerol-3-phosphate (GPAT) in different tissues of *Brassica napus* (rape) var. Jet Neuf (R) and High Erucic Acid Rape (HR), *Arabidopsis* leaf, *Tropaeolum majus* L. (Nasturtium) embryo and *Elaeis guineensis* (oil palm) leaf, mesocarp and kernel from fruit, were examined using the *Arabidopsis* soluble GPAT cDNA as a radioactive probe in Northern analysis.

In the *Brassica napus* varieties a single mRNA species, of approximately 1.8-1.9 kb., cross-hybridised with the probe in total RNA from embryo, root and leaf tissue (Figure 4.3). As expected for a chloroplastic GPAT mRNA, the steady state mRNA level in leaf tissue is the highest. Also in *Arabidopsis* leaf total RNA, a single soluble GPAT mRNA species of a similar size seems to be present. It is known that the *Arabidopsis* plastid-located GPAT coding sequence is 1377 nucleotides and the size of the full length RNA transcript is further determined by the 5'- and 3'- flanking, untranslated sequences. The 5' and 3'-untranslated sequences were found to be 57 and 442 nucleotides, respectively (Nishida, I. et al., 1993). This would generate a mRNA species of 1876 nucleotides long and this corresponds to the sizes of the bands cross-hybridising on the Northern blot in Figure 4.3.

In this experiment, the use of the *Arabidopsis* GPAT cDNA as a heterologous probe, to cross-recognise GPAT mRNA from other distantly related species, was also tested. An interesting observation was that in total RNA of Nasturtium (*Tropaeolum majus* L.) embryo two mRNA species seemed to cross-hybridise with the probe. The largest mRNA detected has a similar size to the soluble GPAT mRNA in other species but a smaller band of approximately 1.4 kb was observed. The band could represent a transcript of another isoform of a GPAT or could be a stable degradation product of the 1.8 kb mRNA species.

Unexpectedly, in leaf, mesocarp (111 DAF) and kernel (82 DAF) total RNA of oil palm, no mRNA cross-hybridising to the probe could be detected. Unfortunately, in figure 4.3 there was less total RNA from oil palm leaf (expected to have the highest steady state GPAT mRNA level) present in the Northern gel, but it seems likely that the mRNA of putative soluble oil palm GPAT is only present at a very low level in the examined tissues.

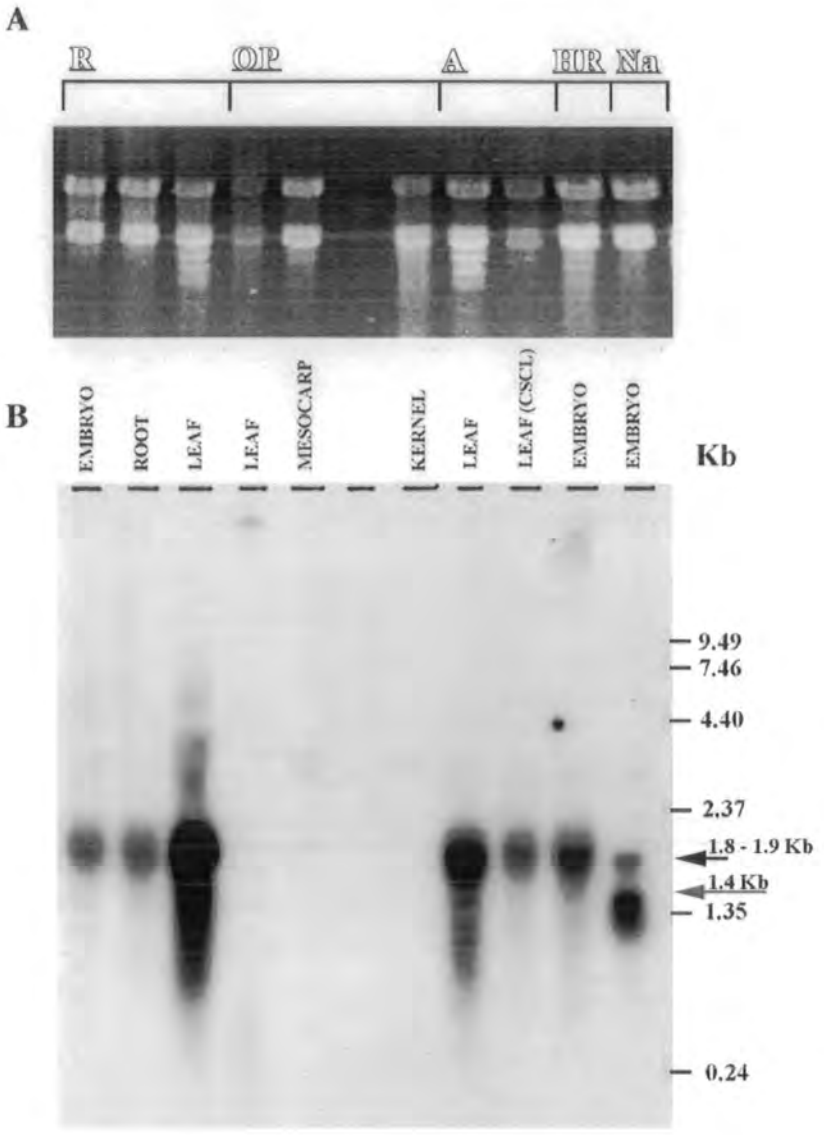

Figure 4.3 Northern analysis of plastid-located soluble glycerol-3-phosphate acyltransferase (GPAT) mRNA in tissues from *Brassica napus* (rape), *Arabidopsis*, *Tropaeolum majus* (Nasturtium) and *Elaeis guineensis* (oil palm)

(A) 10 μg of total RNA from different tissues of rape (*Brassica napus*) vars. Jet Neuf (R) and High Erucic Acid (HR), oil palm (*Elaeis guineensis*) (OP), *Arabidopsis thaliana* var. C24 (A) and Nasturtium (*Tropaeolum majus)* (Na) was fractionated in a 1.2% agarose/formaldehyde gel and transferred to an Hybond-N membrane (Amersham) as described. Ethidium bromide-stained rRNA is shown for loading comparison between lanes.

(B) Northern blot showing the presence of mRNA hybridising to a ^{32}P-labeled 1445 bp. *Eco*RI cDNA fragment of *Arabidopsis* GPAT (p 2-6). The blot was washed with 2 x SSC/0.1% SDS up to 60 °C (low stringency conditions) and autoradiographs were exposed for 1 wk. with intensifying screens at –70 °C. RNA markers are indicated on the right. The tissues from which the RNA was isolated are indicated above the blot. The arrows on the right indicate the approximate size of the hybridising bands.

4.3.2 The cloning of a novel cDNA and gene for a soluble GPAT from oil palm (*Elaeis guineensis*) and functional expression of the cDNA in *E. coli*.

Heterologous screening and subcloning

An oil palm (*Elaeis guineensis*) genomic library (section 4.3.6) was screened for cross-hybridisation with a 1445 bp. *Eco*RI cDNA fragment of *Arabidopsis* GPAT as a ^{32}P-labeled probe. From approximately 2 x 10^5 recombinant clones, three putative positive clones were obtained and were purified in three subsequent rounds of plating and re-screening as is illustrated in Figure 4.4.

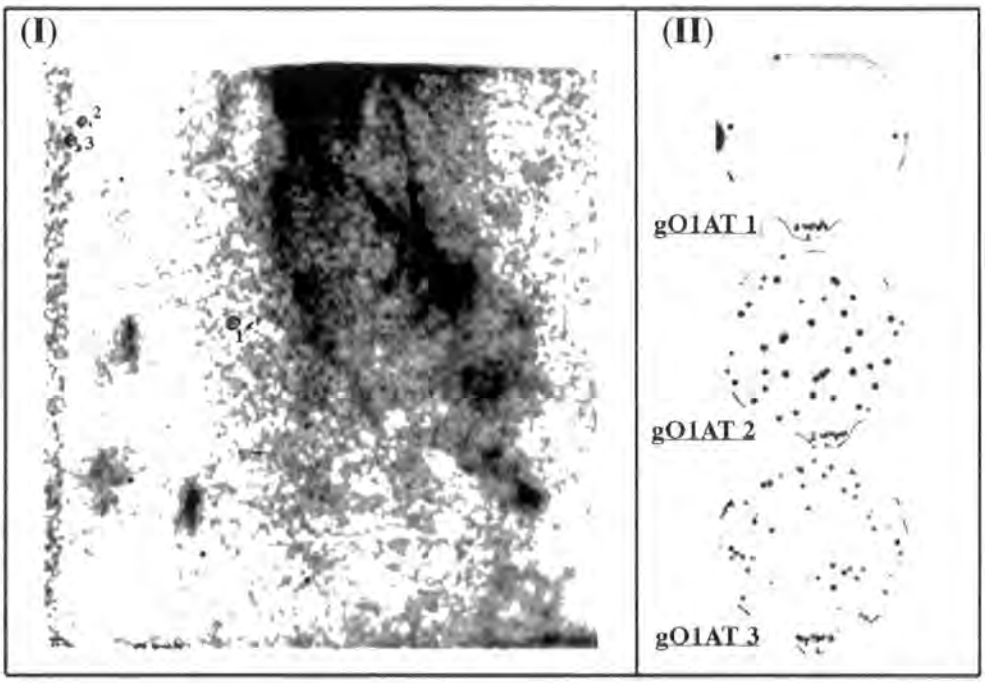

Figure 4.4 Heterologous screen of an oil palm genomic library for GPAT genes

200.000 recombinant pfu's of an oil palm genomic library in λBLUESTAR were screened via heterologous hybridisation with a ^{32}P-labeled 1445 bp. *Eco*RI cDNA fragment of *Arabidopsis* GPAT. All blots (not to scale in the figure) were hybridised at 60 °C, washed under low stringency conditions (2 x SSC/0.1% SDS , 60 °C) and autoradiographs were exposed for 117 hr. (primary screens) or 14 hrs. (rescreens) with intensifying screens at –70 °C. **(I)** a primary screen. **(II)** hybridisation of the second round of rescreen/purification of the positively hybridising phage vector.

Two positive clones, putatively encoding (parts of) oil palm GPAT gene(s), were obtained and designated gO1AT 2 and gO1AT 3. Due to a higher priority to obtaining putative oil palm soluble GPAT cDNA sequences, the genomic clones were not further characterised at the time and stored at 4 °C (section 4.2.6). However, the result of these experiments, in combination with the Southern analysis results (4.3.1), suggested that the *Arabidopsis* GPAT cDNA probe could be successfully employed in heterologous phage-library screens for putative oil palm GPAT sequences.

At least 2 x 10^5 recombinant clones from the amplified oil palm (*Elaeis guineensis*) mesocarp cDNA library were screened with the 1445 bp. *Eco*RI cDNA fragment of *Arabidopsis* GPAT as a ^{32}P-labeled probe. Four putative positive clones, designated cOA1-4, were further re-screened to confirm the hybridisation signal and the selected clones were purified in three subsequent rounds of plating and re-screening as is illustrated in Figure 4.5.
Two clones (cOA1 + 2) were confirmed to cross-hybridise with the probe, subcloned and they were designated JKO1AT.1 and JKO1AT.2. After *Eco*RI digest analysis and sequence determination, it was found that both clones were identical and that the cDNA inserts were 2043 bp in length (Figure 4.5).

The DNA sequence of **JKO1AT.1** is shown in Figure 4.6. The largest open reading frame (ORF) present within this DNA sequence covers 460 codons from nucleotide 262 up to nucleotide 1641 encoding a polypeptide with a predicted molecular mass of 51.3 kDa. The reported consensus sequence for translation initiation in plants, 5'-TAAACAATGGCT- (Joshi, C.P., 1987), was not present in the nucleotide sequence flanking the putative initiation codon in JKO1AT.1, 5'-ACGGCGATGCTG-. This is also the case for the cDNA sequence of the plastid-located *Arabidopsis* GPAT (Nishida, I. et al., 1993).
The deduced amino-acid sequence of the putative oil palm mesocarp soluble GPAT, exhibited the highest score for significant alignment with the gapped BLAST program (Altschul, S.F. et al., 1997), with 70% and 72% identity to those of the plastid-located GPAT from squash (*Cucurbita moschata*: Acc.Nr. P10349) and cucumber (*Cucumis sativus*: Acc.Nr. Q39639), respectively. The identity between the DNA and protein sequences of the oil palm GPAT and the plastid-located *Arabidopsis* GPAT was 78% and 67%, respectively.

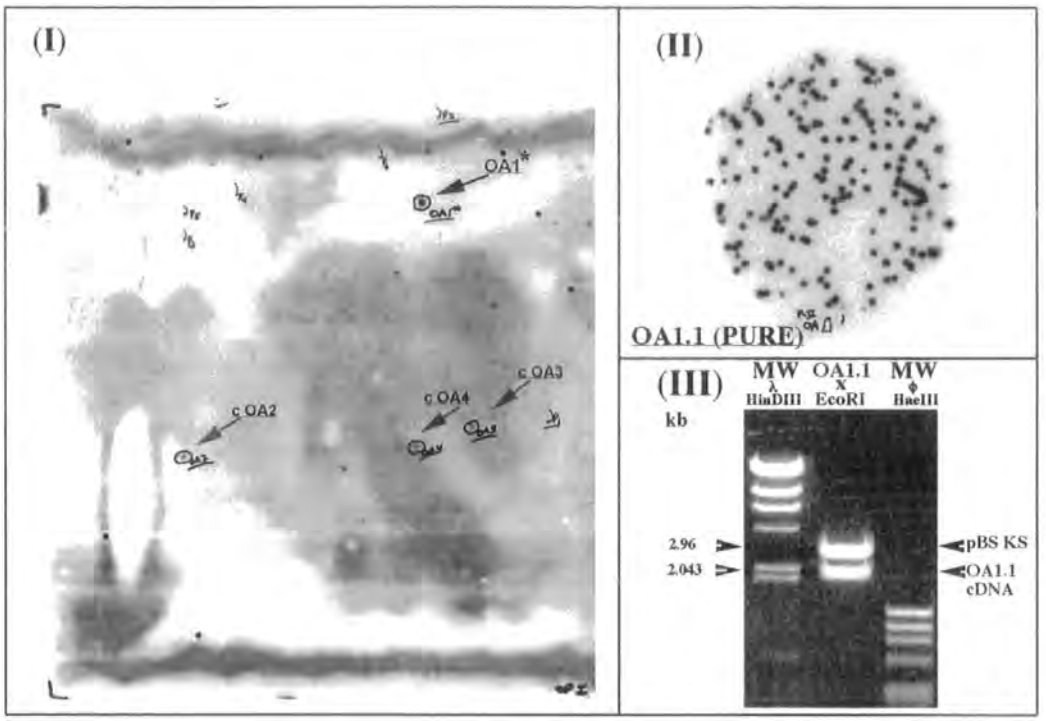

Figure 4.5 Heterologous screen of an oil palm mesocarp cDNA library for soluble GPAT clones

At least 200.000 recombinant pfu's of an amplified oil palm mesocarp (111 DAF) cDNA library in λZAPII were screened via heterologous hybridisation with a ^{32}P-labeled 1445 bp. *Eco*RI cDNA fragment of *Arabidopsis* GPAT. All blots (not to scale in the figure) were hybridised at 60 °C, washed under low stringency conditions (2 x SSC/0.1% SDS , 60 °C) and autoradiographs were exposed for 72 hr. (primary screens) or 14 hrs. (rescreens) with intensifying screens at –70 °C.

(I) a primary screen with four putative positively hybridising clones indicated by cOA1-4.

(II) hybridisation of the second round of rescreen/purification of the positively hybridising phage vector designated cOA1.1.

(III) a 1% agarose gel electrophoresis for analysis of an *Eco*RI digest of the subclone in the pBS vector. DNA molecular weight markers are separated in the flanking lanes and the sizes of the empty vector DNA band and the 2043 bp. cDNA insert are indicated by arrows.

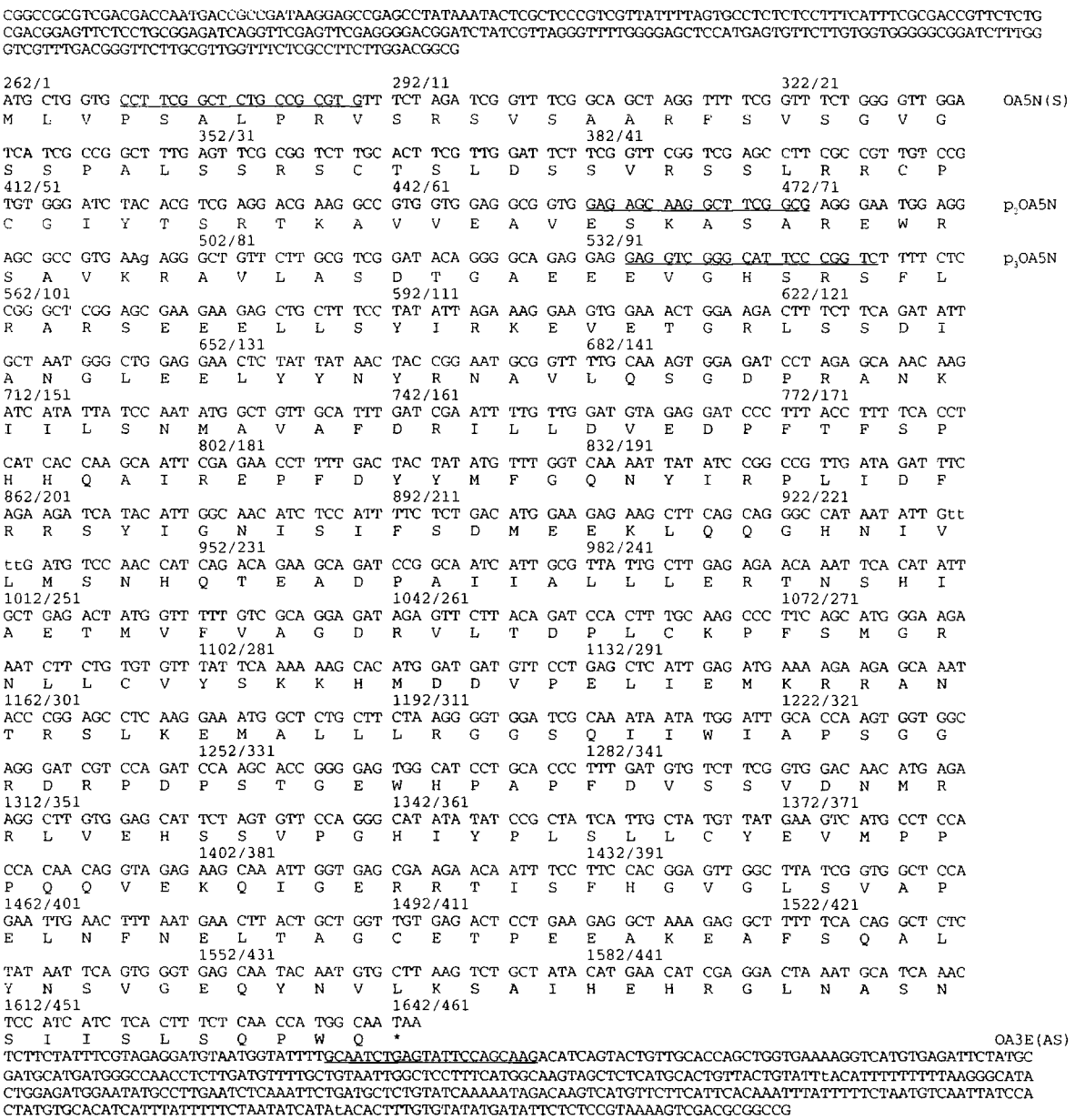

Figure 4.6 Nucleotide and amino acid sequence of the oil palm (*Elaeis guineensis* var. *tenera*) cDNA clone JKO1AT.1, encoding a soluble glycerol-3-phosphate acyltransferase (GPAT)

The 2043 bp long nucleotide sequence (Genbank: AF 251795) is shown with the deduced amino acid sequence of the longest open reading frame depicted above the DNA sequence. The sequences which were complementary to the PCR primers employed to create the three clones used in the overproduction studies in *E. coli* are underlined and the names of the respective primers indicated on the right of the figure. Nucleotides and amino acids are numbered and the respective numbers are shown above the sequences in a modified DNA Strider 1.3f program output.

Studies of functional expression of the putative oil palm GPAT in E. coli

To establish unequivocally whether the cDNA sequence in JKO1AT.1 does encode a functional GPAT enzyme, versions of the putative oil palm GPAT were expressed in *E. coli*. Also, to investigate the influence of the length and composition of the N-terminal sequence upon enzymatic activity and the acyl-chain selectivity, three different constructs in the vector pET24a (*NheI/Eco*RI) were created as described in section 4.2.7, and the analysis is illustrated in Figure 4.7.

The constructs OA5N/1.9 (encoding the preprotein with a minor modification concerning the N-terminal three amino acids), p2OA5N/2.2 (encoding the mature protein in close alignment to 'the predicted processing site*') and p3/OA5N/3.4 (encoding the truncated mature protein in alignment with 'the previously reported processing site**'), were transformed and overproduced in *E. coli* BL21(DE3) pLysS. The bacterial overproduction of the respective recombinant oil palm GPAT proteins was analysed and confirmed via 10% SDS-PAGE and is shown in Figure 4.7 (B). The relative molecular mass of the proteins was as anticipated for the fusion proteins encoded by the respective pET24a based clones. From the Coomassie Blue stained SDS-PAGE gels it was estimated that the overproduced GPAT proteins accounted for approximately up to 5% of the total *E.coli* protein content after induction with IPTG. The soluble protein fractions (or crude cell-free extracts (CCE)) from the BL21(DE3) pLysS cells, in which the respective recombinant GPAT proteins were overproduced, were prepared and analysed as described (4.2.7, 5.2.2 and 5.2.3).

The results from the standard GPAT enzyme activity determination (section 3.2.2) of the overproduced recombinant oil palm mesocarp GPAT proteins is shown in the Table of Figure 4.7 (C), and suggests that fractions of all three GPAT enzymes are active. The absolute enzymatic activities per μg of crude cell-free extract (CCE) total protein were calculated to be 2.76 pmol/min. for OA5N/1.9, 9.40 pmol/min for p2/OA5N/2.2 and 26.24 pmol/min for p3/OA5N/3.4. It could be concluded that all enzymes, including the preprotein, are capable of proper protein folding in *E. coli* , resulting in active GPAT enzyme. The result also suggested that, assuming the presence of equal amounts of recombinant GPAT in the CCE of the respective overproduced proteins, the length of the N-terminal part of the protein influences the absolute enzymatic activity negatively. This could be explained by relatively less efficient, or slower protein folding into an active protein in *E. coli* or a perturbation of the overall enzymatic activity by longer N-terminal sequences (especially in the preprotein), altering kinetic parameters of the enzyme. However, in analogy to a study on a *Brassica napus* enoyl-ACP reductase, of which also a preprotein (pEAR1) was overproduced in *E. coli* and assayed *in vitro* (Kater, M.M., 1994), there is a possibility that the GPAT preprotein has not folded into an active enzyme but that the leader peptide is considerably modified or degraded in *E. coli* and by chance resulting in an at least partially active GPAT enzyme.

Figure 4.7 Creation of recombinant oil palm mesocarp GPAT clones and their functional expression in *E. coli*

(A) 1% (w/v) agarose gel electrophoresis of analytical *NheI/Eco*RI digests of the recombinant GPAT clones in pET24a. The samples in the lanes are indicated above the gel. DNA molecular weight markers are fractionated in the first two lanes and their sizes indicated on the left. The sizes of the pET24a vector (5.310 kb) and the sizes of the respective cDNA inserts of the recombinant oil palm GPAT clones are indicated by arrows on the right.

(B) Coomassie Blue stained 10% SDS-PAGE of total *E. coli* extract before (lanes 1, 3 and 5, respectively) and after 3 hr induction (lanes 2,4 and 6 respectively) of overproduction of the recombinant oil palm GPAT (clones indicated above the lane numbers) in BL21(DE3)pLysS. The predicted molecular masses of the recombinant GPAT proteins are depicted in outlined lettertype below lanes 2,4 and 6 and the putative GPAT proteins are indicated by arrows. Molecular weight markers are shown on the left.

(C) a table with data relevant for the standard GPAT enzyme activity (sections 3.2.2 and 5.2.3) determination of the partially purified (CCE) of the overproduced oil palm GPAT enzymes.

(A)

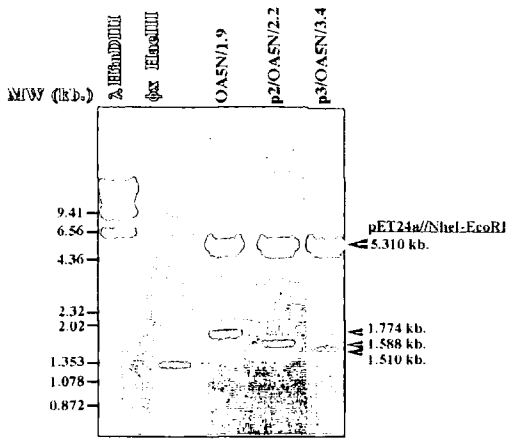

(B)

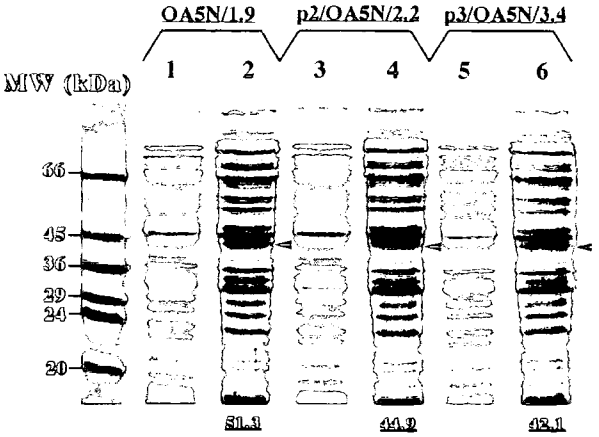

(C)

Table 1-AT Standard Activity Assay using 2 μl CCE.				
Conditions: 80 μl //0.25 M Hepes pH 8.0/ 5 mg./ml. BSA/ 2 mM [U-^{14}C] G3P (2000 dpm./nmol)/ 0.4 mM 16:0-CoA//25 °C				
Sample	Concentration total soluble protein in CCE (μg/ μl)	Time (min.)	^{14}C dpm. ORGANIC PHASE	Volume CCE with standard 1-AT activity of 6000 dpm./ 5 min. (μl)
Background		0	384.21	
OA5N/1.9	31.8	2 5	835.91 1446.72	6.84
p2/OA5N/2.2	32.4	2 5	1935.87 4124.02	1.97
p3/OA5N/3.4	32.2	2 5	4793.71 10619.40	0.71

Determination of the selectivity factor of the recombinant oil palm GPAT enzymes; is there an influence of the N-terminal protein sequence?

With the results of the standard GPAT enzymatic assays it was shown that the oil palm cDNA clone JKO1AT.1 encoded a functional GPAT enzyme. The selectivity factor (SF) of the bacterially overproduced, recombinant enzymes (encoded by) OA5N/1.9, p2/OA5N/2.2 and p3/OA5N/3.4, was determined in the standard selectivity assay (SSA) as described in Chapter III, section 3.3.3. The amounts of soluble GPAT enzyme in the crude cell-free extracts (CCE) used as the enzyme source in the SSA, are shown in the last column of the table in figure 4.7 (C).

It was found that, despite differences in the length and composition of the N-terminal protein sequences, the three different recombinant oil palm GPAT enzymes did not display a significantly different selectivity for the 18:1- and 16:0-ACP substrates. An average selectivity factor (SF) of 1.163, similar to the non-selective squash GPAT (SF = 1.1), was obtained. Typical results of the standard selectivity assay (SSA) of the three respective oil palm GPAT recombinant enzymes is shown in Figure 4.8.

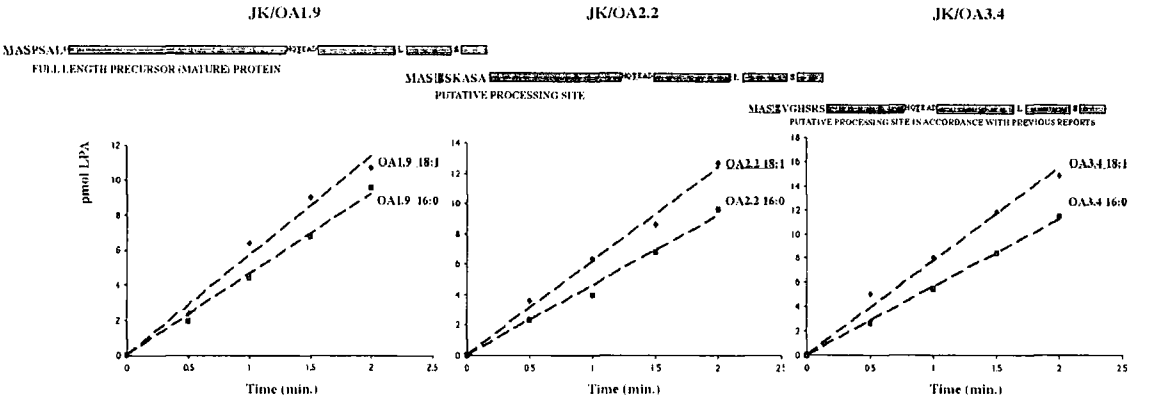

Figure 4.8 Differences in the N-terminal sequence of recombinant soluble oil palm GPAT does not influence the selectivity for 18:1-ACP and 16:0-ACP

Schematic representations of the recombinant oil palm GPAT proteins examined in this study are indicated above the graphs. The amino acid sequences on the N-terminal part of the proteins are depicted with the residues encoded by the pET vectors underlined. The significance of the other residues will be explained elsewhere.

The amount of LPA formed is depicted against time, the lines illustrate the initial rates of the enzymes when using the 18:1-ACP or 16:0-ACP substrate

4.4 Conclusion

A wide availability of primary structures (sequences) of the genes, cDNAs (RNA) and proteins involved in plant lipid biosynthesis provides the tools for molecular investigation of their genetic organisation, their biochemical organisation (supramolecular complex, metabolon or dissociated proteins), evolutionary aspects, molecular, structural and biochemical diversity (substrate selectivities and structure-function relationships) and regulatory aspects.
At the present time especially the upper hierarchy level regulatory aspects of plant glycerolipid metabolism is still a bit of an enigma. No transcription factors or their alleles, involved in regulating (sub-) sets of lipid biosynthesis structural genes have been characterised as yet. It is possible that lipid biosynthesis mutants of this type of alleles affecting multiple enzymatic steps, with analogy to for instance the *An1*, *An2*, *An4* and *An 11* loci of the anthocyanin biosynthesis in *Petunia* (Quattrocchio, F.M. et al., 1993), will be lethal to the plant and will be hard to identify via mutational approaches.
The availability of *cis*-regulatory gene sequences (promoters) of a wider range of genes of plant glycerolipid biosynthesis, may allow significant comparative analysis, transgenic experiments and studies such as DNA mobility gel shift assays, to identify specific DNA regions or specific transcription factors functioning in transcriptional regulation of these genes and the metabolism they are involved in. Some transgenic studies involving β-glucuronidase (GUS) gene fusions, have been reported for promoter analysis of FAS genes, namely ACP (De Silva, J. et al., 1992), stearoyl-ACP desaturase (Slocombe, S.P. et al., 1994) and enoyl-ACP reductase genes (De Boer, G.-J. et al., 1996).

The squash GPAT cDNA was used as a probe for the heterologous cloning of the gene for the precursor to the plastid-located GPAT of *Arabidopsis thaliana* and its structure described (Nishida, I. et al., 1993). However, a study of *cis* and *trans* regulatory elements of the gene have not been reported to date. In this Chapter the isolation of two genomic clones for a putative soluble oil palm GPAT gene was reported, but due to time constraints and a higher priority for isolation and functional identification of the cDNA/protein, the further molecular characterisation of these genomic clones had to be delayed.
From the Southern analysis in this study it appears that the putative soluble oil palm (*Elaeis guineensis*) GPAT is likely encoded by one, but possibly two, genes.
Another relatively unclear aspect of the molecular biology of plant fatty acid synthesis is the existence, specific regulation and role of isofunctional forms (isoforms) of enzymes and multiple genes. In different plant species there appears to be a range in the number of genes encoding different proteins involved in plant fatty acid and glycerolipid synthesis. For example, in several plant species, tissue specific desturases and other enzymes are controlling seed fatty acid composition (Chapter I; Ohlrogge, J.B. et al., 1991) and even within the small genome of *Arabidopsis*, ACP and stearoyl-desaturases are each encoded

by at least five genes. However, many other enzymes such as enoyl-ACP reductase (EAR) or soluble GPAT are encoded by only one gene.
Although the presence of a multigene family could be advantageous for an extra regulatory mechanism of fine tuned developmental- or tissue-specific gene expression, it does not appear to be essential for some of the lipid biosynthesis genes.

The Northern blot analysis of the soluble GPAT mRNA in tissues of different plant species indicates that the relative steady state levels of expression of the RNA for these enzymes is low. This observation seems supported by analysis of gene expression patterns of a number of lipid biosynthesis enzymes (Dr. Paul O'Hara (University of Durham), personal communication, Chalifour, L.E. et al., 1994) and the findings that the plastidial soluble GPAT enzyme amount seems to be low in plant cells (Chapter III; Douady, D. et al., 1990). From the observation that the *Arabidopsis* soluble GPAT cDNA probe did not cross recognise mRNA species in the amounts of total RNA from the different oil palm tissues, it was concluded that the steady state level of putative oil palm GPAT mRNA was low, and in any case below detection level of this heterologous Northern analysis. The nature of the ~1.4 kb putative GPAT mRNA in Nasturtium embryo total RNA remains unknown at present.

The isolation and characterisation of the cDNA and protein for a novel, natural variant of soluble GPAT from oil palm, is of value for greater insight into the structure-function relationships of this type of enzymes.
The primary structures of a number of other plant soluble GPAT proteins have now been reported and although they have a high degree of overall sequence conservation, their substrate preferences can differ. The protein sequence conservation is illustrated by a protein alignment as is shown in Figure 4.9. The oil palm soluble GPAT, which was not published before the production of this thesis, was incorporated in the alignment.

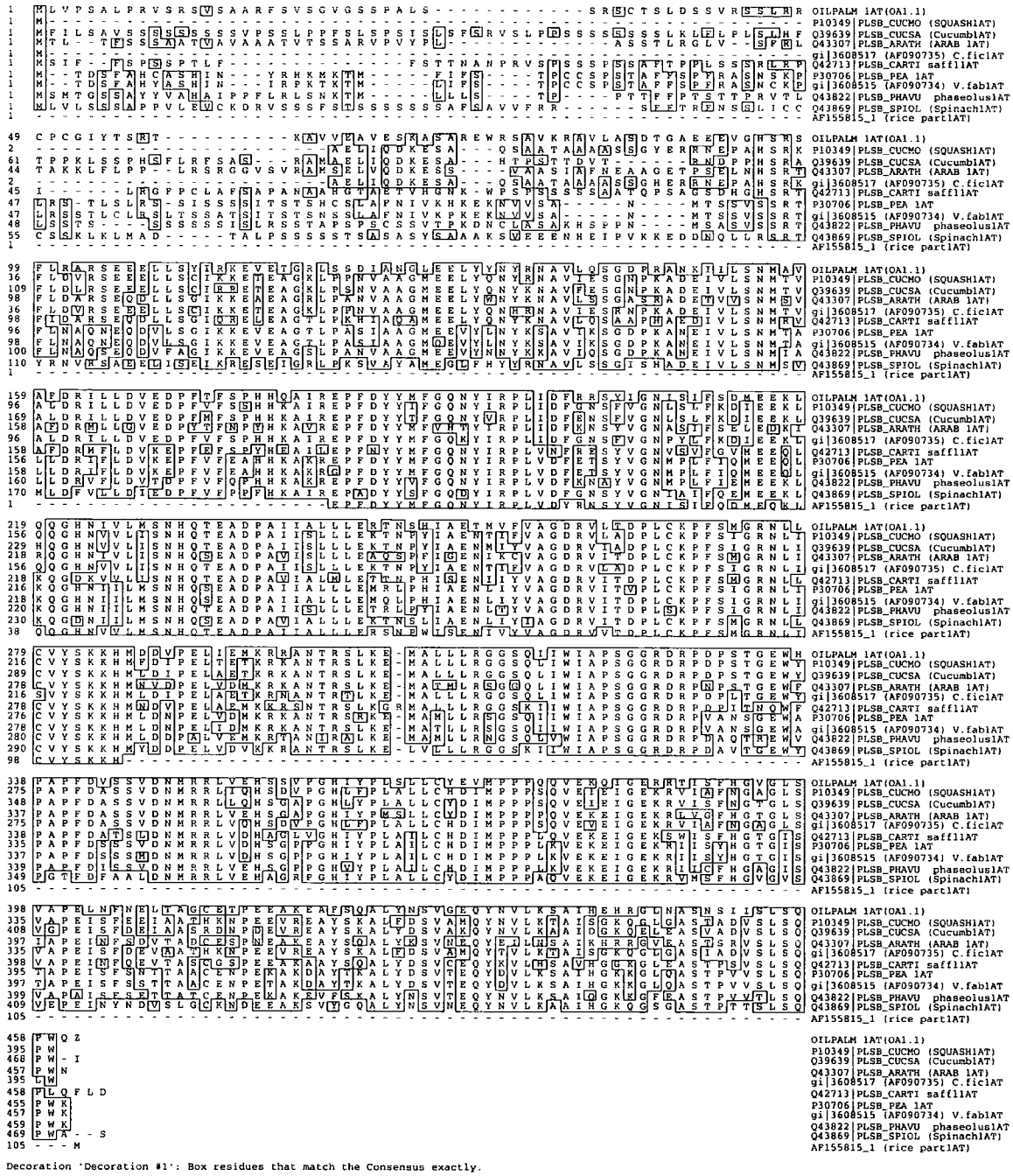

Figure 4.9 Protein alignment of plant soluble GPAT enzymes using the Clustal algorithm

The amino acid sequences of the open reading frame of the oil palm mesocarp soluble GPAT clone (JKO1AT.1) and all known other plant soluble GPAT proteins in the database, were aligned and identical residues were boxed. The Swiss-Prot Accession number followed by the designation for the GPAT is depicted on the right of the sequences.

Interestingly, evolutionary relationships illustrated by a phylogenetic tree depiction of the Clustal protein alignment in Figure 4.10, places the oil palm soluble GPAT in an ancestral group of mainly chilling sensitive plants such as squash, figleaf gourd and cucumber. The exception to this relationship is the soluble GPAT from *Arabidopsis*, which is a chilling resistant plant.

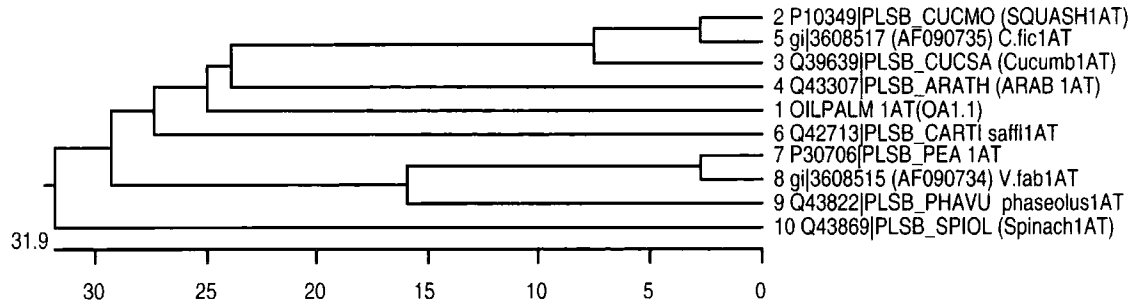

Figure 4.10 Phylogenetic tree of the plant soluble GPAT protein alignment of Figure 4.9, using the Clustal method with PAM250 residue weight table. The software used was DNA Strider 1.3f

The functional expression of three recombinant oil palm mesocarp soluble GPAT proteins in *E. coli*, unequivocally demonstrated that all the CCE fractions had GPAT enzyme activity and that the enzyme appeared to be **non-selective** (SF = 1.163) for 18:1-ACP and 16:0-ACP substrates. The soluble GPAT from chilling sensitive plants such as squash is also demonstrated to be non-selective. It was shown that the length and composition of the N-terminal portion of the soluble GPAT did not have a significant influence on the substrate selectivity.

Chapter V

∞∞∞∞∞

Substrate Selectivity Modification and Kinetic Parameters of Recombinant Glycerol-3-Phosphate Acyltransferase Chimeras and Mutants

5.1 Introduction

The structure-function relationship is one of the key problems in protein chemistry. Often a single amino acid residue alteration can dramatically affect catalytic rate and selectivity of an enzyme. Valuable clues for amino acid residues, or regions of amino acid residues ('domains') in the primary structure, which have an effect on functional properties, could come from identifying conserved residues via straightforward alignments of the sequences of different orthologous (or maybe even paralogous) proteins. Also, with respect to the plant soluble GPAT enzymes, the availability of different natural variants of the enzymes then becomes important (Chapter IV). However, although the plastid soluble GPAT enzymes have obvious differences in their substrate preferences, their overall primary structures are highly similar and therefore it is quite difficult to exactly identify all the structural requirements for their function, particularly relating to selectivity, in this way.

Amino acid residues, which are not necessarily organised in domains in the primary structure, can be organised together by polypeptide folding, in such a way as to form secondary and tertiary structure elements which form the basis for the catalytic region and other requirements for the functional properties of the enzyme. On basis of models of the enzyme 3D-structure, revealing for instance regions with specific overall hydrophobicity, charge and molecular spacing, in combination with the knowledge of the chemical properties of the substrates, it will be possible to identify specific residues potentially involved in the reactions. Some of the amino acid residues identified in this way are currently being targeted for site directed mutagenesis by other researchers in the laboratory.

In another approach, large segments of different GPAT proteins can be exchanged ('swapped') from one GPAT protein to an other, and potentially transfer variations in secondary and tertiary structure important for their functional properties. Ferri and Toguri (Ferri, S.R. and Toguri, T., 1997) took such an approach, using the spinach and squash GPAT. These respective GPAT proteins were divided in three domains and six chimeras were constructed. One conclusion from their *in vitro* studies was that, although the amino (N-) terminal domain may play some role, the central third of the GPAT proteins seems to contain the structural features which determine the substrate preference of the wild-type GPAT enzymes.

Of importance in all such *in vitro* studies is the physiological relevance of the conditions used. Any selectivity result could be obtained *in vitro* but the test is really whether they correlate with *in vivo* conditions and observed *in vivo* selectivities. In this study it was deliberately chosen to pay attention to this.

The prevalent *in vivo* conditions are [glycerol-3-phosphate] ~ 0.15 – 0.7 mM, [acyl-ACP] ~ 0.6 – 3 μM, pH dark ~7.4 and pH light ~8.0 (Chapter III). Whilst many investigators have used acyl-CoA substrates in their studies, this is a non-physiological substrate for the enzyme and may give a wrong representation of the substrate selectivity. From previous work it was concluded that the observed preference of spinach and pea for oleic acid from mixtures of acyl-ACPs, were in agreement with other experiments carried out with acyl-CoA thioesters (Bertrams, M. and Heinz, E., 1981) and that the GPAT selectivity could not be ascribed to differences in the physical state of the substrates (Frentzen, M. et al., 1983). However, it was found that the following sets of conditions would not reflect the *Arabidopsis* GPAT selectivity clearly. In the study of Bertrams and Heinz (Bertrams, M. and Heinz, E., 1981) 1 mM G3P, no BSA, and 20 μM acyl-CoAs at pH 7.4 were used, comparable to panel A in figure 3.10. Ferri and Toguri (Ferri, S.R. and Toguri, T., 1997) measured acylation rates under non-physiological conditions, with substrate analogues being provided at very high concentrations (0.3 – 2.2 mM G3P, 6 mg/ml BSA, and single acyl-CoA substrate at 0.4 mM, at pH 7.4) and this could roughly be compared to panel B in figure 3.10. In the study of Frentzen, M. et al. (Frentzen, M. et al., 1983) 1 mM G3P , 0.5 mg/ml BSA, and 4-6 μM acyl-ACP mixtures at a pH 7.4, were used. Besides a potential pH effect (the only major difference is pH 8.0) this situation would be comparable to the results shown in panel C, figure 3.10.

In Chapter III of this study, a range of conditions was tested, using both acyl-CoAs and acyl-ACPs, to design the standard selectivity assay (SSA) and it was found that under physiologically relevant conditions (300 μM G3P, a mixture of acyl-ACP (1 μM each), 5 mg/ml BSA, at pH 8.0), the observed substrate selectivities was reflecting the known phenotypic (*in vivo*) behaviour of the examined GPAT enzymes.

Due to their experimental assay set up, Ferri and Toguri (Ferri, S.R. and Toguri, T., 1997) could only explain their results on basis of affinity of the GPAT enzymes for G3P. Single substrate assays were performed using non-physiological conditions, namely at a pH 7.4 and with the substrate analogue acyl-CoA. On this basis, also kinetic constants of the recombinant GPAT enzymes for G3P were determined.
In this way it is only possible to investigate a 'specificity' of the enzyme. The term specificity is used to denote comparisons of acylation rates measured in the presence of single acyl-donors. They theoretically integrated the specificities of one recombinant GPAT by looking at the ratio of the Vmax with 18:1-CoA over Vmax 16:0-CoA and made assumptions about the enzymes selectivity for G3P.
However, the term selectivity is used when the acylation rates are actually measured in the presence of thioester mixture (Frentzen, M. et al., 1983).

When assaying *E. coli* extract expressing the wild-type squash GPAT they found that the enzyme seemed to use 16:0-CoA three times faster than 18:1-CoA. If this result would be used to make predictions for selectivity of the squash GPAT the enzyme, it would be thought to be selective for palmitic acid chains. This would be in contradiction to actual selectivities determined for the squash enzyme (Frentzen, M. et al., 1987) and its phenotypic behaviour in transgenic tobacco plants from which it is clear that the squash GPAT is a non-selective enzyme. A similar argument holds true for the spinach GPAT, the spinach GPAT used 18:1-CoA only 1.5 times faster than 16:0-CoA. From previous experiments with equimolar mixtures of C 16:0-ACP/ C 18:1-ACP (the physiological substrates), it was reported that spinach GPAT is a very oleophylic enzyme and selects 18:1 acyl chains with a factor (SF) nine times more preferred over 16:0 acyl chains (Frentzen, M. et al., 1983). Ferri and Toguri concluded that the relative affinity for the type of acyl chain (16:0 or 18:1) did not appear to be a major determinant of the substrate specificity of the enzyme.

The experiments in this study were aimed at assaying the soluble GPAT enzymes in a manner reflecting physiological conditions and functional GPAT behaviour *in vivo*. It is thought that the standard selectivity assay (SSA) in which the enzyme selects its natural substrate (acyl-ACP) from a mixture, reveals more of its phenotypic behaviour than when only examining specificity.
It is clear however that in plant cells, sub-cellular concentrations of substrates and the physiological state of the enzyme (which is unknown at present) will have important influences on its function *in vivo*. Therefore, determination of selectivity- and also kinetic data for all physiological substrates of the GPAT enzymes under these conditions will provide valuable insight into the functional properties.
In this Chapter determinations of this sort of data are reported for the acyl-ACP substrates of a series of recombinant GPAT enzymes. The structure-function relationship was examined at the molecular level by constructing chimeric recombinant proteins of *Arabidopsis* and squash GPAT, and of spinach and squash GPAT respectively.
The influence of variations in the N-terminal domain and two single amino acid substitutions in the C-terminal domain of the recombinant squash GPAT on the selectivity, was investigated. It was found that in some cases the substrate selectivities of the enzymes were dramatically changed.

5.2 Materials and methods

5.2.1 Plasmid construction for 'domainswapping' to create chimeric GPAT enzymes

To be able to objectively evaluate the findings from similar type of experiments by Ferri, S.R and Toguri, T. (Ferri, S.R. and Toguri, T., 1997) on spinach and squash GPAT, it was aimed to create the chimeric GPATs of *Arabidopsis* and squash as identical to their constructs as possible. Also two of their chimeras were re-created in exact same fashion, in order to objectively compare their findings to the results of this study. Spinach GPAT was cloned via a polymerase chain reaction (PCR) cloning strategy. Spinach leaves were purchased from the local supermarket (Sainsbury) and polyA mRNA was isolated according to described methods (home made 1 ml oligodT-cellulose spin column with LiCl based salt-solutions). Double stranded cDNA was synthesised according to instructions with the TimeSaver cDNA System (Pharmacia) and used as a template in amplification of spinach GPAT with Vent DNA Polymerase (NEB, 254 L) using the oligonucleotides: pSP1S; 5'-ACAT GCTAGC CAT TCT CGC ACT TAT CGT AAC GTT CG –3', and pSPxAS; 5'- CAT GAATTC CTCTACAAGACTACAAGTATGC –3'. To insert the GPAT cDNA fragments into pET based overexpression vectors (pET17b or pET24a, Novagen) all the primer oligonucleotides for PCR amplification in these procedures, could be designed to encode a *Nhe*I restriction endonuclease site on the 5' part of the sequence (N-terminal site of the protein) and an *Eco*RI site on the 3' part (C-terminal end of the protein). As in the experiments of Ferri, S.R and Toguri, T, the *Hin*DIII and *Kpn*I restriction endonuclease site, conserved between spinach and squash GPAT, were used to create two chimeric GPATs (PPQ and QQP).

The *Hin*DIII and *Kpn*I restriction endonuclease sites are not conserved between *Arabidopsis* and squash GPAT. However, the conserved *Ava*II and *Eco*RV (RV) restriction endonuclease sites between these two enzymes are in similar regions as the *Hin*DIII and *Kpn*I restriction endonuclease sites of spinach and squash GPAT, and were used to create six chimeras of domains of both enzymes.

Three letter-names were given to the recombinant 'wild-type' GPAT proteins and the GPAT chimeras to indicate the origin of the GPAT domains, using the same nomenclature as Ferri and Toguri. For spinach and squash GPAT, the names were composed of the second letters (P and Q respectively) but for *Arabidopsis* GPAT the first letter was used (A). For example QAA corresponds to a chimeric protein consisting of the N-terminal third of the squash GPAT and the central- and carboxyl third of the *Arabidopsis* GPAT. In some cases, for practical reasons to distinguish between certain constructs, an alternative name for the 'wild-type' GPAT recombinant proteins was also used. In this case the whole protein was indicated by the relevant letter followed by the number of the type of pET overproduction vector used, for example squash GPAT = QQQ or Q17b (in pET17b) or Q24a (in pET24a).

The DNA sequence for the GPAT of squash was re-cloned from plasmid pNA4 and that of *Arabidopsis* from plasmid p2-6. For re-cloning purposes and to be able to insert the GPAT DNA sequences in the a *Nhe*I and *Eco*RI sites of pET17b, the following oligonucleotides were designed and used in PCR amplification catalysed by Vent DNA Polymerase (NEB): to create QQQ$^{(*)}$ (or Q17b$^{(*)}$): pSQ1S; 5'- CAT CGCTAGC CAC TCC CGC AAA TTT CTC GAT G –3' and pSQ2AS; 5'- GAAAGAATTC GGTTTTATCTTACAG –3', to create AAA (or A17b): pAR1S; 5'- CATCGCTAGC CAT TCC CGT ACT TTC TTG GAT G –3' and the standard T3 promoter primer, to create A-20/17b: pAR-20S; 5'- CATCGCTAGC GAA TCG TCC GCT GCG GCG AG –3' and the T3 promoter primer. All PCR DNA fragments were analysed and purified via 1% agarose gel electrophoresis using the GFX DNA Purification System (Pharmacia), digested with *Nhe*I and *Eco*RI in the appropriate salt mix (Boehringer Mannheim) at 37 °C overnight, purified as above and inserted into the *Nhe*I and *Eco*RI. Sites of pET17b (Figure 5.1). These constructs encoded proteins in which the first three amino acid residues on the amino (N-) terminus of the mature squash GPAT (**EPA**), *Arabidopsis* GPAT (**ELN**) ('previously reported processing site', see Figure 3.1) and spinach GPAT (**QLL**) (Acc. Nr. 43869) were replaced by the first three residues encoded by the ϕ10 fragment of the pET vector (**MAS**). All DNA fragments and clones were analysed and confirmed by nucleotide sequencing of the entire DNA sequences.

5.2.2 Overproduction and recombinant GPAT enzyme preparation; the crude cell-free extract (CCE)

All constructs (and as a control the unmodified pET17b or pET24a vectors) were transformed to *E. coli* BL21 (DE3) pLysS. This *E. coli* BL21 (DE3) pLysS strain was chosen for overexpression of all constructs for two reasons: 1) Using a pLysS host prevents unwanted production of the recombinant GPAT proteins which could impair cell growth; the pLysS plasmid encodes a small amount of T7 lysozyme which binds to T7 RNA polymerase and prevents unwanted transcription before induction (Studier , F.W., 1991) and 2) the presence of T7 lysozyme, which cuts a specific bond in the peptidoglycan layer of the *E. coli* cell wall (Inouye, M. et al., 1973) and only acts after the inner membrane is disrupted, helps to lyse the cells efficiently during preparation of soluble protein extract.

Growth of the transformed hosts and induction of overproduction of the recombinant proteins was performed as described in Materials and Methods section 3.2.1, usually in 50 ml cultures. After washing of the induced cells and harvesting via centrifugation, pellets were stored at – 80 °C without significant loss of GPAT activity. The success of the overproduction procedure was confirmed by 10% SDS-PAGE analysis (section 3.2.11) and Coomassie Blue staining.

Crude cell-free extract (CCE) of induced *E. coli* cell pellets of 25 – 50 ml original culture volume were prepared according to the following protocol; cells were thawed on ice and resuspended in 2.5 ml of homogenisation mix (HM) containing: 20 mM Tris-HCl, pH 8.0, 20 mM DTT, 10% glycerol, 10 mM MgCl2, 5 μg/ml DNAseI, and 0.5 μg/μl lysozyme (chicken egg white, SIGMA L-6876). Cell suspensions were then incubated with occasional gentle mixing at 0 °C for 1 hr and at 4 °C for an extra hr. All subsequent steps were performed at 4 °C . The lysates were centrifuged at 40 000 x g for 10 min. (Beckman Table Top Ultracentrifuge; rotor TLA 100.4) and the supernatants ultracentrifuged at 150 000 x g for 1 hr. In this soluble *E. coli* protein extract, the endogenous (membrane bound) *E. coli* GPAT is seemingly completely removed as measurements in control experiments were not significantly different from background values in GPAT assays. Supernatants (CCE) were aliquoted and could be kept on ice for one night or were snap-frozen and stored at – 80 °C without significant loss of GPAT activity.

5.2.3 Protein analysis and quantitation of amount of CCE for use in the standard GPAT activity assay and in the standard selectivity assay (SSA)

Total protein concentrations were determined using the BioRad dye binding assay according to instructions with the reagent, with bovine serum albumin (BSA) as a standard (Bradford, M.M., 1976).

Routinely, the following analyses were performed in order to quantify the bands corresponding to recombinant GPAT, to determine the absolute recombinant GPAT enzyme activity and the amount of CCE to use in the standard selectivity assay **SSA** (section 3.3.3). After 10-12% SDS-PAGE analysis of 10 μg total protein,the level of the new recombinant GPAT protein in the CCE was quantified using an Imaging Densitometer (Model GS-690; BioRad, in combination with MacIntosh software for BioRad's Image Analysis System: MultiAnalyst version 1.0.2) and additionally 3 μg total CCE protein was tested for enzyme activity in the standard GPAT assay (section 3.2.2). As noted in section 3.3.3, it was found that, in general, the amount of GPAT with an absolute activity of **6000 dpm per 5 min**. in the standard GPAT assay, would have a linear initial reaction rate in the **SSA** with acyl-ACP as substrates. Therefore, enzyme activity determinations with the standard GPAT assay were recalculated towards the number of microlitres of CCE to use in the SSA. Unless otherwise stated, these standard activity values were **corrected to account for the total reaction products formed**. This meant that the dpm.value of the radioactive *sn*-1-LPA formed after 5 min. was corrected by subtracting background dpm. and subsequently corrected for the total volume of the aqueous lower

phase (times a factor 0.625). It was found empirically, that this usually corresponded to GPAT amounts in the range of 50 – 100 ng.

The selectivity factors (SF, section 3.3.3) of the recombinant GPAT enzymes was determined by the standard selectivity assay (SSA). It was found that these CCE preparations of recombinant GPAT did not contain significant hydrolytic (thioesterase-) activities, which could compromise the acyl-ACP substrate integrity

The amounts of enzyme used in the assays maintained the product concentration below 10% of maximum (to prevent substrate concentration influences on the assay) in the time range used in all experimental assays in this study.

Figure 5.1 The construction of chimeric GPAT enzymes

(A) Schematic drawings of the recombinant mature regions of GPAT from *Arabidopsis* (A17b and A-20/17b), squash (Q17b*) and spinach (P17b).

All the depicted cDNAs were cloned in the *Nhe*I and *Eco*RI sites of pET17b. The conserved restriction sites used in creation of chimeras between *Arabidopsis* (A) and squash (Q) GPAT are indicated as RV (*Eco*RV) and AVAII (*Ava*II) in underlined characters above the amino acid residues, encoded by codons which are located at the restriction sites. The conserved *Hin*DIII (HdIII) and *Kpn*I sites conserved between squash (Q) and spinach (P), used to create PPQ and QQP are depicted in the same way. The percentage of amino acid similarity between the individual domains of the respective sequences are shown as outlined characters between the schematic drawings. Amino acid sequences on the N-terminal part of the recombinant proteins are shown in bold characters. The first three or four N-terminal amino acid residues in italics are encoded by the pET vector and replace the first three amino acid residues of the mature GPAT enzyme as based on the previously reported processing site. Also indicated are a HX_4D configuration which is conserved in a number of membrane-bound and soluble GPAT and is thought to play a role in catalysis (Heath, R.J. and Rock, C.O., 1998). Two amino acid residues in the C-terminal domain are indicated in many schematic representations of GPAT sequences for the same reason.

(B) a simplified representation of the three domains in the chimeras and the restriction sites used in their creation, with the number of the amino acid residues they encode depicted in outlined characters below the lines.

5.3 Results

5.3.1 The creation of chimeric GPAT enzymes and preparation and analysis of *E. coli* crude cell-free extracts (CCE)

The cDNA sequences encoding the mature soluble GPAT, based on the previously reported processing site (denoted by comparison, see Figure 3.1 and Murata, M. and Tasaka, Y., 1997) from spinach, squash and *Arabidopsis* were (re-) cloned (5.2.1). Two chimeras of spinach (P) and squash (Q) GPAT, namely PPQ and QQP, were created by making use of the conserved *Hin*DIII and *Kpn*I restriction endonuclease sites in the spinach and squash GPAT cDNA sequences. As is depicted in figure 5.1, six chimeras between *Arabidopsis* (A) and squash (Q) could also be constructed in a similar way, when using the conserved *Ava*II and *Eco*RV (RV) restriction endonuclease sites between the two enzymes.

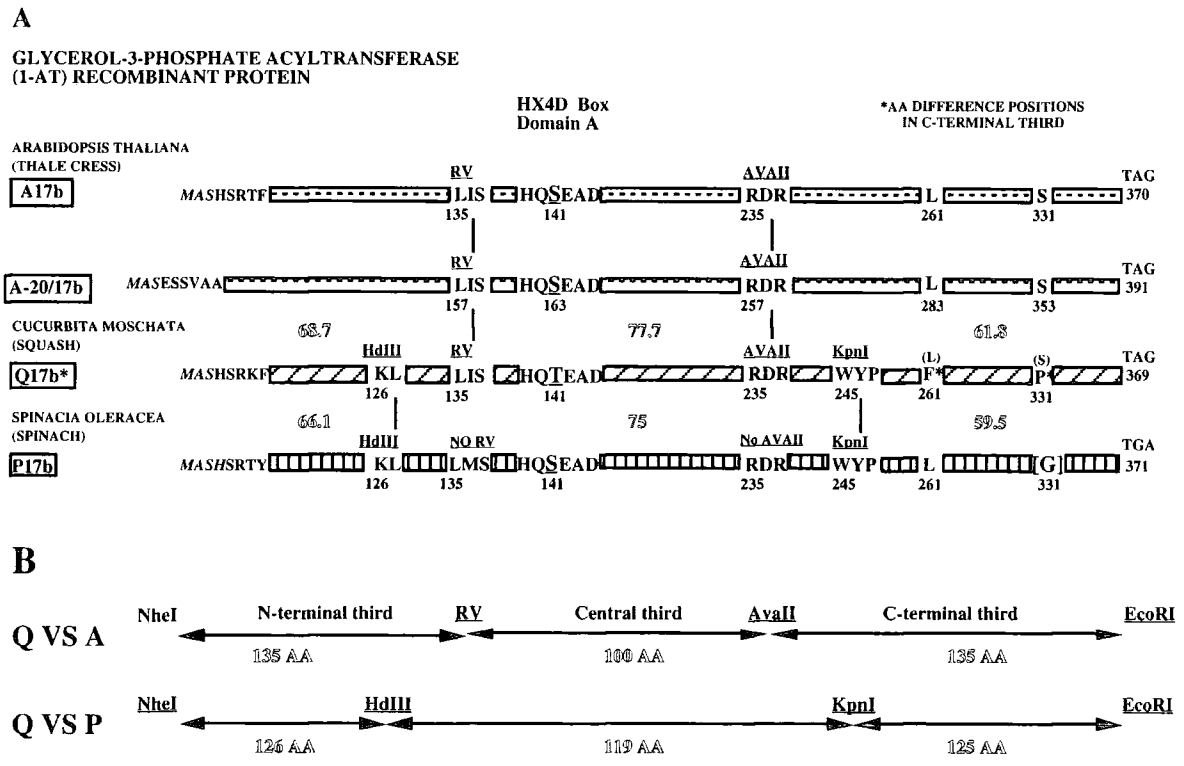

In order to study if alterations to the amino (N-) terminus affected selectivity of recombinant *Arabidopsis* GPAT, a N-terminal region which was 20 amino acids longer was also created (A-20/17b, section 5.3.1). Although, in previous studies (Frentzen, M. et al., 1994; Ferri, S.R. and Toguri, T., 1997) it is reported that small alterations of the amino terminal had no significant effect on the enzymes' absolute activity and substrate preference, but this has been only tested to a limited extend. It is still controversial which amino acid is truly the first on the N-terminus of the mature imported chloroplast protein and it may even be so that for individual (different) GPAT enzymes, there could be some influence on activity/property.

All the GPAT cDNAs were cloned in the *Nhe*I and *Eco*RI sites of pET17b and analysed by restriction digest analyses and confirmation of the nucleotide sequences of the entire cDNA inserts from all respective clones, namely: P17b, A17b, Q17b*, PPQ*, QQP, AAQ*, A+AQ*, QQA, QAQ*, AQA, QAA, and AQQ*. All DNA sequences were confirmed to be identical to the previously published cDNA sequences, with one exception.
It was found that in the carboxyl (C-) terminal domain of the recombinant squash (Q) GPAT, and therefore in all the respective chimeras containing this C-terminal domain, three nucleotide substitutions occurred. These nucleotide aberrations, presumably introduced during the PCR-based cloning procedure, caused two amino acid alterations in the C-terminal domain of Q17b*. The **asterisks** in the terminology of recombinant enzymes in this study is meant to indicate that the two amino acid substitutions are present in that particular GPAT protein. These amino acid substitutions in the primary sequence of the C-terminal domain of the squash GPAT construct Q17b* are: a L 261 to F 261(*) substitution and a S 331 to
P 331(*) substitution. The amino acid number designations are based on the protein sequence encoded by the Q17b* construct. Initially it was assumed that these amino acid substitutions would not have a significant influence on the GPAT selectivity or activity, based on findings by Ferri, S.R and Toguri, T. (Ferri, S.R. and Toguri, T., 1997) for spinach and squash GPAT and other studies implicating the central domain of GPAT proteins (with a conserved HX_4D box (Heath, R.J. and Rock, C.O., 1998) to contain the structural features which determine the major functional properties. However, it was decided to clone non-altered squash GPAT sequence in a pET24a vector in an identical manner to Q17b*. This clone was called Q24a and is identical to the published sequences of this region of squash GPAT. Also the *Arabidopsis* (A24a) and spinach GPAT (P24a) were re-cloned into the pET24a vector.

All constructs were transformed to and overproduced in *E. coli* BL21 (DE3) pLysS (section 5.2.2). The success and extend of the bacterial overproduction was confirmed via 10% SDS-PAGE analysis and is shown in figure 5.2.

Figure 5.2 Overproduction of recombinant stromal GPAT proteins; chimeras of *Arabidopsis*, squash and spinach GPAT

Compilation of Coomassie Blue stained 10% SDS-PAGE gels of crude total proteins from *E. coli* BL21 (DE3) pLysS cells, showing induction of overproduction of GPAT proteins.

Lanes 1 and 2 show total *E. coli* protein fractions at T = 0 hr. and T = 3 hr. respectively before and after induction of GPAT overproduction via IPTG addition.

(A) the results profiles for the 'wild-type' recombinant GPAT proteins.

(B) the induction profiles for chimeric GPATs.

The terminology is described in the text (also in section 5.2.1). Molecular weight standards are depicted in outlined numbers in the flanking lanes. Below the lanes, the outlined and underlined values indicate the molecular weight of the overproduced GPATs and the protein bands are indicated by arrowheads.

(A)

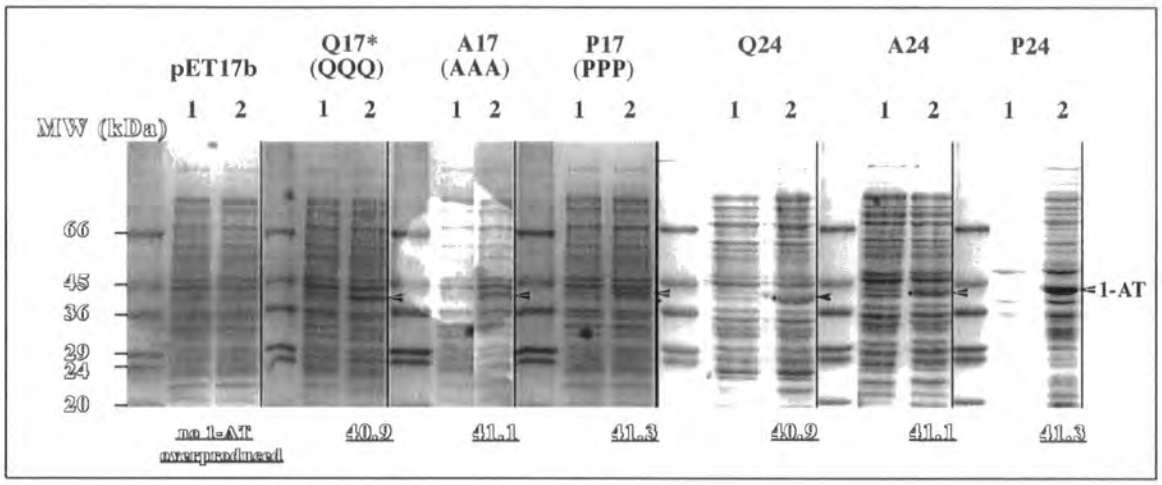
pET17b
Q17* (QQQ)
A17 (AAA)
P17 (PPP)
Q24
A24
P24
1 2
MW (kDa)
66
45
36
29
24
20
1-AT
no 1-AT overproduced
40.9
41.1
41.3
40.9
41.1
41.3

(B)

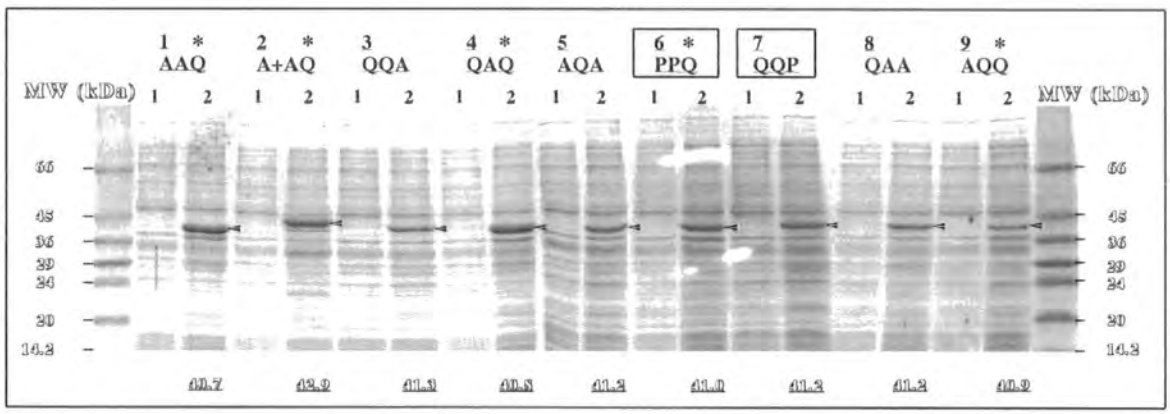
1 * AAQ
2 * A+AQ
3 QQA
4 * QAQ
5 AQA
6 * PPQ
7 QQP
8 QAA
9 * AQQ
MW (kDa)
1 2
66
45
36
29
24
20
14.3
40.7
42.9
41.3
40.8
41.2
41.0
41.2
41.2
40.9

As is previously described in the legend of Figure 3.1, the predicted squash GPAT pre-protein processing site (predicted protein processing site*) is currently thought to be before amino acid residue A43. There have been speculations (Nishida, I., personal communication) that the length, and/or, composition of the N-terminal sequence of the GPAT enzyme could have an influence on the substrate preference. To evaluate if these speculations could be true, a cDNA clone was constructed **identical** to the published sequences, and created to encode a mature squash GPAT enzyme on basis of the currently predicted protein processing site* with no residues attached originating from the overproduction vector.

In PCR-based cloning procedures (similar to section 5.2.1), the plasmid p4-1 (a pTZ18R based clone containing the 1781 bp. *Eco*RI cDNA sequence deposited in the computer database under Accession number Y00771; kindly provided by Nishida, I. for this study) was used as a DNA template for PCR. The primer oligonucleotides were designed to flank the resulting squash GPAT amplified DNA product with a *Nde*I site on the 5' end and a *Eco*RI site on the 3' end; pJKSQ5Nd1: 5'- CATTATA CATATG GCG GAG CTT ATC CAG GAT AAG G –3' and pSQ2AS: 5'- GAA AGA ATT CGG TTT TAT CTT ACA G –3'. The amplification product was purified, digested with *Nde*I and *Eco*RI and after purification subcloned to pET17b digested with the same restriction endonucleases. This construct was named **JKSQ+/17** and would encode a mature squash GPAT of 43.84 kDa, starting at the N-terminal flank with the residues MA(43)ELIQDKESAQSAAT-etc as is shown in figure 5.3 together with a comparison of the N-terminal residues of other squash GPAT proteins used in this study.

Figure 5.3 Creation and bacterial overproduction of the predicted mature squash GPAT protein encoded by JKSQ+/17

In the top part of the figure, schematic representations of the recombinant squash GPAT proteins from this study are depicted with their designation on the left. Amino acid sequences on the N-terminal part of the recombinant proteins, encoded by the respective pET vectors and cloning junctions, are in bold and underlined. The non-bold residues represent true GPAT protein residues. Also indicated are the HX_4D configuration and the position of two amino acid residues in the C-terminal domain which are aberrant in Q17b* encoded GPAT.

On the bottom left : a Coomassie Blue stained 10% SDS-PAGE of total *E. coli* extract before (lane 1) and after 3 hr. induction (lane 2) of overproduction of the GPAT protein encoded by construct JKSQ+/17.

The bottom left panel shows a table with results of the standard GPAT enzyme activity determination of the partially purified (CCE) overproduced JKSQ+/17 GPAT protein (5.2.3).

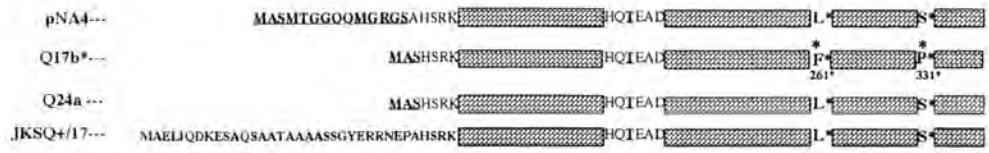

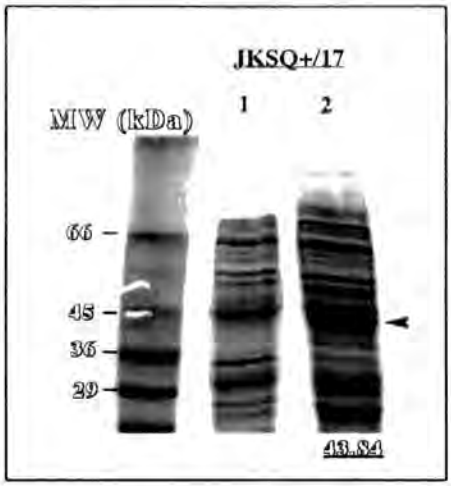

Table 1-AT Standard Activity Assay of JK/SQ+/17 CCE.				
Conditions: 80 µl //0.25 M Hepes pH 8.0/ 5 mg./ml. BSA/ 2 mM [U-^{14}C] G3P (2000 dpm./nmol)/ 0.4 mM 16:0-CoA//25 °C				
Sample	Concentration total soluble protein in CCE (µg/ µl)	Time (min.)	^{14}C dpm. ORGANIC PHASE	Volume CCE with standard 1-AT activity of 6000 dpm./ 5 min. (µl)
Background		0	186.95	
JKSQ+/17 2 µl	11.21	2	85245	0.07 - 0.1
		5	137317	
JKSQ+/17 4 µl	11.21	2	114003	0.1
		5	184037	

Crude cell-free extracts (CCE) of the *E. coli* BL21 (DE3) pLysS strains, overproducing the respective GPAT enzymes, were prepared (Materials and methods section 5.2.2). Total protein in the centrifuged lysates were quantitated via the Bradford method (BioRad dye reagent). As is illustrated in figure 5.4, volumes of CCE containing 10 µg total protein were electrophoretically separated on 10% SDS-PAGE gels and after Coomassie staining, the GPAT protein bands quantified via densitometry with known amounts of BSA present in lanes on the gels.

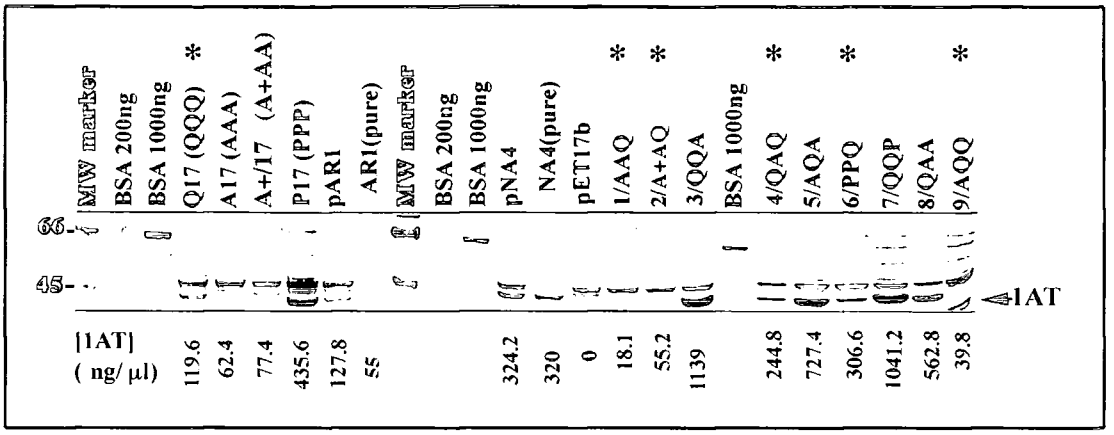

Figure 5.4 Coomassie Blue stained 10% SDS-PAGE gels of 10 µg total protein of CCE expressing soluble GPAT

Compilation of Coomassie Blue stained 10% SDS-PAGE gels containing standard amounts of CCE (10 µg total protein) of *E. coli* BL21 (DE3) pLysS strains, overproducing soluble GPAT enzymes (three gels were generated in one single experiment and treated identical). The identity of the samples is depicted above the lanes. The names for the recombinant GPAT enzymes are described in the text. As a standard for the densitometry determinations of the amount of GPAT protein per band (indicated by the arrow on the right), 200 ng and one thousand ng of BSA was run on the same gels. Control CCE was prepared from cells containing unmodified pET17b and molecular weight markers are depicted in kDa by outlined lettertype. The amounts of GPAT protein in the bands visible in these samples are indicated below the figure (in ng/µl CCE).

Additionally (routinely), 3 µg total CCE protein was tested for enzyme activity in the standard GPAT assay (section 3.2.2). From these determinations, the amounts of CCE (with quantitated amounts of GPAT protein) with an absolute activity of 6000 dpm per 5 min. in the standard GPAT assay, which would have a linear initial reaction rate in the SSA (standard selectivity assay) with acyl-ACP as substrates, were derived.
Results from standard GPAT activity determinations and the subsequently derived volumes of CCE, which were used in subsequent standard selectivity assays (SSA) and in kinetic experiments of the GPAT enzymes, are depicted in **Table 5.1**.

Table 5.1 The protein concentrations of *E.coli* crude cell-free extracts (CCE) and standard GPAT enzyme activities determine the amounts of GPAT protein to use in selectivity assays (SSA) and kinetic studies

ROW 1	2	3	4	5	6	
Conditions: 80 µl //0.25 M Hepes pH 8.0/ 5 mg./ml. BSA/ 2 mM |U-^{14}C| G3P (2000 dpm./nmol)/ 0.4 mM 16:0-CoA// 25 °C						
Sample	Concentration total soluble protein// concentration 1-AT in CCE (µg/ µl)	Assay 3µg total CCE protein (in µl)	^{14}C dpm. ORGANIC PHASE (not corrected) after 5 min.	Volume CCE with standard 1-AT activity of 6000 dpm/5 min.		
				(µl) used in competetive/selectivity studies	corrected values (µl) / amount of 1-AT enzyme (ng.) used in determination of kinetic parameters	
					(µl)	(ng. 1-AT)
pET17b	3.5	35 µg = 10 µl	298	-	-	-
Q17* (QQQ*)	2.1 // 0.1196	1.43	11706	0.75	0.134	16.03
A17 (AAA)	1.7 // 0.0624	1.76	6666	1.6	0.438	27.33
A+17 (A+AA)	1.95// 0.0774	1.54	6972	1.35	-	-
P17 (PPP)	3.6 // 0.4356	0.83	12623	0.4	0.665	289.7
pAR1	2.2 // 0.1278	1.5	6211	1.35	0.325	41.54
AR1 (pure)	- // 0.055	-	-	-	-	-
pNA4	2.5 // 0.3242	1.2	20529	0.35	0.033	10.7
NA4 (pure)	- // 0.320	-	-	-	-	-
1/AAQ*	2.07// 0.0181	1.5	1347	6.7	8.85	160.19
2/A+AQ*	1.93// 0.0552	1.6	857	11.22	-	-
3/QQA	3.03// 1.139	1	26862	0.22	0.017	19.36
4/QAQ*	1.74// 0.2448	1.7	19143	0.53	0.604	148
5/AQA	4.3 // 0.7274	0.7	16957	0.25	0.029	21.1
6/PPQ*	3.32// 0.3066	0.9	1702	3.17	5.09	1561
7/QQP	4.83// 1.041	0.6	42699	0.09	0.009	9.4
8/QAA	1.87// 0.5628	1.6	41947	0.23	0.045	25.33
9/AQQ*	3.57// 0.0398	0.9	1629	3.32	0.67	26.7

The term 'corrected value' refers to the volume of CCE which produces radiolabeled reaction product (LPA) corresponding to 6000 dpm./5 minutes in the standard GPAT assay, after correction for the background counts and the total volume of the lower aqueous phase containing the reaction products. This amount of GPAT enzyme preparation has a linear reaction velocity when using acyl-ACP as substrates under the assay conditions used.

5.3.2 Determination of the selectivity factor of recombinant chimeric GPAT and a squash GPAT mutant

Using the amounts of GPAT enzyme in crude cell-free extract (CCE) (as depicted in table 5.1) with a linear initial reaction velocity up to at least 2 minutes, the selectivity factor (SF) of the enzymes was determined in the standard selectivity assay (SSA). As described in Chapter III, section 3.4.3., the conditions for this assay are as close to physiological relevance as possible (300 μM G3P, 5 mg/ml BSA, an equimolar mixture of [1-^{14}C] 16:0-ACP and [9,10(n)-^{3}H] 18:1-ACP at 1 μM each, at pH 8.0) and reflect the *in vivo* behaviour of squash GPAT and *Arabidopsis* GPAT in the best way (Figure 3.10, panel D). The selectivity factor (SF) was calculated on basis of the ratio between the initial reaction velocity with 18:1-ACP over the initial reaction velocity with 16:0-ACP.

When assaying the CCE with the different recombinant squash GPAT enzymes, a surprising and unexpected selectivity of Q17b* was observed (Figure 5.5).
The squash GPAT encoded by the **pNA4** was also described and tested in Chapter III and, as in previous studies, was confirmed to be a non-selective enzyme with a SF of about 1.1. Like the enzyme encoded by pNA4, the GPAT encoded by **Q24a** was based on the previously reported protein processing site** (E70) (Chapter III, figure 3.1) and its sequence was identical to the published sequences for this region of the protein (Acc. Nr. Y00771 or P 10349). However, the N-terminal residues encoded by the overexpression vectors and cloning junctions differed, and less residues were attached to the Q24a based protein, as is illustrated in figure 5.5 (A). The protein was created in this manner, to be identical to the recombinant fusion protein used by Ferri and Toguri (Ferri, S.R. and Toguri, T., 1997) and to be able to relate both studies. It was shown that the enzyme from Q24a had a similar SF (0.9) to the one encoded by pNA4, indicating that a small alteration on the N-terminus did not affect the selectivity.
To investigate a potential influence of a larger N-terminal sequence and to create the GPAT protein thought to be the actual mature enzyme, based on a newly predicted protein processing site* (A43), **JKSQ+/17** was constructed. It was found that the protein encoded by JKSQ+/17 was also non-selective and on basis of absolute activity (little difference in the velocity of the reaction) and a SF of 1.2, was functioning in the same way as the squash GPATs from pNA4 and Q24a. Again this illustrated that moderate variation of the N-terminal sequence of the mature squash GPAT enzymes, does not have a significant influence on the substrate selectivity under these conditions.

Figure 5.5 One or two amino acid substitutions in the C-terminal protein domain of squash soluble GPAT (1-AT) dramatically changes substrate selectivity

(A) schematic diagrams of the squash GPAT proteins used in this study and is a similar illustration to the one shown in figure 5.3, but this is meant for easy identification of the recombinant proteins used in the SSA (for description see the legend of figure 5.3 and the text). The HX_4D configuration and the position of two amino acid residues in the C-terminal domain which are aberrant in Q17b* encoded GPAT are also indicated.

(B) The results from (at least three repeats) standard selectivity assays (SSA) of recombinant soluble squash GPAT proteins in *E. coli* crude cell-free extracts (CCE). The initial reaction velocities of the GPAT proteins with the substrates are indicated by the lines. The amount of reaction product (pmol LPA) is plotted against the time (minutes). The lines represent a regression calculation of the various points in the time series and the name of the GPAT and the substrate used, are indicated beside the lines. The selectivity factor (SF) for each of the GPAT enzymes boxed in the top left corner of each of the graphs.

A Schematic diagrams of the recombinant squash 1-AT proteins examined in this study

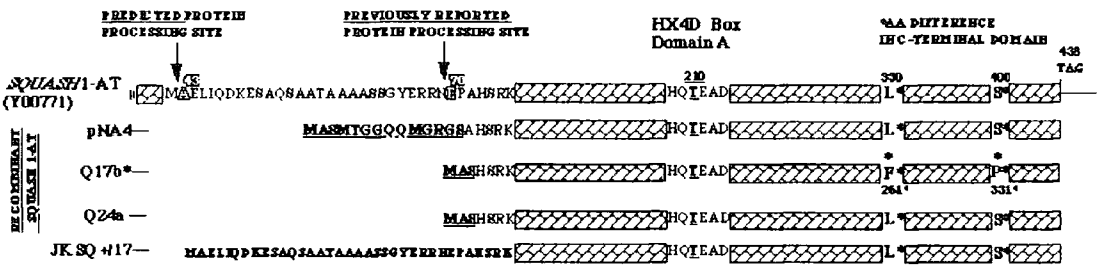

B Dual Selectivity Assay on Recombinant Squash 1-AT enzymes:
Ratio: rate of transfer of 18:1-ACP over 16:0-ACP

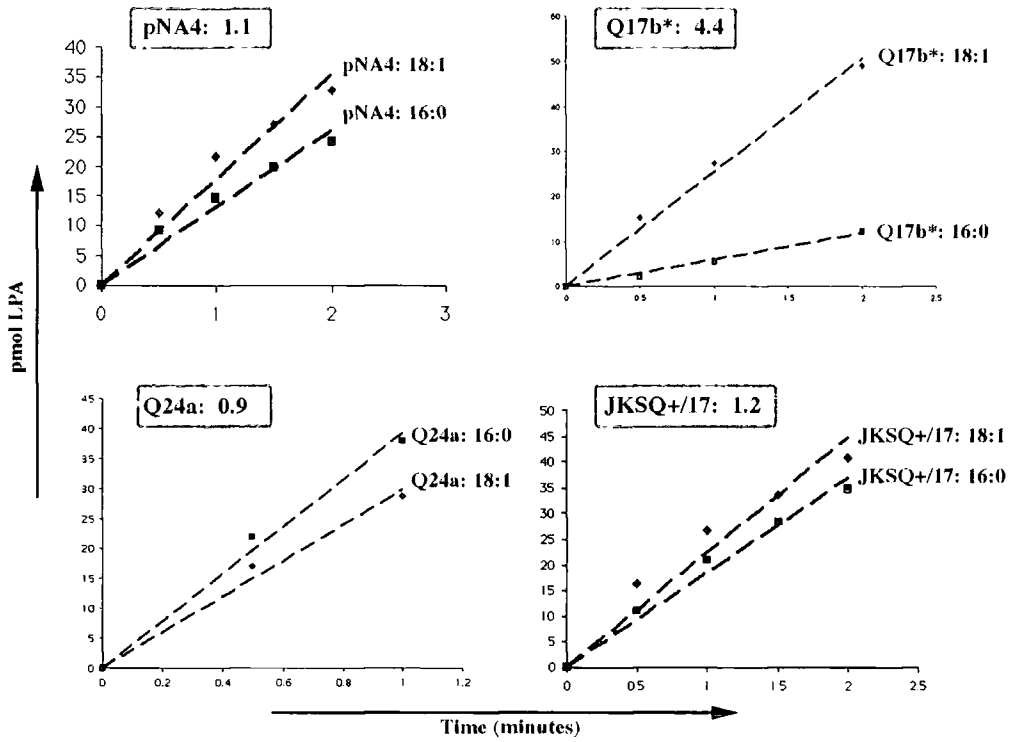

The squash GPAT enzymes encoded by **Q24a and Q17b*** are identical, except for the two amino acid substitutions in the carboxyl (C-) terminal third of the Q17b* based GPAT protein.
It was determined that the **Q17b*** encoded GPAT enzyme had a **SF of 4.4**, which is similar to the selectivity factor found for the *Arabidopsis* derived soluble GPAT protein (Figure 3.10 and below) and indicates that the mutant enzyme has four times higher selectivity for unsaturated (18:1-) acyl chains. It seems that either one or both of the amino acid substitutions **L (Leucine) 261 to F (Phenylalanine) 261** and/or **S (Serine) 331 to P (Proline) 331**, introduces a variation in the secondary or tertiary structure of the GPAT enzyme which influences its substrate selectivity.

The most extreme differences in selectivity factors (SF), determined in the standard selectivity assay (SSA) of CCE of the overproduced chimeric GPAT enzymes, are summarised in figure 5.6 and all selectivity factors are depicted in Table 5.2.

The P17b based spinach GPAT displayed a 15 fold preference (SF = 15) for 18:1-ACP and clearly shows that spinach GPAT is an extremely oleophylic enzyme (a factor 9 x was determined by Frentzen, M. et al. (1983). Also the 'wild-type' pAR1 and A17b encoded *Arabidopsis* GPAT is selective for 18:1 chains with a SF of about 4.3. Both these findings would be expected for the soluble GPAT of these chilling resistant plants.

Chimeric GPAT enzymes created during this study contained the mutant C-terminal region of the Q17b* encoded enzyme and this was proven to have an effect on the overall selectivity of the, normally non-selective, squash GPAT. However, it was found that certain domainswaps between the *Arabidopsis* and squash GPAT, and between spinach and squash GPAT, had dramatic effects of the substrate selectivity of the enzymes.
Substitution of the amino (N-) terminal domain appeared to have no significant or only a very small influence on the selectivity of the enzymes. This is illustrated by analysis of A17b (AAA) with and SF=4.3 and QAA with a SF= 4.4, or Q17b* (QQQ*) with SF=4.4 and AQQ* with SF=4.4 (Table 5.2).
Also the transfer of the carboxyl (C-) terminal third domain of the spinach or *Arabidopsis* GPAT on their own, did not have a significant influence on the selectivitiy. Illustration of this is by comparing Q24a (QQQ) (or pNA4 or JKSQ+/17) with SF~ 1.0 to QQA with SF=1.6 or QQP with SF=2 (Table 5.2).

Figure 5.6 Extreme variations in selectivity of recombinant soluble GPAT enzymes and chimeras for acyl-ACP substrates

Depiction of representative results from (at least three repeated) standard selectivity assays (SSA) of different recombinant soluble GPAT proteins and their chimeras, in *E. coli* crude cell-free extracts (CCE).

The initial reaction velocities of the GPAT proteins with the substrates, are indicated by the lines. The amount of reaction product (pmol LPA) is plotted against the time (minutes). The lines represent a regression calculation of the various points in the time series and the name of the GPAT and the substrate used are indicated beside the lines. The selectivity factor (SF) for each of the GPAT enzymes are shown in the squared box in the top left corner of each of the graphs.

Row **(I)** illustrates the effect of the combination of the C-terminal of the Q17b* based squash GPAT with the central domain of the oleophylic A17b based *Arabidopsis* GPAT.

Row **(II)** the effect of the 2 amino acid substitutions in the C-terminal domain of squash GPAT proteins (Q24a versus Q17b*), together with the influence on the selectivity by a domainswap with the central domain of the oleophilic *Arabidopsis* GPAT.

Row **(III)** illustrates the same effect as described for row (I), on the oleophylic spinach (P17) GPAT enzyme.

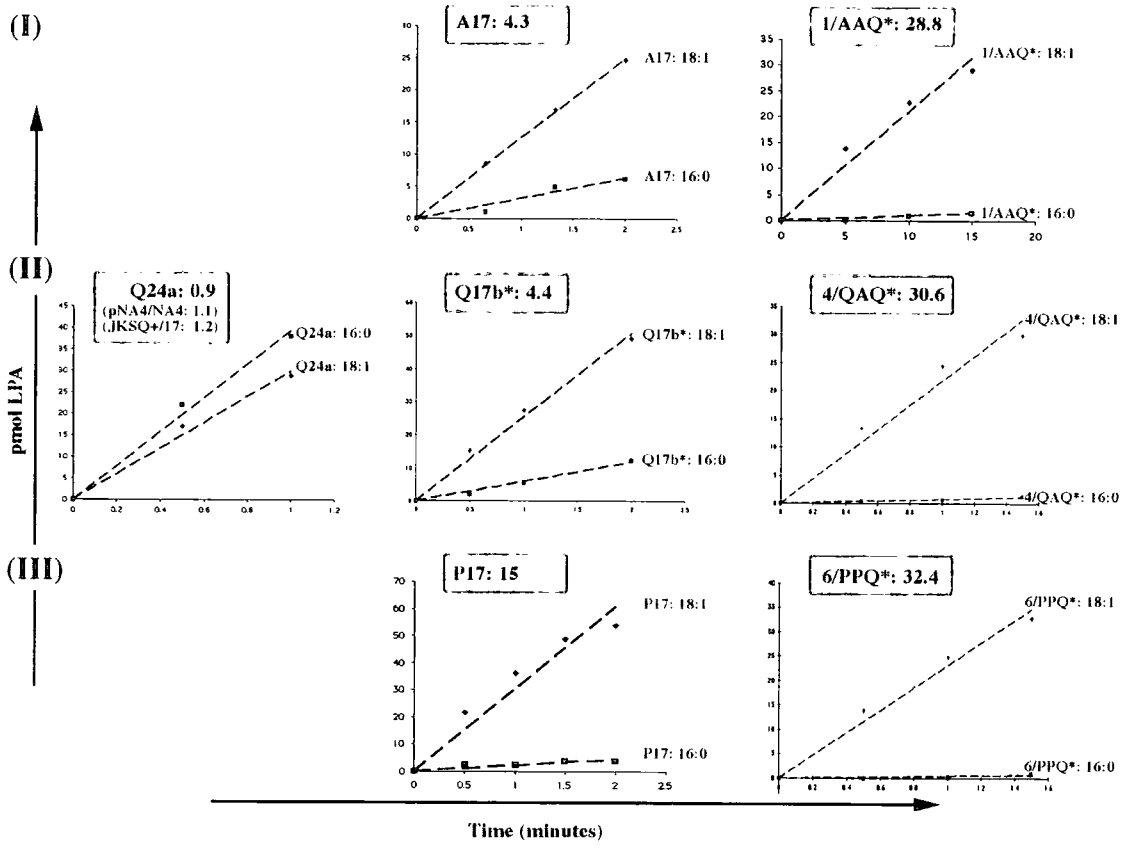
(I)
(II)
(III)
pmol LPA
A17: 4.3
A17: 18:1
A17: 16:0
1/AAQ*: 28.8
1/AAQ*: 18:1
1/AAQ*: 16:0
Q24a: 0.9
(pNA4/NA4: 1.1)
(JKSQ+/17: 1.2)
Q24a: 16:0
Q24a: 18:1
Q17b*: 4.4
Q17b*: 18:1
Q17b*: 16:0
4/QAQ*: 30.6
4/QAQ*: 18:1
4/QAQ*: 16:0
P17: 15
P17: 18:1
P17: 16:0
6/PPQ*: 32.4
6/PPQ*: 18:1
6/PPQ*: 16:0
Time (minutes)

The most striking findings of these experiments were that the **central domains** of the respective GPAT enzymes conferred the functional property (selectivity) of the GPAT from which the domain originated, to the domainswap chimeric molecule. A clear illustration of this finding is, for instance, the influence on the selectivity of a substitution of the central domain of the A17 (AAA) based GPAT with SF= 4.3, with a squash GPAT central domain. This seems to confer the selectivity of the 'wild-type' squash GPAT (Q24a/pNA4 or JKSQ+/17 based GPAT with SF~ 1.0) onto the chimera AQA (SF=1.5).

Interestingly, when the **C-terminal domain** of squash GPAT was combined with the central third of an oleophilic GPAT from *Arabidopsis* or spinach, the oleophylicity conferred by the central domain was even more pronounced. Similar findings were reported by Ferri, S.R. and Toguri, T. (1997). For instance, the selectivity of Q17b* (QQQ*) based GPAT reconstructed to QAQ* changed from SF=4.4 to SF= 30.6 respectively. The same effect was illustrated by the reconstruction from A17b (AAA) (SF=4.3) to AAQ* (SF=28.8), or P17b (PPP) (SF=15) to PPQ* (SF=32.4). It does appear that the central regions of the GPAT enzymes do contain essential structural features, which give the GPAT enzymes their most important functional properties, such as selectivity for their substrates. However, also amino acid residues in the C-terminal domain of the enzyme appear to dramatically influence the affinity or selectivity for its substrates. It seems likely that there are secondary or tertiary variations in the C-terminal domain which influence the ability of (at least the squash-) GPAT to use 16:0- acyl chains as a substrate.

5.3.3 Determination of apparent kinetic constants of recombinant chimeric GPAT and a squash GPAT mutant for 18:1-ACP and 16:0-ACP

The apparent kinetic properties of recombinant soluble GPAT , the Q17b* encoded mutant squash GPAT and the chimeric GPAT enzymes, were studied under steady-state conditions.
The GPAT enzymatic reaction seems to follow Michaelis-Menten kinetics. Under the assay conditions used the reactions were determined to have linear initial reaction velocities for at least 2 minutes, with occurrence of less than 10 –20% of total substrate consumption. Crude cell-free extracts (CCE) of *E. coli*, in which the recombinant GPAT enzymes were overproduced, were used as the enzyme source. The volumes of CCE and the amount of enzymatically active GPAT protein (in ng.) present in that CCE sample (as determined by densitometry of Coomassie stained 10% SDS-PAGE gels, with BSA as standards) which were used in the kinetic studies, are depicted in the last column of Table 5.1.

The apparent kinetic parameters of recombinant GPAT enzymes for 18:1-ACP and 16:0-ACP were determined under the reaction conditions specified in the legend for Figure 5.7 (B). The assay reactions were generally manipulated as for the standard GPAT assay and important to note is that the pH was 8.0.

In first instance it would be interesting to investigate, if the differences in selectivity between the recombinant *Arabidopsis* GPAT (A17), the squash GPAT (pNA4) and the mutant squash GPAT (Q17b*) correlate to differences in the apparent kinetic data for the acyl-ACP substrates.

Lineweaver-Burke plots for both sets of data for A17-GPAT, pNA4-GPAT and Q17b*-GPAT are shown in Figure 5.7 (B).

Figure 5.7 Substrate selectivity and apparent kinetic constants for acyl-ACP shows an obvious Km effect for 16:0-ACP in the Q17b* encoded squash GPAT

(A) Results from (at least three repeated) standard selectivity assays (SSA) of soluble GPAT proteins encoded by pAR1 and A17 (*Arabidopsis*) (row **(I)** and pNA4 (mature squash 'wild-type') and Q17b* (mature squash mutant) (row **(II)**, in *E. coli* crude cell-free extracts (CCE). The principle of the figure description is identical to figure 5.6 The selectivity factor (SF) for each of the GPAT enzymes are boxed in the top left corner of each of the graphs.

(B) Lineweaver – Burke plots of initial velocity, with a fixed glycerol-3-phosphate concentration versus varying concentrations of acyl-ACP (in μM) using CCE preparations of GPAT. Standard assay conditions were used, except the pH was 8.0, with 0.30, 0.44, 0.76 and 2.2 μM 18:1-ACP or 16:0-ACP using a fixed concentration of G3P (20 mM).

Initial velocity was measured over 1 minute for

(I) *Arabidopsis* GPAT (A17 ; 0.438 μl. = 27.33 ng) and

(II + III) recombinant squash GPAT (pNA4 ; 0.033 μl CCE = 10.7 ng or

Q17b*; 0.134 μl = 16.03 ng).

The Vmax values were calculated in pmol.min $^{-1}$ per microgram of GPAT protein and the apparent Km values are calculated in μM for acyl-ACP.

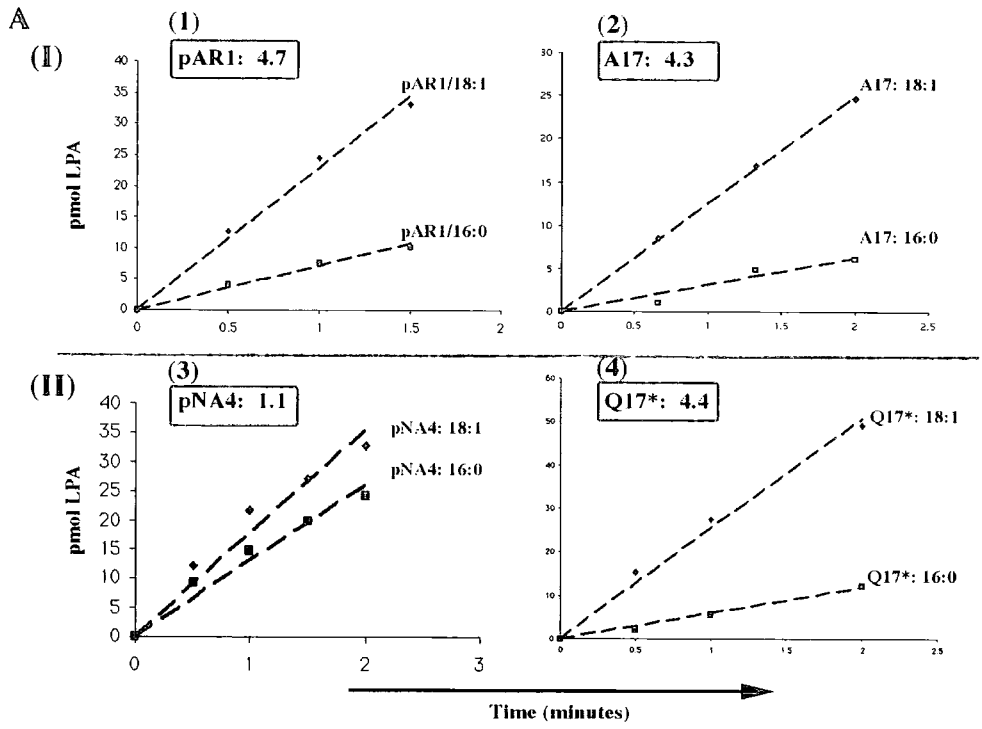
A
(I)
(1)
pAR1: 4.7
pAR1/18:1
pAR1/16:0
pmol LPA
(2)
A17: 4.3
A17: 18:1
A17: 16:0
(II)
(3)
pNA4: 1.1
pNA4: 18:1
pNA4: 16:0
pmol LPA
(4)
Q17*: 4.4
Q17*: 18:1
Q17*: 16:0
Time (minutes)

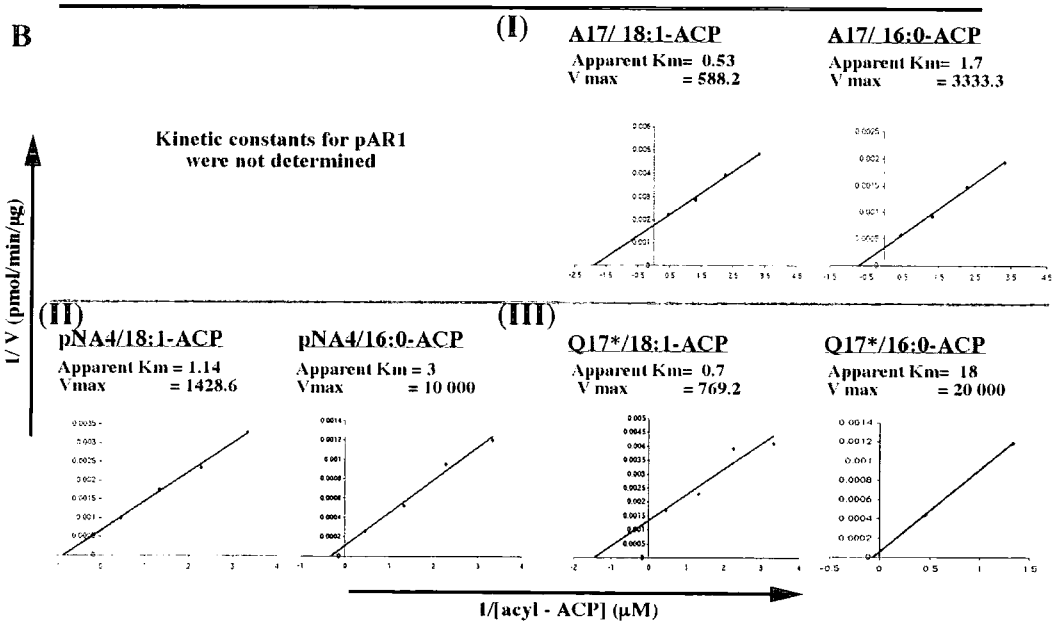
B
(I)
A17/ 18:1-ACP
Apparent Km= 0.53
V max = 588.2
A17/ 16:0-ACP
Apparent Km= 1.7
V max = 3333.3
Kinetic constants for pAR1
were not determined
1/ V (pmol/min/µg)
(II)
pNA4/18:1-ACP
Apparent Km = 1.14
Vmax = 1428.6
pNA4/16:0-ACP
Apparent Km = 3
Vmax = 10 000
(III)
Q17*/18:1-ACP
Apparent Km= 0.7
V max = 769.2
Q17*/16:0-ACP
Apparent Km= 18
V max = 20 000
1/[acyl - ACP] (µM)

In the standard selectivity assay (SSA), acyl-ACPs were present at a total concentration of 2 μM. In the kinetic determinations, the concentrations of acyl-ACP were in the range 0.3 – 2.2 μM. In plant cells (*in vivo*) acyl-ACPs are present in a concentration range of 0.6 – about 3 or 4 μM. In predictions for the selectivity of the GPAT enzymes in a physiological environment this situation has to be taken into account.

When considering the **Km values for the acyl-ACPs** in Figure 5.7, all Km values are within a **physiological concentration range**, with one major exception.
An apparent Km of 18 μM for 16:0-ACP for the mutant squash GPAT encoded by **Q17b*** was 6 fold higher than that of the 'wild-type' GPAT encoded by pNA4 and greatly out of a physiological concentration range. This will have a major influence on the enzymes affinity for 16:0-ACP which is demonstrated by its effect on the selectivity. The Q17b* encoded GPAT enzyme became oleophylic (SF=4.4). It seemed that 18:1 activity was almost normal but 16:0 activity was reduced under the levels of acyl-ACP in the assays.

When considering both the recombinant **squash GPAT** enzymes, it was interestingly to observe the following results.

Although it was determined that 'wild-type' squash GPAT (**pNA4**) is a non-selective enzyme (SF=1.1), the apparent Km of 3 μM for 16:0-ACP was at least two times higher than its apparent Km of 1.14 μM for 18:1-ACP. However, it seemed that the velocity for its usage of 16:0-ACP (Vmax = 10 000 pmol.min $^{-1}$ per microgram) was about 7 fold higher than the Vmax for 18:1-ACP (1428.6 pmol.min $^{-1}$ per microgram). In a physiological environment the kinetic properties of the enzyme may well balance out against each other and effectively make squash GPAT a non-selective enzyme.

Although the mutant squash GPAT (**Q17b***) had an even higher Vmax for 16:0-ACP (20 000 pmol.min $^{-1}$ per microgram), its Km was extremely high.
When considering the kinetic data for the recombinant ***Arabidopsis* GPAT (A17)**, it was found that also for this enzyme, the Vmax for 16:0-ACP was higher than that for 18:1-ACP. But again also the Km for 16:0-ACP (1.7 μM) is higher than that for 18:1-ACP (0.53 μM).

The apparent kinetic data of the Q17b* based GPAT for 18:1-ACP were very similar to the ones for the recombinant *Arabidopsis* GPAT (A17) however the kinetic constants for 16:0-ACP are strikingly different.
Interestingly, under the conditions used in the standard selectivity assay (SSA) their selectivity factor (SF) was almost identical (about 4.3).

Generally, it appears that GPAT enzymes have a greater affinity for 18:1-acyl chains but seem to be able to use 16:0-acyl chains with greater speed during catalysis. A fine balance of the kinetic parameters of the GPAT enzymes (determined by their structure) and the accessibility to substrates may well determine their selectivity under physiological conditions. Therefore, in an *in vivo* situation (in plant cells) not only the physical state of the enzyme but also the pool size, distribution and physical presentation (association with proteins) of the substrates G3P and acyl-ACPs are of major importance.

The apparent kinetic parameters for 18:1-ACP and 16:0-ACP of **all** the recombinant GPAT enzymes examined are summarised, together with the selectivity factors, in Table 5.2.

Table 5.2 Substrate Selectivity and Kinetic Constants of Recombinant Wild-Type - and Chimeric 1 - ATs for Acyl-ACPs

1-AT (G3P-AT)	Substrate Selectivity Ratio of initial rate of transfer $\frac{V_{18:1\text{-ACP}}}{V_{16:0\text{-ACP}}}$	* Apparent V_{max} | K_m 18:1-ACP		* Apparent V_{max} | K_m 16:0-ACP	
pNA4 (NA4)	1.1	1429	1.14	10 000	3
JKSQ+/17	1.2	ND	ND	ND	ND
Q24a	0.9	ND	ND	ND	ND
Q17b*	4.4	769	0.7	20 000	18
4/QAQ*	30.6	2500	6	1111	11.9
3/QQA	1.6	769	0.54	3333	1
9/AQQ*	4.4	385	0.46	5000	8
pAR1(AR1)	4.7 (4.3)	ND	ND	ND	ND
A17	4.3	588	0.53	3333	1.7
5/AQA	1.5	500	0.2	1429	0.43
1/AAQ*	28.8	2000	5.2	213	6.7
8/QAA	4.4	667	0.27	3333	1.67
P17	15	1000	4.2	2000	8.6
7/QQP	2	1429	0.43	16 666	3.33
6/PPQ*	32.4	204	5.2	104	11.35

ND = not determined; 1-AT = glycerol-3-phosphate acyltransferase (GPAT)

5.4 Conclusion

In this study, an examination of the structure-function relationship of the soluble glycerol-3-phosphate acyltransferase (GPAT) from *Arabidopsis* , spinach and squash, is presented. Chimeric recombinant proteins of *Arabidopsis* and squash GPAT, and of spinach and squash GPAT respectively, were constructed. Also the influence of variations in the N-terminal domain and two single amino acid substitutions in the C-terminal domain of the recombinant squash GPAT on the selectivity, was investigated. The selectivity and kinetic constants for the 18:1-ACP and 16:0-ACP substrates of the recombinant GPAT enzymes were determined.

Some striking alterations of the selectivity and kinetic parameters for some of the newly created recombinant GPAT enzymes were observed. The central domains of the respective GPAT enzymes appeared to contain essential structural requirements which confer the main functional properties to a soluble GPAT protein. The amino (N-) terminal domains appears to play only a minor role on catalytic and other functional properties. However, when the carboxyl (C-) terminal domain of the non-selective squash GPAT was combined with the central third of an oleophilic GPAT (from *Arabidopsis* or spinach), the oleophylicity determined by the central domain was even more pronounced.

The two, coincidentally introduced, amino acid substitutions L 261 to F 261 and S 331 to P 331 in the C-terminal domain of the mutant squash GPAT (**Q17b***), appeared to cause an apparent increase in the Km for 16:0-ACP (up to 18 μM). This greatly reduced the capacity of the enzyme to select 16:0-ACP under physiological conditions and effectively caused the Q17b* based GPAT enzyme to become as oleophylic (SF=4.4) as an *Arabidopsis* GPAT (A17 or pAR1 encoded).

Recently, other researchers in our laboratory are systematically using site directed mutagenesis to substitute amino acid residues, which are thought to play a vital role in determining the properties of the soluble GPAT enzymes. It has been shown that only the single amino acid substitution L 261 to F 261 substitution in the Q17b* based squash GPAT, causes the reported effect upon acyl-ACP substrate selectivity

It is quite obvious that under physiological conditions, a refined balance of the kinetic parameters of the GPAT enzymes, as is dictated by their overall structure, in combination with their physical environment, determine their functional properties and phenotypic behaviour.

As is illustrated by the data in **Table 5.2**, a general conclusion is that **all** soluble GPAT enzymes have a greater affinity for 18:1-acyl chains, as is demonstrated by their lower Km for 18:1-ACP substrate.
However, most GPAT enzymes, seem to be able to use 16:0-acyl chains with greater speed during catalysis, as can be concluded from their higher Vmax values for 16:0-ACP substrates.
The notable exceptions to this generalisation were occurring when carboxyl (C-) terminal domain of the non-selective squash GPAT was combined with the central third of an oleophylic GPAT enzyme. In this type of chimeras it may well be that there are certain secondary and tertiary structure variations in the enzyme, generally causing the Km values for both acyl-ACP substrates to increase but more strikingly, reducing the Vmax values for the 16:0-ACP substrate. The overall effect of this was that the selectivity for 18:1-ACP, determined by the central domain, was even more pronounced.

From the studies by Ferri, S.R. and Toguri, T. (1997) and in the work presented in this thesis, it is quite clear that the, highly conserved, central domain of soluble GPAT enzymes, contains most of the major structural requirements for its overall activity. Lewin, T.M. et al. (1999) reported on the analysis of amino acid motifs diagnostic for the *sn*-glycerol-3-phosphate acyltransferase reaction. Alignments of amino acid sequences from various acyltransferases revealed four regions of strong homology, designated blocks I – IV. Conserved residues in blocks I – IV have been shown to be potentially involved with GPAT catalysis and glycerol-3-phosphate binding from site directed mutagenesis and chemical modification studies. However, the soluble GPATs cloned from several plant species were not included in their homology table, which represented mainly membrane-bound enzymes from bacteria, nematodes and mammals, because they lacked blocks III and IV. This suggests a difference in the catalytic domain of these soluble plant GPATs and membrane-bound GPATs. Homology based comparisons of primary sequences seems not to suffice to identify membrane-bound GPATs in plants. Indications for amino acid residues which may play a vital role in the catalytic mechanism of GPAT enzymes in general also come from, for instance, some reported studies of membrane-bound GPAT from *Escherichia coli* (*plsB*) and the bifunctional 2-acyl-glycerophosphoethanolamine acyltransferase/ acyl-ACP synthetase (*Aas*) (Heath, R.J. and Rock, C.O., 1998) and mitochondrial GPAT from rat (Bhat, G.B. et al., 1999).
Primary sequence comparisons of membrane-bound and some soluble GPAT proteins revealed that that these proteins share a highly conserved domain in the central third of the

protein. The H4XD configuration, also designated as 'Block I' in Lewin, T.M. et al. (1999) contains an invariant histidine (H) and aspartic acid residue (D) which have been proven to be important for acyltransferase activity.

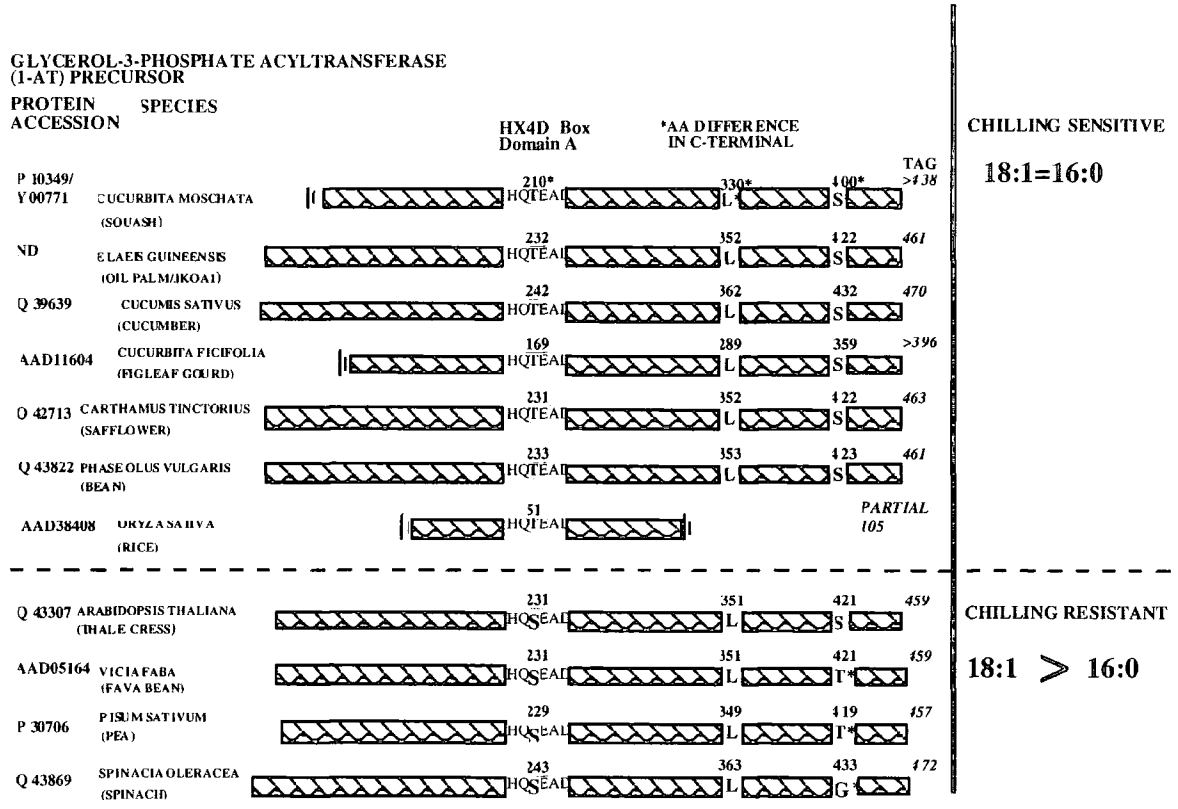

Figure 5.8 The H4XD configuration in the central domain of GPAT is vital for the acyltransferase activity

Schematic representation of the soluble GPAT proteins from plants. The protein sequences were aligned to illustrate the difference of the third amino acid residue within the H4XD configuration, between the enzymes from chilling resistant plants and non-selective enzymes, mostly from chilling sensitive plants. Genbank Accession numbers are indicated on the left.

Another interesting speculation is that the H4XD domain might be somehow involved in determining the selectivity for 18:1-ACP or 16:0-ACP. When comparing the primary sequences of the known soluble GPAT enzymes from chilling-sensitive plants with those from known chilling-resistant plants, the third amino acid residue within the H4XD domain appears to be a threonine (T) in non-selective GPAT and a serine (S) in 18:1-ACP preferring GPAT enzymes (Figure 5.8). The importance of this amino acid in this context and other amino acid residues important for GPAT catalysis, G3P binding, acyl-ACP selection and maybe even other properties such as binding to inhibitors, subcellular localisation or interaction with other proteins, can be tested by site directed mutagenesis.

Chapter VI

∞∞∞∞∞

Developing Ribozyme Technology for Specific Gene Inactivation of Endogenous Glycerol-3-Phosphate Acyltransferase in *Arabidopsis*

6.1 Introduction

Originally, this study was in context of an industrially funded project (Nickerson Biocem, now: Biogemma) aimed at engineering increased content of erucic acid (22:1 Δ^{13}) in oilseed rape. Limitations on the levels of erucic acid attainable in oilseed rape are due to the inability of rape LPAT to put this fatty acid at the *sn*-2 position of triacylglyceride. It was projected that the levels of erucic acid in the seed could be elevated via a dual strategy of isolating the membrane bound 1-acyl-*sn*-glycerol-3-phosphate acyltransferase (2-AT or LPAT [E.C. 2.3.1.51) from *Limnanthes douglassii*, and, after introduction of this gene into an HEAR (High Erucic Acid Rape) cultivar, to isolate the endogenous rape LPAT and subsequently use ribozyme (Rz) technology for downregulation of its gene product (Brown, A.P. et al., 1995; Brough, C.L. et al., 1996; Bourgis, F. et al., 1999). At the time, the project was not in a sufficiently advanced stage to evaluate ribozyme technology directed against LPAT, mainly because these membrane bound LPAT enzymes, from rape, involved in the storage triglyceride pathway had not been isolated yet. Research on ribozyme technology and the *in vivo* application in plants are still relatively not very advanced areas in science.
Therefore a series of experiments was designed to examine the efficacy of ribozyme technology in specifically downregulating another type of acyltransferase within a plant-system, reflecting a very similar concept.

The basic strategy was to develop a plant-system in which the effect of *in vivo* activity of ribozymes directed against an endogenous stromal glycerol-3-phospate acyltransferase (1-AT; GPAT) [E.C. 2.3.1.15] could be phenotypically recognised.
This approach could be divided in two sets of experiments. First, the creation, analysis and selection of transgenic *Arabidopsis* plants, expressing a squash soluble GPAT and the evaluation of the suitability of a severe chilling treatment protocol for use in phenotypic scoring experiments is described in this Chapter. Second, as described in Chapter VII, the design and construction of hammerhead ribozymes (Rz) for *in vitro* Rz activity testing and for use in the second plant-transformation (gene-stacking) of a selected transgenic plant (squash GPAT transgene) for *in vivo* Rz activity evaluation.

The considerations for the strategy of the experiments, the design of the constructs, the analysis of constructs and plants and the results are described.

The chilling sensitivity of a considerable range of plants is a phenomenon of agricultural interest as well as a topic of some scientific controversy and questions. Chilling-sensitive plants, among which many economically important crops such as soybean, maize, rice, cotton and also squash, cucumber, green bean, green pepper and castor bean, undergo reductions in development, growth rate, stress symptoms and some could even die at low temperatures (between 0 and 12 °C). In contrast, most plants originally of temperate climates, such as *Arabidopsis*, spinach, fava bean and pea, are able to grow at these chilling temperatures and are termed chilling-resistant.
One of the most enduring hypotheses concerning the physical and physiological change of certain plants under exposure to low temperatures, proposes that molecular species of chloroplast phosphatidylglycerol (PG) containing saturated fatty acid (16:0 or 18:0) or 16:1-*trans* at both the *sn*-1 and *sn*-2 position of the glycerol backbone confer this chilling sensitivity on plants (Murata, N. and Yamaya, J., 1984; Murata, N. et al., 1992). Because the *sn*-2 position of chloroplastic PG contains 16:0 and 16:1-*trans* (physically similar to saturated fatty acids) exclusively, the amounts of these disaturated, high-melting-point PG (HMP-PG) molecular species mainly depends on the selectivity of the plastidial GPAT. Therefore, the substrate selectivity of plastidial soluble GPAT has been shown to be an important determinant of chilling sensitivity in higher plants (Murata, N., 1983; Murata, N. et al., 1992; Wolter, F.P. et al., 1992). The soluble GPAT in chilling-resistant plants has a dominant preference for 18:1-ACP. The soluble GPAT in chilling-sensitive plants appears non-selective and uses both 18:1 and 16:0 at similar rates and so higher levels of HMP-PG are produced in these species.

Recently, it has become clear that the phenomenon of chilling-sensitivity is likely to be more complex and it has been suggested that HMP-PG alone cannot account for chilling-sensitivity of plants in general (Wu, J. and Browse, J., 1995). The increased content of HMP-PG molecular species (from 20% to 42%) in the leaf PG of the *fatty acid biosynthesis* (*fab1*) mutant of *Arabidopsis*, is a higher percentage than that is found in many chilling-sensitive plants. Nevertheless, compared to wild-type controls, the *fab1* mutants are unaffected by a range of 'short exposure' chilling (low temperature) treatments that lead quickly to the death of cucumber and other chilling-sensitive plants. These treatments included a relatively severe treatment by exposure to 2 °C for up to 7 days under constant light. However, after a severe chilling treatment by prolonged exposure (beyond two weeks) to low temperature also the *fab1* plants eventually showed damage (chlorosis and further deterioration). This latter observation was important because it prompted the researchers to consider a different view of chilling-sensitivity. It may be that some tropical and subtropical plant species, that evolved in warmer habitats, acquired traits only affecting plant performance after extended cold treatment (the GPAT mediated effect) and others would undergo damage on the shorter time scale normally associated with 'classical' chilling-sensitivity (Wu, J. and Browse, J., 1995).

The delayed damage observed in these experiments may be mediated through a requirement for certain PG species in long term maintenance processes in the chloroplast (Nishida, I. and Murata, N., 1996; Wu, J. et al., 1997). Thus, even though elevated levels of HMP-PG do not lead to rapid plant damage and death, they may be incompatible with (long term) growth in a cold climate.

This perception of chilling-sensitivity did not directly compromise the practical approach of the experimental strategy within this study. The severe, prolonged low-temperature exposure, chilling treatment protocol for experiments with *Arabidopsis* appeared to be the most suitable for use in phenotypic scoring experiments, to investigate the effect of potential variations in the HMP-PG levels of transgenic plants induced by differences in soluble GPAT activity.

It has been demonstrated that it is possible to genetically manipulate the fatty acid unsaturation in PG by the introduction of an appropriate acyltransferase (GPAT) and consequently that this can alter plant chilling-sensitivity.

Tobacco plants transformed with a cDNA of soluble GPAT from squash, a chilling-sensitive plant, had a higher content of HMP-PG and the chilling-sensitivity was also increased. When a cDNA of soluble GPAT from *Arabidopsis*, a chilling-resistant plant, was introduced in tobacco, the relative level of HMP-PG and also the chilling-sensitivity of the plants was decreased (Murata, N. et al., 1992). Also, rice plants transformed with a similar *Arabidopsis* GPAT construct displayed decreased percentage of HMP-PG and decreased chilling-sensitivity (Yokoi, S. et al., 1998).

Even, normally chilling-resistant, *Arabidopsis* plants transformed with a modified version of the *Escherichia coli* GPAT gene (*plsB*), showed an increase of 16:0 in all the membrane lipids. The fraction of HMP-PG was elevated and transgenic plants were more susceptible to chilling-treatments of 7 days incubation at 4 ^{0}C and return to standard growth conditions (Wolter, F.P. et al., 1992).

The main aim of the experiments described in this Chapter was to initially genetically engineer an *Arabidopsis* plant to express a squash soluble GPAT at a high level and still maintain chilling resistance. A second transformation, or gene-stacking, of a selected plant line with an *in trans* working hammerhead ribozyme (Rz), constructed to specifically target the endogenous *Arabidopsis* soluble GPAT mRNA, could result in a chilling sensitive phenotype if the Rz functions *in vivo*.

6.2 Materials and methods.

6.2.1 Procedures used during construction of the plasmid pJKD5.1

These procedures are illustrated in Figures 6.3 and 6.4.

The coding region of the squash GPAT corresponding to the predicted processed mature protein (Ishizaki, O. et al., 1988) has been cloned in a pET3A overexpression vector and the overexpressed recombinant protein from this plasmid (pNA4; kindly provided for this study by Nishida, I., 1993) was proven to have GPAT enzymatic activity. A similar mature protein region of the squash GPAT was encoded by the constructs used for transgenic experiments with tobacco (Murata, N. et al., 1992).

The plasmid p4-1 contains a 1781 bp. cDNA insert cloned in the *Eco*RI site of pTZ18R. The DNA sequence corresponds to that deposited under Genbank Accession Nr. P10349 and encodes the main portion of the squash GPAT preprotein (Ishizaki, O. et al., 1988; Nishida, I., personal communication, 1993). The 'predicted mature coding region' for the squash GPAT was isolated as a 1220 bp. *Nae*I-*Eco*RI cDNA fragment of this insert.

***Nae*I and *Eco*RI restriction endonuclease recognition sequences:**

5'-GCC/GGC-3'	**5'-G/AATTC-3'**
3'-CGG/CCG-5'	**3'-CTTAA/G-5'**

The vector pJIT116, a pUC19 based vector made by J.F. Guerineau and L. Brooks (John Innes Institute) and obtained from the industrial partner (Nickerson Biocem, Cambridge), encodes a RNA polymerase II transcription 'cassette' consisting of a double cauliflower mosaic virus (CaMV) 35S constitutive promoter (767 bp), the 204 bp cDNA of the transit region for the small subunit of pea Rubisco (Schreier, P.H. et al., 1985; Van den Broeck, G., 1985), and a 749 bp cauliflower mosaic virus (CaMV) polyadenylation sequence. In the cloning strategy it was anticipated that in a later stage the entire recombinant 'cassette' had to be excised (using restriction endonucleases which would not cut in the internal sequences) and prepared for subloning in a binary plant vector. Therefore the pJIT 116 was modified to alter the existing *KpnI/Asp*718 site at the 5' cloning junction of the double CaMV 35S promoter sequence to a *XhoI* site.

***(Kpn*I)*Asp*718 restriction endonuclease recognition sequence:**

5'-G/GTACC-3'
3'-CCATG/G-5'

Alteration of pJIT116 to create pJKD1.1

(step1) 3 µg of the plasmid pJIT116 was digested with the restriction endonuclease *Asp*718 in 50 µl reaction volume according to standard method. A fraction of the digestion was analysed via 1% (w/v) agarose gel-electrophoresis to monitor the success of the reaction and the rest of the digestion was purified, concentrated by a standard phenol/chloroform (v/v. 1:1) extraction followed by a salt/ethanol precipitation and resuspension in an appropriate amount of sterile water or TE. Approximately 1 µg of pJIT 116/*Asp*718 was blunt ended by 5'-3' polymerase activity of VENT DNA polymerase (New England Biolabs, NEB).

The digested DNA was combined with 1X VENTbuffer (10 mM KCl, 10 mM $(NH_4)_2.SO_4$, 20 mM Tris-HCl pH8.8 (@25 °C), 2 mM $MgSO_4$, 0.1% Triton X-100), each dNTP at 200 µM and 4 Units VENT DNA polymerase (NEB, at 2U/ µl) in a reaction volume of 50 µl and incubated at 55 °C for 15 min. The polymerase was inactivated and removed via phenol/chloroform extraction followed by an ethanol precipitation as above and resuspended in 10 µl sterile water (milliQ). To prevent re-ligation of the vector in subsequent steps, the DNA termini were dephosphorylated using Shrimp Alkaline Phosphatase (SAP) (USB, at 1 Unit/ µl: catalyses the hydrolysis of 5'-phosphate groups from DNA, RNA and ribo- and deoxyribonucleoside triphosphates). The pJIT116/*Asp*718/Blunt DNA was incubated with 1 x SAP buffer (20 mM Tris-HCl pH 8.0, 10 mM $MgCl_2$) and 1 Unit (1 µl) SAP in 40 µl total reaction volume at 37 °C for 30 min. The phosphatase was heat-inactivated at 65 °C for 15 min. and after phenol/chloroform extraction and ethanol precipitation, resuspended in 11 µl sterile water (milliQ). A fraction (1 µl) was analysed to examine the quality and amount (recovery) of DNA after these procedures. To engineer *Xho*I restriction sites at the 5' cloning junction of the double CaMV 35S promoter sequence, the pJIT116/*Asp*718/Blunt and dephosphorylated DNA was ligated with 1 µg *Sal*I-*Xho*I adaptor (Stratagene #901125, at 1 µg/µl) in a reaction volume of 30 µl, also containing 1 x ligation mix (1 x LM: 30 mM Tris-HCL pH 7.8, 10 mM $MgCl_2$, 10 mM DTT, 1 mM ATP) and 3 Units T4 DNA Ligase (Promega: catalyses the joining of of two DNA strands between the 5'-phosphate and 3'-hydroxyl groups), at 15 °C overnight. Directly after the ligation reaction , the DNA termini of the ligation products were phosphorylated (kinased) by adjusting the reaction mixture with 1 x Kinase buffer (70 mM Tris-HCl pH 7.7, 10 mM $MgCl_2$,5 mM DTT), 0.1 mM ATP and 10 Units (1U/ µl) T4 polynucleotide kinase (Promega: catalyses the transfer of the γ-phosphate from ATP to the 5'-terminus of polynucleotides or mononucleotides) to 40 µl and incubation at 37 °C for 40 min. To help in subsequent recovery of small amounts of DNA, carrier nucleic acid (yeast tRNA to a final concentration of 50 µg/ml) was added and unincorporated adaptors and other contaminants were removed by gel filtration. The reaction was purified over a 1 ml. Sephacryl S-400 spin-column (4 min centrifugation at 800 x g.) and subsequently extracted with phenol/chloroform and ethanol precipitated. The purified pJIT116/*Asp*718 Blunt x *Sal*1-*Xho*I adaptor was religated in a standard 20 µl ligation as described above and a sample (0.25 volume) of the reaction was transformed into *E. coli* XL1-Blue (Stratagene) and selected (LB-AMP50 plates) and analysed according to standard methods. In this case, from appropriate plates, 20 colonies were selected for plasmid isolation and plasmids were examined to confirm the re-engineering of the restriction site (*Asp*718 to *Xho*I) by analytical digests with *Xho*I, or *Asp*718, or *Sal*I.

The recreated restriction site would consist of the following DNA sequence:

5'---- CTCGAGGTCGACCTCGAG---- 3'
3'---- GAGCTCCAGCTGGAGCTC---- 5'
*Xho*I *Sal*I *Xho*I

Therefore, the ultimate confirmation of the creation of **pJKD1.1** was the release of a 980 bp *Sal*I fragment from pJKD5.1 (consisting of the double CaMV 35S promoter and the pea rbscSSU transit peptide region).

Subcloning of the *Nae*I-*Eco*RI squash GPAT cDNA fragment in frame with the chloroplast target peptide coding region

(step2) 3 µg of the plasmid pJKD1.1 was digested with *Pst*I in the appropriate salt mix (Boehringer Mannheim) in 100 µl according to standard method. The DNA was purified by organic solvent extraction and ethanol precipitation and a fraction of the digestion was analysed via 1% agarose gel electrophoresis.

***Pst*I restriction endonuclease recognition sequence:**
5'-CTGCA/G-3'
3'-G/ACGTC-5'

The 3'- overhang was converted to a blunt end terminus by making use of the 3'-5' exonuclease activity of T4 DNA Polymerase (Promega # M4211). The T4 DNA polymerase has a 3'-5' exonuclease activity that will, in the presence of excess dNTPs, convert a 3'-protruding end to a blunt end. With a high dNTP concentration (100 µM), degradation of single-strand DNA will stop at the duplex DNA. pJKD1.1/ *Pst*I DNA (2.5 µg) was incubated with 1 x T4 DNA Polymerase I buffer (33 mM Tris-acetate pH 7.9, 66 mM potassium acetate, 10 mM magnesium acetate, 0.5 mM DTT), 100 µM of each dNTP, 0.1 mg.ml BSA and 12.5 units of T4 DNA PolymeraseI, in a total volume of 30 µl for 10 min at 37 °C and 15 min. at 12 °C. The reaction was stopped by heat inactivation at 75 °C for 10 min. and the DNA was purified and concentrated purified by organic solvent extraction and ethanol precipitation. Subsequently, the pJKD1.1/*Pst*IBlunted DNA was digested with 20 units *Eco*RI in 100 µl according to standard protocol and after 4 hrs digestion, purified and concentrated by organic solvent extraction and ethanol precipitation.

(step3) The vector DNA was further purified by gel band purification from a preparative 0.9% agarose gel and subsequently used in a standard ligation (overnight at 15 °C) with an equimolar amount of the *Nae*I-*Eco*RI squash GPAT cDNA fragment. Due to the fusion of the blunt-ended *Pst*I site of the vector (around the processing-site of the transit peptide) with the *Nae*I site of the squash GPAT cDNA fragment, the *Nae*I restriction site would be recreated. In conjunction with the appropriate procedural controls, 0.25 volume of this ligation was transformed into *E. coli* XL1-Blue (Stratagene) with selection (LB-AMP50 plates) and analysed according to standard methods. In this case, from appropriate plates, 20 colonies were selected for plasmid isolation and plasmids were examined to confirm the sub-cloning by analytical digests and compared to similar digests of unmodified pJKD1.1. In this manner the plasmid **pJKD3.1** was constructed and the cloning junction

of the fusion of the pea rbscSSU chloroplast targetting presequence and the mature squash GPAT sequence was confirmed via nucleotide sequence analysis using a custom primer:
SQAT3 (AS); 5'-CCATTCCTGCAGCAACATTTGG-3'

Construction of the binary plant-transformation plasmid pJKD5.1

(step 4) The RNA polymerase II expression cassette was excised from the plasmid pJKD3.1 by a large scale digest (25 µg DNA) with 50 units *Xho*I in 200 µl at 37 °C for 4 hr, and the DNA fragments separated by preparative 0.8% agarose gel electrophoresis. The top band (2945 bp) was purified by gel band purification using QIAEX silica resin (QIAGEN). An agarose slice containing the DNA band was cut out of the gel using a sterile scalpel blade and placed in a sterile 1.5 ml Eppendorf tube. 400 µl of NaI solution (per litre: 90.8 gr NaI and 1.5 gr Na_2CO_3 dissolved in sterile water, filter sterilised and saturated with 0.5 gr Na_2SO_3, and stored at 4 °C in a light-proof bottle) was added and the tube placed at 55 °C for >10 min. with mixing by inversion, to dissolve the agarose. After being allowed to cool to room temperature, 10 µl of the silica resin was added and the solution left at room temperature for 15 min. with continuous mixing by inversion. The chaotropic agent (NaI) promotes the binding of double-stranded DNA to the silica resin via differential ionic interaction between the different molecules in the mixture. The resin was pelleted by 30 sec centrifugation, washed with 70% ethanol and the resin (air dried) was resuspended in 20 µl sterile water. Following incubation at 42 °C, the resin was pelleted and the supernatant, containing the DNA, was collected, transferred to a new sterile 1.5 ml Eppendorf tube and a sample analysed via 1% agarose gel electrophoresis. Usually, the concentration of DNA isolated by this method was in the range of 10- 100 ng/µl. depending on the size and the amount originally present in the gel slice.

***Xho*I restriction endonuclease recognition sequence:**

***Xho*I: 5'-C/TCGAG-3'**
3'-GAGCT/C-5'

The 3'-recessed DNA termini of the *Xho*I fragment were filled in (blunted) using VENT DNA Polymerase in a similar procedure as described above (for step 1). To engineer a *Bam*HI site on the flanks of the fragment, for cloning into a *Bgl*II site of the basic binary plant transformation vector pSCV 1.2, a *Bam*HI-*Sma*I adaptor (Stratagene # 901112) was ligated to the blunt ended *Xho*I sites, according to similar procedures described above (step 1).

***Bam*HI-*Sma*I adaptor sequence**
5'-GATCCCCCGGG-3'
3' GGGGCCC-5' –P

The resulting fragment was phosphorylated in a reaction with T4 Polynucleotide Kinase as described for step 1.

The **binary plant transformation vector pSCV 1.2** (8.5 kb) encodes an ampicillin (AMP) resistance marker for selection in *E.coli*, a kanamycin/gentamycin (KAN/GM) resistance marker for *E.coli* and also plant selection, a RK2 origin of replication for *Agrobacterium tumefaciens* and a COL E1 origin of replication for propagation in *E.coli*. A multiple cloning site was encoded between the left and the right T-DNA (transfer-DNA) borders and an O/D sequence (OverDrive) sequence was present, flanking the right T-DNA border sequence on the outside. The pSCV 1.2 (pShell Cloning Vector 1.2) was constructed by Glyn A. Edwards and obtained via the industrial partner Nickerson Biocem, with permission.
The binary vector pSCV 1.2 was digested with *Bgl*II, dephosphorylated and ligated to the *Bam*HI- flanked RNA Polymerase II expression cassette encoding a preprotein consisting of the pea RbscSSU chloroplast transit peptide and a mature portion of the squash GPAT, according to standard methods. Taking the appropriate controls into account, the resulting ligation reaction was transformed to electrocompetent *E.coli* DH10B cells (Electromax; Gibco BRL # 18290-015) by electroporation.

Electroporation was performed using a BioRad Electroporater with dial settings at 25 μF and 125 μF, resistance at 100 Ω (for *E. coli*, or 200 Ω for *Agrobacterium tumefaciens*) with pulse control. Button settings were; set V = 2.5 V, actual V = 0, Capacitance = 25 and TC (time constant) =0. Cell-Porator (BRL) settings were: Voltage 400 (delivers 2.5 hV), Capacitance 330 μF, independence; low, charge rate; fast, BRL; booster settings, resistance on voltage booster = 4.000 ohms.
Electrocompetent cells were thawed on ice and 20 – 40 μl cells were mixed with DNA (for instance; with whole or part of ligation reaction in a volume < 10 μl) and transferred (without air bubbles) to micro-electrocuvettes which were pre-cooled in ice. The electrocuvettes were then placed between the electrodes and a pulse was given after which the TC (time constan) was monitored (usually 2.4 for a successful transformation procedure). Cells were removed from the electrocuvette and prewarmed SOC (or 2 xYT) medium was added (500 – 950 μl). Cells were incubated at 37 °C for 1 –3 hrs to recuperate before aliquots were plated to selective LB agar media plates. For pJKD5.1 cloning, LB agar + 50 μg/ml AMP, 5 μg/ml GM plates were used for selection and for the subsequent colony hybridisation procedure.

For **colony hybridisation**, colonies resulting from the transformation procedure, were picked using sterile toothpicks and streaked on replica plates. The master plate (90 mm petridish+ LB agar+ antibiotics) had a numbered grid marked on the bottom. The replica plate was overlayed with a 70 mm Colony/Plaque Screen Hybridisation Transfer Membrane (NEN) with an identical grid drawn on and numbered with a pencil. Colonies were streaked on identical numbered positions on the two grids. The plates were incubated at 37 °C overnight. The master plate was stored at 4 °C and the hybridisation membrane was peeled from the replica plate and placed, colony side up, on a piece of Whatmann 3 MM filterpaper saturated with the appropriate buffers for denaturing, neutralisation and equillibration, according to the instructions of the supplier. After colony lifting procedures and washing with 4 x SSC to remove bacterial debris, the filters were air dried and the DNA was covalently linked to the membrane by UV irradiation (Stratalinker; Stratagene) or oven baking at 80 °C for 2 hr.

For hybridisation to radiolabelled DNA probes, standard methods were used according to instructions with the membranes.

In subcloning procedures of pJKD5.1, at least 150 colonies were screened, using the purified *Nae*I-*Eco*RI squash GPAT cDNA fragment as a radiolabelled probe. Four clones were selected and grown in selective LB media at 37 °C overnight and plasmids were isolated according to the protocol with the Promega Wizard Miniprep System (based on binding of plasmid DNA from bacterial lysates to a glass fibre matrix). Plasmids were examined to confirm the sub-cloning by analytical digests and compared to similar digests of unmodified pSCV 1.2. Extra confirmation was obtained by Southern blot analysis of the restriction digests using the above probe and matching hybridising bands on an autoradiograph with the bands expected to contain the appropriate squash GPAT cDNA regions.

6.2.2 Procedures used during plant transformation of *Arabidopsis thaliana*, ecotype Columbia-C24 and other manipulations of seeds and plants

6.2.2.A Preparation of electrocompetent Agrobacterium tumefaciens

Agrobacterium tumefaciens strain C58C1 (pGV2260) was grown to OD_{600nm} = 0.5-0.7 100 ml LB+ 50 μg/ml AMP + 50 μg/ml RIF(Rifampicin) for ~36 hr at 28 °C. Cells were pelleted by centrifugation at 6000xg for 10 min at 4 °C. The cell pellets were resuspended in 1 original culture volume (100 ml) of ice cold 10% (v/v) glycerol and centrifuged as above. This cell pellet was resuspended in 0.5 volume of ice cold 10% (v/v) glycerol and these steps were repeated with decreasing volumes of glycerol solutions, 0.2, 0.02 and 0.01 volume respectively. Aliquots of 40 μl were snap frozen in liquid nitrogen and stored at –80 °C.

6.2.2.B Transformation of a binary vector to A. tumefaciens

Electrotransformation of electrocompetent cells of *Agrobacterium tumefaciens* strain C58C1 (pGV2260) with a binary vector was as described above (section 6.3.1 step4) with only exceptions that dial settings for resistance were at 200 Ω for *Agrobacterium tumefaciens* and the TC (time constant) was then monitored at 4.8. *A. tumefaciens* was grown at 28 °C for 2 days and selection of transformants was on LB agar + 50 μg/ml AMP+35 μg/m GM + 50 μg/ml RIF(Rifampicin). Transformed colonies were identified by total nucleic acid isolation and appropriate restriction digest analysis.
Total nucleic acid was prepared according to a mini prep method descibed for *Agrobacterium tumefaciens* by Draper, J. et al. (Draper, J., Scott, R., Armitage, P., and Walden, R., Eds., 1988)

6.2.2.C Plant material

Transgenic as well as control plants (for instance *Arabidopsis thaliana*, ecotype Columbia-C24) were kept, as a standard, under 16 hr light/8 hr dark regime (140 μmol. quanta $m^{-2}.sec^{-1}$) at 22 °C and 60% humidity. All transgenic plants were germinated under selective conditions in order to ensure antibiotic (50 mg/l KAN or 40 mg/l Phleomycin) resistance.
Seeds for *Arabidopsis thaliana*, ecotype Columbia-C24 (N906), ecotype Landsberg and the ecotype Columbia *fad6* (*fad C*-1) mutant (N207), were obtained from the Nottingham *Arabidopsis* Stock Centre, U.K.

6.2.2.D *Arabidopsis thaliana*, ecotype Columbia-C24 transformation

Media (per litre)

Germination medium (ATG): 1 x MS (Murashige and Skoog) salt mixture (SIGMA M55244), 3% (w/v) sucrose, 0.05% MES (SIGMA M-8250; 2-[N-morpholino] ethane sulfonic acid), 0.8% Difco Bacto agar, 1 mg/l thiamine-HCl (SIGMA T-3902), 0.5 mg/l pyridoxine-HCl(SIGMA P-9755), 0.5 mg/l nicotinic acid (SIGMA N-0765), 100 mg/l myoinositol (SIGMA I-7508), adjusted to pH 5.7 with 1 N KOH. **Callus Inducing Medium (CIM):** 1 x MS (Murashige and Skoog) salt mixture + Gamborg's B5 vitamins (SIGMA M0404), 2% glucose, 0.05% MES, 0.8% Difco Bacto agar, 0.5 mg/l 2,4-D (2,4-dichlorophenoxyacetic acid; 10 mg/ml stock in DMSO), 0.05 mg/l kinetin (5 mg/ml stock in DMSO), adjusted to pH 5.7 with 1 N KOH . **Selective Shoot Inducing Medium (SIM):** 1 x MS (Murashige and Skoog) salt mixture + Gamborg's B5 vitamins (SIGMA M0404), 2% glucose, 0.05% MES, 0.8% Difco Bacto agar, 5 mg/l 2-IP (SIGMA D-7674; N^6-(2-isopentenyl)adenine, 20 mg/ml stock in DMSO), 0.15 mg/l IAA (SIGMA I-2886; indole-3-acetic acid, 1.5 mg/ml stock in DMSO), 400 mg/l Augmentin (Beecham Research 7794.000.5), adjusted to pH 5.7 with 1 N KOH. **Medium for rooting (ATIM):** 1 x MS (Murashige and Skoog) salt mixture + Gamborg's B5 vitamins (SIGMA M0404), 2% glucose, 0.05% MES, 0.8% Difco Bacto agar), adjusted to pH 5.7 with 1 N KOH.

All media were used in 9 cm diameter Optilux 1005 Petri dishes (Falcon), except for ATG which was used in 15 cm 1013 (2.5 cm high) Petri dishes (Falcon). All Petri dishes were sealed with Urgopore (France) medical gas-permeable tape during tissue culturing. Sometimes Nescofilm was used but was found to lower regeneration efficiencies at all stages. Hormones were dissolved in DMSO (dimethyl sulfoxide); antibiotics were dissolved in water and subsequently filter-sterilised. Hormones, some vitamins and antibiotics were added after autoclaving and cooling the media to 65 °C.

Seed sterilisation and growth of Arabidopsis plants

Seeds were put in a 1.5 ml Eppendorf tube and 70% ethanol was added for 1 min. after which the ethanol was removed with a pipette. Subsequently 15% Domestos (commercial bleach) or 5% NaOCl was added and seeds were left in this solution for 15 min with occassional inversion. The liquid was pipetted off and seeds were washed five times with sterile water for 5 min. After the last wash, seeds were kept in 0.5 – 1 ml sterile water and could be put on tissue culture medium (ATG) as 'drops with seed' or as single seeds by using a low volume tip. For growth of seedlings, seeds were incubated on ATG in a cold room (4 °C in the dark) for a 3-4 day vernalisation period and subsequently in a culture room (22 °C; 16 hr light/8 hr dark regime (140 $\mu mol.m^{-2}.sec^{-1}$)) for 7-10 days.

Cotyledonary seedlings were transferred to fresh ATG medium plates (15 – 30 seedlings per 15 cm dish).

Transformation of root explants

For one round of transformation, 5 of such plates were usually used. For both regeneration and transformation white roots of any age can be used. After 8 weeks of growing, however, the roots will eventually start to turn green. Usually after 3-5 weeks, plantlets were gently pulled out of the ATG medium using a forceps and put in a sterile Petri dish. Root-systems were cut off the plantlet (with a sterile scalpel) so that no green parts remained attached to the roots. 10-15 root-systems were then incubated on solid CIM medium, taking care that the roots were entirely in contact with the medium, for 3 days. Three to five callus-induced root systems were stacked in a sterile Petri dish and cut into 0.5 cm root explants. The root explants were then transferred to a sterile Petri dish containing 20 – 30 ml liquid CIM medium. For *Agrobacterium* infection, 0.5 – 1.0 ml of an overnight grown *Agrobacterium* culture (28 – 30 °C, 200 rpm, in LB (Luria Broth)+ appropriate antibiotics) was added and followed by incubation with gentle shaking for 5 min. Root explants were then blotted on sterile filter paper to remove most of the liquid and subsequently put on solidified CIM medium. Up to 50 explants per 9 cm Petri dish (CIM) were incubated under standard conditions in a growth room for 2 –3 days. After 2 days coculture the explants are completely overgrown by *Agrobacteria*. The explants were pooled in a 150 ml capped sterile container and washed five times with 20 – 100 ml liquid SIM + 1 g/l cefotaxim, shaking vigorously to wash off *Agrobacteria*. After the last wash, root explants were blotted on sterile filter paper for a few sec. and transferred to 9 cm Petri dishes with solidified SIM + appropriate antibiotics (5 root explants/ dish). After 3 weeks incubation in standard growth conditions, tiny green calli appear on the yellowish root explants. Calli were then transferred to fresh 9 cm Petri dishes with solidified SIM + appropriate antibiotics and after about 2 weeks the green calli would form shoots. These shoots were initially often vitreous but turn into normal structures a few days later. Shoots (~0.5 cm) were transferred to 15 cm Petri dishes with solidified ATIM (10 shoots/ dish) to allow for root formation and further development. Roots started to appear after 3 weeks and when the roots were about 1 cm long, plantlets were transferred to soil (4 volumes commercial compost/1 volume sand were sieved and sterilised before plantlets were potted) and grown under standard conditions.

Plants were grown to seed in a growth room (22 °C; 16 hr light/8 hr dark regime (140 $\mu mol.m^{-2}.sec^{-1}$); 60 % humidity) in 12 cm pots or making use of the Arasystem (βeta Tech) for growth and seed harvesting for *Arabidopsis*.

6.3 Results

6.3.1 Evaluation of the suitability of a prolonged low-temperature exposure, chilling treatment protocol for phenotypic scoring experiments with *Arabidopsis*

Literature on research involving the use of chilling treatments of *Arabidopsis* and the effect on the visible plant phenotype was evaluated.

The main purpose of this was to compile a severe chilling treatment procedure which potentially would indicate changes in chilling resistance of transgenic plants due to, for instance, changes in chloroplast membrane fatty acid composition, but would not significantly affect the phenotype of wild-type *Arabidopsis* plants.

A directly visible phenotype can be observed on the biology and appearance of plants as a clear-cut consequence of mutations affecting three loci for structural lipid synthesis genes of *Arabidopsis*, namely ***fad5* (*fadB*), *fad6* (*fadC*) and *fab1*.**

fad5

The ***fad5*** *(fadB)* (for fatty acid desaturasion) gene product is a chloroplastic Δ7 desaturase. It is highly substrate specific, using 16:0 acyl chains on MGDG and possibly DGDG (Browse, J. et al., 1985; Kunst, L., et al., 1989a).

fad6

The chloroplastic 16:1/18:1 ω-6-desaturase is encoded by the ***fad6*** (*fadC*) gene (Browse, J. et al., 1989). Although the *fad5* and *fad6* mutants exhibit substantial changes in chloroplast fatty acid composition and also have differences in the size of the chloroplast (McCourt,P.J. et al., 1987) and in the organisation of the thylakoid membranes (Hugly, S. et al., 1989; Kunst, L. et al., 1989b), they do not exhibit a visible phenotype under normal growth conditions. Both mutants show chlorosis of the leaves and a 20 to 30 % reduction in their growth rate compared to wild type plants when grown at the lower temperature of 5 °C (Hugly, S. and Somerville, C., 1992). The **'chilling treatment'** by Hugly and Somerville involved germination of plants at 22 °C under continuous fluorescent illumination (100-150 μmol. quanta $m^{-2}.sec^{-1}$) and plants at the cotyledon stage (7 days after germination) were either maintained at 22 °C for 10 days or given a chilling treatment by transfer to 5 °C for 3 weeks with continuous, but lower energy, fluorescent illumination at 20 μmol. quanta $m^{-2}.sec^{-1}$. Although the **phenotypes** show some parallels to the physiology of naturally chilling-sensitive plants, it has been demonstrated that the low temperature response was likely due to impaired chloroplast development rather than to reduced membrane stability. Both the mutants continued to grow and eventually, although 'battle scarred', would complete their life cycles even at the lower temperatures. As such, these mutants would not represent ideal models for processes involved in chilling injury. It was clear, however, that chloroplast membrane unsaturation is a factor that affects the low-temperature responses of plants.

fab1

The overall level of glycerolipid unsaturation is also affected by mutations that control other steps of fatty acid biosynthesis, for instance in the ***fab1*** mutant (for fatty acid biosynthesis) of *Arabidopsis*. The *fab1* mutant is characterised by increased levels of 16:0 or 18:0, respectively, in seed and leaf tissues (Lightner,J. et al., 1994a; Wu, J. et al., 1994) and appears to be caused by a reduction in 16:0 to 18:0 elongation (condensing) activity by a isozyme for KAS II. The increased level (from 20 to 42 %) of HMP molecular species (16:0, 16:1-*trans* and 18:1) in the leaf PG of the *fab1* mutant is a higher percentage than that is found in approximately 50% of chilling-sensitive plants that have been examined (Wu, J. and Browse, J., 1995). Wu and Browse examined the effect of **a number of chilling treatments**, which will be further referred to as '**less severe or rapid response**'.

The standard growth conditions were defined as plant growth on commercial potting mix in controlled environment chambers at 22 °C under continuous illumination (150 µmol. quanta $m^{-2}.sec^{-1}$) and 60-70% humidity.

Treatment A) involved plant growth under standard conditions and transfer of rosette plants (17 days after sowing) to a growth chamber at 10 °C, with standard lighting conditions, for 10 weeks.

Treatment B) was similar to the chilling-treatment used by Wolter and co-workers (Wolter, F.P. et al., 1992) for *Arabidopsis* transformed with *plsB* (GPAT) cDNA from *E. coli*, and involved the following: at first, plant growth was in a 9 hr day 21 °C / 15 hr night 16 °C cycle, 70% humidity and lighting at 150 µmol. quanta $m^{-2}.sec^{-1}$. Twenty-four-day-old plants were then kept at 4 °C for 7 days in the dark and were then returned to 20 °C for 7 days.

Treatment C) involved the transfer of standard grown, 15 day old, plantlets to 2 °C under continuous high light for 7 days. Plants were then transferred to standard growth conditions for 7 days.

The observation of the researchers was that the mutant was completely unaffected by this range of low-temperature treatments that quickly killed some known, naturally chilling-sensitive plants.

However, it was shown that the increased 16:0 content in the membrane lipids of *fab1* plants affected **longer-term** survival of the mutant plants at low temperature. Growth of the mutant was severely affected and the leaves gradually became chlorotic after **prolonged exposure to low temperature**. Plants were germinated and grown at standard

conditions and for the prolonged chilling treatment, 15 days old plantlets were transferred to 2 °C under continuous illumination for 28 days. After this time, plants were either returned to 22 °C or kept at 2 °C for an additional 7 to 28 days. It was observed that during the first 2 weeks of the chilling treatment, *fab1* plants were indistinguishable from the wild type. The effects on the mutant's appearance were seen beyond this period. Plants left at 2 °C continued to deteriorate and eventually died without producing seed. However, 4 weeks treated plants, which were returned to 22 °C, quickly recovered and produced seed.

∞∞∞∞

Generally, a chilling treatment, involving a combination of **high light** (150 µmol. quanta $m^{-2}.sec^{-1}$) and **low temperature** (2-4 °C), is considered to be more severe. Also the return to warmer (standard) conditions can have an effect on the physiological response. Naturally chilling-sensitive plants commonly develop symptoms after rewarming. However, although even *Arabidopsis fab1* plants are dramatically affected by such low temperature treatment during 3 – 4 weeks, the mutants did demonstrate a remarkable capacity for recovery when returned to 22 °C (Wu, J. et al., 1997).

It was decided to **evaluate the use of a severe chilling treatment**, combining these elements, of *Arabidopsis* plants for a prolonged period. The first objective was to try and calibrate experimental procedures to optimise the observation of physical responses of *Arabidopsis* plants to such a severe chilling treatment.
Symptoms of chilling damage would be patches of necrosis, anthocyanins or even death of the plants.
The *Arabidopsis*, ecotype Columbia, ***fad6*** (*fadC*) mutant was chosen as **a chilling susceptible control** and the *Arabidopsis*, ecotype Columbia-C24 and ecotype Landsberg were tested for their resistance against developing visible chilling damage. This experiment would ensure that the selected wild type variety for use in the subsequent plant transformations was not sensitive to the cold stress conditions used and was performed in collaboration with Dr. J. Coventry at Nickerson Biocem (the industrial partner).
Seeds of each plant genotype, were planted (17 seeds spaced 0.5 inch apart) in commercial potting mixture in 4 inch pots. Plants were germinated and grown in controlled environment chambers under standard conditions defined as; at 22 °C under continuous illumination (140 µmol. quanta $m^{-2}.sec^{-1}$) and 60-70% humidity. The two chilling-treatments tested, to phenotypically distinguish between the mutant and the wild type plants (and subsequently the squash GPAT-transgenic plants) involved the transfer of 15-20 days old plantlets to the following conditions:

Control) control pots (one of each genotype) were maintained at standard conditions
Treatment 1) pots were subjected to 4 °C in the dark for 7 days, after which they would be returned to standard conditions, similar to treatment B in experiments of Wu, J. and Browse (1995) and Wolter, F.P. et al. (1992), and
Treatment 2) pots were placed at 4 °C under constant illumination (140 μmol. quanta $m^{-2}.sec^{-1}$) and 60-70% humidity, and monitored for 29 days. After this time, plants were returned to standard conditions.

By **day 7**, all genotypes continued to develop but with lower rate than the standard control plants. For the cold/dark treatment 1 all plants remained small and less developed but with no obvious changes in colouration. For the cold/light treatment 2 reddish patches (anthocyanins) were observed on leaves of the *fad6* (*fadC*) mutant.
At **day 14** the main observations were the following. For both treatment 1 and 2 there were no visible chilling damage symptoms for the C24 plants, which remained green. However, in the cold/light treatment 2, obvious patches of necrosis and chlorosis were observed on leaves of the *fad6* (*fadC*) mutant and some small patches of necrosis were seen for the Landsberg plants.
By **day 17**, the control plants of C24 were bolting and some started flowering with a small amount of necrosis on the leaf tips, possible due to overwatering. The *fad6* (*fadC*) genotype did not show signs of damage but the Landsberg genotype plants also showed a small amount of necrosis on the leaf tips, possible due to overwatering. In the meantime, the plants for the cold/dark treatment 1, were returned to standard conditions and the following was observed: the C24 plants were beginning to bolt and did not display signs of damage, the *fad6* (*fadC*) plants were very green without signs of anthocyanins or leaf damage. However for the cold/light treatment 2 the observations were more pronounced: the C24 plants were not bolting yet and displayed a small amount of chlorosis/necrosis around the edges of the older leaves and minor darker coloured patches on the tips of the newest leaves, the Landsberg plants were not bolting yet and showed more pronounced chlorosis/necrosis around the edges of the older leaves and appeared to be dying back from the edges. There were no obvious signs of anthocyanin patches, except in the buds, but this could be due to the relatively darker-green shade of this genotype.
As is illustrated in Figure 6.1, the *fad6* (*fadC*) plants were flowering but their leaves displayed obvious chlorosis and patches of necrosis and anthocyanin accumulation, especially in the older leaves.

None of the genotypes showed obvious chilling damage symptoms due to the **cold/dark treatment 1** other than an overall delay in development affecting all plants.

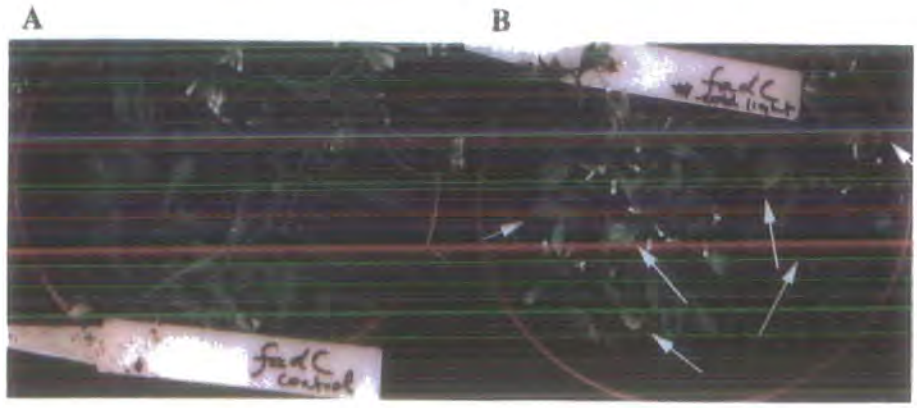

Figure 6.1 Response of the *fad6* (*fadC*) *Arabidopsis* plants to cold/light treatment 2

Details of growth conditions preceding the chilling treatment are given in the text. Fifteen-day-old plants were maintained under standard conditions (**A**) or were subjected to a cold/light treatment 2 (4 °C under constant illumination (140 µmol. quanta $m^{-2}.sec^{-1}$)) for 29 days (**B**). The visible phenotype of the plants by day 17 are shown, with obvious signs of chilling damage indicated by white arrows.

Although the C24 and *fad6* (*fadC*) are both derived from the Columbia ecotype, during the **cold/light treatment 2**, the appearance of the ecotype Landsberg plants was more similar to the *fad6* (*fadC*) plants than C24 was to *fad6* (*fadC*) plants. Although *fad6* (*fadC*) plants displayed more pronounced chilling damage respons, the Landsberg plants also developed minor discolouration and signs of chlorosis/necrosis.
The C24 Columbia ecotype of *Arabidopsis* was the cultivar of choice for the subsequent plant transformations because the plants did not show symptoms of chilling stress and remained bright green throughout the relatively severe cold/light treatment 2.

By using the cold/light treatment 2 it was perceived possible to distinguish chilling-sensitive from chilling-tolerant *Arabidopsis* C24 transformants and, because plants were able to recover after returning them to standard conditions, to obtain seeds from the transformants.

Ideally a very large number of individuals of different SQ GPAT-transgenic lines could be phenotypically screened as such and it was expected that the experiment could potentially generate two main phenotypes, including chilling-tolerant but also chilling-sensitive plants. The latter phenotype would directly proof the concept that due to an extremely high expression of a 'competetive' squash GPAT transgene the plant would be rendered chilling sensitive.

6.3.2 Transformation of *Arabidopsis* C24 with the binary vector pJKD5.1 and selection of a chilling-resistant line expressing squash GPAT at a high steady state level

The main overall objective of this part of the study was to create transgenic *Arabidopsis* C24 plants, which are naturally chilling-resistant, transformed with a construct expressing a chloroplastic GPAT from the chilling-sensitive plant squash (*Cucurbita moschata*). Due to the nature of plant transformation, it was expected that a range of levels of expression of the transgenic squash GPAT would occur, and the intention was to obtain a transgenic *Arabidopsis* line expressing squash GPAT at a very high level but maintaining chilling-resistance.
Trangenic lines would be analysed and phenotypically screened, by subjecting them to the cold/light chilling treatment 2, and selected for the next round of plant transformation with a ribozyme (Rz) expressing construct. Therefore, it was also imperative that in a later stage, putatively chilling-sensitive plants subjected to such treatment, would not die but able to recover and eventually set seed for further investigations, which was proven to be possible (6.3.1).

Creation of the binary plant transformation vector pJKD5.1 and Arabidopsis C24 transformation

The mature protein region, according to the previously reported processing site**, of the cDNA for the soluble glycerol-3-phosphate acyltransferase (GPAT) from squash was ligated with the amino-terminal transit region of the cDNA for the small subunit of pea Rubisco (section 6.2.1). This transit peptide has been proven to direct transport of the fusion protein into plant chloroplasts and is then cleaved by a site specific protease (Schreier, P.H. et al., 1985; Van den Broeck, G. et al., 1985). The construct was inserted between a strong constitutive double CaMV (35S) promoter and a CaMV polyadenylation sequence of pSCV 1.2 to form the binary vector pJKD5.1.

The exact nature of the mature protein region of the squash GPAT used in this study is shown schematically in Figure 6.2

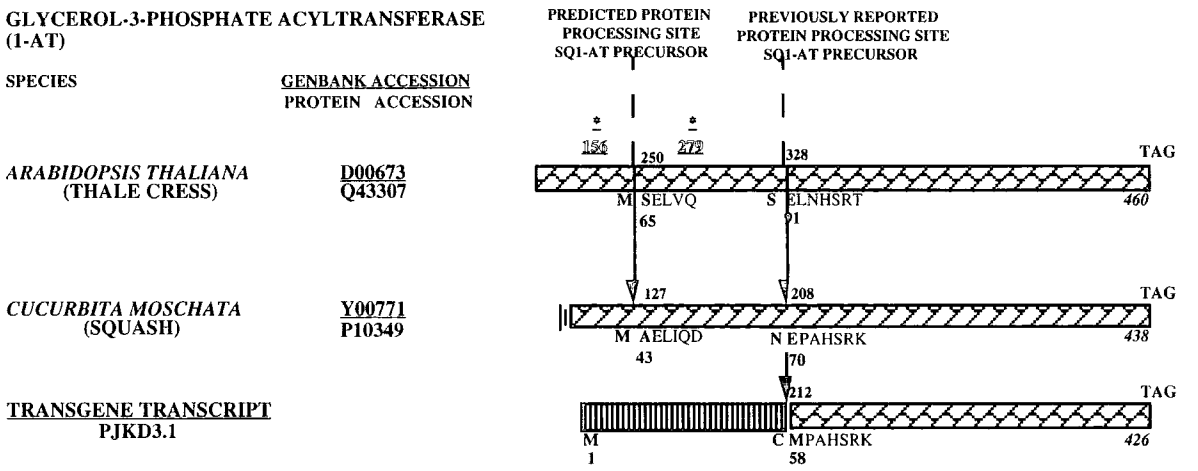

An illustration of the entire cloning procedure to create the binary plant transformation vector pJKD5.1 (section 6.2.1), is depicted in Figure 6.3 and 6.4.

The construct pJKD5.1 (and as a control the empty binary pSCV1.2 vector) was introduced into *Agrobacterium tumefaciens* C58C1 (pGV2260) and selected for resistance to kanamycin and on basis of restriction enzyme analysis as described (section 6.2.2A+B + Figures 6.3 and 6.4). In collaboration with Dr. J. Coventry of the industrial partner (Nickerson Biocem Cambridge), *Arabidopsis thaliana* ecotype Columbia-C24 was transformed by the root-explant method as described in section 6.2.2D. Transformed calli were selected on Murashige-Skoog (MS) based medium containing kanamycin (50 mg/l). After shooting and rooting, transformants were grown in dedicated environment chambers at 22 °C; 16 hr light/8 hr dark regime (140 $\mu mol.m^{-2}.sec^{-1}$); 60 % humidity and after approximately 3 weeks they were transferred to soil and grown to seed under the same controlled conditions.

Figure 6.3 The construction and analysis of pJKD3.1 and further engineering towards the binary vector pJKD5.1

Flow diagram of cloning procedures and schematic representations of intermediary constructs used or created during engineering towards the construct pJKD5.1. Cloning steps (1 to 4) are indicated and described in detail in section 6.2.1. The schematic drawings of the constructs represent DNA sequences and restriction sites, relevant for interpretation of the cloning or analysis procedures are indicated above the drawings. Designation of restriction sites in outlined characters is meant to accentuate that they were important in the procedures. The designation for the different portions of the DNA constructs and their respective size (underlined and illustrated by horizontal double arrows) are depicted below the drawings and the boxes they represent are filled in with different patterns to clarify the distinction within the diagram. Nucleotide positions corresponding to relevant restriction sites and also indicating the sizes of the different DNA regions are shown directly below the drawings. **Panel A** illustrates the nucleotide and protein sequence around the *Nae*I site in the squash GPAT (1-AT) used in the cloning procedure. The amino acid residues in the region of the squash GPAT (1-AT) protein are indicated above the nucleotides, with the residues which will be represented in the final squash GPAT fusion protein encoded by pJKD5.1, indicated by outlined characters. **Panel B** the nucleotide and amino acid sequence around the newly created fusion site of the amino terminal pea SSU Rbsc transit peptide region and the mature squash GPAT (1-AT) protein region. This sequence was confirmed to be correct by nucleotide sequence analysis using the primer SQAT3, which is indicated in the diagram of the pJKD3.1 construct. Restriction sites encoded by the fusion sequence are indicated. **Panel C** illustrates the restriction digest analysis of the pJKD3.1 construct to confirm the success of the cloning procedure. DNA was size fragmented in a 1.2 % (w/v) agarose gel electrophoresis and the samples are indicated above the lanes. Molecular weight markers (M1 = λ*Hin*DIII and M2 = λ*Pst*I) were run in the flanking lanes and are indicated in base pairs on either side of the gel. The sizes (in base pairs) of the respective DNA fragments are shown below the lanes.

p4 - 1
Squash 1-AT cDNA (ACC. nr. P10349)
//1781 bp. EcoRI in pTZ18R

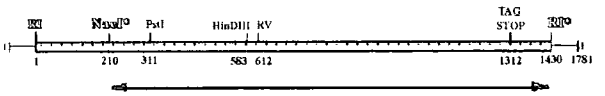

1220 bp NaeI - RI DNA fragment

1 pJKD 1.1: modified pJIT116, a pUC9 based vector
encoding a RNA polymerase II expression cassette with a chloroplast targetting/transit peptide

Panel A: DNA and Protein sequence around the NaeI- site in Squash 1-AT

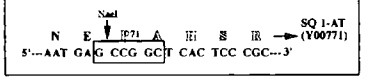

pJIT116
(KpnI/Asp718)*

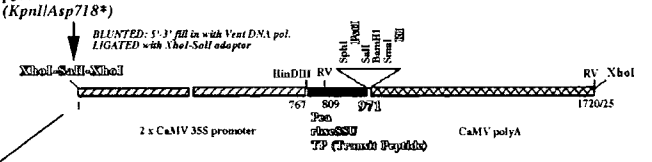

2

Panel B: Fusion of Pea rbcSSU chloroplast targetting presequence with mature SQ 1AT sequence.

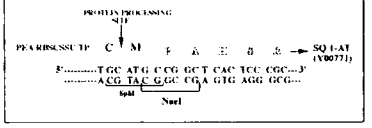

PstI *Blunted via 3' - 5' exonuclease activity of T4 DNA pol.*

3

pJKD 3.1: RNA polymerase II expression cassette encoding a mature Squash 1-AT protein fused to a chloroplast targetting peptide

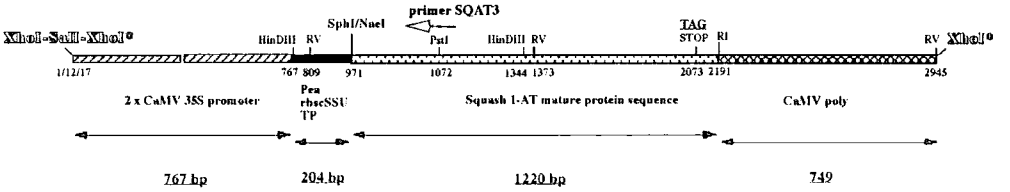

Panel C: RESTRICTION ANALYSIS pJKD 3.1

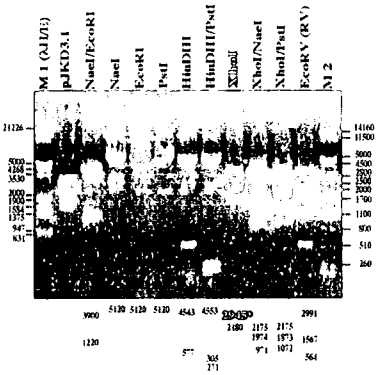

4

2950 bp. XhoI DNA fragment
BLUNTED 5'-3' fill in with Vent DNA pol.
LIGATED with a BamHI-SmaI Adaptor (Stratagene 901112)
LIGATED to BglII site of pSCV 1.2

pSCV 1.2: Binary plant transformation vector encoding a Neomycin(Kanamycin) selection marker

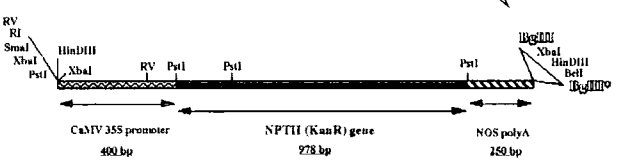

Figure 6.4 Schematic representation of the T-DNA region of the plant binary vector pJKD5.1 and illustration of restriction enzyme analysis of the vector compared to the 'empty' vector control (pSCV1.2)

The depiction of restriction sites, DNA regions, the functions they encode and their size, is described in the legend of figure 6.3.

The nucleotides are numbered from the start of the first 'cassette' at the *Hin*DIII restriction enzyme site, which flanks the CaMV 35S promoter of the neomycin phosphotransferase-encoding cassette conferring a kanamycin resistance for use as a selection marker. This was meant to facilitate interpretation of restriction enzyme analyses.

Restriction enzymes used in the restriction analysis illustrated in Panel D, are shown in outlined characters. On either side of the diagram the left (LB) and the right border (RB) of the T-DNA (transfer-DNA) are indicated. Also the overdrive sequence (O/D) flanking the right border, is shown.

Panel D the restriction digest analysis of the pJKD5.1 construct, compared to the 'empty' vector control (pSCV1.2), to confirm the success of the cloning procedure. DNA was size fragmented in a 1.2 % (w/v) agarose gel electrophoresis and the samples are indicated above the lanes. Molecular weight markers (M1 = λ*Hin*DIII /*Eco*RI) were run in the flanking lane and are indicated in base pairs on the left side of the gel.

The sizes (in base pairs) of the respective DNA fragments are shown below the lanes. The gels were Southern blotted and hybridised with a radioactive labeled *Nae*I-*Eco*RI cDNA fragment of the squash GPAT and bands which hybridised with the probe are indicated with an outlined asterisks next to the size indication below the gel.

pJKD 5.1 : Binary plant transformation vector encoding a kanamycin selection gene and a mature Squash 1-AT protein fused to a chloroplast targetting peptide

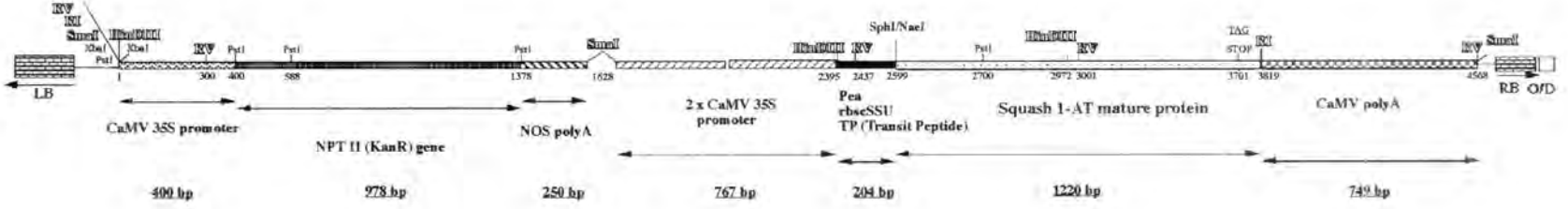

Panel D: RESTRICTION ANALYSIS pJKD 5.1

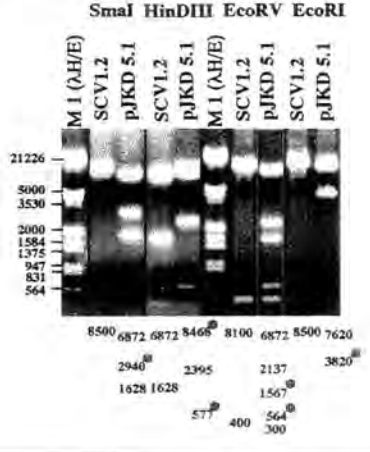

It was expected that a range of expression levels of the transgenic squash GPAT would occur, due to the nature of plant-transformation and possibly due to potential homology-dependent gene silencing effects (Matzke, M.A. and Matzke, A.J.M., 1995a; Meyer, P., 1995 a+b; Meyer, P. and Saedler, H., 1996).
To test the original idea that transgenic *Arabidopsis* lines with variable levels of expression of squash GPAT, may possibly lead to the observation of chilling-resistant and chilling-sensitive phenotypes, it was thought that it would be ideal if a relatively large number of trangenic lines was generated and examined.

In two rounds of *Arabidopsis thaliana* ecotype Columbia-C24 transformations by the root-explant method (section 6.2.2D), 40 independent, kanamycin resistant transformants were obtained. The primary transformed plants were very fragile and it was decided that they were not suitable for a direct phenotypical screen involving exposure to the cold/light chilling treatment 2. In first instance it was thought to be imperative to establish if they were true transformants (and not 'escapes') and to maintain the lines by growing them to produce seed.

PCR confirmation of transformants

Total nuclear DNA was isolated from two small leaves of each primary transformant via a miniprep procedure of the CTAB based method described in Chapter IV, section 4.2.1. Using standard procedures, the presence of the kanamycin resistance gene (present within the T-DNA region of construct pJKD5.1) was confirmed by PCR analysis using the primers: TN5 KAN1; 5'-CGCAGGTTCTCCGGCCGCTTGGGTGG-3' and TN5 KAN2; 5'-AGCAGCCAGTCCCTTCCCGCTTCAG-3', which lead to the amplification of a 255 base pair DNA fragment if the transgenic construct is present in the genome. In a similar PCR procedure the presence of the CaMV 35S promoter was tested by using the primers: CaMVPCR1; 5'-AGATACAGTCTCAGAAGACCAAAGG-3' and CaMVPCR2; 5'-ACGTCAGTGGAGATATCACATCAAT-3', amplifying a 298 bp. DNA fragment. The data resulting from this analysis is not shown but all 40 primary transformants were confirmed to be transformed. Plants were grown to seed (self fertilisation), transferred to the Durham laboratory and this batch of seed was designated T1 seed.

Further testing of transformants

Part of the T1 seed was experimentally tested for the following:

1) germination frequency on ATG medium, indicating their viability
2) germination frequency on ATG medium + 50 mg/l kanamycin, indicating segregation of the transgene in the next (T1) population and indicating the presence of a single or multiple insertion of the transgene. When a single copy was present in the genome, the heterozygosity of the dominant kanamycin resistance marker in the primary transformant would then result in a 3:1 Mendelian segregation in the next population. This is shown in Figure 6.5.

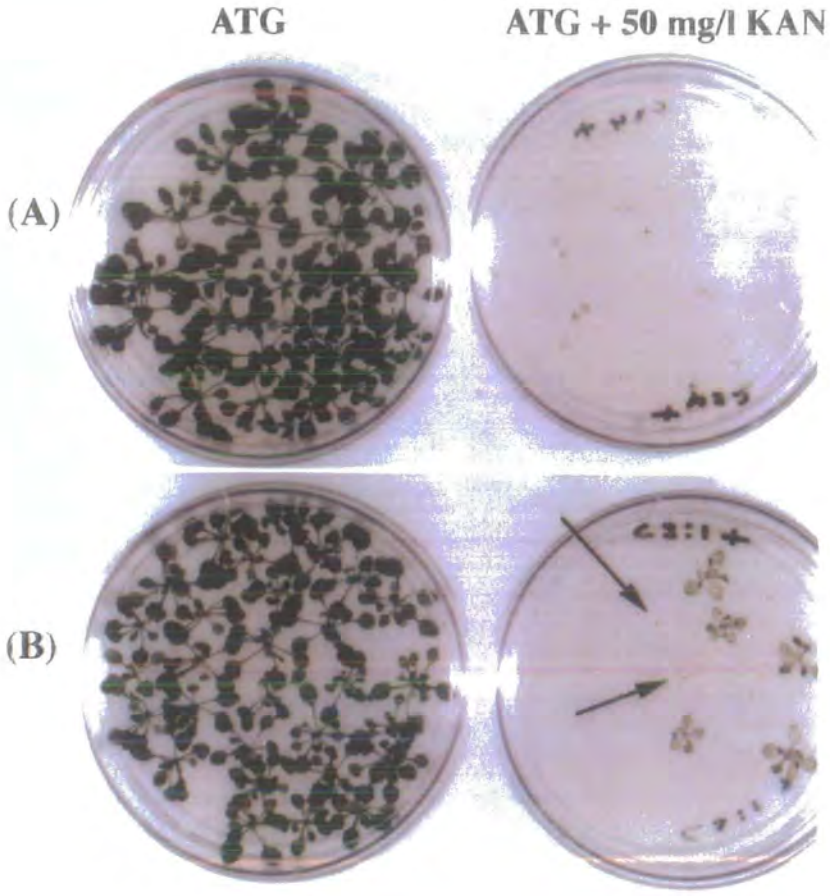

Figure 6.5 Seed viability and selection for kanamycin (KAN) resistance of plants generated from T1 seed (the F1 generation)

Approximately 25-30 T1 seeds, originating from control plants or from selfing of the primary plants transformed with pJKD5.1, were sterilised, germinated and grown in tissue culture (section 6.2.2.D). The figure shows an example of the germination of seed on 90 mm plates containing non selective ATG medium (on the left) or ATG medium with 50 mg/l kanamycin (on the right). Plants which are not resistant against the antibiotic, do not develop past the early cotyledonary two-leaf stage, turn chlorotic and die. In **(A)** the growth of *Arabidopsis* C24 is shown, without and with selection pressure and in **(B)** an example of a segregation of the kanamycin resistance in T1 seed of a known single copy, heterozygote for the kanamycin resistance gene is shown. The arrows indicate the appearance of non-resistant plants after 7-10 days.

In this manner, 40 T1 seed batches, each originating from an independent transformation event, were investigated. Seventeen of the 40 seed batches did not germinate or the few seeds which did germinate, died rapidly due to the presence of 50 mg/l kanamycin in the ATG medium.

The test screening for the segregation of the kanamycin resistance marker in 25-30 seeds was considered to be just a rough indication for the genetic status of the plants. For only a small number of T1 plants an assumption for the possible genetic status could be made beyond reasonable doubt. A kanamycin resistant/kanamycin-sensitive ratio of 3/1 indicated heterozygosity for a single copy insertion of the transgene and this was observed for the T1 generation of the lines: a, 2, 15b, 21, 23 76,651 and 1001. The lines: 7c, 10, 22a, 602 and 604 were scored as double copy transgene heterozygotes (~16:1 or all kanamycin resistant) or possible single copy homozygotes. In segregation tests of T2 seed, several individuals of the T1 generation were scored as single copy homozygotes and the most conclusive observations (all kanamycin resistant in the T2 population) were for the lines: **7a-4**, 8-4, 15b-2, **15b-3**, 15b-4, **22a-2**, 22a-3, 26-1 and 76-2.

An average of 8 plants of each of the 23 viable lines, resistant against kanamycin, were transferred to soil after 10 days and grown to seed. It was the intention to grow each individual plant to produce seed and therefore only a limited amount of tissue could be taken without compromising the growth of the plantlets. One to three leaves were taken from each individual plant of each generation and stored at –80 °C for use in later analyses.
Due to working with a larger number of individual plants of different squash GPAT-transgenic lines, growth of the plants in soil was now performed in the Aracon system and not in pots, as before. The T1 generation of plants, produced seed batches which were then designated as T2 seed. Individual plantlets in each generation were designated according to a numbering system, for example: 15b-3-2, in which 15b is the designation for the original primary independent transformant, 3 indicates that it is plant number 3 out of the T1 generation, and 2 indicates that it is plant number 2 out of the T2 generation (resulting from growth of T2 seed originating from a selfing of plant 15b-3).

The phenotypical, visible appearance of the individual plants from each generation was monitored and compared to wild-type C24 plants. It was observed that lines originating from the different independent transgenic *Arabidopsis* plants had distinctive differences in appearance including plants which were very healthy and green, plants which were fragile with small leaves and many inflorescens, stunted growth, and overall differences

Figure 6.6 Phenotypes of wild-type C24 and transgenic (pJKD5.1) *Arabidopsis* plants

T2 plants were grown in tissue culture (ATG medium + 50 mg/l KAN for transgenic plant-lines and non-selective ATG medium for C24 plants) in dedicated environment chambers at 22 °C; 16 hr light/8 hr dark regime (140 $\mu mol.m^{-2}.sec^{-1}$); 60 % humidity. Plantlets in the four-leaf stage (~10 days after germination) were transferred to soil and grown to seed in the Aracon system under the same controlled conditions.

The phenotypes for the T2 plants of the wild-type *Arabidopsis* C24 plants are well represented by the two plants on the left in each panel. The plants are well developed with a number of tall inflorescens and the plants were flowering.

(A) the phenotypes of T2 plants of the transgenic lines 15b-1,2,3,4 and 5. Plants were very healthy with multiple leaves in the rosettes, but were not bolting yet. In a later stage the plants started bolting with one compact inflorescens out of the centre of the rosette. Overall, plants were healthy and produced relatively good amounts of seeds.

(B) the phenotype of T2 plants from the lines 22a-2,3 and 5 (five middle plants) and one plant (completely on the right) from 76-5. Overall, these plants developed very similar to the C24 control plants but with a slight delay in bolting time. The plant of the line 76-5 was more similar to plants from the lines 15b but with a more pronounced 'lettuce-like' rosette. **(C)** T2 plants for 7a-2 and 7a-4 and these lines developed as fragile plants with relatively small leaves and usually with multiple inflorescens. Bolting and flowering times were similar to the C24 plants with the difference that development of the inflorescens was slower.

in bolting times. Figure 6.6 illustrates the visible appearance of plants of the T2 generation of a number of the transgenic *Arabidopsis* lines. The visible differences in appearance of the plants could be caused by several factors. Ideally it would indicate physiological differences due to functional expression of the transgene (in pJKD5.1, the squash GPAT) but similar variations in physical appearance could also be due to somaclonal effects during growth in tissue culture or insertion of the transgene in positions of the nuclear genome, influencing the expression of approximate genes.

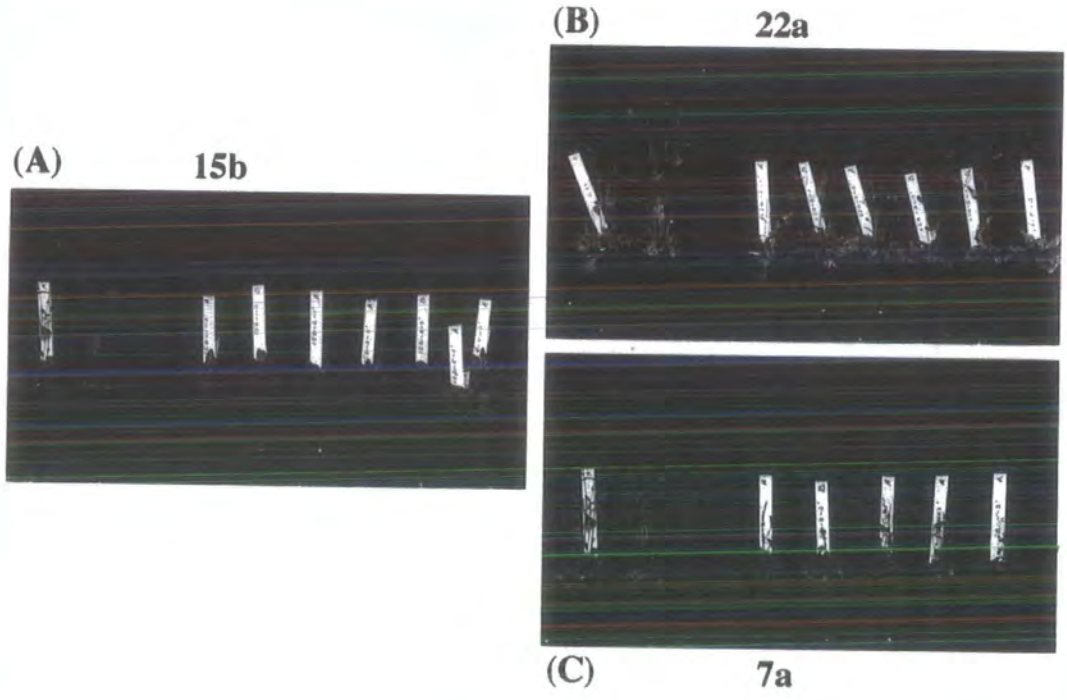

Molecular analysis

Only a relatively small amount of leaf tissue from each individual plant could be collected. This would limit the number of analyses, which could be performed during the experiment. Also because of time constraints (time scales and interaction with an industrial partner), it was the intention to try and obtain minimal essential molecular information concerning the growing transgenic plant lines, enabling the selection of candidate lines for use in the phenotypic screening experiment. Plant lines could then be selected for the subsequent double-transformation with a 'gene-downregulation' tool (a ribozyme) targeted against the endogenous *Arabidopsis* GPAT mRNA.

For interpretation of the results of later experiments, it was desirable to work with transgenic *Arabidopsis* lines which were genetically stable and preferrably with knowledge of the copy number of integrated transgene (pJKD5.1 T-DNA) and expression level of the squash GPAT.

A probe differentiating between *Arabidopsis* GPAT and squash GPAT

The nucleotide sequences of the *Arabidopsis* GPAT gene (the exons) and the squash GPAT cDNA (in the transgene) have a high level of overall similarity. To circumvent the need for development of PCR protocols, using specific primers for the squash GPAT transgene and the endogenous *Arabidopsis* GPAT gene (or their mRNA transcripts), it was evaluated if a fragment of the transgene squash GPAT cDNA could be used as a radioactive probe, which could differentiate between the *Arabidopsis* GPAT gene fragments and the squash GPAT transgene.

Equimolar amounts of the plasmid encoding the squash GPAT transgene (pJKD3.1, as shown in Figure 6.3) and the plasmid p2-6, encoding the full length *Arabidopsis* GPAT cDNA as a 1445 bp. *Eco*RI fragment in pBluescript SK(-) were Southern blotted in duplicate, to Hybond-N membranes according to standard procedures.

One blot was hybridised with ^{32}P-labeled 1572 bp. *Eco*RV cDNA fragment of the squash GPAT transgene encoded by the plasmid pJKD3.1. This cDNA fragment comprises 818 bp of the 3'-part of the squash GPAT cDNA fused to 754 bp of the CaMV polyadenylation sequence. This latter cDNA is only present in the pJKD5.1 encoded transgene T-DNA. The main poly adenylation site, encoded by the CaMV polyadenylation sequence, is thought to be approximately 190 bp distal from the *Eco*RI site of the fusion junction with the 3'-end of the squash GPAT cDNA. The 3'-untranslated sequence of the mRNA transcript of the transgene pJKD5.1 would thus be encoded by at least 190 bp. of the CaMV polyadenylation sequence of the transgene. The duplicate blot was probed with the 1445 bp *Eco*RI *Arabidopsis* GPAT cDNA fragment under identical hybridisation conditions.

Probes were calibrated to equal amount and specific activity, using standard labelling conditions (rediprime system of Amersham/Pharmacia) and by monitoring the incorporation of label using DE81 paper. The probes were added to equal amounts (15 ml) of hybridisation buffer and corresponded to 50 ng labeled DNA with a specific activity of 3.10^8 cpm/μg. It was found that moderate to high stringency washes of the blots (1 x SSC/0.1% SDS to 0.1 x SSC/0.1% at 65 °C), were sufficient to obtain specific hybridisation with the respective probes and to differentiate between the two different constructs, as was visualised by autoradiography (data not shown).

Genomic DNA analysis of transgenic plants

Total genomic DNA from part of the leaf samples of a number of individual T3 plants (usually 4 plants) of each line was isolated using a miniprep procedure of the CTAB method (section 4.2.1). Southern blot hybridisation (section 4.2.2) of 2 μg genomic DNA from leaves of these transformants digested with a number of restriction enzymes and probed with one of the two specific probes described above, showed that in the majority of lines, the transgene squash GPAT cDNA (pJKD5.1) was stably integrated into the genome.

In the majority of the examined lines in the T3 generation, only one copy was integrated. However, in three investigated lines, 10, 602 and 604, the number of integrated copies was estimated to be at least two (data not shown).

Figure 6.7 shows such a Southern hybridisation experiment for individual plants (1 to 4) from the T3 generation of the transgenic lines 15b and 7a and a C24 contol. The restriction enzymes used in the experiment were chosen because it was known that they would digest the *Arabidopsis* GPAT gene with *Nde*I (not with *Xba*I or *Pst*I) and the transgenic squash GPAT-T-DNA (from pJKD5.1) with *Pst*I (not with *Nde*I or *Xba*I).

These Southern blot experiments, with at least 4 different individual T3 plants per transgenic line displaying an identical hybridisation profile and a similar hybridisation signal intensity on autoradiograms, suggested that the transgenic plant lines were genetically stable. Germination and survival of all T3 seed of these lines on ATG medium containing kanamycin, together with the above results, suggested that the examined lines were homozygote for a single copy insertion of the transgene.

Figure 6.7 Genomic Southern blot analysis of transgene squash GPAT (pJKD5.1) and *Arabidopsis* GPAT (1-AT) in two different T3 generation *Arabidopsis* C24 transformants

Southern blot analysis of individual transgenic *Arabidopsis* plants from the T3 generation of plants transformed with a binary plant-vector (pJKD5.1) encoding a fusion protein of squash GPAT (1-AT). Transgene copy number and genetic status of a number of transgenic plant lines (second row from the top: 15b or 7a and C24 control are shown) was examined. (A) Approximately 2 µg of genomic DNA, extracted from leaves of individual plants (T3 plant number indicated third row from the top) or pools of 10 plants (indicated by POOL), was digested with the enzymes *Nde*I, *Xba*I or *Pst*I (indicated in the first row on the top). DNA was fractionated in a 0.8 % agarose gel and transferred to an Hybond-N membrane (Amersham). (B) The membrane was hybridised at 60 °C with a ^{32}P-labeled 1572 bp. *Eco*RV DNA fragment of the squash GPAT construct pJKD3.1. (C) After exposure to film, the membrane was stripped once and re-probed with a ^{32}P-labeled 1445 bp. *Eco*RI cDNA fragment of *Arabidopsis* GPAT (p2-6).

Blots were washed at a moderate stringency at 1 x SSC/0.1% SDS // 60 °C and autoradiographs were exposed for 90 hr. with intensifying screens at –70 °C. DNA markers are indicated as MW (= λ*Hin*DIII).

Under these washing conditions, the probes display minor cross-hybridisation (up to 5%), which is illustrated by the hybridisation of the squash GPAT (pJKD3.1x*Eco*RV) probe with the endogenous*Arabidopsis* GPAT gene for instance in the wild-type C24 samples and in the background of other samples (B). The blot shown in (C), appeared to be not totally stripped of the probe used in a previous hybridisation (B) and therefore residual hybridisation signals to the DNA fragments in (B) are still visible.

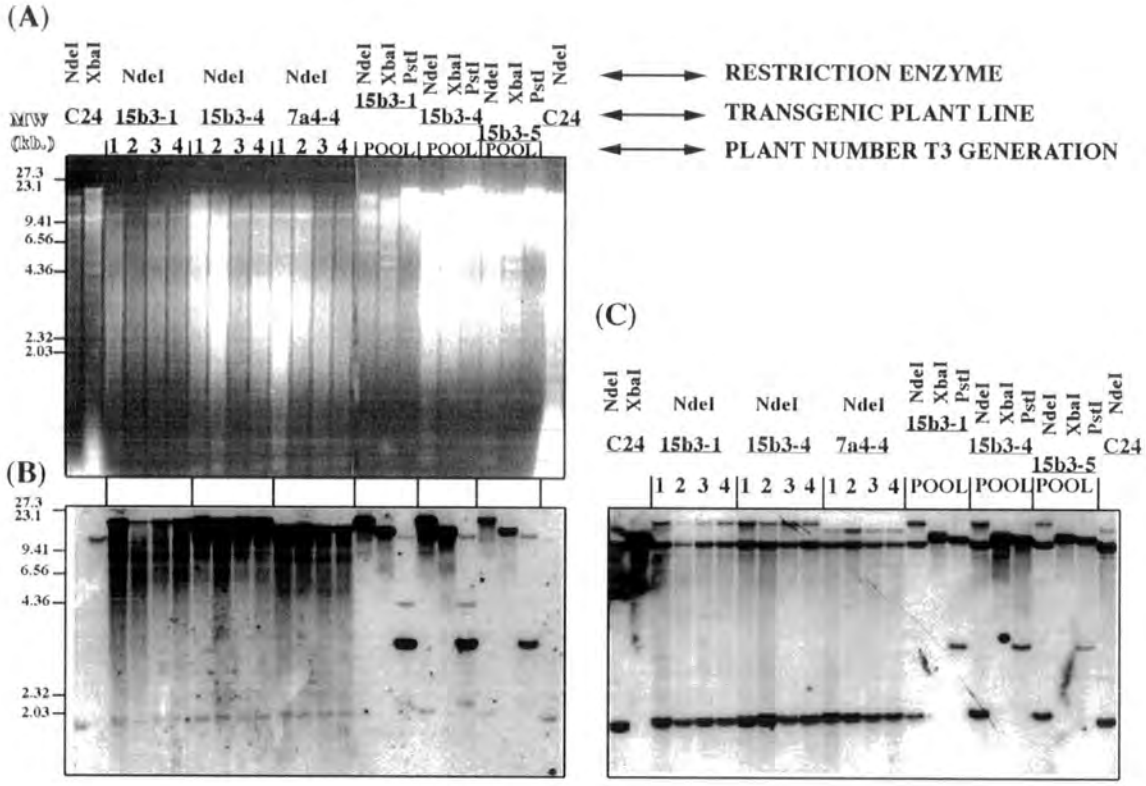
(A)
(B)
(C)
RESTRICTION ENZYME
TRANSGENIC PLANT LINE
PLANT NUMBER T3 GENERATION
MW (kb.)
C24
15b3-1
15b3-4
7a4-4
15b3-5
POOL
27.3
23.1
9.41
6.56
4.36
2.32
2.03

Total RNA analysis of transgenic plants

The steady state level of transgenic squash GPAT mRNA and the endogenous *Arabidopsis* GPAT mRNA, was examined via Northern blot analysis (section 4.2.4). Total RNA was isolated (Trizol, Gibco BRL) from part of the leaf samples collected from individual plants of the T2 generation, transgenic *Arabidopsis* C24 lines. Due to limited tissue material, only small amounts of total RNA per individual plant could be obtained (10-100 μg). It has been shown that the endogenous *Arabidopsis* GPAT mRNA is present only at moderate to low steady state levels in leaf. Although as much as 5 μg polyA$^+$ mRNA demonstrated the presence of a 1.9 nucleotides long mRNA, no cross-reactive band with an *Arabidopsis* GPAT cDNA probe was detected on a Northern blot with 30 μg total RNA (Nishida, I. et al., 1993).

The use of a dextrane sulphate containing hybridisation mix (JODEX: 1M NaCl/10% dextrane sulphate) was found to improve the sensitivity of RNA-DNA hybridisation in a semi-quantitative Northern analysis in this study.

Duplicate Northern blots of 5 μg total RNA from leaf samples of individual T2 transgenic plants were prepared. The ^{32}P-labeled probes, synthesised from the1572 bp. *Eco*RV DNA fragment of the squash GPAT and of a 1445 bp *EcoRI Arabidopsis* GPAT cDNA fragment , were standarised to 50 ng labeled DNA with a specific activity of 3.10^8 cpm/μg. High stringency washes of the blots (0.1 x SSC/0.1% at 65 °C) after hybridisation with the respective probes resulted in specific mRNA detection as is illustrated in Figure 6.8. In this way, a semi-quantitative analysis of the relative steady state levels of the squash GPAT transgene and the endogenous *Arabidopsis* GPAT mRNA in each total RNA sample was obtained. The signals on autoradiography film were quantified via densitometry and volume integration using a BioRad Image Analysis System and software. These experiments demonstrated that the transgenic squash GPAT mRNA was highly expressed and in most examined lines, to be over 5 fold higher compared to the endogenous *Arabidopsis* GPAT mRNA levels.

Figure 6.8 shows that in the transgenic *Arabidopsis* line 10, an aberrant larger transcript was present in leaves at a relatively high steady state level. The nature of this transcript was unknown and was not further investigated.

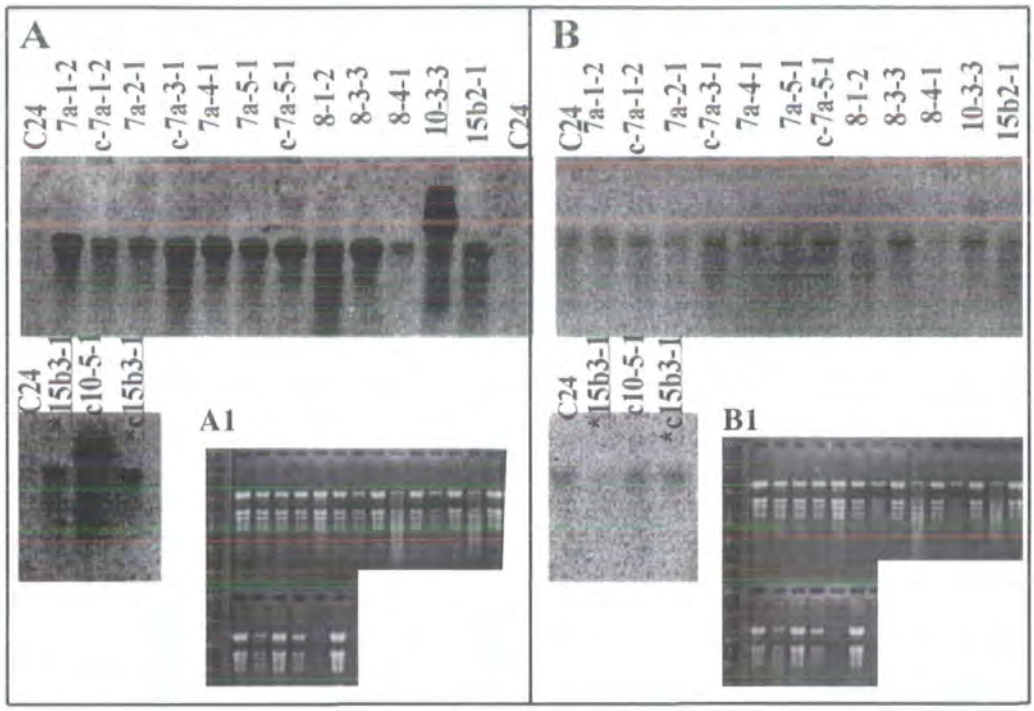

Figure 6.8 Relative steady state levels of mRNA due to expression of the transgene squash GPAT and the endogenous *Arabidopsis* GPAT in leaves from T2 generation plants

Duplicate Northern blots showing the presence of mRNA hybridising to
(A) a ^{32}P-labeled 1572 bp. *Eco*RV cDNA fragment of the squash GPAT construct pJKD3.1 (comprising 818 bp. of squash GPAT and 754 bp. of CaMVpolyA DNA sequence) and
(B) a ^{32}P-labeled 1445 bp. *Eco*RI cDNA fragment of *Arabidopsis* GPAT (p 2-6). These probes were equalised to 50 ng labelled DNA with a specific activity of 3.10^8 cpm/µg and proven to differentiate between the GPAT cDNA nucleotide sequences of both species. 5 µg of total RNA from developing leaf of individual transgenic *A. thaliana* plants (C24 + pJKD5.1/T2 generation, plant lines are indicated above the blot) was fractionated in a 1.2% agarose/formaldehyde gel and transferred to an Hybond-N membrane (Amersham). **(A1)** and **(B1)** ethidium bromide-stained rRNA, shown for loading comparison between lanes on the duplicate blots. A semi-quantitative measure of relative steady state levels of transgene squash GPAT mRNA over *Arabidopsis* GPAT mRNA was obtained via densitometry and volume integration of the signals using a BioRad Image analysis System. The prefix 'c-' before a plant line number, indicates that the plant was subjected to cold/light treatment 2 before leaves were harvested.

Phenotypic screening by cold/light treatment 2

The main objective of this part of the study was to engineer a transgenic *Arabidopsis* C24 line, expressing squash GPAT at a very high level but maintaining chilling-resistance. However, it was expected that a possibility would exist that a limited number of transgenic *Arabidopsis* plants could become chilling-sensitive and would not be suitable for the subsequent double transformation.

A number of transgenic *Arabidopsis* lines were chosen for a first phenotypic screening by subjecting developing T3 plants to cold/light chilling treatment 2. Fourteen T2 seed batches, representing 4 selected primary transgenic lines and T2 control seed of wild-type C24 and the *fad6* (*fadC*) *Arabidopsis* mutant were selected. The transgenic seed batches were of the following lines: 15b-2, 15b-3, 15b-4, 15b-5, 7a-1,7a-2, 7a-3, 7a-4, 7a-5, 8-1, 8-3, 8-4, 10-3 and 10-5. Testing such a large number of individual plants of different squash GPAT-transgenic lines could only be performed practically in the Aracon system. However, it was not clear if the plants would respond to the chilling treatment in the same way as plants in pots. All seed batches were germinated and grown in duplicate pots and in duplicate Aracon systems. One of each was maintained under standard growth conditions and the other set of pots and Aracons were subjected to cold/light chilling treatment 2. An example of the experimental set up is illustrated in Figure 6.9.

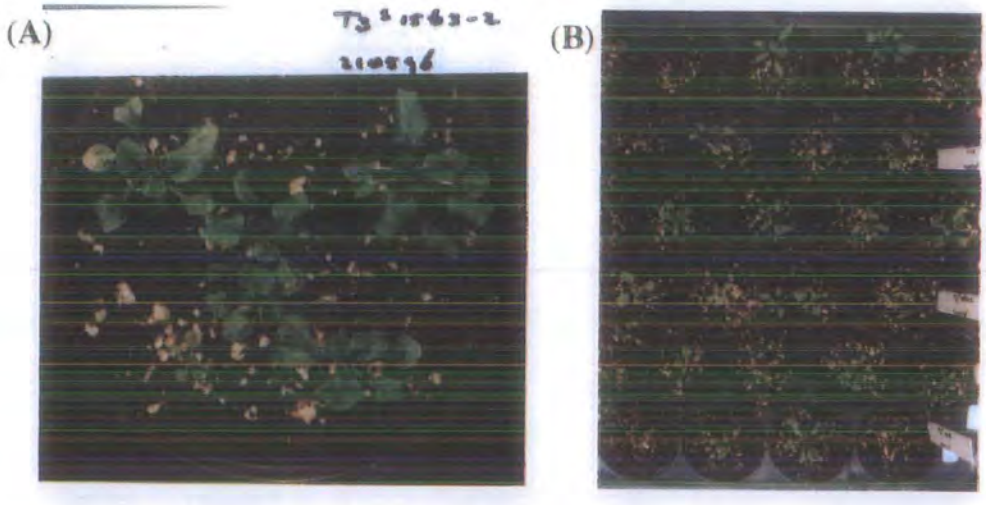

Figure 6.9 Chilling treatment of transgenic (pJKD5.1) *Arabidopsis* line 15b-3-2 in pots and in the Aracon system

Phenotypes of individual plantlets of *Arabidopsis* line 15b-3-2, expressing transgene squash GPAT mRNA and subjected to a cold/light chilling treatment. Plants were grown in pots (A) and in the Aracon system (B) at 22 °C under continuous illumination (140 µmol. quanta $m^{-2}.sec^{-1}$) and 60-70% humidity and 15-20 days old plantlets were subjected to 4 °C under constant illumination (140 µmol. quanta $m^{-2}.sec^{-1}$) and 60-70% humidity, and monitored for 29 days. Plants at day 28 of chilling are shown.

It was found that none of the transgenic plants examined, appeared to be susceptible to the relatively severe chilling treatment. No significant chilling injury was observed but an expected overall delay in growth and bolting rate, relative to the control plants (under standard conditions), was obvious. The cold/light treatment 2 on the *fad6 (fadC) Arabidopsis* mutant plants resulted in a similar chilling damaged phenotype as before (Figure 6.1) but had a more pronounced effect on the plants which were grown in pots compared to the ones (10 plantlets) grown in the Aracon system.

Due to time constraints, it was not possible to evaluate the other transgenic lines at that time.
Western blot analysis to evaluate the relative protein expression levels of the transgenic squash GPAT protein could not yet be performed at the time because the development of specific polyclonal antibodies was still in progress. Techniques for fatty acid content analysis and analysis of the possibly altered composition of chloroplastic phosphatidyl glycerol (PG) were being developed in the laboratory but could not yet be practically employed.

In was considered to be a priority to proceed with the development and evaluation of the ribozyme (Rz) mediated, specific *Arabidopsis* GPAT down regulation of expression.

The following transgenic *Arabidopsis* lines, expressing the squash GPAT mRNA at high levels, were considered to be prime candidates for the double transformation (gene-stacking) with a ribozyme construct, specifically targeted against the endogenous *Arabidopsis* GPAT mRNA: 15b-3 (1 to 5), 22a-2 (1 to 5) and 7a-4 (1 to 5). All three lines appeared to be genetically stable and seem to contain a single copy transgene squash GPAT insertion. The transgenic plants, with exception of the 7a line, had robust and healthy growth phenotypes (Figure 6.6). It was decided to select the transgenic *Arabidopsis* line 15b-3 for the subsequent double transformation.

6.3.3 Creation and application of ribozyme (Rz)-expressing plant vectors

A second plant transformation of the selected transgenic *Arabidopsis* C24 plant line, transformed with pJKD5.1, was intended to down regulate the expression of the endogenous *Arabidopsis* GPAT. The genetically stable plant line 15b-3 was selected because it was shown by Northern analysis, that the plants were expressing the 'foreign' squash GPAT fusion product at relatively high levels but they still appeared to be chilling-resistant. By down regulating the expression of the endogenous GPAT *in vivo*, the transgene squash GPAT may effectively compete in the plant and possibly confer chilling-sensitivity upon the *Arabidopsis* plants by changing the fatty acid composition of membranes.

The gene-downregulation of one out of multiple, sequence-similar acyltransferase genes, required the development and use of a molecular tool which would be very specific for its intended target. An approach to use an *in trans* working hammerhead ribozyme (Rz) to specifically target the endogenous *Arabidopsis* soluble GPAT mRNA, was evaluated. The design and construction of hammerhead ribozymes (Rz) for use in the double plant-transformation (gene-stacking) of the selected transgenic plant (squash GPAT transgene) and for testing of the *in vitro* Rz activity, is described in Chapter VII.

Ribozymes, or catalytic RNA's, are RNA's with the capacity to cleave covalent phosphodiester bonds catalytically and sequence specific in a target RNA (Zaug, A.J. et al., 1986; Uhlenbeck, O.C., 1987; Haseloff, J. and Gerlach, W.L., 1988; Symons, R.H., 1992; Pyle, A.M., 1993); therefore, they have enormous potential to inhibit gene expression. Specific endonucleolytic ribozymes, based on the naturally occurring class of self-cleaving RNA's, the hammerhead, have received most attention thus far because of its early discovery, small size and potential to cleave almost any RNA molecule (Bratty, J. et al., 1993). It is possible to engineer artificial ribozymes, which could cleave practically any target RNA molecule *in trans*. The first published reports concerning the use of ribozymes as therapeutic agents by Haselhoff and Gerlach (Haseloff, J. and Gerlach, W.L., 1988) defined general design rules for simple hammerhead ribozymes capable of acting *in trans*.

In principle, this strategy can be used to alter the level of any biological RNA in a living organism and research towards achieving this goal has been a major focus of ribozyme research (Usman, N. and Stinchcomb, D.T., 1996; Symons, R.H., 1991). Despite much effort, the progress has been slow in attaining highly efficient cleavage of target molecules in living cells. In no reported studies to date, has complete or nearly complete cleavage been observed *in vivo* for any *trans*-acting ribozyme (Cotton, M., 1990; Sarver, N. et al., 1990; Sullenger, B.A. and Cech, T.R., 1993; Burke, J.M., 1997; Montgomery, R.A. and

Dietz, H.C., 1997). For the realisation of the full potential for modulating gene expresssion with ribozymes, overcoming the factors that limit the ribozyme efficiency in living cells is critical.

To achieve efficient cleavage *in vivo*, three key conditions can be identified and must be satisfied:

1) a high degree of colocalisation of the ribozyme in the same subcellular compartment(s) as the target molecule(s) (Symons, R.H., 1991; Sullenger, B.A. and Cech, T.R., 1993; Ding, D. and Lipshitz, H.D., 1993; Burke, J.M., 1997),

2) a high, non-limiting intracellular concentration of ribozyme. This requires a high transcription rate and/or a high metabolic stability of the ribozyme (Marschall, P. et al., 1994), and

3) highly effective ribozyme-target(substrate) interaction, i.e., a good accessibility and turn-over of the relevant RNA sequences in the catalytic and substrate molecules

The latter point continues to be a major point of limitation because the potential for interference effects can be high; either or both RNA molecules may be large, complex and interacting with proteins. At the moment, there is a lack of detailed information about the *in vivo* dynamics and structures of the interacting RNAs (Fedor, M.J. and Uhlenbeck, O.C., 1990; Pachuk, S.J. et al., 1994; Chen, H. et al., 1997).

In this study it was sought to try and satisfy these criteria as much as practically possible. Endonucleolytic ribozymes based on the hammerhead were designed to specifically bind and cleave at two different GUC motifs within the projected target *Arabidopsis* GPAT mRNA (Accession number D00673). To monitor potential anti-sense effects (Nellen, W. and Lichtenstein, C., 1993), a mutated version of each ribozyme (MRz1 and MRz2) was created by means of an A-14-G transition within the ribozyme domain known to inactivate RNA catalysis *in vitro* (Chapter VII).

For effective endogenous delivery and thus intracellular transcription of the ribozymes in plant cells, the U1.1snRNA expression system was chosen.

This system has a number of important advantages and may satisfy many of the key considerations for effective *in vivo* ribozyme efficacy:

--- gene expression appears to occur in all tissues and is an order of magnitude higher than for many other genes,

--- the required gene constructs are smaller and therefore easier to manipulate,

--- multiple copies of ribozyme genes can be included in each construct to increase enzyme dose, and ribozyme sequence can be varied in order to aim for more than one site in the target RNA,

--- the embedded ribozymes are likely to be more stable and sequestered in the same cellular compartment as the target mRNA

Hammerhead ribozyme 1 (Rz1), which was demonstrated to be target specific and cleave *Arabidopsis* GPAT mRNA in a cell free system (Chapter VII), and its catalytically inactive A14G mutated version (MRz1), were embedded in a potato U1.1 snRNA (Vaux, P. et al., 1992) as described in Chapter VII.

U1snRNAs occur in the nucleus of plants and animals and smaller eukaryotes and are generally the most abundant of the spliceosomal UsnRNAs. The major role of U1snRNP is the recognition of intron 5' splice sites via base-pairing of the 5' single-stranded region of U1snRNA to the 5' splice site of the pre-mRNA in the nucleus. In plants the U1snRNA genes seem to be highly homologous (between 80 and 90%) between different species and U1snRNA transcripts are present in high levels in the nucleus!
Selected U1.1 snRNA-ribozyme constructs (generally referred to as pU-Rz, in this study) were cloned in the SCV-based plant transformation vector pDH 69.

The binary plant transformation vector pDH69 was constructed by D. Hird at the Botany Department in the University of Leicester and was obtained via the industrial partner (Nickerson Biocem) with permission. The megaplasmid encodes a kanamycin/gentamycin resistance (amino-glycoside phosphotransferase (APH(3')II) gene and also an ampicillin resistance (β-lactamase) gene for selection in *E.coli* or *Agrobacterium* (used 25 μg/ml kanamycin or 5 μg/ml gentamycin and/or 50 μg/ml ampicillin). For propagation in *E. coli*, a COL E1 origin of replication is encoded and for *Agrobacterium*, a RK2 origin was present. Within the left- (LB) and right border (RB) of the transfer (T)-DNA region, two RNA polymerase II transcription cassetes were represented (see also the schematic drawing of pDU 1.9-5 in Figure 6.11). One cassette encoded a β-glucuronidase (GUS) gene, under control of the pea plastocyanin promoter (Pwee, K.H. and Gray, J.C., 1993) and the mRNA was stabilised by the CaMV polyadenylation sequence. This cassette was still being experimentally tested for use as a (extra) reporter for successful plant transformation, but was not used as such in this study. The other transcription cassette encoded a phleomycine resistance as a dominant selectable marker for the double transformation of the, already kanamycin resistant, transgenic *Arabidopsis* plant line 15b-3 (Perez, P. et al., 1989). The gene conferring resistance for bleomycin and phleomycin was isolated from *Streptoalloteichus hindustanus* (designated *She-Ble*) and placed under control of the nopaline synthase (NOS) promoter and polyadenylation sequence.

Figure 6.10 ***Arabidopsis*** **plantlet viability assay ('kill-curve') on selective medium with phleomycin (Phleo)**

Approximately 25-30 F3 seeds, originating from control plants (C24) or from selfings of the plant line 15b-3-2, transformed with pJKD5.1, were sterilised, germinated and grown in tissue culture (section 6.2.2.D). The figure shows an example of the germination of seed on 90 mm plates containing ATG medium with a concentration range of 0, 20, 30 and 40 mg/l phleomycin D1. Plants which are not resistant against the antibiotic, appear to develop slower as indicated by the rate at which the different leaves appear. Some plants turned chlorotic and died eventually, especially when the concentration of phleomycin is greater than 20 mg/l. The photographs were taken approximately after 18 days after germination.

Before undertaking transformation experiments, the sensitivity of the wild-type *Arabidopsis* C24 and the transgenic 15b-3-2 (F3 generation) cells to phleomycin, under germination and rooting conditions, were determined. The recommendations of the supplier of phleomycin D1 (Cayla; Centre Commercial de Gros, Avenue de Larrieu, 31094 Toulouse cedex, France) indicated that Phleo^{R} transformed plant cells could be selected in the concentration range between 5 and 25 μg/ml. Perez and co-workers (Perez, P. et al., 1989), performed experiments in the range of 10 to 50 μg/ml. A 'kill-curve' was determined by germinating sterilised seed of both plant lines on ATG medium (section 6.2.2.D) with phleomycin present at 0, 10, 20, 30, 40 and 50 μg/ml. The germination frequency, viability and phenotype of the plantlets during growth in tissue culture and incubation at 22 °C; 16 hr light/8 hr dark regime (140 μmol.m^{-2}.sec^{-1}), 60 % humidity, was examined (Figure 6.10).

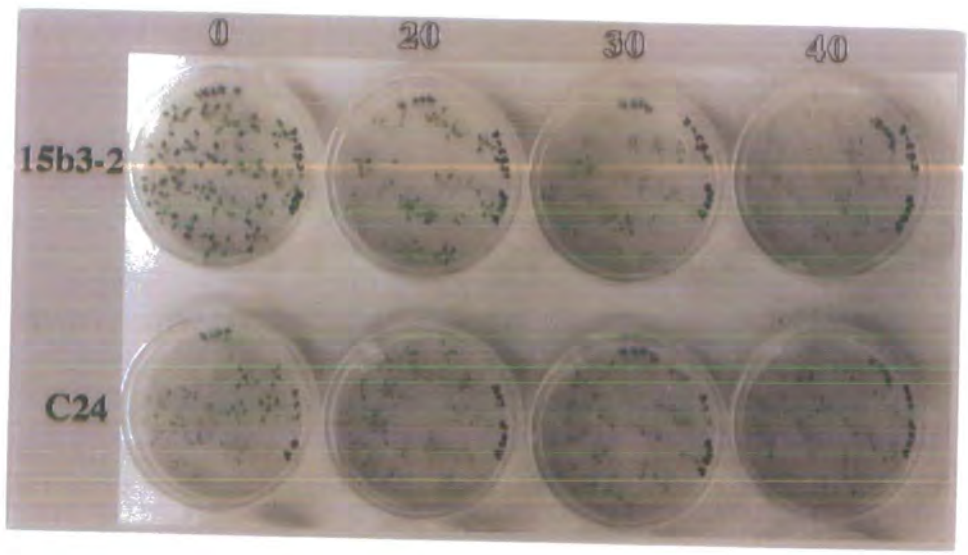

It was observed that in this 'plantlet viability assay', the plants, which do not encode a phleomicin resistance, developed slower at higher concentrations of phleomycin. It appeared that sensitivity was displayed by slow development of the seedlings and some would eventually die on concentrations of phleomycine at 30 mg/l and above. Although this was not a direct test of sensitivity versus resistance of regenerative tissue, during for instance a transformation procedure, it did indicate a 'working-concentration' for selection, in a similar range found by the few researchers who also used this selection marker. With consideration for the nature of phleomycin action (cleavage of DNA), it was decided to perform transformation/selection experiments at the relatively high concentration of 30 µg/ml phleomycin, to select for true transformants in a stringent manner.

The construction of the clones pDU 1.9-5 (one copy Rz1), pDU 1.2-1 (double copy Rz1) and pDU 2.4-1 (one copy of A14G MRz1) is described below and the cloning procedures are illustrated in Figures 6.11 and 6.12.

Ribozymes, which were embedded in the 5' single-stranded region of a potato U1.1 snRNA gene, were cloned in the *Hin*DIII and *Eco*RI site of the basic transcription vector pGEM-3Zf(+) (Promega) and are generally designated pU-Rz (Figure 6.11). In this collaborative study of ribozyme mediated gene-inactivation, the clone with the potato snRNA (U1.1-65) was kindly provided by Dr. J. Brown of the Scottish Crop Research Institute (Invergowrie, Dundee, Scotland). The detailed design of the ribozymes and their construction, is described in Chapter VII. Approximately 10 µg of the pU-Rz vectors: pU1.1-1.2-1, pU1.1-1.9-5 or pU1.1-2.4-1, were digested with 50 units of each of the restriction endonucleases *Hin*DIII and *Eco*RI in a total reactionvolume of 200 µl. After 3 hr. incubation at 37 °C, the DNA was purified and concentrated by a standard phenol/chloroform (v/v, 1:1) extraction followed by a salt/ethanol precipitation and resuspended in 20 µl of sterile water (milliQ). The 3;-recessed termini were filled-in (blunt-ended) by 5' – 3' polymerase activity of VENT DNA polymerase (New England Biolabs, NEB) in a reaction as described before (section 6.2.1). Half of the blunt-ended DNA products were purified by standard gel band purification from a preparative 0.9% agarose gel and were eluted in an end-volume of 25 µl. After analysis of a sample by 1.0% agarose gel electrophoresis, to estimate the recovery and the concentration, approximately 2 µg DNA fragment was ligated to 1 µg *Xba*I-*Xmn*I conversion adaptor (New England Biolabs, NEB: #1133 + #1140) in a standard ligation of 30 µl total reaction volume.

_Xba_I-_Xmn_I conversion adaptor:

5'-CTAGCGAAGGGGTTCG-3'
3' GCTTCCCCAAGC-5'-P

The DNA termini of the modified ligation products were phosphorylated with T4 polynucleotide kinase (Promega) as described before (section 6.2.1) and final products were purified via agarose gel band extraction. The megaplasmid pDH69 was digested with *Xba*I, deposphorylated with Shrimp Alkaline phosphatase (SAP; USB) and ligated (in an equimolar vector:insert ratio/ 200 ng vector 12 ng insert) to the *Xba*I-flanked U1.1-Rz fragment, according to described procedures (section 6.2.1). The *Xba*I site was the only unique cloning site left within the T-DNA sequence of pDH69 and was located between the two transcription cassettes (described above and illustrated in Figure 6.11).

The resulting ligation reactions were transformed to electrocompetent *E. coli* DH10B cells (Electromax; Gibco BRL) by electroporation (section 6.2.1) and selected on LB plates containing 50 µg/ml AMP and 25 µg/ml KAN. Approximately 40 of the resulting colonies were analysed for integration of the U1.1-Rz DNA fragment by a colony hybridisation procedure as described in section 6.2.1. Concatemerised ribozyme 1 (Rz 1) (Chapter VII, section 7.2.2) was used as a ^{32}P-labeled probe and hybridising clones were identified via exposure to autoradiography film. Three selected clones of each of the respective cloning excercises were grown in selective LB medium and plasmids were isolated and analysed via nucleotide sequence analysis using a primer directed against the U1.1 snRNA gene. The oligonucleotide used for sequencing was designated pU1 280S: 5'- GACTTACTCCCACATCGCTAAG-3', and it's position is indicated in the schematic drawings in Figure 6.11 and 6.12 A.

The resulting clones had to be further examined for the possibility of single or multiple insertions of the U1.1-Rz fragments in the vector and also for the orientation of the insertion, relative to the two existing transcription cassettes in the megaplasmid pDH6.9. Using different combinations of oligonucleotide primers, a PCR approach was employed to investigate the different clones (pDU 1.9-3, pDU 1.9-5, pDU 1.2-1, pDU 2.4-1 and pDH69 as a control) and the results are illustrated in Figure 6.12.
In standard polymerase chain reactions (PCRs) the following oligonucleotides were employed:
pU1 280S: described above;
pNOSpA: 5'- GAATCCTGTTGCCGGTCTTGC-3';
pPCI: 5'-CGTTGTAAGTTGCATATGTCC-3',
pRz1: 5'-GACGCGAAACGAAGCGAGTG-3' and
pU1d: 5'-GGCCCCCACTGCAACAAATT-3'.

It was found that all the investigated clones had the intended single insertions of the U1.1-Rz. The orientation of the insertions, as defined by the direction of transcription, relative to the phleomycine resistance and the GUS transcription cassette is indicated by the arrows below the gel picture in Figure 6.12. The direction of transcription of the U1.1-Rz insertion in the clones DU 1.9-5, DU 1.2-1 and DU 2.4-1 was parallel to the other transcription cassettes but the clone DU 1.9-3 directed transcription in the opposite direction.

Figure 6.11 Cloning of a ribozyme (Rz), embedded in a potato U1.1 snRNA gene, in the megaplasmid plant transformation vector pDH69

Flow diagram of cloning procedures and schematic representations of the construct pU-Rz1 (top), a pGEM-3Zf(+) vector with ribozyme 1 (Rz1) embedded in an introduced *Bgl*II site of the potato U1.1-65 snRNA gene (Vaux, P. et al., 1992) and the resulting plant transformation vector pDU 1.9-5.

Cloning steps are described in detail in the text. The schematic drawings of the constructs represent DNA sequences and restriction sites, relevant for interpretation of the cloning or analysis procedures, are indicated above the drawings. Designation of restriction sites *Hin*DIII and *Eco*RI in outlined characters is meant to accentuate that they were important in the following steps. The designation for the different portions of the DNA constructs are depicted below the drawings and the boxes they represent are filled in with different patterns to clarify the distinction within the diagram. Nucleotide positions corresponding to relevant restriction sites, the primer positions and the positions of other DNA sequence elements, are shown directly below the drawings. USE = Upstream Sequence Element and TATA depicts the U1.1 TATA box (Vaux, P. et al., 1992). The primers used in nucleotide sequencing (pU1 280S) and in PCR analysis are indicated by arrow points. Below the drawing of pDU 1.9-5, the designation for the different DNA sequences and their respective sizes (underlined and illustrated by horizontal double arrows) is shown.

Figure 6.11 Construction of pDU-Rz plantvectors

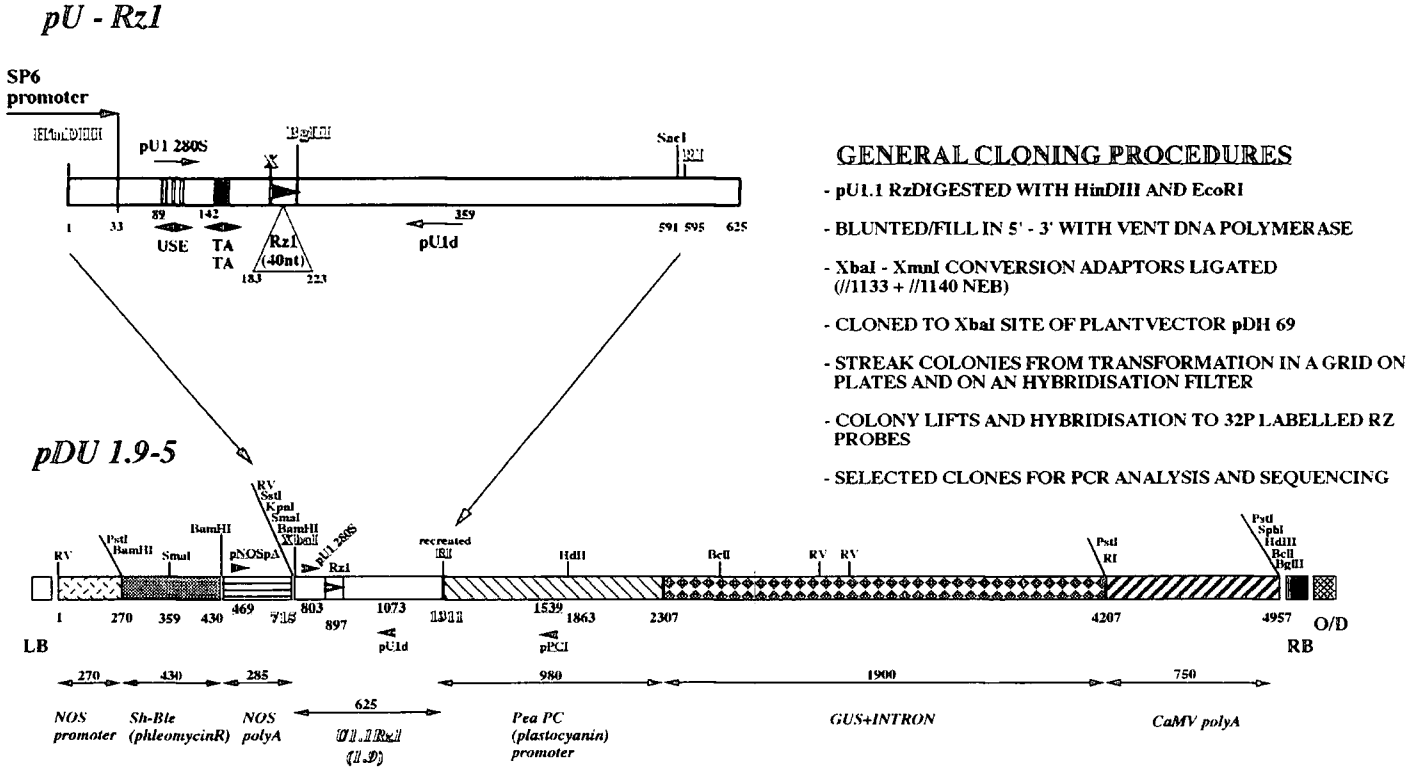

Figure 6.12 Schematic representation of the U1.1-Rz region of the plant binary vectors pDU-Rz and illustration of PCR analysis of different constructs compared to the 'empty' vector control (pDH69)

(𝔸): The two possible orientations of the cloned U1.1-Rz, relative to the neighbouring transcription cassette (phleomycin resistance), is illustrated. The depiction of restriction sites, primers and primer positions, is described in the legend of Figure 6.11. The nucleotides are numbered from the start of the NOS polyadenylation DNA sequence for simpler interpretation of the size of DNA fragments resulting from PCR amplifications using the different combinations of primers.

(𝔹): Samples of different, analytical PCR reactions were size fragmented in a 1.2 % (w/v) agarose gel electrophoresis and the samples are indicated above the lanes. Designation for the samples is by the primer combinations used in the respective PCR reactions. The oligonucleotide sequences are given in the text. Molecular weight markers (M1 = λ*Hin*DIII and M2 = λ*Pst*I) were run in the flanking lanes and are indicated in base pairs on the left side of the gel. The sizes (in base pairs) of the respective DNA fragments are shown below the lanes. The cross (𝕏) indicates that only 'background' (a-specifically amplified DNA) was present.

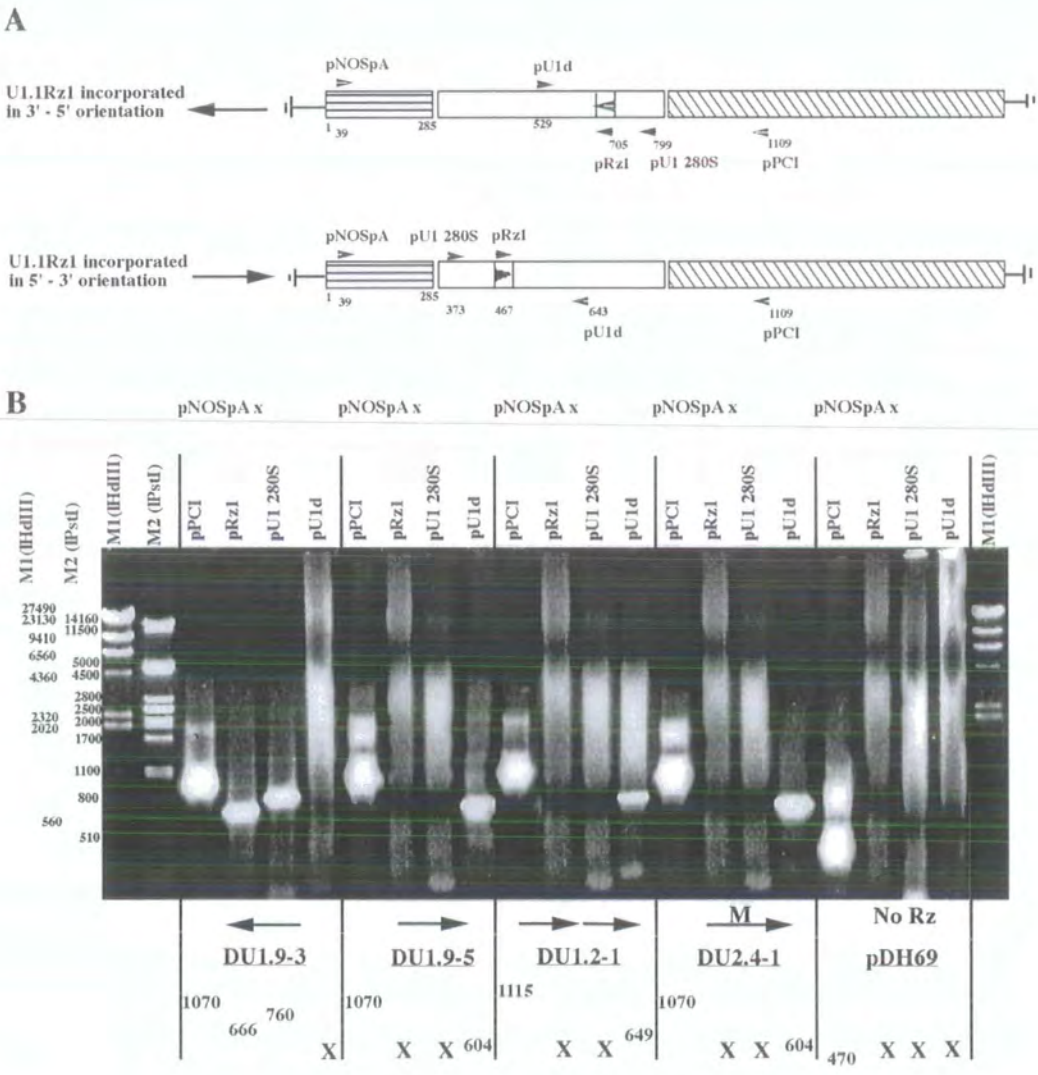
A
U1.1Rz1 incorporated in 3' - 5' orientation
pNOSpA
pU1d
1
39
285
529
705
799
1109
pRz1
pU1 280S
pPCI
U1.1Rz1 incorporated in 5' - 3' orientation
pNOSpA
pU1 280S
pRz1
1
39
285
373
467
643
1109
pU1d
pPCI
B
pNOSpA x
M1(HdIII)
M2 (PstI)
pPCI
pRz1
pU1 280S
pU1d
27490
23130
9410
6560
4360
2320
2020
14160
11500
5000
4500
2800
2500
2000
1700
1100
800
560
510
DU1.9-3
DU1.9-5
DU1.2-1
M
DU2.4-1
No Rz
pDH69
1070
760
666
X
1070
X
X
604
1115
X
X
649
1070
X
X
604
470
X
X
X

The F3 generation of plants of the genetically stable *Arabidopsis* line 15b3-2-(2,4+5), expressing transgenic squash GPAT mRNA at a high level, was double-transformed via the *Agrobacterium* (C58C1//pGV2260) mediated root-transformation (section 6.2.2D), with the exception that selection was now for resistance against 30 μg/ml phleomycin in the tissue-culture media.
A large number (~100) of green calli were regenerated and approximately 50 were forming shoots on selective medium (+ phleomycin).

After transfering tissue-culture plates to a larger growth chamber, which also harbored other species of flowering plants (*Brassica napus*), a major problem occurred with contaminations on the plates. It was established that the medical micropore tape, with which the tissue-culture plates were sealed, did not prove to exclude a minority of spores in the atmosphere of the growth chamber. Many attempts to rescue the putatively transformed plantlets, by regular subculturing to fresh plates containing phleomycin, were in vain. Repeated transfer and challenges with fresh doses of phleomycin as a antibiotic selection marker was thought to be detrimental to the survival of even putatively resistant plants.

6.4 Conclusion

A common goal of many efforts in plant biotechnology is the overexpression of an endogenous or introduced trait. The experiments within this project were designed to initiate the examination of a double strategy aimed at modifying fatty acid composition. The focus was on the ectopic expression of a heterologous acyltransferase enzyme and the subsequent down-regulation of the gene expression of the homologous, endogenous acyltransferase gene of the plant species under investigation. Overexpression of a plant-derived enzyme does not always lead to an increased enzymatic activity *in vivo*. The newly introduced transgene and/or its product may be subject to endogenous regulatory mechanisms including cosuppression (see Appendix A), metabolic or posttranslational control. Also, to have a substantial effect upon the physiology of the engineered plant cells, the transgenic enzyme has to be able to compete effectively with the endogenous enzyme for local concentrations of substrates and other necessary factors. The transgenic enzyme may overcome the likely advantage of the endogenous enzyme in its natural cell environment, when the gene expression of the resident gene would be down regulated.
In this study it was envisaged that a rigorous biological test of these concepts could come from experiments in which the functioning of a highly substrate-selective endogenous acyltransferase (*Arabidopsis* GPAT), may be overcome by the overexpression of biological activity of a transgenic non-selective enzyme (squash GPAT) and followed by the effective *in vivo* down-regulation of the endogenous gene expression.

Transgenic *Arabidopsis* plant lines were generated which were transformed with a squash GPAT cDNA. A number of transformed lines were examined and the stable integration of the transgene into the genome (Southern analysis) was confirmed. It was found that in many lines the transgenic squash GPAT mRNA was present at more than 5 fold higher steady state levels than the endogenous GPAT mRNA.
Due to a combination of time constraints, alternative priorities and the fact that two important analytical techniques were still in a development stage within the laboratory, some analytical experiments could not yet be satisfactory performed at the time. The presence and level of expression of the transgenic squash GPAT protein in the chloroplast fractions of the transgenic *Arabidopsis* plants would also have to be examined. A specific antiserum against each of the proteins would be ideal (Chapter III) to investigate the relative protein levels of both GPAT enzymes in leaf cells by Western blot experiments. The antisera were in the process of being developed but a specific, low background and high titer antiserum seemed to be needed to be able to detect GPAT proteins in crude extracts of *Arabidopsis* leaves (Chapter III).

It would also be of importance to investigate if the expression of the introduced squash GPAT transgene has had an influence upon the fatty acid content and/or the composition of chloroplastic phosphatidyl glycerol (PG). It has been shown that the biological, phenotypic property of chilling-sensitivity of plants, can be genetically altered by varying the levels of disaturated chloroplastic PG (HMP-PG) molecular species due to expression of GPAT enzymes with different substrate selectivities.

One of the main objectives of this study was to convert a (still) chilling-resistant transgenic *Arabidopsis* plant (expressing a non-selective GPAT from the chilling-sensitive plant squash at high levels) into a chilling-sensitive plant. This may be achieved by down-regulation of the endogenous GPAT gene by ribozyme-mediated cleavage of *Arabidopsis* GPAT mRNA *in vivo* (see below). It was expected that the possibility would exist that amongst a relatively large number of transgenic (+ squash GPAT) *Arabidopsis* plants from the first transformation, chilling-sensitive phenotypes could be found. It was shown however, that none of the examined transgenic plants were sensitive to a relatively severe, prolonged exposure chilling-treatment. When considering the evidence from previous studies concerned with the evaluation of the correlation between the level of HMP-PG molecular species and chilling-sensitivity, the following speculation could be made. Variation in the specific levels of HMP-PG molecular species in chloroplastic membranes of different plant species, might only lead to a biological effect, i.e. chilling-sensitivity, when a certain critical level, specific for that particular plant species has been reached. When elevated levels of HMP-PG are engineered in leaves of chilling-sensitive plants, such as tobacco transformed with squash GPAT (Murata, N. et al., 1992), this may only affect the extend of damage and dramatise the chilling-sensitivity. However, to convert a chilling-resistant plant, such as *Arabidopsis*, into a chilling-sensitive plant may require a relatively very high level of disaturated HMP-PG in the chloroplast membranes. The *fab1* mutant of *Arabidopsis* was found to contain an increased content of HMP-PG molecular species in the leaf PG (from 20-42%) but was found only to be susceptible to a prolonged exposure chilling treatment (Wu, J. and Browse, J., 1995). Short exposure low temperature treatments did not affect this *fab1* mutant but were found to be sufficiently effective to damage (wilting and necrosis) transgenic *Arabidopsis* plants containing HMP-PG more than 50% of the total leaf PG (Wolter, F.P. et al., 1992). However, it has been considered (Wu, J. and Browse, J., 1995) that these *Arabidopsis* plants, transformed with a modified *E. coli plsB* (membrane bound GPAT), show damaging effects of low temperature exposure because of some other aspect of transgenic *plsB* expression. It would therefore be very interesting to investigate the level of HMP-PG in the plants generated in this study and ideally, after potentially down regulating the endogenous GPAT gene expression, to monitor the effects upon the level of chloroplast HMP-PG and the chilling-sensitivity in those double transformants.

Alteration in the expression of endogenous plant genes allows the study of their function and contribution to plant growth and physiology. However, in contrast to prokaryotic cells, deletion-mutants or conditional-mutants in specific loci are hard to acquire in eukaryotic cells when the mutation is lethal, when the phenotype can not be predicted or because mutations are not effective when a multigene family is transcribed.
The application of reverse genetics to suppress or modify eukaryotic gene expression, has been shown to be a powerful tool in determining gene function, identification of 'cryptic' genes and in genetic improvement of crops with altered properties and desirable traits (controlling virus and parasitic infections and manipulation of metabolic pathways). A mini-overview of tools of reverse genetics is presented in Appendix A.

In this study and described in detail in Chapter VII, hammerhead ribozymes were designed aimed at two different GUC triplets in the mRNA sequence of the endogenous chloroplastic *Arabidopsis* GPAT, encoding the chloroplast targeting polypeptide.
These target sequences were not present in (and in any case, least similar to) the homologous transgenic squash GPAT previously introduced into the plant (Figure 6.2). It was envisaged that when the ribozyme would effectively function *in vivo* (*in planta*), the *Arabidopsis* GPAT mRNA would be destroyed before it could be translated or targeted as a functioning protein and that the transgenic squash GPAT would confer the property of chilling-sensitivity upon the transgenic *Arabidopsis* line.

The realisation of the full potential of highly efficient ribozyme-mediated endogenous gene down-regulation in living cells (*in vivo*), and especially in plants, has not as yet been achieved. A number of conditions for potentially efficient target cleavage *in vivo* has to be met, as outlined in section 6.3.3. In this study the cellular delivery of the ribozyme was aimed to be an endogenous delivery, i.e. aimed at intracellular transcription of a ribozyme encoding gene integrated into the genome. This would allow genetic stability of the ribozyme and continual expression.
A ribozyme against the *Arabidopsis* GPAT mRNA (Rz1) was embedded in a (potato) snRNA gene, ensuring a high level of expression and localisation of the U1.1-Rz transcripts mainly in the nucleus (Cotton, M. and Birnstiel, M.L., 1989), hopefully in co-localisation with newly transcribed *Arabidopsis* GPAT (pre-) mRNA. This colocalisation could be even more stimulated by the presence of introns in the pre mRNA of nuclear encoded, chloroplastic *Arabidopsis* GPAT (Nishida, I. et al., 1993) with respect to the natural function of U1.1 snRNA. U1snRNA is an abundant component of U1 snRNP and the 5' single-stranded region, in which the Rz1 was embedded, base-pairs with intron 5' splice sites.
U1.1-Rzs were cloned in a plant transformation vector and transformed to F3 generation plants of the transgenic *Arabidopsis* line 15b-3, expressing squash GPAT at a high steady state mRNA level.

Unfortunately, the first rounds of *Agrobacterium* mediated root-explant transformations failed due to a combined problem of contamination and of working with phleomycin as a second selectable marker for the double transformation. The contamination occurred when tissue culture plates, with regenerating transformed plantlets and sealed with gas-permeable medical tape (Urgopore), were transferred to an environmental chamber with multiple and flowering *Brassica napus* plants. It became painfully obvious that the tape could not totally exclude fungal spores, which were clearly airborn and saturating the growth chamber environment (Sanyo). Phleomycin belongs to the glycopeptide group of the bleomycin group of antibiotics. Their toxicity is exerted by breaking of DNA at specific sites and the mode of action for resistance is based on a one-to-one ratio binding of the *She-Ble* protein to the antibiotic, which then can no longer cleave DNA. In attempts to rescue putatively transformed plants from contaminated plates, they were repeatedly transferred to fresh selective media. However, it seemed that the level of (suspected) resistance, could not 'keep up' with repeated challenge with fresh doses of phleomycin. Although the *She-Ble* encoded phleomycin resistance has been used as a selectable marker (Perez, P. et al., 1989), on basis of experiences within this study, it was found that phleomycin does not seem the most practical and selective to work with for the acquisition of transformed plants. Other selectable marker genes encoding resistance to toxic drugs (hygromycin, chloroamphenicol, streptomycin, gentamycin, methotrexate, phosphinotricin) could be used as alternatives.

Chapter VII

∞∞∞∞∞

In Vitro Ribozyme Action on *Arabidopsis* Glycerol-3-Phosphate Acyltransferase mRNA.

7.1 Introduction

Ribozymes are small RNA molecules capable of highly specific catalytic cleavage of RNA (Zaug, A.J. et al., 1986; Uhlenbeck, O.C., 1987; Haselhoff, J. and Gerlach, W.L., 1988) and therefore, they have enormous potential in basic molecular biology research and biotechnology to inhibit gene expression. Although much research effort and success has been achieved *in vitro* for ribozyme-mediated gene inhibition, progress to attain highly efficient ribozyme effectivity *in vivo* has been markedly slower. Recent examples include inhibition of gene expression in mammalian cells for C-*fos* (Scanlon, K.J. et al., 1991), α-lactalbumin (Huillier, P.J.L. et al., 1992), β2-microglobulin (Larsson, S. et al., 1994) and tumor necrosis factor (Sioud, M. et al., 1992), in *Xenopus* oocytes for 28S rRNA (Saxena, S.K. and Ackerman, E.J., 1990) and U7 snRNA (Cotton, M. and Birnstiel, M.L., 1989), as well as reduction in viral RNA replication of HIV-1 (Sarver, N. et al., 1990; Ojwang, J.O. et al., 1992; Homann, M. et al., 1993) and a potato spindle tuber viroid (PSTVd) with a nuclear replication phase (Yang, X. et al., 1997). In plant systems even fewer reports document the application of ribozymes to reduce gene expression. They have been shown to down regulate neomycin phosphotransferase (*npt*) activity in transient assays of tobacco protoplasts (Steinecke, P. et al., 1992). Also decreased enzymatic activity of the endogenous gene-targets encoding UDP-glucose pyrophosphorylase in potatoes and lignin-forming peroxidase in tobacco, was observed (Borovkov, A.Y. et al. 1996; McIntyre, C.L. et al., 1996). Recently, it was demonstrated that a multimer hammerhead ribozyme targeted to stearoyl-ACP D9 desaturase mRNA can be used to modulate the expression of the endogenous gene in transgenic maize leaves. Heritable increases of leaf stearate correlated with the presence of the ribozyme gene and decreases in D9 desaturase mRNA and protein (Merlo, A.O. et al., 1998).

The best characterised ribozymes are hydrolytic nucleases that perform site-specific cleavage of a target RNA (Symons, R.H., 1991 and 1992; Bratty, J. et al., 1993) and thus far, the class of naturally occurring hammerhead ribozymes, has received most attention. The hammerhead is a functional RNA motif that characterises a class of self-cleaving RNAs. It can be found in certain plant pathogenic RNAs (reviewed in Symons, R.H., 1997), including at least eight different satellite RNAs that accompany some plant viruses. They are also present in RNA transcripts of satellite DNAs in schistosome (Ferbeyre, G. et al., 1998) and newt (Luzi, E. et al., 1997). Some aspects of the mechanism of autocatalytic cleavage are still under debate but it is clear that RNA cleavage requires Mg^{2+} and results in cleavage products with a 2',3'-cyclic phosphate and with a 5'-hydroxyl group (Buzayan, J.M. et al., 1986; Pontius, B.W. et al., 1997: Lott, W.B., 1998). The hammerhead structure consists of three base-paired stems or RNA helices, I, II and III, which are linked by two short stretches of conserved single-stranded sequences and by a single nucleotide after which (3') cleavage occurs (Figure 7.1).

A uniform conventional numbering system for hammerheads has been established (Hertel, K.J. et al., 1992) and is illustrated in Figure 7.1. The three dimensional structure of the hammerhead has been solved (Tuschl, T. et al., 1994; Pley, H.W. et al., 1994; Scott, W.G. et al., 1995).

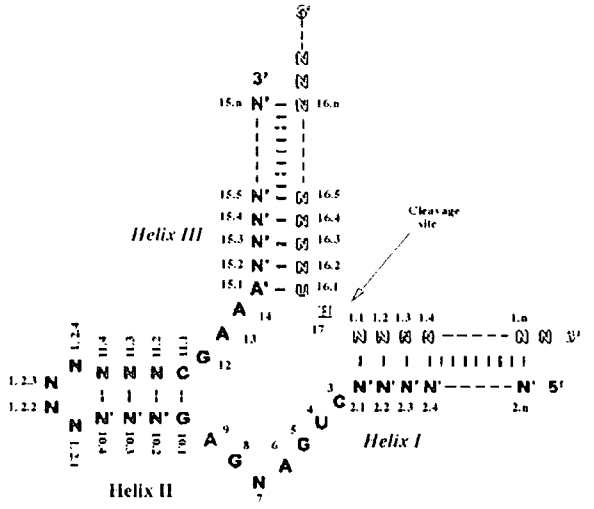

Figure 7.1 Numbering system for a hammerhead ribozyme associated with a target RNA

Two dimensional representation of the hammerhead ribozyme with its sequence given in filled letters and the substrate RNA sequence in open letters. Residues indicated by N can be any base and N' indicates the complement of the base with which it is paired. The H at the cleavage site means: any base but G. The numbering system is according to convention introduced by Hertel, K.J. et al., (1992).

Although in natural self-cleaving RNAs, cleavage occurs *in cis*, it is possible to engineer ribozymes to cleave another RNA molecule *in trans*, after intermolecular association via helices I and III (Uhlenbeck, O.C., 1987; Haselhoff, J. and Gerlach, W.L., 1988). Aspects of the function and application of hammerhead ribozymes have been reviewed in several publications (Symons, R.H., 1991 + 1992; Stull, R.A. and Szoka,C., Jr., 1995; Birikh, K.R. et al., 1997; Sun, L.-Q. et al., 1997). In principle, specific endonucleolytic hammerhead ribozymes can be designed for any target RNA. There is a minimal sequence requirement for cleavage 3' to a three-nucleotide motif NUH, in which H is anything but G (guanine), and N is any nucleotide but included to discriminate between 12 possible NUH motifs that differ in their reactivity (Zoumadakis, M. and Tabler, M., 1995). However, most researchers have worked with the GUC triplet, since it is most common amongst the natural hammerheads and it has been reported to cleave particularly efficiently (Perriman, R. et al., 1992; Nakamaye, K.L., and Eckstein, F., 1994). The recognition of a particular cleavable target and thus the specificity of the ribozyme, originates from the engineered antisense arms which form helices I and III by complementary base pairing.

The length and sequence of the arms can be selected as desired and the ribozyme can then be thought of as antisense oligonucleotide, but with the added advantage of the capability to destroy the target after recognition. Although the ultimate goal is the application of ribozymes in *in vivo* systems, a substantial body of work has concentrated on the *in trans* hammerhead reactions *in vitro* and the testing of variants of ribozyme constructs against potential RNA targets. It has been recognised that the type (G:C or A:U) and the number of base pairs (the length of the arms) would affect the specificity, affinity (Km) and turnover (Kcat) of the ribozyme and thus there are different concepts about what is an ideal arm-length. If the ribozyme should act in a truly catalytic fashion there would be a multiple turnover, i.e. one ribozyme molecule would cleave more than one substrate RNA molecule. Besides effective cleavage, for multiple turnover, the association and dissociation must proceed efficiently and is therefore influenced by the length of the helices I and III. Short arms and short, structureless substrate RNAs will have the highest catalytic efficiencies (Rittner, K. et al., 1993). However, when testing for applications in *in vivo* gene suppression, other considerations for the RNA partners apply. The RNA substrate under *in vivo* conditions will usually be considerably longer and will have secondary structures, which might interfere with the accessibility of the target RNA for the ribozyme or the ribozyme may even become 'kinetically trapped'. Although progress is being made in this field, currently it is still difficult to predict reliably by computer analysis which regions of a target are best accessible (Patzel, V. and Sczakiel, G., 1998). Despite the possibilities for detailed kinetic analyses of the cleavage reactions *in vitro*, it is not certain that *in vitro* transcripts are good reflections of the *in vivo* situation. Besides complicating factors of cellular localisation, relative concentrations of the target RNAs, ribozymes and co-factors (Mg^{2+}), molecular stability and secondary structures, proteins could shield the target but could also facilitate the docking of the ribozyme to the target (Tsuchihashi, Z. et al., 1993). The probability that turnover under *in vivo* conditions will be limited, has posed the question whether stoichiometric cleavage may be sufficient to inhibit gene expression. The concept of catalytic antisense RNAs, which are characterised by relatively long antisense sequences that also carry an additional hammerhead catalytic domain, was therefore investigated (Homann, M. et al., 1993; Hormes, R. et al., 1997). Even when the major emphasis of an experiment is on an *in vivo* application, the particular ribozyme design is usually still tested on projected target (substrate) RNAs *in vitro*.

In such an experiment, the extend of the contribution of the possible antisense effect of a ribozyme design (Nellen, W. and Lichtenstein, C., 1993), can be determined using a control ribozyme which has been inactivated by exchanging one (or more) of the invariant nucleotides in the central core domain.

In this study the design and hydrolytic activity of essentially two different hammerhead ribozymes, targeted against the chloroplast *Arabidopsis* GPAT mRNA, was tested *in vitro*.

7.2 Materials and methods

7.2.1 Plasmid constructions

Construction, growth and subcloning of clones were done by a variety of standard techniques (Sambrook, J. et al., 1989; Promega: Protocols and Applications Guide 2nd or 3rd edition). A detailed description of the ribozyme design and plasmid constructions is given in the results section of this chapter. Synthetic oligonucleotides were made by Cruachem Ltd. (Cruachem Ltd., Todd Campus, West of Scotland Science Park, Acre Road, Glasgow G20 0UA). All plasmid constructs used for *in vitro* transcription of RNA of the projected target substrate (*Arabidopsis* GPAT RNA) and the ribozymes were verified by DNA sequencing. Plasmid DNA was usually purified using the Wizard *Plus* Minipreps Plasmid Purification Systems (Promega).

For cloning of ribozymes, two oligonucleotides (oR-sense (S) and oR-antisense (AS)), corresponding to complementary strands of the ribozyme sequence, the flanking antisense sequences against *Arabidopsis* GPAT (1-AT) mRNA and appropriate restriction sites for cloning, were phosphorylated, annealed and cloned in corresponding restriction sites of two types of vector. Non-embedded ribozymes (designated KS Rzs) were cloned in pBS KS$^+$ (*Bgl*II—Rz—*Bam*HI-*Hd*III) for *in vitro* testing of hydrolytic activity of the ribozyme design, without supplementary sequences. The same hammerhead ribozymes were embedded in a potato U1.1 snRNA gene (Vaux, P. et al., 1992) in the vector pU1.1-5' *Bgl*II (*Bam*HI—Rz—*Bgl*II) , designated U1.1 Rz's, and were tested *in vitro*, to assay if structural interactions with the supplementary sequence would influence the ribozyme hydrolytic activity. Oligonucleotides used in this study are named as follows: o (=oligo), M (=mutant), Rz (ribozyme) followed by the oligo number and indication for sense (S) or antisense (AS) strand. Sequences in italics correspond to restriction endonuclease sites, underlined sequences are involved in formation of the helices I, II and III, the sequences in bold indicate the position which can be mutated (A 14 G) to create a catalytically inactive hammerhead ribozyme.

For cloning of the **KS Rzs** (in pBS KS$^+$ --*Bgl*II—Rz—*Bam*HI-*Hd*III), the following oligonucleotides were used:

- for **KS Rz 1 and KS MRz 1** (against position 156 (in *Arabidopsis* GPAT mRNA (genbank Access. Nr.: D00673) or position 183 in the *in vitro* target RNA -p2-6T):

oRz1-9(S): 5'-*GATCT* GAAGAGTCCTGATGA CGG GTGA CGC GAA ACGAAGCGAGTG *GGATCCA*-3'

oRz1-10(AS); 5'-*AGCTTGGATCC* CACTCGCTTCGT TTC GCG TCAC CGC TCATCAGGACTCTTC *A*-3'

oMRz1-11(S); 5'-*GATCT* GAAGAGTCCTGATGA GCG GTGA CGC GAG ACGAAGCGAGTG *GGATCCA*-3'

oMRz1-12(AS); 5'-*AGCTTGGATCC* CACTCGCTTCGT CTC GCG TCAC CGC TCATCAGGACTCTTC *A*-3'

- for **KS Rz 2 and KS MRz 2** (against position 279 (in *Arabidopsis* GPAT mRNA (genbank Access. Nr.: D00673) or position 306 in the *in vitro* target RNA -p2-6T):

oRz2-13(S); 5'-*GATCT* CGC-ACGCTGATGA GCG GTGA CGC GAA ACGATTCTTTATC *GGATCCA*-3'

oRz2-14(AS); 5'-*AGCTTGGATCC* GATAAAGAATCGT TTC GCG TCAC CGC TCATCAGCGT-GCG *A*-3'

oMRz2-15(S); 5'-*GATCT* CGC-ACGCTGATGA GCG GTGA CGC GAG ACGATTCTTTATC *GGATCCA*-3'

oMRz2-16(AS); 5'-*AGCTTGGATCC* GATAAAGAATCGT CTC GCG TCAC CGC TCATCAGCGT-GCG *A*-3'

For cloning of the **U1.1 Rz's** (in pU1.1-5' *Bgl*II - *Bam*HI—Rz—*Bgl*II), the following oligonucleotides were used:

- for **U1.1 - Rz 1 and U1.1 - MRz 1** (against position 156 (in *Arabidopsis* GPAT mRNA (genbank Access. Nr.: D00673) or position 183 in the *in vitro* target RNA - p2-6T):

oRz1-1(S); 5'-*GATCC* GAAGAGTCCTGATGA GCG GTGA CGC GAA ACGAAGCGAGTG *A*-3'

oRz1-2(AS); 5'-*GATCT* CACTCGCTTCGT TTC GCG TCAC CGC TCATCAGGACTCTTC *G*-3'

oMRz1-3(S); 5'-*GATCC* GAAGAGTCCTGATGA GCG GTGA CGC GAG ACGAAGCGAGTG *A*-3'

oMRz1-4(AS); 5'-*GATCT* CACTCGCTTCGT CTC GCG TCAC CGC TCATCAGGACTCTTC *G*-3'

- for **U1.1 - Rz 2 and U1.1 - MRz 2** (against position 279 (in *Arabidopsis* GPAT mRNA (genbank Access. Nr.: D00673) or position 306 in the *in vitro* target RNA - p2-6T):

oRz2-5(S); 5'-*GATCC* CGC-ACGCTGATGA GCG GTGA CGC GAA ACGATTCTTTATC *A*-3'

oRz2-6(AS); 5'-*GATCT* GATAAAGAATCGT TTC GCG TCAC CGC TCATCAGCGT-GCG *G*-3'

oMRz2-7(S); 5'-*GATCC* CGC-ACGCTGATGA GCG GTGA CGC GAG ACGATTCTTTATC *A*-3'

oMRz2-8(AS); 5'-*GATCT* GATAAAGAATCGT CTC GCG TCAC CGC TCATCAGCGT-GCG *G*-3'

7.2.2 Concatemerisation of ribozyme cDNA for use in radioactive probe synthesis

The complementary oligonucleotides oRz1-9(S) and oRz1-10(AS) (to create RZ1 probe) or oRz2-13(S) and oRz2-14(AS) (to create RZ2 probe) or oRz1-1(S) and oRz1-2(AS) (to create U1.1 RZ1 probe) or oRz2-5(S) and oRz2-6(AS) (to create U1.1 RZ2 probe) were phosphorylated, annealed (as described in the result section) and used in a ligation reaction to concatemerise the molecules. To 2 µg (U1.1-) Rz 1 or (U1.1-) Rz 2 cDNA (in 20 µl), 5 µl 10 x Ligation Buffer (Promega; 1 x =: 30 mM Tris-HCL pH 7.8, 10 mM $MgCl_2$, 10 mM DTT,
1 mM ATP) and 3 Units T4 DNA Ligase (Promega: catalyses the joining of of two DNA strands between the 5'-phosphate and 3'-hydroxyl groups) was added in a total volume of 50 µl and incubated at 15 °C overnight. After the ligation, 0.5 M EDTA was added to 5 mM and 20% SDS was added to 0.5%. The reaction was then extracted with phenol/chloroform and ethanol precipitated according to standard protocol. After centrifugation for 10 min. in a microcentrifuge (13000 g), the DNA pellet was resuspended in 12 µl sterile water and 2 µl was used to synthesise a ^{32}P-labeled probe according to instructions with the *redi*prime DNA labeling system (Amersham; RPN1633/1634). Probes were purified by Bio-Gel P-6 (gel filtration) chromatography (BioRad). Mostly, these probes were used in colony hybridisations during cloning procedures or selections of clones (see also Materials and methods of Chapter V, section 6.2.1, step4).

7.2.3 ^{32}P-labeled Molecular size markers for use in PAGE analysis

5 µl (50 ng/µl) of dephosphorylated ϕx 174 bacteriophage DNA, digested with *Hinf*I, was phosphorylated in a 9.5 µl reaction containing 1 µl 10 x Kinase Buffer (Promega; 700 mM Tris-HCl pH 7.6, 100 mM MgCl2, 50 mM DTT), 1.5 µl γ-^{32}P ATP (3.3 pmol/µl; Amersham), 1.0 µl cold ATP (5 pmol/µl) and 1.0 µl T4 Polunucleotide Kinase (10 u/µl; Promega). Reactions were incubated for 20 min. at 37 °C and the reaction was terminated by heat-inactivation for 10 at 70 °C. 90 µl of TE buffer (10 mM tris-HCl pH 7.5/1 mM EDTA) was added and usually 1 – 3 µl was loaded per lane on a PAGE gel.

7.2.4 Generation of ribozymes and target substrate *Arabidopsis* GPAT(1-AT) RNA from plasmids; RNA transcription *in vitro*.

Plasmid DNA was purified using the Wizard *Plus* Minipreps Plasmid Purification Systems (Promega) and strict precautions against ribonuclease were maintained. Plasmids were linearised prior to *in vitro* transcription to produce RNA of defined lengths. Only restriction enzymes which produced 3'-recessed ends were used for the respective templates. The use of restriction enzymes which produce 3'-protruding ends should be avoided, as extraneous transcripts have been reported to appear in addition to the expected transcript when such templates are transcribed. If no alternative is available, the linearised template ends can be converted to blunt ends (filled-in) with Klenow DNA polymerase. The digestion reactions with the linearised DNA templates were cleaned-up by using a Qiaex II Gel Extraction Kit (Qiagen) for DNA extraction from agarose gels. This involved examination of the purified linear DNA by agarose gel electrophoresis to verify complete linearisation and the presence of a discrete DNA fragment of the expected size.
The plasmid p2-6T, encoding 501 bp. of the start of the open reading frame (ORF) of the *Arabidopsis* GPAT (in the vector pBS SK$^+$ - *Eco*RI-*Bam*HI), was linearised with *Bam*HI and was transcribed *in vitro* using T7 RNA polymerase as described below. This resulted in the *Arabidopsis* GPAT RNA target RNA substrate with a length of 586 nt.
The KS Rzs (in pBS KS$^+$ -*Bgl*II—Rz—*Bam*HI-*Hd*III) were linearised with *Hin*DIII and transcribed *in vitro* using T7 RNA polymerase. This resulted in a transcript of 119 nt. (when 1 Rz was cloned) and 159 nt (when 2 Rzs were cloned—etc.).
The U1.1 Rzs (in pU1.1-5' *Bgl*II - *Bam*HI—Rz—*Bgl*II) were linearised with *Eco*RI and transcribed *in vitro* using SP6 RNA polymerase. This resulted in a transcript of 595 nt. (when 1 Rz was cloned) and 635 nt (when 2 Rzs were cloned—etc.).

For RNA transcription *in vitro*, the Riboprobe Gemini II Core System (Promega; P1270) was used with minor modifications of the instructions of the manufacturer. Instead of [α-^{32}P]CTP (400 Ci/mmol, 10 mCi/ml), radiolabeled UTP (Amersham; PB 10163: [α-^{32}P]UTP, 400 Ci/mmol, 10 mCi/ml) was used and the standard protocol was adjusted to accommodate this. A typical protocol for the generation of radiolabeled *in vitro* RNA transcripts from the linearised templates was as follows: the final reaction volume of 20 µl contained 0.2-0.4 µg (1 µl) of the linearised template DNA and 1.0 µl of either T7 or SP6 RNA polymerase (at 15 – 20 u/µl), 4.0 µl Transcription Optimized 5X Buffer (200 mM Tris-HCl pH 7.5, 30 mM $MgCl_2$, 10 mM spermidine, 50 mM NaCl), 2 µl 100 mM DTT, 20 units Rnasin Ribonuclease Inhibitor, 4.0 µl rRNTP mix (with ATP, GTP and CTP at 2.5 mM each), 2.4 µl 100 µM UTP and 5.0 µl [α-^{32}P]UTP (400 Ci/mmol, 10 mCi/ml). When it was the intention to generate a non-radiolabeled *in vitro* RNA transcript, the same protocol was used with the exception that the radioactive ribonucleotide and the 2.4 µl of

cold (100 μM) UTP was omitted and instead, an rNTP mix containing all four ribonucleotides at 2.5 mM was used.
The reaction was allowed to proceed for 60-90 min. at 37 °C after which a 1 μl aliquot was removed for determination of the specific activity.

The **specific activity** (total incorporated cpm/total μg of RNA synthesised) and the percentage incorporation was determined according to standard procedures (see Promega Protocols and Applications Guide, or Sambrook, J. et al., 1989) using DE81 (Whatmann) filter papers. A 1:10 dilution of the labeled probe in water was prepared (aliquot was 1 μl). 1 μl of the 1:10 dilution was spotted on duplicate filters and the filters were air dried. These were then counted directly to determine the total cpm.
1 μl of the 1:10 dilution was spotted on duplicate filters and the filters were washed 3 times (5 min.) with 0.5 M NaPhosphate buffer pH 7.6 (45.2 gr. Na_2HPO_4.2H2O + 6.42 gr NaH_2PO_4.H2O in 600 ml). Subsequently the filters were washed 3 times with copious amounts (20 ml) of ice-cold 5% TCA followed by a rinse with acetone and were then air dried before counting (= incorporated cpm). Total cpm incorporated = incorporated cpm x dilution factor (=10) x reaction volume (=20)/volume counted (=1). Nmol of labeled rNTP = μCi rNTP in reaction (= 50 μCi)/ isotope concentration (= 400 μCi/nmol) =0.125 nmol. Nmol of limiting cold rNTP = μl of limiting cold rNTP (=2.4 μl) x 100 μM rNTP x 10^3 nmol/1μmol x 1 l./10^6 μl = 0.24 nmol. Total nmol of limiting rNTP = nmol of labeled rNTP (0.125) + nmol of limiting cold rNTP (0.24) = 0.365 nmol. Maximum theoretical RNA yield = total nmol of limiting rNTP (= 0.365) x 4 rNTPs x 330 ng/nmol rNTP = 0.482 μg. Total μg of RNA synthesised = % incorporation x maximum theoretical RNA yield (=0.482 μg).
Specific activity = total incorporated cpm/ total μg of RNA synthesised.
For conversion from μg to pmol the following formula was used: pmol = μg x 10^6 pg/1μg x pmol/330 pg x 1/N (length of transcript in nt).

Following the transcription reaction, the **DNA template was removed** by digestion with DNAseI. RQ1 RNAse-free DNAseI was added to a concentration of 1 u/μg template DNA and the reaction was incubated for 15 min at 37 °C. The reaction was extracted with 1 volume of acid (pH 4.5) phenol: chloroform: isoamyl alcohol (25:24:1). After vortexing for 1 min. the tube was centrifuged at 12000 x g for 2 min and the upper aqueous phase (RNA remains in the aqueous phase whereas the DNA is selectively partitioned into the organic or interphase) was transferred to a fresh tube. The RNA was precipitated by addition of 0.5 volume of 7.5 M ammonium acetate and 2.5 volumes of 100% ethanol,

mixed and placed at –70 °C for 30 min. After centrifugation at 12000 x g, the RNA pellet was washed with 1 ml of 70% ethanol.

In the most relevant procedures to determine the *in vitro* ribozyme hydrolytic activity, the *Arabidopsis* GPAT (p2-6T) *in vitro* target RNA substrate was radiolabeled and was purified by band purification from a polyacrylamide gel (as described below). In contrast, it was determined empirically that the final analyses of the cleavage reactions were of highest quality when the ribozymes were synthesised in the absence of radiolabel (to monitor the success of *in vitro* RNA transcription reactions and to quantify the products, pilot reactions in the presence of [α-^{32}P]UTP were then run along side the experimental syntheses and taken through exactly the same manipulations).

For **removal of unincorporated nucleotides** from non-radioactively labeled *in vitro* RNA transcripts, the RNA pellets were resuspended in 100 µl 1 M ammonium acetate and 2.5 volumes of 100% ethanol was added. After mixing and precipitation at –70 °C for 30 min., the RNA was pelleted at 12000 x g for 10 min. The pellets were resuspended in a volume of sterile (RNAse-free) water, corresponding to 160.000 cpm/µl (calculated on basis of the radioactive products from the pilot reactions. The molarities of the ribozymes were then calculated on basis of these values.

For **gel-band purification** of the ^{32}P-labeled *Arabidopsis* GPAT (p2-6T) *in vitro* target RNA, the RNA pellets were resuspended in 16 µl (RNAse-free) water and fractionated by electrophoresis on a 5% polyacrylamide gel (BioRad Protean II gel system) containing 7 M urea. An equal volume of 2 x Formamide Loading Buffer (FLB: 80% deionised formamide,10 mM EDTA, 1 mg/ml XCFF (Xylene Cyanol FF) and 1 mg/ml BB (Bromophenol Blue)) was added prior to loading the samples for PAGE gel electrophoresis.
The gel was 1.0 mm thick and contained 5% Acrylamide, 7M urea and 1 x TBE (10 x TBE per litre = 108 g Tris, 55 g boric acid, 9.3 g $Na_2EDTA.H_2O$, pH 8.3), with 240 µl 25% APS (ammonium persulfate) and 80 µl TEMED added to 150 ml. gel-mix for polymerisation. Prior to loading samples the gel was pre-run for 30 min at 300 V followed by 500 V for 15 min. (constant voltage) (Powerpack was BioRad 3000 Xi). Samples were boiled for 2 min prior to loading onto the gel and the samples were electrophoretically separated at 300 V (constant voltage; 22 mA and 7 W). After the run, the gel system was dismantled and the gel was covered with plastic wrap, followed by exposure to film for a few minutes. After processing the film, the film was re-orientated on the gel and a window was cut in the film corresponding to the band of interest, using a clean scalpel. The gel

slice was placed in a microcentrifuge tube and the RNA was eluted by passive diffusion (16-24 hrs at room temperature) in elution buffer (0.5 M ammonium acetate, 10 mM magnesium acetate, 0.1% SDS, 10 mM EDTA). The RNA was extracted with 1 volume of acid (pH 4.5) phenol: chloroform: isoamyl alcohol (25:24:1) and precipitated from the aqueous phase by addition of 0.5 volume of 7.5 M ammonium acetate and 2.5 volumes of 100% ethanol, mixed and placed at –70 °C for 30 min. After centrifugation at 12000 x g, the RNA pellet was washed with 1 ml of 70% ethanol and resuspended in sterile (RNAse-free) water at approximately 3 x 10^5 cpm/µl.

7.2.5 Preparation of an analytical, denaturing polyacrylamide sequence gel for analysis of ribozyme cleavage reactions

The gel system needed to provide maximum resolution with high reproducibility and therefore it was decided to use sequencing gels. The Sequi-Gen Nucleic Acid Sequencing Cell of BioRad was employed. This is a modular, high-resolution, vertical slab electrophoresis instrument for DNA/RNA sequencing. Assembly, casting, setting up for operation, loading and running of the gel were according to the manufacturers recommendations. The gel system used in almost all analyses, was a 38 cm wide/ 50 cm high, 5% polyacrylamide - 8 M urea gel, cast with 0.4 mm spacers and prepared and run with 1 x TBE buffer.

Before loading and electrophoresis of samples, the gel was pre-run for at least 1 hr. This is meant to remove traces of salt (catalyst) and to stabilise the gel temperature near 55 °C. Approximate voltage settings for operating Sequi-Gen Cells, according to the manufacturers recommendations, were maintained; for a (38cm x 50cm x 0.4 mm) 5% polyacrylamide gel run in 1 x TBE the constant voltage was approximately 1800 V. In these experiments, the powerpack was a BioRad 3000 Xi and the runs were at constant power of 45 W with limit settings of max 1900 V; 100 mA and 45 W. An equal volume of 2 x Formamide Loading Buffer (FLB: 80% deionised formamide,10 mM EDTA, 1 mg/ml XCFF (Xylene Cyanol FF) and 1 mg/ml BB (Bromophenol Blue)) was added to the samples. The samples were then denatured at 95 °C for no longer then 3 min and placed on ice, prior to loading. Sample loading is a key step for high-resolution gels and the wells were cleaned immediately (removal of dissolved urea) before loading a sample directly on top of the acrylamide gel. In this study, gels were usually run until the XCFF marker was approximately 60% run down from the top of the gels (XCFF runs at approximately 260 nt, BB at approximately 65 nt). The radiolabeled oligonucleotides were visualised by drying the sequencing gels with a slab gel dryer, followed by autoradiography. After the run, the gel system was disassembled and the sequencing gel was transferred to a sheet of Whatmann 3MM filter paper. The gel was wetted (misted) slightly with water, the dry filter paper was laid on top of the gel and was picked up by lifting the filter paper carefully

from one end. The sequencing gel was then covered with plastic wrap (no air bubbles or folds) and trimmed to fit the slab gel dryer. A model 583 gel dryer (BioRad) was set to sequencing cycle and the gel was dried for 30 min at 80 °C with an applied vacuum of 30 inches of mercury (> 125 torr). The gel was autoradiographed with X-ray film in a suitable film cassette. No intensifying screens were used and usually a 5 hr - overnight exposure was satisfactory.

7.3 Results

7.3.1 Construction of the plasmids encoding the target *Arabidopsis* GPAT (1-AT) RNA sequence and the hammerhead ribozyme genes

7.3.1.A The Arabidopsis GPAT projected ribozyme target template

The plasmid p2-6, containing a 1445 bp. *Arabidopsis* GPAT cDNA clone as an *Eco*RI fragment in pBluescript SK(-) (Nishida, I, personal communication; sequence is identical to deposition under Genbank accession Number D00673), was re-cloned to create plasmid p2-6T (T stands for 'target' and encoded 501 bp. from the start of the open reading frame). The plasmid p2-6 was digested with *Bam*HI, which would cut at position 559 (calculated from the *Eco*RI cloning site at the 5' end) and downstream of the *Eco*RI site in the vector, on the 3' end of the cDNA. This released a cDNA fragment of 1224 bp and the vector + 5' *Eco*RI-*Bam*HI part of the *Arabidopsis* GPAT cDNA sequence, was purified via gel band extraction using Qiaex II silica-gel particles (Qiagen). This DNA was re-ligated and subcloned according to standard procedures. The clone was verified by dideoxy-nucleotide sequencing. After linearisation with *Bam*HI, *in vitro* transcription of this plasmid with T7 RNA polymerase (as described in section 7.2.4) yielded a 586 base-long *Arabidopsis* GPAT (1-AT) mRNA fragment. This is illustrated in Figure 7.2 together with an indication of the position of the two ribozyme target sites tested in this study. Two GUC triplets within the *Arabidopsis* GPAT cDNA fragment, encoding the chloroplast targeting polypeptide, were selected. These GUC triplets were chosen as ribozyme target sites for two reasons: first, GUC triplets have been reported to cleave particularly efficient (Perriman, R. et al., 1992; Nakamaye, K.L., and Eckstein, F., 1994) and second, these sites would not be present in the transgenic squash GPAT mRNA, produced in the transformed *Arabidopsis* plants, described in Chapter VI (see also Figure 6.2).

The length of the generated target sequence and the lengths of the cleavage products, allowed the use of high-resolution analysis of the respective sequences on 5% polyacrylamide - 8 M urea denaturing sequence gels (section 7.2.5). Ribozymes directed against the GUC triplet at position 183 in the target template, were designated 1 (KS Rz1 or U1.1 Rz1) and ribozymes against GUC at position 306 were named 2 (KS Rz2 or U1.1 Rz2). Sequence-specific *in vitro* hydrolytic cleavage of the target by Rz1 would generate fragments of 183 and 402 bases long. Rz2 sequence specific activity would result in a fragment of 306 nucleotides and a fragment 279 bases long (Figure 7.2).

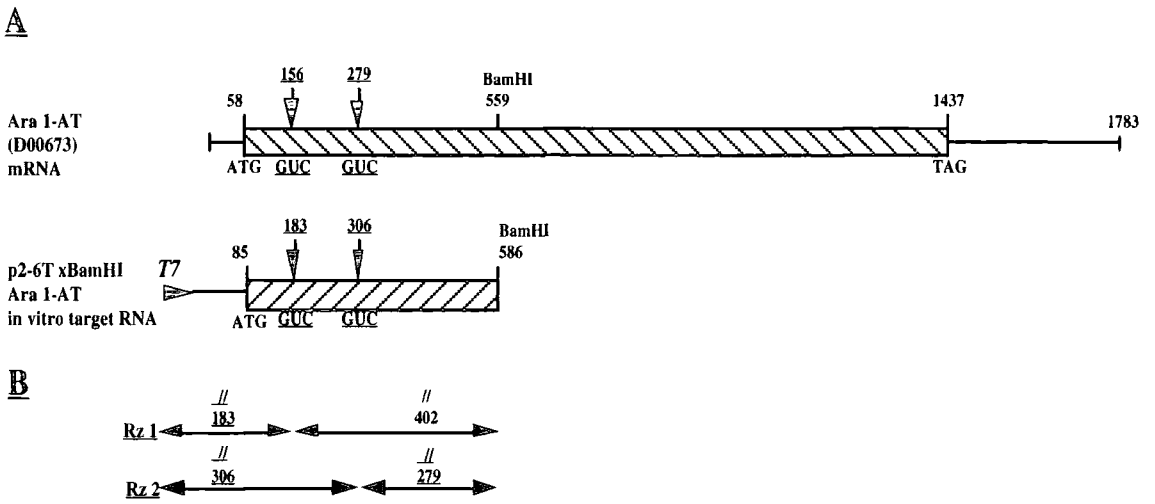

Figure 7.2 Selection of the location of target sites on the *Arabidopsis* GPAT (1-AT) mRNA and the sizes of the sequence-specific cleavage products of *in vitro* GPAT (1-AT) mRNA substrate

(**A**) The GUC targets (underlined) of the two different ribozyme constructs (Rz1 and Rz2) are indicated in the top diagram of the full length *Arabidopsis* (Ara) GPAT (1-AT) mRNA (identical to the *Ara* 1-AT cDNA sequence with Genbank Accession nr.: D00673) and also in the lower diagram of the 586 base long *in vitro* transcribed *Ara* 1-AT mRNA. The numbered arrows indicate the position of the GUC targets within the reference sequence (or; *in vivo*) and substrate sequence (Rz 1: position 156 (ref.) is 183 (sub.)/ Rz 2: position 279 (ref.) is 306 (sub.). (**B**) The numbers indicate the sizes of the expected cleavage products when the 586 base long *in vitro* transcribed *Ara* 1-AT mRNA from plasmid p2-6T is used for the substrate.

7.3.1.B The design of two different hammerhead ribozymes

Hammerhead ribozymes can be designed to work *in trans*, which means that they can be assembled from two different RNA strands; one acting as the ribozyme and the other as the substrate. This has two major advantages: first, the ribozymes can be designed to theoretically cleave any (cellular or viral) RNA at defined posiions (Haselhoff, J., and Gerlach, W., 1988), and secondly, the separation of the RNA strands permits kinetic and mechanistic studies of the cleavage reaction. The three base-paired stems (RNA helices, I, II and III) of the complex of a designed ribozyme with its target RNA, are specially arranged in formats and with a conventional numbering system as described by Hertel, K.J. et al., (1992) (see also for example figure 7.1).

Helix II, which is entirely within the ribozyme, is not likely to affect the specificity of cleavage, but its main function is in achieving an active conformation and to stabilise the active structure of the conserved domain (Hendry, P., et al., 1995; personal communication with the industrial partner in this project: Geneshears, CSIRO Plant Industry). As the achievement of an active conformation could be a rate-limiting step, there may be scope for improvement of the ribozyme efficacy by modulating the stability of Helix II. It has been shown that helix II can be shortened to a minimum of 2 base pairs, closed by a 4 base pair loop (loop II), without a significant decrease in the catalytic efficiency (Tuschl, T. and Eckstein, F., 1993). It was determined empirically (CSIRO Plant Industry) that a modified, smaller helix II, resulted in faster ribozyme cleavage *in vitro*.

Helix II in nature is: 5'-GUCC but in this study it was decided to design the
3'-CAGG

ribozymes (1 and 2) with the modified Helix II: 5'-GCG
3'-CGC

The general structure of the ribozymes with the modified Helix II used in this study, is illustrated in Figure 7.3, which is drawn in the same format as the general 'natural' structure in Figure 7.1.

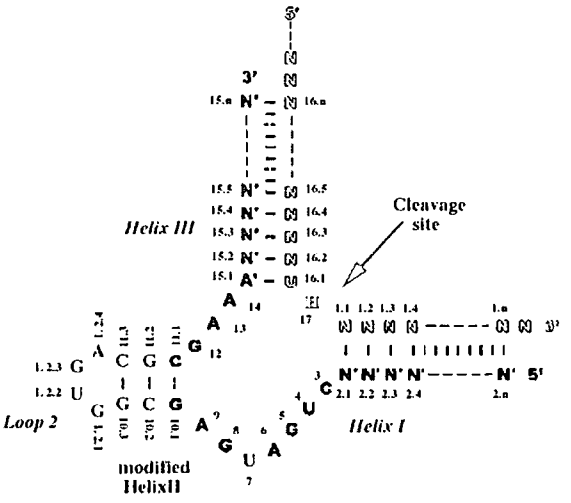

Figure 7.3 Two dimensional general representation of the hammerhead ribozyme sequences and their numbering, used in this study

The numbering system of the ribozyme associated with a target RNA is according to convention introduced by Hertel, K.J. et al., (1992). The ribozyme sequence is represented in filled letters and the substrate RNA sequence in open letters. Residues indicated by N can be any base and N´ indicates the complement of the base with which it is paired. The H at the cleavage site means any base but G. The natural Helix II (5'-GUCC-3') (see Figure 7.1) is changed to a smaller Helix II (5'-GCG-3') which presumably cleaves faster.

The tetraloop (loop 2), connects the strands of helix II. In large structured RNAs these tetraloops, with a consensus sequence of 5'-GNRA (where N is any nucleotide, and R is either G or A) are unusually frequent and have been thought to mediate intramolecular tertiary interactions (Pley, H.W. et al., 1994). It has been observed that the thermodynamic stability of the tetranucleotide loop 2 was not of great influence on the catalytic efficiency (for example: Tuschl, T. and Eckstein, F., 1993). Loop 2 is likely involved in transition state stabilisation since changes in the loop, seem to be reflected in k_{cat} (turnover) rather than the Km values (affinity). This would be mainly visible in studies were the cleavage step, rather than product release, is the rate-limiting step. The length of the loop 2 seems to be a major requirement for activity. In this study and illustrated in the figures 7.4 and 7.5, the sequence of loop 2 was chosen to be as in the ('standard') design by Haselhoff, J. and Gerlach, W.L. (1988) and is identical to naturally occurring ribozymes, such as that one of the avocado sunblotch viroid (ASBV).

The efficacy of binding of the hammerhead ribozyme to its cleavage site in target RNA is crucial for its use as a specific, molecular gene down-regulation tool or therapeutic agent. This efficacy can be influenced by several factors, such as mRNA secondary structures and the base composition and the length of the helices I and III.
The helices I and III comprise the base-pairing between ribozyme and substrate and do not need to be long. In natural viral ribozymes, where cleavage is *in cis* (or intramolecular), they are only 4 – 6 bp each. However, for ribozyme efficiency *in trans*, even at the current state of the art, it is still difficult, if not impossible, to theoretically predict the ideal helix (arms) lengths. Herschlag (Herschlag, D., 1991) concluded that there must be an optimal length of arms for specificity and that adequate specificity might even be impossible. For hammerheads to bind and cleave a specific mRNA in a large pool of intracellular RNA molecules (*in vivo*), the specificity of the reaction is crucial.
It is clear that for an optimal ribozyme activity at least three major steps are in balance with each other: 1) association, 2) cleavage, and 3) dissociation.
Longer substrate-recognition arms might enhance the rate of association with substrate and also the specificity (the ability to discriminate between the correct substrate and a-specific RNA sequences) depends on the difference in the affinities of binding between matched and mismatched targets. On the other hand, arms longer than approximately 7 – 14 bp could potentially lead to loss of catalytic turnover. Kinetic models for hammerhead ribozyme activity and thermodynamic parameters analysis predict that ribozymes with short arms have a high turnover when compared to their counterparts with long arms (Bertrand, E. et al., 1994; Hertel, K.J., 1994). However, in some cases it was found that hammerhead ribozymes with longer arms were more active *in vivo* when compared with shorter derivatives (Crisell, P. et al., 1993). Optimal cleavage is only achieved if the cleavage rate is in the same range as the rate of substrate dissociation. Arm sizes longer than 5 bp each seem to shift the rate-limiting step from the chemical-cleavage step to the

product release step. The affinity can be adjusted with the length and base-composition of the helices I and III but substrate recognition arms which are too long, will potentially reduce the specificity.

For this study, with the ultimate goal to down-regulate the expression of the endogenous, nuclear encoded, chloroplastic *Arabidopsis* GPAT activity *in vivo* (Chapter VI), it was decided to test two different ribozyme designs, each directed against a different region of the substrate, *in vitro*.
Ribozymes directed against the GUC triplet at position 183 in the target template encoded by p2-6T and corresponding with position 156 in the cDNA sequence deposited under Genbank Accession number D00673, were designated 1 (KS Rz1 or U1.1 Rz1 + mutants).
Ribozymes, designated 2 (KS Rz2 or U1.1 Rz2 + mutants), were directed against GUC at position 306 in the target template (position 279 in D00673). The main structural difference between the design of the two hammerhead ribozymes was the length and composition of the arms involved in the formation of helix I.

Helix I is formed by the annealing of the 5' sequence of the ribozyme with the substrate sequence 3' of the target codon. It has been suggested that only three nucleotides, absolutely paired next to the cleavage site, are required for helix I (Tabler, M. et al., 1994; communications with the industrial partner: Geneshears; CSIRO Plant industry). Following these first three bases, less stable sequences could be improving catalytic efficiency, due to faster product release. However, within this study it is also important to maintain optimal specificity for the target sequence. It was therefore decided to construct ribozyme 1 derivatives with a helix I-arm of 8 nucleotides, perfectly matched with the corresponding region of the substrate (Figure 7.4). The helix I-arm of ribozyme 2 derivatives were designed to have the first three nucleotides next to the GUC-cleavage site perfectly paired, followed by a de-stabilising deleted base in the ribozyme arm and another set of 3 perfectly paired nucleotides (Figure 7.5).
Helix III is formed by annealing of the 3' sequence of the ribozyme with the sequence 5' of the substrate. This helix contains the target GUC site, paired with CA-5', with the C of the GUC substrate triplet left unpaired. As noted before, it might be that a longer arm would improve the efficacy of the ribozyme but an arm which is too long would presumably reduce the potential turnover. A compromise, that has been made by many researchers, is to use a perfectly matched arm of 10 to 20 nucleotides long. In this study it was chosen to construct ribozyme 1 and ribozyme 2 derivatives with respectively 12 and 13 perfectly paired nucleotides for formation of helix III (Figures 7.4 and 7.5).

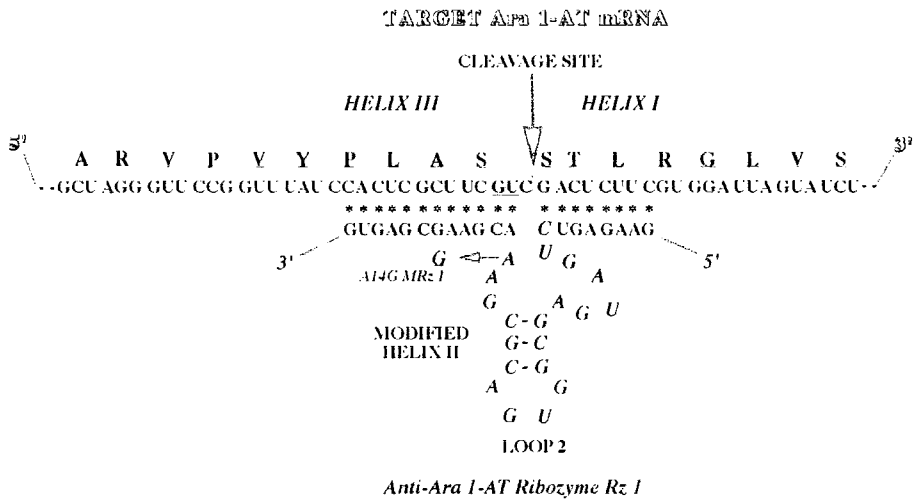

Figure 7.4 Ribozyme 1 in association with its target substrate

Predicted secondary hammerhead structure of ribozyme 1 (Rz 1) derivatives (lower sequence) associated with the target sequence of the *Arabidopsis* GPAT (1-AT) mRNA (upper sequence). The location of the cleavage site after the GUC target sequence (boxed) within the *Ara* 1-AT mRNA (position 155: Accession D00673) is indicated by a vertical arrow. The nucleotide which is substituted (A 14 G) to abolish catalytic activity is marked by an horizontal arrow and resulted in the non-catalytic MRz1.

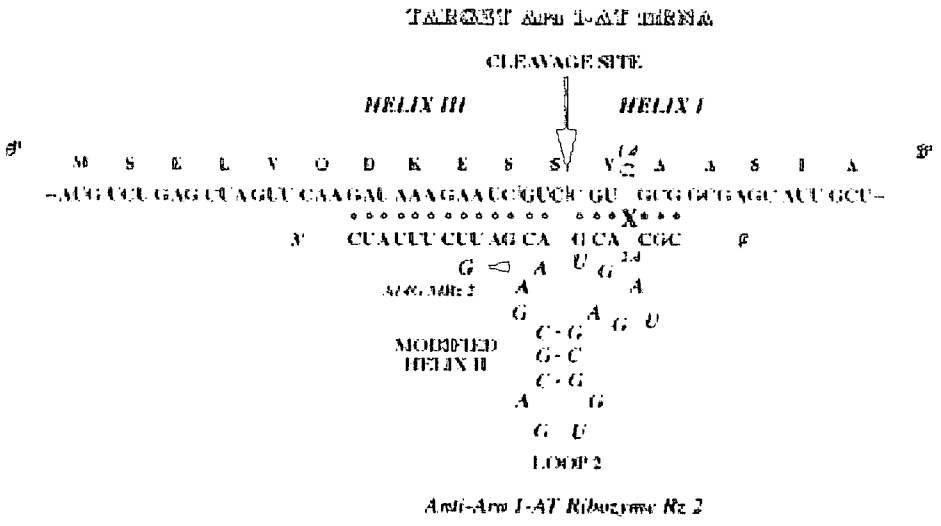

Figure 7.5 Ribozyme 2 in association with its target substrate

Predicted secondary hammerhead structure of ribozyme 2 (Rz 2) derivatives (lower sequence) associated with the target sequence of the *Arabidopsis* GPAT (1-AT) mRNA (upper sequence). The location of the cleavage site after the GUC target sequence (boxed) within the *Ara* 1-AT mRNA (position 278: Accession D00673) is indicated by a vertical arrow. Another GUC sequence within this target region is underlined. Rz 2 was designed with a deletion in Helix I at position 1.4/2.4 and is indicated by X. The nucleotide which is substituted (A 14 G) to abolish catalytic activity is marked by an horizontal arrow and resulted in the non-catalytic MRz2.

To monitor potential anti-sense effect of the ribozymes *in vivo* in the study described in Chapter VI, an A 14 G transition was introduced in a version of each of the ribozymes (MRz1 and MRz2), which was known to inactivate RNA hydrolytic activity fully *in vitro* (Ruffner, D.E. et al., 1990; Lamb, J.W. and Hay, R.T., 1990).

7.3.1.C. Construction of the nonembedded ribozymes in pBS KS⁺ (BglII—Rz—BamHI-HdIII): the KS Rz's

Ribozymes of the KS Rz series, without supplementary sequences, were cloned in pBS KS⁺.

To prepare the vector for cloning, approximately 10 μg of pBS KS⁺ was digested with 50 units each of *Bam*HI and *Hin*DIII in a 150 μl reaction volume containing the appropriate restriction enzyme buffer (1 x B; Boehringer Mannheim). After 2 hr incubation at 37 °C the reaction was extracted with phenol/chloroform, precipitated with ethanol and resuspended in 20 μl sterile water according to standard procedures. To prevent re-ligation of the vector in the cloning procedure, the DNA termini were dephosphorylated using Shrimp Alkaline Phosphatase (SAP) (USB, at 1 Unit/ μl). The pBS KS⁺ - *Bam*HI /*Hin*DIII was incubated with 1 x SAP buffer (20 mM Tris-HCl pH 8.0, 10 mM $MgCl_2$) and 2 units SAP in 50 μl total reaction volume at 37 °C for 30 min. The phosphatase was heat-inactivated at 65 °C for 15 min. and after phenol/chloroform extraction and ethanol precipitation, resuspended in 20 μl sterile water. 1 μl was analysed to examine the quality and recovery of DNA after these procedures.

For cloning of KS ribozymes, two oligonucleotides corresponding to complementary strands of the intended ribozyme sequence were phosphorylated, annealed and cloned in the *Bam*HI /*Hin*DIII sites of the dephosphorylated pBS KS⁺ vector. The DNA sequences of all oligonucleotides used in this study are given in section 7.2.1.

The different KS Rz's were formed by combination of the following complementary oligonucleotides:

oRz1-9(S) and oRz1-10(AS)	form:	KS Rz 1
oMRz1-11(S) and oMRz1-12(AS)	form:	KS MRz1
oRz2-13(S) and oRz2-14(AS)	form:	KS Rz 2
oMRz2-15(S) and oMRz2-16(AS)	form:	KS MRz 2

Phosphorylation reactions were performed for 2 μg (10 μl) of each individual oligonocleotide in a 50 μl reaction mixture with 1 x Kinase buffer (50 mM Tris-HCl pH 8.2, 10 mM $MgCl_2$, 0.2 mM DTT, 5 mM spermidine), 1 mM ATP and 16 Units (8U/ μl) T4 polynucleotide kinase (Boehringer Mannheim) and incubation at 37 °C for 60 min. The phosphorylation reactions with the appropriate oligonucleotides were then mixed together. The annealling of the oligonucleotides was performed according to the following protocol, making use of a Perkin Elmer thermocycler Model 9600: 2 min. at 85 °C, 5 min at 90 °C, 1 hr at 65 °C, 15 min at 37 °C, 15 min at room temperature and followed by 15 min on ice.

The annealing-mixtures were then extracted with phenol/chloroform, precipitated with ethanol and resuspended in resuspended in 40 µl sterile water, assuming full recovery of the DNA which would correspond to 4 µg. The pBS KS^+ - *BamH*I /*Hin*DIII vector (240 ng) was then ligated with the respective ribozyme genes (*Bgl*II—Rz—*Bam*HI-*Hd*III; 100 ng) in a reaction volume of 20 µl, also containing 1 x ligation mix (1 x LM: 30 mM Tris-HCL pH 7.8, 10 mM $MgCl_2$, 10 mM DTT, 1 mM ATP) and 3 Units T4 DNA Ligase (Promega), at 15 °C overnight. Twenty percent of the ligation reaction was transformed to electrocompetent *E.coli* DH10B cells (Electromax; Gibco BRL # 18290-015) by electroporation and selected by blue-white color selection and colony hybridisation as described in section 6.2.1 (step 4), using the appropriate concatemerised ribozymes (RZ1 or RZ 2) as a radiolabeled probe (section 7.2.2). Selected clones were further analysed and confirmed by dideoxynucleotide sequencing using the standard forward and reverse primer. The flow diagram for the cloning procedures used is illustrated for KS Rz 1 in figure 7.6.

Figure 7.6 Cloning and selection of KS Ribozymes

Flow diagram of cloning procedures used for construction of ribozyme genes from the KS series, with Rz 1 as an example.

In the top part of the figure, the DNA sequence of the two annealed oligonucleotides which make up KS Rz 1 is shown, with the restriction enzyme sites (outlined) and the structural features within the hammerhead motif (above the sequence). The position of the nucleotide involved in creating a hydrolytically inactive mutant ribozyme (here: MRz1) by an A 14 G transition, is indicated by an asterisks above the residue.

In the bottom part of the figure, a schematic diagram of the region of the vector in which the ribozyme is cloned, is depicted. The numbering is relative to the start of the T7 promoter in the vector and the T 7 primer, used in the *in vitro* transcription of the ribozyme, is annealed from nucleotide position 26 to 53. The 5 '-*Bgl*II site of the ribozyme gene was ligated to the *Bam*HI site of the vector and resulted in the abolition of either restriction site (indicated by a cross). This would allow repeated cloning of similarly constructed ribozymes, to be integrated in the engineered *Bam*HI site immediately adjacent to the ribozyme motifs on the 3'-end, resulting in multimeric ribozyme clones. The restriction sites in this region are indicated above the diagram, with the *Hin*DIII site used in the cloning procedure and in linearisation of the plasmid, before *in vitro* transcription, depicted in outlined characters.

The inserted picture shows an autoradiogram (O/N exposure) of a colony hybridisation for selection of clones with KS Rz 1 in pBS KS^+, with one negatively- and one positively-hybridising colony indicated by an arrow for illustration.

pKS Rz cloning - for IN VITRO ACTIVITY ANALYSIS

Rz 1 oligomers phosphorylated and annealed

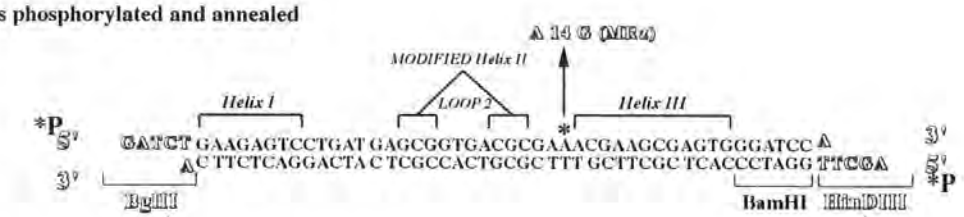

GENERAL CLONING PROCEDURES

pBS KS+ //BamHI - HinDIII + BglII - Rz - BamHI-HinDIII

- PHOSPHORYLATED OLIGOMERS ANNEALED AND LIGATED IN pBS KS+
- BLUE/WHITE SELECTION OF COLONIES AFTER TRANSFORMATION
- SELECTED WHITE AND LIGHTBLUE COLONIES STREAKED IN A GRID ON PLATES AND ON AN HYBRIDISATION FILTER
- COLONY LIFTS AND HYBRIDISATION TO 32P LABELLED RZ PROBE
- SELECTED POSITIVE CLONES FOR SEQUENCE ANALYSIS

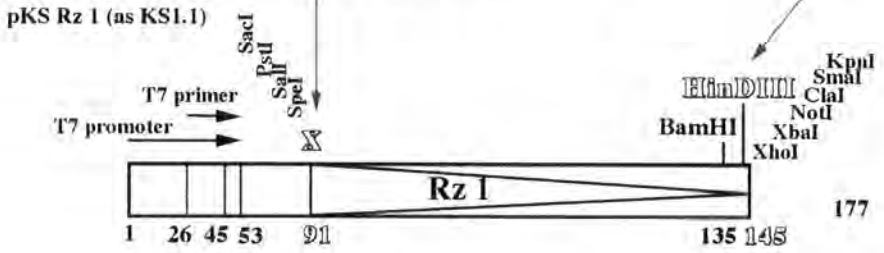

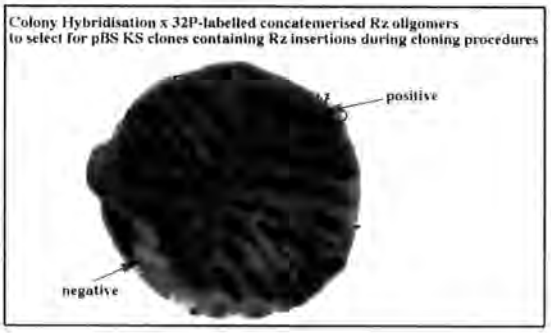

After nucleotide sequence analysis of clone, it was observed that a wide range of unexpected sequence aberrations occurred. This seem to be more frequent in the cloning of the KS Rz 2 series and the main sequence aberrations seem to involve extra nucleotide insertions (at various positions) and an obvious sequence-rearrangement (KS 3.9 in Table 7.1). These observations are shown in Table 7.1.

Table 7.1 : Sequence aberrations occurring during cloning processes of ribozymes to pBS KS+ (KS Rz series) in this study: Examples of observed sequence variations in KS Rz 2 clones

Secondary structure prediction of ribozyme 2 (this study) associated with the Ara 1-AT target sequence as illustration of the convention for definition of Helices I and III and II and loops (boxed).

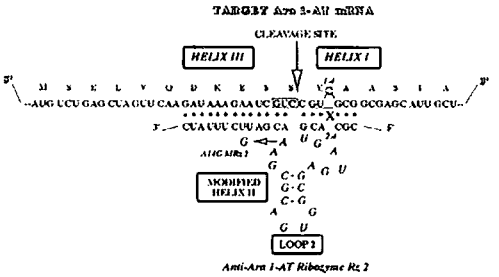

Anti-Ara 1-AT Ribozyme Rz 2

5'→3' (BglII)	Helix I			Helix II	Loop 2	Helix II		Helix III	(BamHI - HinDIII)
STANDARD		CUGA	UGA	GUCC	GUGA	GGAC	GAA	AC	
RZ 2 (KS 3 SERIES)		CUGA	UGA	GCG	GUGA	CGC	GAA	AC	
	GATCT CGC ACG	CUGA	UGA	GCG	GUGA	CGC	GAA	AC GAUUCUUUAUC	GGAUCCA
KS 3.1	GATCT CGC ACG	CUGA	UGA	GCG	GUGA	CCGC	GAA	AC GAUUCUUUAUC	GGAUCCA
KS 3.2*	GATCT CGC ACG	CUGA	UGA	GCG	GUGA	CGC	GAAA	AC GAUUCUUUAUC	GGAUCCA
KS 3.5	GATCT CGC ACG	CUGA	UGA	GCG	GGUGA	CGC	GAA	AC GAUUCUUUAUC	GGAUCCA
KS 3.6	GATCTCGGC ACG	CUGA	UGA	GCG	GUGA	CGC	GAA	ACAAUUCUUUAUC	GGGAUCCA
KS 3.7*	GATCT CGC ACG	CUGA	UGA	GCG	GUGA	CGC	GAA	AC GAUUCCUUUAUC	GGAUCCA
KS 3.9	GATCT CGC ACG	CUGA	UGA	GCCGCG			GAA	AC GAUUCUUUAUC	GGAUCCA
KS 3.10	GATCT CGC ACG	CUGA	UGA	GCG	GUGACCGC		GAA	AC GAUUCUUUAUC	GGAUCCA
KS 3.11	GATCT CGC ACG	CUGA	UGA	GCG	GUGAACGC		GAA	AC GAUUCUUUAUC	GGAUCCA
KS 3.12	GATCT CGC ACG	CUGA	UGA	GCCG	GUGA	CGC	GAA	AC GAUUCUUUAUC	GGAUCCA
KS 3.27/30 AND 31	CORRECT// IN LATER, PERSISTENT CLONING ATTEMPTS (NOT TESTED IN VITRO)								

In Table 7.1, the triangle indicates the mismatch with the target mRNA in the arm associated with helix I in the ribozyme 2 design. The aberrant nucleotides are in outlined/underlined characters. 'Standard' refers to the design used by, for instance, Haselhoff, J. and Gerlach, W.L., 1988.

7.3.1.D. Construction of ribozymes embedded in potato U1 snRNA in pU1.1-5' BglII (BamHI—Rz—BglII: the U1.1 Rz's

Ribozymes of the U1.1 Rz series, were cloned in the vector pU1.1-5' *Bgl*II. The hammerhead ribozymes were essentially identical to the ones used in the creation of the KS Rz's, but were embedded in an engineered *Bgl*II site in a potato U1.1 snRNA gene in the DNA sequence encoding the U1.1 snRNA 5' single-stranded region (Vaux, P. et al., 1992).

The basic pU1.1-5' *Bgl*II vector was pGEM 3Zf$^+$, containing a 520 bp *Hin*DIII/*Eco*RI cDNA fragment encoding U1.1-65 (Vaux, P. et al., 1992) and was kindly provided for this study by Dr. John Brown of the Scottish Crops Research Institute.

Cloning of ribozymes in this vector may allow for effective endogenous cellular delivery of the ribozymes to transgenic *Arabidopsis* plants.

In the study in this Chapter, it was the intention to assay *in vitro*, if structural interactions with the supplementary sequence would influence the ribozyme hydrolytic activity and/or specific recognition of the target substrate RNA sequence. An illustration of a ribozyme (Rz 1) integrated in this RNA polymerase III expression system is shown in Figure 7.7

The vector pU1.1-5' *Bgl*II was digested with *Bgl*II and dephosphorylated according to similar procedures as described in section 7.3.1.C. and the linearised DNA was resuspended at 60 ng/µl in sterile water (milliQ). For cloning of U1.1 ribozymes, two oligonucleotides corresponding to complementary strands of the intended ribozyme sequence were phosphorylated, annealed and cloned in *Bgl*II site of the dephosphorylated pU1.1-5' *Bgl*II vector. These procedures were performed as described in section 7.3.1.C., with the exception that the final products were resuspended in 60 µl sterile water (at 66.6 ng//µl), assuming full recovery of the DNA which would correspond to 4 µg.

The different U1.1 Rz's were formed by combination of the following complementary oligonucleotides:

oRz1-1(S) and oRz1-2(AS)	form:	U1.1 Rz 1
oMRz1-3(S) and oMRz1-4(AS)	form:	U1.1 MRz1
oRz2-5(S) and oRz2-6(AS)	form:	U1.1 Rz 2
oMRz2-7(S) and oMRz2-8(AS)	form:	U1.1 MRz 2

The DNA sequences of all oligonucleotides used in this study are given in section 7.2.1.

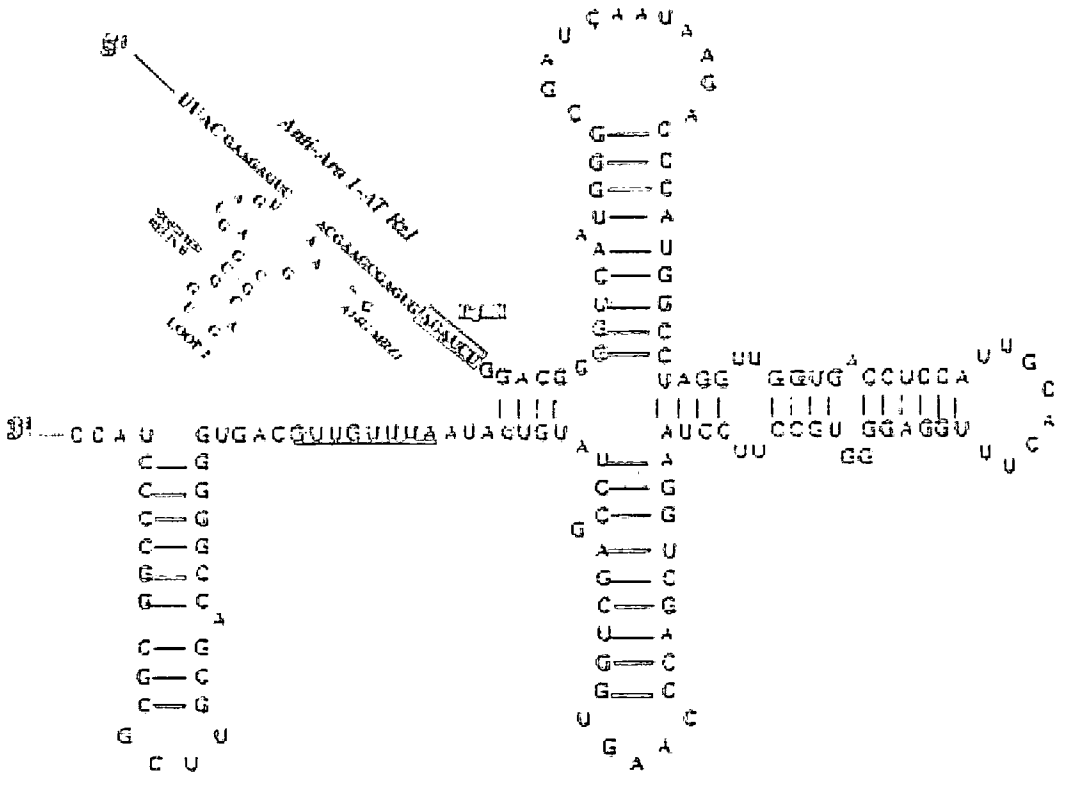

Figure 7.7 **Two dimensional representation of the secondary structure of ribozyme 1 (Rz 1) integrated in the 5' single-stranded region of potato U1.1. snRNA**

The potato U1.1 snRNA secondary structure is based on the model of Branlant, C. et al. (1981) and was derived from Figure 4 in the publication by Vaux, P. et al. (1992). U1.1 Rz 1 was inserted in an engineered *Bgl*II site in the 5' splice site recognition region (boxed). The sequence which is underlined represents the Sm antigen-binding site (the site where the UsnRNP core proteins bind) but was not directly relevant for this study.

The vector pU1.1-5' *Bgl*II (240 ng) was ligated with the respective ribozyme genes (*Bam*HI—Rz—*Bgl*II; 66.6 ng) in a reaction volume of 20 µl (section 7.3.1.C). Twenty percent of the ligation reaction was transformed to electrocompetent *E.coli* DH10B cells (Electromax; Gibco BRL # 18290-015) by electroporation and clones were selected by colony hybridisation (section 7.3.1.C.), using the appropriate concatemerised ribozymes (U1.1 RZ1 or U1.1 RZ 2) as a radiolabeled probe (section 7.2.2). Selected clones were further analysed by restriction analysis using double digests with *Hin*DIII and *Bgl*II.

This analysis allowed an examination of the clones for single or multiple insertions and at the same time would determine the orientation of the inserted U1.1 Rz relative to the SP6 promoter, from which the *in vitro* transcription for synthesis of the U1.1 Rzs would be initiated.
A flow diagram for the cloning procedures used is illustrated for U1.1 Rz 1 in Figure 7.8.

Selected clones were confirmed by dideoxynucleotide sequencing using the primers pU1 280S and pU1d, which are indicated in the schematic drawing of a U1.1 Rz construct in figure 7.8 and are described in section 6.3.3.
The clones U1.1-1.9 (single copy insert of U1.1 Rz 1 in 5'-3' orientation relative to the SP6 promoter), U1.1-1.2 (double copy insert of U1.1 Rz 1in 5'-3' orientation relative to the SP6 promoter), U1.1-3.7 (single copy insert of U1.1 Rz 2 in 5'-3' orientation relative to the SP6 promoter) and U1.1-1.5, with a single copy insert of U1.1 Rz 1 in the 'anti-sense' 3'-5' orientation relative to the SP6 promoter, were singled out as main candidates for investigation of specific, *in vitro* hydrolytic activity assays, although also other clones (including the mutated versions) were tested.

Figure 7.8 Cloning and selection of U1.1 Ribozymes

Flow diagram of cloning procedures used for construction of ribozyme genes from the U1.1 series, with Rz 1 as an example. In the top part of the figure, the DNA sequences of the *Bgl*II and *Bam*HI restriction sites are depicted to illustrate that when a *Bam*HI site is ligated with a *Bgl*II site, neither restriction site is recreated.

- A schematic diagram of the region of the pU1.1 5' *Bgl*II vector, in which the U1.1 ribozyme is cloned. The numbering is relative to the start of the *Hin*DIII site in the vector (the start of the U1.1-65 cDNA fragment) and the last residue of the SP6 primer, used in the *in vitro* transcription of the ribozyme, is at nucleotide position 33. The 5 '-*Bam*HI site of the ribozyme gene was ligated to the *Bgl*II site of the vector and resulted in the abolition of either restriction site (indicated by a cross). This would allow repeated cloning of similarly constructed ribozymes, to be integrated in the engineered *BglII* site immediately adjacent to the ribozyme motifs on the 3'-end. The restriction sites in this region are shown above the diagram. The *Hin*DIII and *Eco*RI sites flank the U1.1-65 snRNA cDNA and are shown in outlined characters. The *Eco*RI site on the 3' end of the U1.1 snRNA cDNA was also used in linearisation of the plasmid, before *in vitro* transcription. The *Bgl*II site, 3' of the ribozyme motif (indicated by the triangle) is also depicted in outlined characters, to indicate its role in the cloning and to emphasise that this site is recreated and available for cloning of multimeric copies of U1.1 Rzs. Arrows indicate the relative position of the primers pU1 280S and pU1d, used in sequence analysis.
- The inserted panel below the diagram illustrates a few possibilities for insertion of U1.1 Rzs in the pU1.1 5' *BglII* vector.
- The inserted picture on the bottom left, shows an autoradiogram (O/N exposure) of a colony hybridisation for selection of clones with U1.1 Rz 1 (left) or U1.1 MRz 1 (right) in pU1.1 5' *Bgl*II, with negatively and positively hybridising colonies clearly distinguishable.
- The inserted picture on the bottom right, shows part of an ethidium bromide stained, 1.8% agarose/TAE gel which illustrates sizes of the *Hin*DIII-*Bgl*II cDNA fragment from U1.1-1.2 (double sense insertion of U1.1 Rz 1) and U1.1-1.9 (single sense insertion of U1.1 Rz 1) compared to the same restriction fragment from the empty pU1.1-5' *Bgl*II vector.

Molecular weight markers are indicated in bp. on the left. The sizes of the DNA fragments in the gel, are indicated (in bp) below the lanes, together with the number and direction of the U1.1 Rz inserts (indicated by arrow heads).

pU1.1 5'BglII Rz cloning

- for in vitro activity analysis AND
- for RNA polymerase III delivery/expression strategy in transgenic plants to downregulate endogenous Ara 1-AT expression

pU1.1 5'BglII + BamHII - Rz - BglII

A GATCT GATCC A
TCTAG A G TCTAG

GENERAL CLONING PROCEDURES

- PHOSPHORYLATED OLIGOMERS ANNEALED AND LIGATED IN PU1.1 5'BGLII VECTOR
- STREAK COLONIES FROM TRANSFORMATION IN A GRID ON PLATES AND ON AN HYBRIDISATION FILTER
- COLONY LIFTS AND HYBRIDISATION TO 32P LABELLED RZ PROBE
- SELECTED CLONES FOR RESTRICTION ANALYSIS AND SEQUENCING

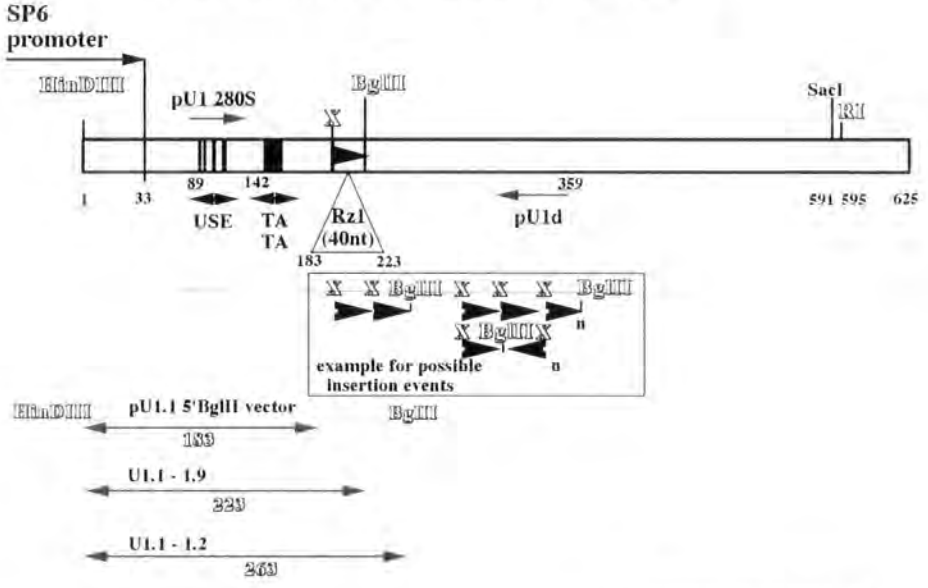

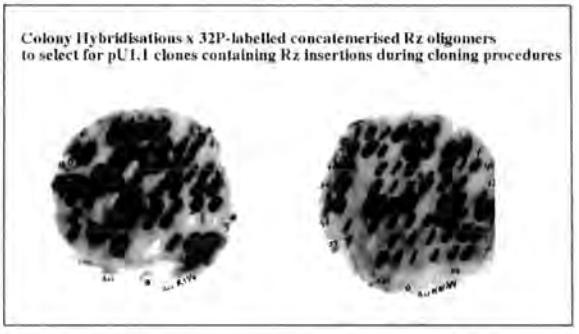

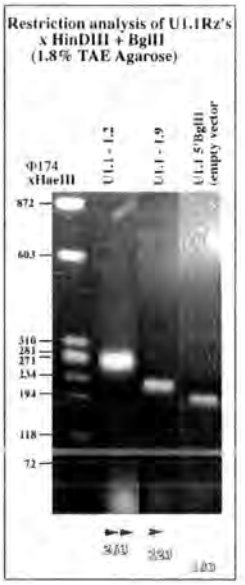

*SEQUENCE ANALYSIS of selected clones was performed using the primer pU1 280S

7.3.2 Sequence-specific and hydrolytic cleavage of Glycerol-3-Phosphate Acyltransferase (GPAT) mRNA *in vitro* by ribozymes

Although major emphasis is currently on *in vivo* systems, ribozyme design is usually tested on projected target RNAs *in vitro*. As a preliminary to the use of ribozymes for the *in vivo* gene down-regulation of the endogenous nuclear encoded, chloroplast *Arabidopsis* GPAT (1-AT) mRNA (Chapter VI), it was decided to test the hydrolytic activity and specificity of the ribozyme-designs *in vitro*.

Two GUC sites in the mRNA sequence, encoding the chloroplast targeting peptide in the preprotein of *Arabidopsis* GPAT, were selected. Figure 7.2 illustrated that these sites are nt 156 (nt 183 in the p2-T target RNA) and nt 279 (nt 306 in the p2-6T target RNA). For the Rz 1 series, 12 nucleotides perfectly matched flanking sequences in the 5' direction (helix III) and 8 nucleotides perfectly matched flanking sequences in the 3' direction (helix I), were used to define the complementary nucleotide regions which are needed to direct the expressed ribozyme to the target GUC site (nt 156). For the Rz 2 series (against nt 279), 13 nucleotides perfectly complementary in helix III and for helix I, 3 nucleotides next to the GUC-cleavage site perfectly paired, followed by a de-stabilising deleted base in the ribozyme arm followed by 3 perfectly paired nucleotides were used. *In vitro* transcription of the plasmid p2-6T after linearisation with *Bam*HI yielded a 586 base-long *Arabidopsis* GPAT RNA target mRNA fragment (Figure 7.2 + section 7.2.4) and, upon cleavage by Rz 1, would yield fragments of 183 bases and 402 bases long. Hydrolytically active Rz 2 would yield products of 306 bases and 279 bases long.
The 586 base-long target mRNA was synthesised in the presence of [α-^{32}P]UTP (400 Ci/mmol, 10 mCi/ml). In a standard *in vitro* transcription reaction of the p2-6T plasmid (described in section 7.2.4), 0.4 µg RNA was synthesised. The substrate RNA, after gel band purification, was calculated to have a specific actitvity of 6.2 x 10^6 cpm/ µg and in the experimental *in vitro* ribozyme cleavage assays, approximately 286000 cpm, which corresponds to 0.24 pmol, was used as the target substrate. The molarity of the amount of substrate in standard cleavage reactions with 15 µl total volume was then approximately 16 nM.
The hydrolytic activity of the ribozyme-design was tested *in vitro* by assaying the sequence specificity and cleavage-capability of the KS Rz's, the **ribozymes without supplementary sequences**, cloned in pBS KS$^+$ (*Bgl*II—Rz—*Bam*HI-*Hd*III). *Arabidopsis* GPAT (1-AT) mRNA-specific ribozymes were synthesised from the linearised plasmids and quantified as described in section 7.2.4. Ribozyme activity was assayed with different molar rations between the substrate and the ribozyme, under different temperatures.

Basically 5 µl of target (286000 cpm/0.24 pmol) was mixed with 0.5 µl (molar ratio substrate:KS Rz (8 x 10^4 cpm) = 1:1) or 5 µl (molar ratio = 1:10) KS Rz (single insert) in 10 µl total volume.

The ribozyme and substrate were first heated at 90 °C, renatured for 5 min at room temperature and then placed on ice. Reactions were started by adding 5 µl of a 3 x concentrated buffer, resulting in final concentrations of 120 mM Tris-HCl pH 7.5, 18 mM $MgCl_2$, 6 mM spermidine and 30 mM NaCl, at desired incubation temperatures. Cleavage reactions were performed at 22 °C, 37 °C and 50 °C. Reactions were stopped by addition of ice-cold EDTA (to 65 mM final concentration). 3 µl of each reaction was mixed with an equal volume of 2 x Formamide Loading Buffer (FLB: 80% deionised formamide,10 mM EDTA, 1 mg/ml XCFF (Xylene Cyanol FF) and 1 mg/ml BB (Bromophenol Blue), boiled for one min. prior to loading the samples for analysis on a denaturing 5% polyacrylamide - 8 M urea gel, run with 1 x TBE buffer (section 7.2.5).
Figure 7.9 illustrates results obtained with KS Rz1 (KS 1.1), the A14G mutant version of Rz 1 (KS MRz 1 (2.6)) and KS Rz 2 (KS 3.2). As is shown in lanes 1, 4, 5, 6 and lanes 23 –30, the sequence for KS Rz 1 was hydrolytically active and cleavage products of the expected sizes of 183 nt and 402 nt were observed. The Rz 1 version (KS1.1) seemed to be active at all temperatures tested but cleavage at 50 °C was most efficient. It was estimated that 40 % of the substrate was cleaved between 60 min and 120 min and that after that period (tested for 12hr) cleavage activity decreased (lanes 28, 29 and 30). The ribozyme 1 mutant (MRz1: KS 2.6), with a point mutation in the most distal nucleotide of the catalytic domain (A 14 G) showed no endonucleolytic activity *in vitro*, as expected (lanes 8 - 17). The ribozyme 2 design (Rz 2 targeted against nt 306 in the target p2-6T RNA) did not seem to have cleavage capability *in vitro* under the experimental conditions tested and this is illustrated for KS 3.2 in Figure 7.9 (lanes 18 - 22). Several other point mutants of Rz 2 were also tested, but none of them seem to be active (data not shown).

Figure 7.9 **Sequence specific *in vitro* cleavage of *Arabidopsis* GPAT (1-AT) mRNA target substrate by different non-embedded ribozymes and time course of the ribozyme-mediated reaction**

In vitro RNA transcription of *Bam*HI-linearised plasmid p2-6T, generated a radioactively labeled 586 base-long target-*Arabidopsis* GPAT mRNA fragment which was used as a substrate for the non-embedded ribozyme1 and 2 derivatives from the KS series (119 base-long non-radioactive *in vitro* transcribed RNA). Ribozyme 1 (Rz1 KS1.1), an A14G mutant of ribozyme 1 (MRz1 KS2.6) and a variant ribozyme 2 (Rz2 KS3.2) and substrate RNA were incubated at 0 °C (15 hr.) (lanes 3, 8, 13 and 18), 22 °C (15 hr.) (lanes 4, 9, 14 and 19), 37 °C (15 hr.) (lanes 5, 10, 15 and 20), 50 °C (4.5 hr.) (lanes 1, 6, 11, 16 and 21) and with added 65 mM EDTA at 50 °C (15 hr.) (lanes 2, 7, 12, 17 and 22).

Standard assays were performed in 120 mM Tris-HCl pH 7.5/18 mM $MgCl_2$/6 mM spermidine/30 mM NaCl with substrate and ribozyme in a molar ratio of 1:1 or 1:10.

To examine if, and with which kinetics, ribozyme 1 (Rz1 KS1.1) causes endonucleolytic cleavage of the substrate, the substrate mRNA was incubated with a 10 fold molar excess of ribozyme 1 at 50 °C and samples were taken at different times (lanes 23 – 31: 0 min., 5 min., 10 min., 15 min., 30 min., 60 min., 120 min., 12 hr. and 12 hr. with 65 mM EDTA added). Lane M, ^{32}P-labelled ϕX174 DNA/*Hinf*I molecular markers (in nucleotides) were prepared as described in section 7.3.3. The terminated cleavage reactions were analysed on 5% polyacrylamide sequence gels (section 7.2.5).

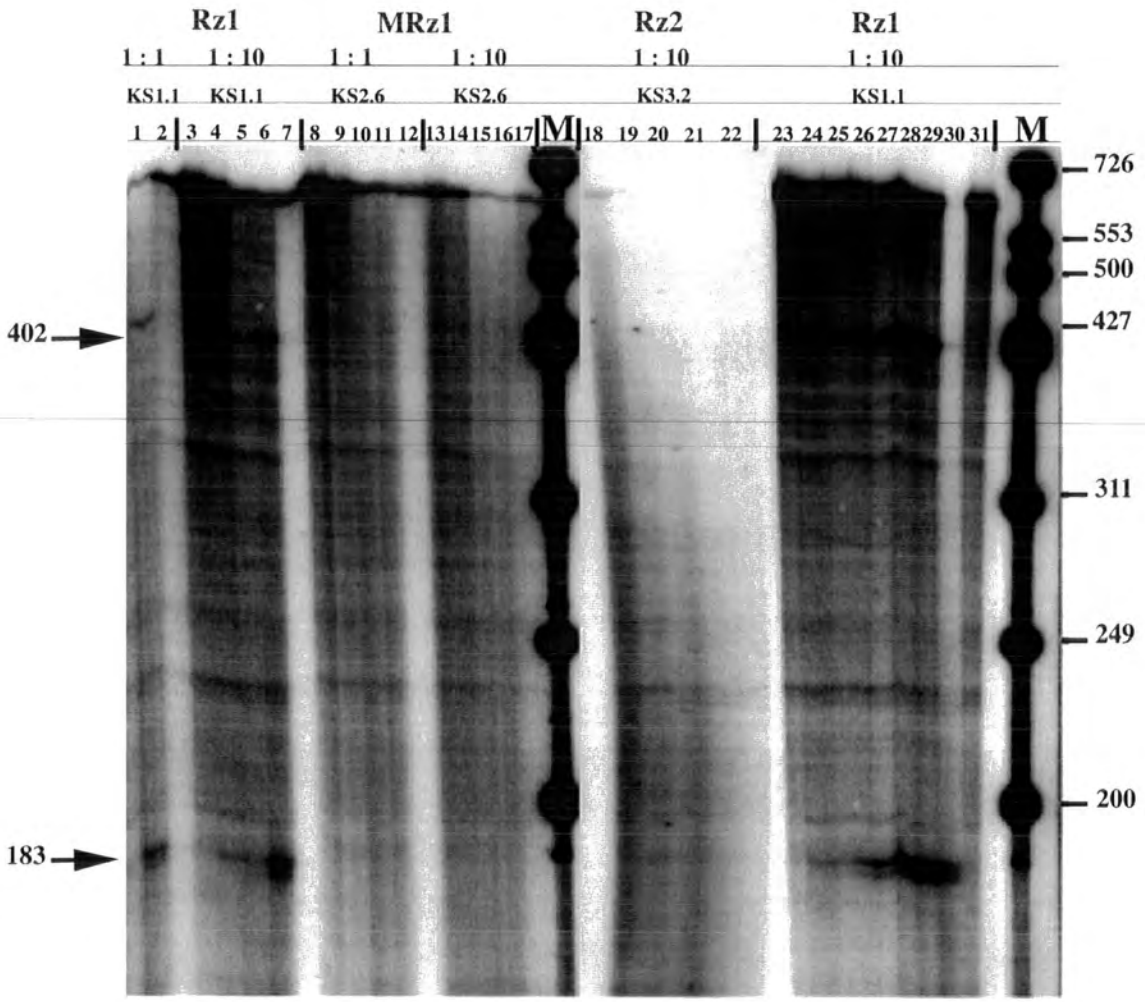
Rz1
MRz1
Rz2
Rz1
1 : 1
1 : 10
1 : 1
1 : 10
1 : 10
1 : 10
KS1.1
KS1.1
KS2.6
KS2.6
KS3.2
KS1.1
1 2 3 4 5 6 7 8 9 10 11 12 13 14 15 16 17 M 18 19 20 21 22 23 24 25 26 27 28 29 30 31 M
726
553
500
427
311
249
200
402
183

An important aim of the *in vitro* assays was to investigate which ribozyme design would be most promising for use as a tool for *in vivo* gene down-regulation of the endogenous *Arabidopsis* GPAT. The same hammerhead ribozyme-designs as in the KS Rz series, were embedded in a potato U1.1 snRNA gene (Vaux, P. et al., 1992) in the vector pU1.1-5' *Bgl*II (*Bam*HI—Rz—*Bgl*II) and evaluated *in vitro*. Structural interactions with the supplementary sequence could influence the ribozyme hydrolytic activity and/or specific recognition of the target substrate RNA sequence.

U1.1-Ribozyme activity was assayed with a molar ratio of approximately 1:2 between the substrate and the ribozyme, under different temperatures and under identical experimental conditions as for the KS Rz's. Basically 5 µl of target substrate (286000 cpm/0.24 pmol) was mixed with 5 µl (molar ratio substrate:U1.1-Rz (approximately 280000 cpm) ~ 1:2) and reactions were started by adding 5 µl of a 3 x concentrated buffer in the same procedures as described above. The equivalent of 3 µl of each reaction was analysed on a denaturing 5% polyacrylamide - 8 M urea sequence gel, run with 1 x TBE buffer. As is shown in Figure 7.10 lanes 30 – 34, when using the complementary sequence for ribozyme 1 (U1.1-1.5; single copy insert of U1.1 Rz1 in the anti-sense 3'-5' orientation) no cleavage products were observed. Also for the ribozyme 2 design (U1.1-3.7; a U1.1 Rz 2 directed against nt 306 in the target p2-6T RNA), none of the expected cleavage products (279 and 308 bases) were observed, as is illustrated in lanes 23 –28 with up to 120 min incubation at 50 °C (lane 28). This corresponded with the results obtained for the non-embedded Rz 2 designs in the KS Rz series previously described. The U1.1 Rz 2 does not seem to have cleavage capability *in vitro* under the experimental conditions tested.

However, the U1.1 Rz 1 transcripts: U1.1-1.9 (single copy of Rz 1 in pU1.1-5' *BglII*: 595 base-long transcript) and U1.1-1.2 (double copy of Rz 1 in pU1.1-5' *BglII*: 635 base-long transcript) seem to form ribozyme-structures which are functional *in vitro*. In a time-series of incubation of the substrate at 50 °C with U1.1-1.9, only in a 2-fold molar excess, the functional U1.1 Rz 1 produced two cleavage products with the expected sizes of 183 and 402 nt., as is illustrated in lanes 1 – 7 of figure 7.10. The increase in the amount of the cleavage product of 183 nt over 120 min. is most apparent. It was also observed that the radiolabeled substrate (586 base-long) visibly decreased over this period of incubation, suggesting efficient and target-specific ribozyme activity *in vitro*.

The transcripts for the U1.1-1.2, with the double inserted Rz 1 in the U1.1 snRNA, seemed to have cleavage capability at 22 °C, 37 °C, but most apparent at 50 °C, at which temperature at least 50 % of the target was cleaved after 12 hr. (Figure 7.10 lanes 9 - 21).

Figure 7.10 Sequence specific *in vitro* cleavage of *Arabidopsis* GPAT (1-AT) mRNA target substrate by different ribozymes embedded in the 5' single stranded region of a potato U1.1 snRNA cDNA and time course of the ribozyme-mediated reaction

In vitro transcribed, 586 base-long ^{32}P-labeled target-*Arabidopsis* GPAT (1-AT) mRNA (p2-6T) was used as a substrate for the ribozyme1 and 2 derivatives embedded in a potato U1.1 snRNA cDNA (595 or 635 base-long *in vitro* transcribed RNA). Standard assays were performed as described in the text, with substrate and ribozyme transcript in a molar ratio of 1:2. A double construct of ribozyme 1 (Rz1: U1.1-1.2) and an antisense version of ribozyme 1 (AS Rz1: U1.1-1.5) and substrate RNA were incubated at 0 °C -15 hr. (lanes 9 and 30), 22 °C -15 hr. (lanes 10 and 31), 37 °C -15 hr. (lanes 11 and 32), 50 °C -4.5 hr. (lanes12 and 33) and with added 65 mM EDTA at 50 °C -15 hr. (lanes13 and 34).

To examine if, and with which kinetics, ribozyme 1 (U1.1-1.9), a double construct of ribozyme 1 (U1.1-1.2) and a variant ribozyme 2 (Rz2: U1.1-3.7) causes hydrolytic cleavage of the substrate, the substrate GPAT (1-AT) mRNA was incubated with only a 2 fold molar excess of the ribozyme transcripts at 50 °C and samples were taken at different times: lanes 1, 14 and 23: 0 min., lanes 2, 15 and 24: 5 min., lanes 3 and 16 : 10 min., lanes 4, 17 and 25: 15 min., lanes 5, 18 and 26: 30 min., lanes 6, 19 and 27: 60 min., lanes 7, 20 and 28: 120 min., lane 21: 12 hr. and lanes 22 and 29: 12 hr. with 65 mM EDTA added. Lane M, ^{32}P-labelled (kinased) ϕX174 DNA/*Hinf*I molecular markers (in nucleotides). The terminated cleavage reactions were analysed on 5% polyacrylamide sequence gels (section 7.2.5).

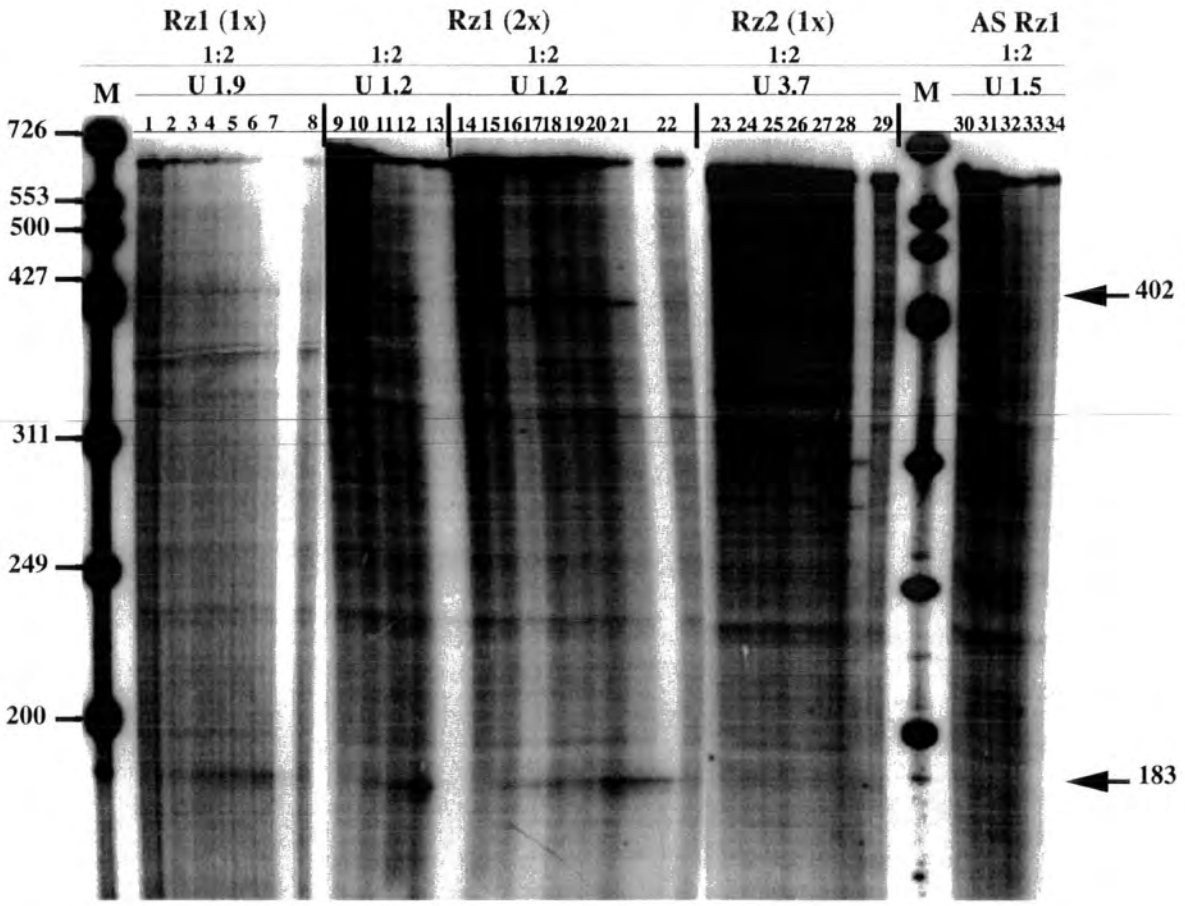
Rz1 (1x)
1:2
U 1.9
Rz1 (2x)
1:2
U 1.2
1:2
U 1.2
Rz2 (1x)
1:2
U 3.7
AS Rz1
1:2
U 1.5
M
M
1 2 3 4 5 6 7 8 9 10 11 12 13 14 15 16 17 18 19 20 21 22 23 24 25 26 27 28 29 30 31 32 33 34
726
553
500
427
311
249
200
402
183

This clearly demonstrated that the U1.1 Rz 1 sequences are capable of considerable hydrolytic cleavage activity *in vitro* and specific recognition of the target GUC codon in the *Arabidopsis* GPAT (1-AT) mRNA. The RNA structures of the potato U1.1 snRNA do not seem to impede the functionality of the structurally integrated Rz 1.

7.4 Conclusion

The ultimate aim of the studies described in chapter and the previous Chapter VI was to start the development and testing of an effective, but specific molecular gene down-regulation tool for acyltransferases in plant cells. The use of hammerhead ribozymes to specifically eliminate or block the function of a gene product may have great advantages. The irreversible destruction of the target mRNA molecule would potentially make an effective ribozyme a more powerful gene down-regulation tool. In contrast to the more frequently used gene silencing (GS) technology, a single ribozyme would have the ability to process a large number of substrate molecules. In this chapter the term 'ribozyme-catalysis' is used in the first instance to describe the involvement of the ribozyme in the promotion of the chemical reaction (endonucleolytic cleavage) and therefore does not strictly mean multiple turnover, i.e. one ribozyme will cleave several substrate molecules. With the experiments described here, no evidence for catalytic turnover in the system is presented. The design and hydrolytic activity of essentially two different, endonucleolytic ribozymes based on the hammerhead, each containing a core catalytic domain with a modified (shorter) helix II and substrate recognition sequences, was tested *in vitro*. The substrate recognition sequences, involved in the formation of helix I and III, were designed to direct the hammerhead ribozymes to two different GUC triplets within the nuclear encoded, chloroplast *Arabidopsis* GPAT (1-AT) mRNA. The substrate recognition sequences (flanking sequences) of the hammerhead ribozymes do not only confer target specificity but also decide the turnover rate of the substrate. Therefore, the length of these sequences is one of the critical factors in designing a successful ribozyme. Under *in vivo* conditions, it is possible that the ribozymes can exert an antisense effect via the formation of a stable complex with the substrate without being involved in catalytic activity. A non-functional version of the ribozymes was constructed by an A 14 G transition (single mutation) in the hammerhead motif, which was shown to result in a ribozyme sequence without hydrolytic activity *in vitro*. These mutant-ribozymes would be used to monitor the contribution of a potential antisense effect *in vivo*. Another major consideration in the design of a specific and effective ribozyme is the target site. Besides the fact that different NUH motifs differ in their reactivity (Zoumadakis, M. and Tabler, M., 1995), the substrate domain which is to be targeted (the "antisense domain") has to be chosen. It is still more luck than an exact science to try and predict the ideal ribozyme target site in a substrate mRNA *in vivo*. Longer RNA substrates in living cells (*in vivo*) are likely involved in secondary structures and may be associated with proteins which might interfere with the accessibility of the target region for the ribozyme. However, some general considerations can be taken into account. First, if at all possible, a cleavage motif in a sequence region, which is unique for the target and does not recur in other RNAs is important. In this study, the sequence region with the two selected GUC sites, was in the part of the mRNA encoding the chloroplast targeting peptide in the preprotein of *Arabidopsis* GPAT.

The corresponding RNA region was not present in the transgenic cDNA construct for squash GPAT, used in the plant-transformations described in Chapter VI. Second, it would be of interest to know whether a cleaved RNA will be functionally inactive or if it may still has some residual function. When a ribozyme would effectively cleave the selected target site of the *Arabidopsis* GPAT mRNA *in vivo*, it was expected that translation of the residual product would not be possible. If, by any chance, a protein would be produced from the cleaved mRNA product, it would lack a transit peptide and thus could not be directed to its subcellular location. Third, it would be helpful to know if a domain has any form of recognised function, for example, a protein binding site, which would render the region inaccessible for a ribozyme (or antisense molecule). Fourth, the ribozyme should avoid RNA domains that are highly structured. Computer analysis may be helpful in identify RNA regions of low local folding potential (Steger, G. et al., 1984; Sczakiel, G. et al., 1993; Ferré-D' Amaré, A.R. and Doudna, A., 1999).

This study described the construction and *in vitro* testing of the hydrolytic cleavage capability and specificity of two hammerhead ribozyme-designs.
Ribozymes were cloned in RNA transcription vectors, via annealing of complementary deoxy-oligonucleotides and selected as single insertions and multimeric versions. During such cloning of the Rz 2 series in particular, a wide range of sequence aberrations occurred. This was thought not to be due to the actual cloning procedures but likely caused by non-homogenous preparations of oligonucleotides of the Rz 2 series. *In vitro* assays were performed and Rz 1 demonstrated to function effectively at 1:1, 1:2 and 1:10 molar ratios (target:Rz) as transcripts from the pBS KS+ vector and embedded in a potato U1.1snRNA transcript respectively. Cleavage was most efficient at 50 °C although cleavage was also apparent after overnight incubation at 37 °C and 22 °C. Variants of Rz2 did NOT cleave under the same conditions. The A14G mutated version of both ribozymes, used to demonstrate the extend of an antisense effect in the *in vivo* situation, proved to be non-catalytic.
Despite the proven cleavage capability of particular ribozymes *in vitro*, it is not certain that the ribozymes will function under *in vivo* conditions. The successful application of a ribozyme strategy *in vivo* will be dependent on a considerable number of circumstances. Besides secondary structures of the ribozyme transcripts and the target RNAs and the possible association with cellular proteins, there are complicating factors such as spatial separation between the site of synthesis of the ribozyme and its target, the molecular stability and relative concentrations of the ribozyme, target RNA and co-factors (Mg^{2+}).
The most important result from the experiments described in this Chapter, was the observation that Rz 1, embedded in a potato U1.1 snRNA gene, has effective cleavage capability *in vitro*. The Rz 1 was inserted in the DNA region of the U1.1 snRNA gene which encodes the 5' single-stranded RNA sequence and would therefore be less likely to be involved in inactive intramolecular interactions with the rest of the gene transcript.

The supplementary sequences around the hammerhead ribozyme did not seem to inadvertently impede the specific recognition of the target substrate and the cleavage capability of the U1.1-Rz 1 transcript.

The method of delivery of the ribozyme into living cells is of major importance but is dependent on the biological system one is working with and the desire for a transient or continuous presence of the ribozyme. In this study the U1.1 snRNA gene was chosen. The major advantages of such a system would be that the U1.1-Rz 1gene expression may be an order of magnitude higher than for RNA polymerase II genes and the ribozymes may likely be more stable and sequestered in the same cellular compartment as the target mRNA.

Therefore, the U1.1-1.2 and U1.1-1.9 ribozymes (Rz 1) were selected for further studies of their use in *in vivo* gene down-regulation of the endogenous, plastidial *Arabidopsis* GPAT.

Summary and general conclusion

∞∞∞∞∞

Lipid biosynthesis results in the formation of a diverse heterogeneous group of compounds, which are essential components of all living cells. The fatty acid and glycerolipid biosynthetic pathways in plants are responsible for the synthesis of the main constituents of cellular membranes and also for the formation of storage oils in seeds. Rapid advances have been made towards understanding the biochemical reactions and the isolation and analysis of genes and enzymes, involved in principle steps of the pathways. A major driving force behind the research is the possibility of rationally designing the lipid composition of plants. In particular, commercial production of unusual and valuable fatty acids in oilseeds is an attractive target.
The biotechnological manipulation of seed oil content has lead to an increasing recognition of the complexities of the regulation of storage and membrane lipid formation. Recent transgenic studies have highlighted a relative ignorance in the areas of regulatory control of gene expression, metabolic partitioning and interaction between components of the lipid biosynthesis pathways and other metabolic pathways *in vivo*. On the other hand, important findings concerning the structure-function relationships and catalytic plasticity of certain lipid enzymes have been reported recently (Broun, P. et al., 1998)

The formation of complex lipids involves specific attachment of fatty acyl groups to a glycerol backbone and these reactions, which are important for the formation of both storage triacylglycerols, as well as structural membrane lipids, are catalysed by acyltransferases. The isolation, characterisation and manipulation of some of these enzymes, has indicated the possibilities for their use in rational modification of plant lipid composition. In other studies, manipulation of, in particular glycerol-3-phosphate acyltransferases, has demonstrated a degree of flexibility in the fatty acid composition of membrane lipids and an alteration in the chilling sensitivity of plants.
De novo synthesised fatty acyl chains are diverted into the prokaryotic pathway of plant lipid biosynthesis by a soluble glycerol-3-phosphate acyltransferase (GPAT [EC. 2.3.1.15]) in the chloroplast. At least in certain plants, it appears to be a rate-limiting step of glycerolipid biosynthesis. GPAT catalyses the acylation at the *sn*-1 position of *sn*-glycerol-3-phosphate to form *sn*-1-acylglycerol-3-phosphate (lysophosphatidic acid; LPA).
The main objective of the work described in this study is to advance our understanding of the biochemical properties and the structure-function relationships of the nuclear encoded, chloroplast glycerol-3-phosphate acyltransferases. This study also details the strategy-

design and experiments carried out to use ribozyme-technology as a molecular tool to down-regulate the gene expression of one out of multiple acyltransferases. At the same time, this strategy would allow for a phenotypic indication of ribozyme-efficacy *in vivo* and may help further contribute to insight into the role of glycerol-3-phosphate acyltransferase in processes determining the phenomenon of chilling-sensitivity of plants.
In **Chapter III**, experiments are described in which the mature protein regions of the soluble plastidial glycerol-3-phosphate acyltransferase (GPAT [EC 2.3.1.15]) from squash and *Arabidopsis* were overproduced in *Escherichia coli* using the pET System. Purification protocols were developed to obtaining relatively large amounts of about 23-fold enriched and approximately 90% pure catalytically active enzyme. This allowed for detailed *in vitro* studies of substrate selectivities of the enzymes using conditions which were physiologically relevant. The pure GPAT enzyme preparations were used to immunise rabbits to raise polyclonal antibodies for use in Western blotting experiments. The overall primary structure (amino acid sequences) of these enzymes has a high degree of similarity (66.9% in 369 AA overlap) and, as anticipated, the immunosera cross-recognised both denatured proteins. Four peptide antigens were designed and used for immunisations of rabbits, with the aim of obtaining very specific polyclonal antibodies distinguishing between both proteins. One of the polyclonal immunosera raised against Ara-PEP2, specifically recognised the purified *Arabidopsis* GPAT enzyme and *Arabidopsis* GPAT enzyme in extracts of *E. coli* in which the respective proteins were overproduced. However, in crude plant leaf extracts there was a persistent high non-specific background. Affinity purification was performed to purify the Ara-PEP2 antiserum.
Using the protein purification protocols, in conjunction with a method developed to create an isomorphon containing heavy metal atoms (selenium), allowed the squash GPAT mature recombinant protein to be made available in sufficient quantities for crystallisation trials. This has allowed the complete 3D-structure of the enzyme to be elucidated in a collaboration with the University of Sheffield. Of particular interest is that only the truncated squash enzyme would crystallise.

The cloning and characterisation of variants of soluble glycerol-3-phosphate acyltransferase enzymes with different substrate selectivities and kinetic parameters is valuable for greater understanding of the structure-function relationships of these enzymes. This is particularly so if this can be extended by appropriate structural studies. With the crystallisation and determination of the complete atomic structure of squash GPAT, this is liable to be a reality in the future. The cloning of a novel GPAT cDNA and gene from oil palm (*Elaeis guineensis* var. *Tenera*) is described in **Chapter IV**. Analysis of an apparent full length cDNA clone of 2043 base pairs long, from a mesocarp-specific λZAP II based cDNA library, revealed that the oil palm soluble GPAT mRNA encodes a 460 amino acids protein with a predicted molecular mass of 51.3 kDa.

The cDNA and protein sequence shares the highest identity (80% and 70% respectively) with a plastid GPAT from squash (*Cucurbita moschata*). Characterisation of the soluble GPAT gene(s) by Southern blotting suggested that oil palm contains one, but possibly two related genes. The clones for the gene (designated gO1AT(2+3)) were isolated by screening a λBluestar based genomic oil palm library for cross-hybridisation with a radiolabeled probe prepared from GPAT cDNA from *Arabidopsis*. Northern blot analysis of soluble GPAT mRNA presence in oil palm mesocarp, kernel and leaf suggested that the steady-state mRNA level in these tissues is very low. An influence of the length and composition of the amino (N-) terminal sequence of the GPAT enzyme on enzymatic activity and acyl-ACP selectivity, was examined by functional expression via bacterial overproduction of three recombinant oil palm GPAT proteins with variable N-terminal regions.

The primary sequences of plastid glycerol-3-phosphate acyltransferases are highly similar, but different GPAT isoforms have variations in substrate preferences. Subtle variations in secondary and tertiary structure of these proteins are likely to be the main determinants of these differences in substrate specificities and selectivities. Aspects of the structure-function relationship were examined at the molecular level in **Chapter V**. Chimeric recombinant proteins of *Arabidopsis* and squash GPAT, and spinach and squash GPAT respectively, were constructed by domain swaps of three fragments of roughly equal size between the respective enzymes. Also the influence on function of variations in the N-terminal domain and two single amino acid substitutions in the C-terminal domain of the recombinant squash GPAT was investigated. The recombinant proteins, overproduced in *E. coli* and partially purified, retained their activity. By means of the standard selectivity assay and determination of apparent kinetic constants for acyl-ACP substrates of most of the enzymes, it was found that in some cases their substrate selectivities were dramatically altered. These data form valuable information for refined analysis of the protein structure by providing a link to phenotypic behaviour of variants of the soluble GPAT enzyme.

In **Chapter VI**, a strategy was designed and experiments were initiated for the development of a molecular tool for specific gene-downregulation of one out of multiple, sequence-similar acyltransferase genes.
It was envisaged that the strong correlation between substrate preference of chloroplast glycerol-3-phosphate acyltransferase and chilling-tolerance may be exploited as a phenotypic identification of such specific gene-downregulation and for evaluation of the efficacy of ribozyme-technology *in vivo*.
Fourty independent transgenic *Arabidopsis* plant lines were generated, transformed with a squash GPAT cDNA, and 23 of these transformed lines were further examined for stable integration of the transgene in the genome (Southern analysis) and expression of the

endogenous and transgene glycerol-3-phosphate acyltransferase (GPAT) mRNA. It was decided to test the use of a prolonged low temperature exposure as a severe chilling treatment protocol for use in these experiments.
Within the overall dual approach aimed at specific acyltransferase gene down-regulation, a strategy for design and delivering ribozyme-activity *in planta* was developed.

Chapter VII describes the design of endonucleolytic ribozymes (Rz's) based on the hammerhead motif, each containing a core sequence, consisting of a modified catalytic domain, and substrate recognition sequences. The substrate recognition sequences were designed to specifically bind and cleave at two different GUC motifs at position 156 (Rz1) and position 279 (Rz2) within the nuclear encoded, chloroplast *Arabidopsis* GPAT mRNA sequence. To monitor potential anti-sense effects *in vivo*, a mutated version of each ribozyme (MRz1 and MRz2) was created by means of an A-14-G transition within the ribozyme domain, known to inactivate RNA catalysis *in vitro*. The ribozymes were subcloned via annealing of complementary phosphorylated deoxy-oligonucleotides and selected as single insertions and multimeric versions in two types of vector. During cloning procedures of such constructs containing ribozyme sequences, a wide range of sequence aberrations occurred. For effective endogenous delivery, intracellular transcription and increased levels of the ribozymes in plant cells, ribozymes were embedded in a potato U1.1 snRNA gene. After linearisation with *EcoRI*, Rz constructs in vector pU1.1-5' *BglII* (*BamHI*—Rz—*BglII*) were used for *in vitro* RNA transcription with SP6 RNA polymerase to assay if structural interactions with the added sequence would influence the ribozyme activity on a projected *Arabidopsis* GPAT mRNA target-substrate *in vitro* .

The results obtained in this work will provide for a greater understanding of the catalytic mechanism and the structural requirements determining substrate preferences of the soluble glycerol-3-phosphate acyltransferases and maybe other acyltransferases.

Publications during the course of this study

A.R. Slabas, C. Brough, J. Kroon, W. Simon, R. Swinhoe, D. Rice, J. Rafferty, R. Winz, A.R. Stuitje and K. Elborough. (1994)
Towards an understanding of enzymes of lipid biosynthesis. in: Plant Lipid Metabolism; Ed. by Jean-Claude Kader and Paul Mazliak; Kluwer Academic Publishers, p.55.

Kieran M. Elborough, Russel Swinhoe, Robert Winz, Johan T.M. Kroon, Lee Farnsworth, Tony Fawcett, Jose M. Martinez-Rivas and Antoni R. Slabas. (1994)
Isolation of cDNAs from *Brassica napus* encoding the biotin-binding and transcarboxylase domains of acetyl-CoA carboxylase: assignment of the domain structure in a full length *Arabidopsis thaliana* genomic clone. Biochemical Journal 301: 599.

Adrian P. Brown, Clare L. Brough, Johan T.M. Kroon and Antoni R. Slabas. (1995)
Identification of a cDNA that encodes a 1-acyl-*sn*-glycerol-3-phosphate acyltransferase from *Limnanthes douglassii.* Plant Molecular Biology 29: 267.

Antoni R. Slabas, Adrian P. Brown, John B. Rafferty, David W. Rice, Clare Baldock, Johan T.M. Kroon, William Simon, Antoine R. Stuitje, Clare L. Brough. (1996)
Soluble and membrane bound components of plant lipid synthesis.
/Composes membranaires et solubles impliques dans la synthese des lipides chez les plantes.
C.R. Acad. Sci. Paris, Sciences de la vie/Life sciences; 319: 1043.
French Academy of Science.

Clare L. Brough, Jane M. Coventry, William W. Christie, Johan T.M. Kroon, Adrian P. Brown, Tina L. Barsby and Antoni R. Slabas. (1996)
Towards the genetic engineering of triacylglycerols of defined fatty acid composition: major changes in erucic acid content at the *sn*-2 position affected by the introduction of a 1-acyl-*sn*-glycerol-3-phosphate acyltransferase from *Limnanthes douglassii* into oil seed rape. Molecular Breeding 2: 133.

J.T.M. Kroon, T.F. Schierer and A.R. Slabas. (May 1998)
Acyltransferases and Function. SEB Annual Meeting. Plant and Cell Biology Abstracts, Journal of Experimental Botany,Volume 49.

T.F. Schierer, J.T.M. Kroon and A.R. Slabas. (July 1998)
In vivo substrate selectivity assays demonstrate that acyl-group preference of plastid acyltransferases is enhanced by attachment to acyl carrier protein. Advances in Plant Lipid Research. The Proceedings of the 13th International Symposium on Plant Lipids. Ed. By Juan Sanchez, Enrique Cerda-Olmedo and Enrique Martinez-Force. Secretariado De Publicaciones, Universidad De Sevilla, Spain

Sipo Vanhanen, Mark West, Johan T.M. Kroon, Nigel Lindner, John Casey, Qi Cheng, Kieran M. Elborough and Antoni R. Slabas. (2000)
A consensus sequence for Long-chain Fatty-acid Alcohol Oxidases from *Candida* identifies a family of genes involved in Lipid ω-oxidation in yeast with homologues in plants and bacteria. J. Biol. Chem. 275 : 4445.

Martin Fisher, Johan T.M. Kroon, Wayne Martindale, Antoine R. Stuitje, Antoni R. Slabas,and John B. Rafferty (2000)
The X-Ray Structure of *Brassica napus* B-Keto Acyl Carrier Protein Reductase and its implications for substrate binding and catalysis.
Structure with Folding and Design Vol. 8, No. 4: 339-347.

A.P. Turnbull, J.B. Rafferty, S.E. Sedelnikova, A.R. Slabas, J.T.M. Kroon, L Nishida, N. Murata, J.W. Simon, T.F. Schierer and D.W. Rice
Analysis of the structure, substrate specificity and mechanism of the glycerol-3-phosphate 1-acyltransferase from Squash (*Cucurbita mosschata*).
(to be submitted)

APPENDIX A

Reverse Genetics in Plants: A Mini Overview

Reverse genetics, or to use the pharmacological term, 'nucleic acid drugs' or nucleic acid polymers, can be used to alter protein function or to interfere with the function of genes encoding the target protein. Depending on their target site and mechanism of action, 'nucleic acid drugs' can be subdivided into four classes: aptamers, antigene molecules (including chimeric RNA/DNA oligonucleotides), homology-dependent gene silencing (HDGS) (antisense suppression, sense co-suppression, oligonucleotides) and ribozymes.

Aptamers are single- or double-stranded nucleic acids, which are capable of binding proteins or other small molecules (Ellington, A.D. and Szostak, J.W., 1990). Aptamers would most likely bind proteins involved in the regulation and expression of genes, i.e. transcription factors, by acting as a sink for the protein factors, preventing their normal function and modulating the expression of the genes dependent upon the activity of the protein. To date, no publications of the application of aptamers in plant cells are known to the author and only a few reports of oligonucleotide aptamers displaying biological effects have been reported for animal systems (Bielinska, A. et al., 1990; Sullenger, B.A., 1990; Bock, L.C. et al., 1992; Lisziewicz, J. et al., 1993).

Nucleic acids designed to bind to single-stranded or double-stranded DNA and targeted to genomic DNA, have been termed **antigene nucleic acids** (Hélène, C. and Toulmé, J.J., 1990). Binding of single-stranded DNA may occur at a replication or transcription bubble and thereby interfering with either of these processes. Alternatively, the antigene may bind the major groove of double-stranded DNA and form a triple helix (or triplex). Triplex formation may prevent the interaction of protein factors required for transcription, or it may physically block the initiation or elongation of the transcription complex. Only a handful of reports on results obtained using antigenes *in vitro* and in living (non-plant) cells (*in vivo*) have been reviewed in Stull, R.A. and Szoka,C. Jr. (1995). However, recently a new strategy for targeted manipulation of endogenous genes by DNA repair (gene conversion) using **chimeric RNA/DNA oligonucleotides** was developed (Yoon, K. et al., 1996; Cole-Strauss, A. et al., 1996) and has been applied to specifically modify genes in maize cells (Beetham, P.R. et al., 1999; Zhu, T. et al., 1999; Zhu, T. et al., 2000). Not only the engineering, but also reverse genetics of endogenous genes in plants seems feasible by using this approach.

Homology-dependent gene silencing (HDGS) is a common phenomenon in transgenic plants. The introduction of transgenes (or a portion thereof) or viral genes into plants can cause inactivation of the introduced gene at the mRNA level, as well as the endogenous genes with sequence homology to the introduced genes (Vaucheret, H., et al., 1998). Currently, the mechanisms of these silencing effects are still under investigation but it is thought that they can regulate gene expression in the nucleus and in the cytoplasm in numerous biological contexts.

Antisense RNA-encoding transgenes have been widely used in plants and animals to suppress the expression of specific genes. Antisense technology was first reported for plants by Van der Krol et al., who showed that the expression of an endogenous gene (chalcone synthase (CHS)) can be effectively inhibited by antisense RNA-producing genes (Van der Krol et al., 1988; Mol, J. et al., 1990). Although some have suggested that antisense suppression may share a similar mechanism to sense co-suppression (Dougherty, W.G., and Parks, T.D., 1995), others have reported that an antisense transgene gave a different pattern of gene suppression to a sense transgene (Jorgenson, R.A., et al., 1996) and many researchers regard both phenomenas as having different and unique mechanisms.

Endogenous genes can also be down-regulated by expression of homologous sense-transcripts, a phenomenon referred to as **sense co-suppression** (Jorgenson, R.A., 1995). This had a substantial impact on applications in agricultural biotechnology in the form of unwanted responses to the introduction of transgenes in genetically engineered crop plants and of 30 companies polled, nearly all reported problems with unwanted silencing of transgenes and/or homologous endogenous genes (Finnegan, J. and McElroy, D., 1994). Insight into the mechanisms behind co-suppression and epigene conversion (Matzke, A.J.M. et al., 1994) have come from analyses of a number of plant genes and has recently been reviewed by Matzke, M.A. and Matzke, A.J.M. (1995b and 2000), Stam, M. et al. (1997), Vaucheret, H., et al. (1998). The inactivation can occur transcriptionally or post-transcriptionally (Vaucheret, H., et al., 1998; Gallie, D.R., 1998; Grant, S.R., 1999). Transcriptional gene silencing **(TGS)** can be a consequence of transcription inactivation by promoter methylation and possibly with a role of the chromatin conformation (Meyer, P., 2000). Post-transcriptional gene silencing **(PTGS)** is characterised by specific reduction of cytoplasmic RNA (Gutiérrez, R.A. et al., 1999), probably through sequence-specific mRNA degradation, with normal rates of nuclear transcription being maintained and is associated with the appearance of specific low-molecular-weight RNA fragments (Hamilton, A.J. and Baulcombe, D.C., 1999). Several models have been proposed to explain PTGS, including the 'threshold level' model, the 'aberrant RNA' models (Wassenegger, M., and Pélissier, T., 1998; Waterhouse, P.M. et al., 1999) and the cyclic RNA degradation model (Metzlaff, M. et al., 1997). Recently, a direct demonstration that PTGS is associated with decreased stability of the silenced transcript has been reported for chitinase and β-1,3-glucanase genes in tobacco (Holtorf, H. et al., 1999). Direct evidence that dsRNA could trigger gene silencing, presumably by inducing RNA degradation, has been obtained from experiments on transgenic tobacco and rice plants. Homologous gene expression is inhibited most effectively in plants that are transformed with construct(s) that produce self-complementary transcripts, in plants producing both sense and antisense transcripts and in plants with tandemly repeated or repetitive (trans-)gene structure (Waterhouse, P.M. et al., 1998; Wang, M.-B., and

Waterhouse, P.M., 2000). It is remarkable that very often (parts of-) genes arranged as inverted repeats (IR) are dominant silencing loci and roles of IRs in HDGS are considered in Muskens, M.W.M. et al. (2000). Recently it was reported that inverted-repeat DNA constructs encoding RNA with a hairpin structure can induce target gene suppression with very high efficacy in primary transgenics and therefore could be used as a new gene silencing tool (Singh, S. et al., 2000).

The *in vivo* down-regulation of the expression of one specific gene out of multiple sequence-similar, homologous genes requires a fine-tuned approach with target site specificity as an important objective. To ensure high sequence-specificity of antisense technology, a relatively short sequence unique in the mRNA population is required and would allow the use of antisense oligodeoxynucleotides or their analogs, which can be prepared by chemical synthesis. When absorbed by cells, they may function in the cytoplasm by blocking translation of the target mRNA and upon penetrating the nucleus, they may interfere with nuclear processing. Much research has been focussed on developing the use of these antisense oligomers and derivatives as specific therapeutic agents, for instance in chemotherapy, neurobiology, antiviral (AIDS) research and possibilities for gene therapy. A second generation of nucleic acid drugs, **the ribozymes**, has evolved as a result of the elucidation of the properties of ribonucleic acids. Ribozymes, are small RNA molecules which similarly rely on the principle of complementary base pair formation but with the added advantage that they are endowed with endoribonuclease activity at enzymatic rates (see references in Chapter VII). In contrast to antisense oligodeoxynucleotides, which inhibit translation, ribozymes cleave the target RNA in a sequence-specific manner, which then leads to degradation (Cech, T.R., 1990; Symons, R.H., 1992). Ribozymes have enormous potential to specifically inhibit gene expression and as such are of importance in basic research and biotechnology (section 6.3.3). A majority of research has been towards the hammerhead ribozyme (Bratty, J. et al., 1993). The cleavage catalysed by the hammerhead ribozyme occurs at a specific nucleotide triplet to generate a nucleoside 2', 3'-cyclic phosphate and a nucleoside with a free 5'-hydroxyl group. Basic prerequisites which must be met are that the cleavage triplet and the 5' and 3' target recognition sequences must be easily accessible to the ribozyme and not otherwise involved in secondary structures or strong interactions with proteins (section 6.4.3). Recognition of the target mRNA by ribozymes is by complementary base pairing between the substrate (target) and the 'arms' of the ribozyme to form helices I and III (Chapter VII). This complementary interaction could be viewed as an RNA antisense approach but with the added advantage of direct degradation of the target and possibly with multiple turnover (catalytic) of the ribozyme.

REFERENCES

Abbot, A. (1999) A post-genomic challenge: learning to read patterns of protein synthesis. Nature 402: 715.

Alban, C., Joyard, J., and Douce, R. (1988) Preparation and characterization of envelope membranes from nongreen plastids. Plant Physiol. 88: 709.

Altschul, S.F., Gish, W., Miller, W., Myers, E.W., and Lipman, D.J. (1990) Basic local alignment search tool. J. Mol. Biol. 215: 403.

Altschul, S.F., Madden, T.L., Schäffer, A.A., Zhang, J., Zhang, Z., Miller, W., and Lipman, D.J. (1997) Gapped BLAST and PSI-BLAST: a new generation of protein database search programs. NAR. 25: 3389.

Arondel, V., Lemieux, B., Hwang, I., Gibson, S., Goodman, H.M., and Somerville, C.R. (1992) Map-based cloning of a gene controlling omega-3 fatty acid desaturation in *Arabidopsis*. Science 258: 1353.

Baldock, C., Rafferty, J.B., Sedelnikova, S.E., Baker, P.J., Stuitje, A.R., Slabas, A.R., Hawkes, T.R., and Rice, D.W. (1996a) A mechanism of drug action revealed by structural studies of enoyl reductase. Science 247: 2107.

Baldock, C., Rafferty, J.B., Sedelnikova, S.E., Bithell, S., Stuitje, A.R., Slabas, A.R., and Rice, D.W. (1996b) Crystallization of *Escherichia coli* enoyl reductase and its complex with diazaborine. Acta Crystallog. Sect. D, 52: 1181.

Bartley, G.E., and Scolnik, P.A. (1995) Plant carotenoids: Pigments for photoprotection, visual attraction, and human health. Plant Cell 7: 1027.

Battey, J.F., and Ohlrogge, J.B. (1990) Evolutionary and tissue-specific control of expression of multiple acyl-carrier-protein isoforms in plants and bacteria. Planta 180: 352.

Beetham, P.R., Kipp, P.B., Sawycky, X.L., Arntzen, C.J., and May, G.D. (1999) A tool for functional plant genomics: Chimeric RNA/DNA oligonucleotides cause *in vivo* gene-specific mutations. Proc. Natl. Acad. Sci. 96: 8774.

Bertrams, M., and Heinz, E. (1981) Positional specificity and fatty acid selectivity of purified *sn*-glycerol-3-phosphate acyltransferase from chloroplasts. Plant Physiol. 68: 653.

Bertrand, E., Pictet, R., and Grange, T. (1994) Can hammerhead ribozymes be efficient tools to inactivate gene function? NAR. 22: 293.

Bhat, B.G., Wang, P., Kim, J., Black, T.M., Lewin, T.M., Fiedorek, F. Jr., and Coleman, R.A. (1999) Rat *sn*-glycerol-3-phosphate acyltransferase: molecular cloning and characterization of the cDNA and expressed protein. Biochim. et Biophys. Acta 1439: 415.

Bhella, R.S., and MacKenzie, S.L. (1994) Nucleotide sequence of a cDNA from *Carthamus tinctorius* encoding a glycerol-3-phosphate acyltransferase. Plant Physiol. 106: 1713.

Bielinska, A., Shivdasani, R.A., Zhang, L., and Nabel, G.J. (1990) Regulation of gene expression with double-stranded phosphorothioate oligonucleotides. Science 250: 997.

Birikh, K.R., Heaton, P.A., and Eckstein, F. (1997) The structure, function and application of the hammerhead ribozyme. Eur. J. Biochem. 245: 1.

Bligny, R., and Douce, R. (1980) A precise localisation of cardiolipin in plant cells. Biochim. Biophys. Acta 617: 254.

Bloch, K., and Vance, D. (1977) Control mechanisms in the synthesis of saturated fatty acids. Annu. Rev. Biochem. 46; 236.

Bock, L.C., Griffin, L.C., Latham, J.A., Vermaas, E.H., and Toole, J.J. (1992) Selection of single-stranded DNA molecules that bind and inhibit human thrombin. Nature 255: 564.

Boehler, B.A., and Ernst-Fonberg, M.L. (1976) *sn*-Glycerol-3-phosphate transacylase activity in *Euglena gracilis* organelles. Arch. Biochem. Biophys. 175: 229.

Borovkov, A.Y., McClean, P.E., Sowokinos, J., Rund, S.H., and Secor, G.A. (1996) Effect of expression of UDP-glucose pyrophosphorylase ribozyme and antisense RNAs on the enzyme activity and carbohydrate composition of field-grown transgenic potato plants. J. Plant Physiol. 147: 644.

Bourgis, F., Kader, J.-C., Barret, P., Renard, M., Robinson, D., Robinson, C., Delseny, M., and Roscoe, T.J. (1999) A plastidial lysophosphatidic acid acyltransferase from oilseed rape. Plant Physiol. 20: 913.

Bradford, M.M. (1976) A rapid and sensitive method for the quantitation of microgram quantities of protein utilising the principle of protein-dye binding. Anal. Biochem. 72: 248.

Branlant, C., Krol, A., Ebel, J.P., Gallinaro, H., Lazar, E., and Jacob, M. (1981) The conformation of chicken, rat and human U1A RNAs in solution. NAR. 9: 841.

Bratty, J., Chartrand, P., Ferbeyre, G., and Cedergren, R. (1993) The hammerhead RNA domain, a model ribozyme. Biochim. et Biophys. Acta 1216: 345.

Briggs, P.B., and Koziel, M. (1998) Engineering new plant strains for commercial markets. Curr. Op. In Biotechn. 9: 233.

Brough, C.L., Coventry, J.M., Christie, W.W., Kroon, J.T.M., Brown, A.P., Barsby, T.L., and Slabas, A.R. (1996) Towards the genetic engineering of triacylglycerols of defined fatty acid composition: major changes in erucic acid content at the *sn*-2 position affected by the introduction of a 1-acyl-*sn*-glycerol-3-phosphate acyltransferase from *Limnanthes douglasii* into oilseed rape. Mol. Breed. 2: 133.

Broun, P., and Somerville, C. (1997) Accumulation of ricinoleic, lesquerolic and densipolic acids in seeds of transgenic *Arabidopsis* plants that express a fatty acyl hydroxylase cDNA from castor bean. Plant Physiol. 113: 933.

Broun, P., Shanklin, J., Whittle, E., and Somerville, C. (1998) Catalytic plasticity of fatty acid modification enzymes underlying chemical diversity of plant lipids. Science 282: 1315.

Broun, P., Boddiyalli, S., and Somerville, C. (1998) A bifunctional oleate 12-hydroxylase:desaturase from *Lesquerella fendleri*. Plant J. 13: 201.

Broun, P., Gettner, S., and Somerville, C. (1999) Genetic engineering of plant lipids. Annu. Rev. Nutr. 19: 197.

Brown, A.P., Brough, C.L., Kroon, J.T.M., and Slabas, A.R. (1995) Identification of a cDNA that encodes 1-acyl-*sn*-glycerol-3-phosphate acyltransferase from *Limnanthes douglasii*. Plant Mol. Biol. 29: 267.

Brown, A.P., Johnson, P., Rawsthorne, S., and Hills, M.J. (1998) Expression and properties of acyl-CoA binding protein from *Brassica napus*. Plant Physiol. Biochem. 36: 629.

Browse, J., McCourt, P.J., and Somerville, C. (1985) A mutant of *Arabidopsis* lacking a chloroplast-specific lipid. Science 227: 763.

Browse, J.A., McCourt, P.J., and Somerville, C. (1986) A mutant of *Arabidopsis* deficient in C 18:3 and C 16:3 leaf lipids. Plant physiol. 81: 859.

Browse, J., Kunst, L., Anderson, S., Hugly, S., and Somerville, C. (1989) A mutant of *Arabidopsis* deficient in the chloroplast 16:1/18:1 desaturase. Plant Physiol. 90: 522.

Browse, J., McConn, M., James, D., and Miquel, M. (1993) Mutants of *Arabidopsis* deficient in the synthesis of α-linolenate. Biochemical and genetic characterization of the endoplasmic reticulum linoleoyl desaturase. J. Biol. Chem. 268: 16345.

Browse, J., and Somerville, C.R. (1994) Glycerolipids. In *Arabidopsis*, ed. E.M. Meyerowitz, C.R. Somerville: Plainview, NY: Cold Spring Harbor, 881-912.

Bucher, P. (1999) Regulatory elements and expression profiles. Curr. Opin. Struct. Biol. 9: 400.

Burke, J.M. (1997) Clearing the way for ribozymes. Nat. Biotechnol. 15: 414.

Buzayan, J.M., Gerlach, W.L., and Brüning, G. (1986) Nonenzymatic cleavage and ligation of RNAs complementary to a plant-virus satellite RNA. Nature 323 (6086): 349.

Cahoon, E.B., Shanklin, J., and Ohlrogge, J. (1992) Expression of a coriander desaturase results in petroselenic acid production in transgenic tobacco. Proc. Natl. Acad. Sci. USA 89: 11184.

Cahoon, E.B., and Ohlrogge, J.B. (1993) Δ^4-hexadecenoyl-acyl carrier protein is the likely precursor of petroselenic acid in *Umbelliferae* endosperm. Plant lipid symposium held in Minneapolis; Minnesota, July: 29-31.

Cahoon, E.B., Cranmer, A.M., Shanklin, J., and Ohlrogge, J. (1994) Δ^6 Hexadecenoic acid is synthesizes by the activity of a soluble Δ^6-palmitoyl-acyl carrier protein desaturase in *Thunbergia alata* endosperm. J. Biol. Chem. 269: 27519.

Cahoon, E.B., Coughlan, S., and Shanklin, J. (1997) Characterization of a structurally and functionally diverged acyl-acyl carrier protein desaturase from milkweed seed. Plant Mol. Biol. 33: 1105.

Cahoon, E.B., Lindqvist, Y., Schneider, G., and Shanklin, J. (1997) Redesign of soluble fatty acid desaturases from plants for altered substrate specificity and double bond position. Proc. Natl. Acad. Sci. USA 94: 4872.

Cahoon, E.B., Shah, S., Shanklin, J., and Browse, J. (1998) A determinant of substrate specificity predicted from the acyl-acyl carrier protein desaturase of developing cat's claw seed. Plant Physiol. 117: 593.

Cech, T.R. (1990) Self-splicing of group I introns. Annu. Rev. Biochem. 59: 543.

Chalifour, L.E., Fahmy, R., Holder, E.L., Hutchinson, E.W., Osterland, C.K., Schipper, H.M., and Wang, E. (1994) A method for analysis of gene expression patterns. Anal. Biochem. 216: 299.

Chen, H., Ferbeyre, G., and Cedergren, R. (1997) Efficient hammerhead ribozyme and antisense RNA targeting in a slow ribosome *Escherichia coli* mutant. Nature Biotechnol. 15: 432.

Chye, M.-L. (1998) *Arabidopsis* cDNA encoding a membrane-associated protein with an acyl-CoA binding domain. Plant Mol. Biol. 38: 827.

Chye, M.-L., Huang, B.-Q., and Zee, S.Y. (1999) Isolation of a gene encoding *Arabidopsis* membrane-associated acyl-CoA binding protein and immunolocalization of its gene product. Plant J. 18: 205.

Clewley, J.P. (1995) MacIntosh sequence-analysis software. Mol. Biotechn. 3: 221.

Cole-Strauss, A., Yoon, K., Xiang, Y., Byrne, B.C., Rice, M.C., Cryn, J., and Kmiec, E.B. (1996) Correction of the mutation responsible for sickle cell anemia by an RNA/DNA oligonucleotide. Science 273: 1386.

Cotton, M., and Birnstiel, M.L. (1989) Ribozyme mediated destruction of RNA *in vivo*. EMBO J. 8: 3861.

Cotten, M. (1990) The *in vivo* application of ribozymes. Trends Biotechnol. 8: 174.

Crisell, P., Thompson, S., and James, W. (1993) Inhibition of HIV-1 replication by ribozymes that show poor activity *in vitro*. NAR. 21: 5251.

Cronan, J.E., Jr., and Roughan, P.G. (1987) Fatty acid specificity and selectivity of the chloroplast *sn*-glycerol-3-phosphate acyltransferase of the chilling sensitive plant *Amaranthus lividus*. Plant Physiol. 83: 676.

Davies, H.M. (1993) Medium chain acyl-ACP hydrolysis activities of developing oilseeds. Phytochemistry 33:1353.

De Boer, G.-J., Fawcett, T., Slabas, A., Nijkamp, J., and Stuitje, A. (1996) Analysis of the *Arabidopsis* enoyl-ACP reductase promoter in transgenic tobacco. Presented at Int. Symp. Plant Lipids, 12th, Toronto.

De Silva, J., Robinson, S.J., and Safford, R. (1992) The isolation and functional characterisation of a *B. napus* acyl carrier protein-5' flanking region involved in the regulation of seed strorage lipid synthesis. Plant Mol. Biol. 18: 1163.

Devereux, J., Haeberli, P., and Smithies, O. (1984) A comprehensive set of sequence-analysis programs for the VAX. NAR. 12: 387.

Ding, D., and Lipshitz, H.D. (1993) Localized RNAs and their functions. BioEssays 15: 651.

Dörmann, P., Spener, F., and Ohlrogge, J.B. (1993) Characterization of two acyl-ACP thioesterases from developing *Cuphea* seeds specific for medium chain acyl-ACP and oleoyl-ACP. Planta 189: 425.

Dörmann, P., Voelker, T.A, and Ohlrogge, J.B. (1995) Cloning and expression in *Escherichia coli* of a novel thioesterase from *Arabidopsis thaliana* specific for long chain acyl-acyl carrier proteins. Arch. Biochem. Biophys. 316: 612.

Douady, D., and Dubacq, J.-P. (1987) Purification of acyl-CoA: glycerol-3-phosphate acyltransferase from pea leaves. Biochim. Biophys. Acta 921: 615.

Douady, D., Passaquet, C., and Dubacq, J.-P. (1990) Immunochemical characterisation and *in vitro* synthesis of glycerol-3-phosphate acyltransferase from pea. Plant Sci. 66: 65.

Dougherty, W.G., and Parks, T.D. (1995) Transgenes and gene suppression: telling us something new? Curr. Opin. Cell Biol. 7: 399.

Draper, J., Scott, R., Armitage, P., and Walden, R., Eds. (1988) Plant genetic transformation and gene expression. Blackwell Scientific Publications: 58. ISBN 0-632-02172-1

Eccleston, V.S., and Ohlrogge, J.B. (1998) Expression of lauroyl-acyl carrier protein thioesterase in *Brassica napus* seeds induces pathways for both fatty acid oxidation and biosynthesis and implies a set point for triacylglycerol accumulation. Plant Cell 10: 613.

Ellington, A.D., and Szostak, J.W. (1990) *In vitro* selection of RNA molecules that bind specific ligands. Nature 346: 818.

Ellman, G.L. (1959) Tissue sulfhydryl groups. Arch. Biochem. Biophys. 82: 7077.

Fedor, M.J., and Uhlenbeck, O.C. (1990) Substrate sequence effects on "hammerhead" RNA catalytic efficiency. Proc. Natl. Acad. Sci. USA. 87: 1668.

Feldmann, K.A., Marks, M.D., Christianson, M.L., and Quatrano, R.S. (1989) A dwarf mutant of *Arabidopsis* generated by T-DNA insertion mutagenesis. Science 243: 1351.

Ferbeyre, G., Smith, J.M., and Cedergren, R. (1998) Schistosome satellite DNA encodes active hammerhead ribozymes. Mol. Cell. Biol. 18: 3880.

Ferré-D' Amaré, A.R., and Doudna, A. (1999) RNA folds: Insights from recent crystal structures. Annu. Rev. Biophys. Biomol. Struct. 28: 57.

Ferri, S.R., and Toguri, T. (1997) Substrate specificity modification of the stromal glycerol-3-phosphate acyltransferase. Arch. Biochem. Biophys. 337: 202.

Finnegan, J., and McElroy, D. (1994) Transgene inactivation: plants fight back! BioTechnology 12: 883.

Fitch Haumann, B. (1997) Bioengineered oilseed acreage escalating. Inform 8: 804.

Frentzen, M., Heinz, E., McKeon, T.A., and Stumpf, P.K. (1983) Specificities and selectivities of glycerol-3-phosphate acyltransferase and monoacylglycerol-3-phosphate acyltransferase from pea and spinach. Eur. J. Biochem. 129: 629.

Frentzen, M. (1986) Biosynthesis and desaturation of the different diacylglycerol moieties in higher plants. J. Plant Physiol. 124: 193.

Frentzen, M., Nishida, I., and Murata, N. (1987) Properties of the plastidial acyl-(acyl-carrier-protein): glycerol-3-phosphate acyltransferase from the chilling sensitive plant squash (*Cucurbita moschata*). Plant Cell Physiol. 28: 1195.

Frentzen, M. (1990a) Comparison of certain properties of membrane bound and solubilised acyltransferase activities in plant microsomes. Plant Sci. 69: 39.

Frentzen, M., Neuburger, M., Joyard, J., and Douce, R. (1990b) Intraorganelle localisation and substrate specificities of the mitochondrial acyl-CoA: *sn*-glycerol-3-phosphate O-acyltransferase and acyl-CoA: 1-acyl-*sn*-glycerol-3-phosphate O-acyltransferase from potato tubers and pea leaves. Eur. J. Biochem. 187: 395.

Frentzen, M. (1993) Acyltransferases and triacylglycerols. In Lipid Metabolism in Plants, T.S. Moor, Jr., ed(Boca Raton, FL: CRC Press): 195-231.

Frentzen, M., Peterek, G., and Wolter, F.P. (1994) Properties and subcellular-localisation of a plastidial *sn*-glycerol-3-phosphate acyltransferase of *Pisum sativum* L. expressed in *Escherichia coli*. Plant Sci. 96:45.

Fritz, M., Heinz, E., and Wolter, F.P. (1995) Cloning and sequencing of a full length cDNA coding for a *sn*- glycerol-3-phosphate acyltransferase from *Phaseolus vulgaris*. Plant Physiol. 107: 1039.

Fu, D.-J., Tang, K., Braun, A., Reuter, D., Darnhofer-Demar, B., Little, D.P., O'Donnel, M.J., Cantor, C.R., and Köster, H. (1998) Sequencing exons 5 to 8 of the *p53* gene by MALDI-TOF mass spectrometry. Nature Biotechn. 16: 381.

Fukuchi-Mizutani, M., Tasaka, Y., Tanaka, Y., Ashikari, T., Kusumi, T., and Murata, N. (1998) Characterization of delta-9 acyl-lipid desaturase homologues from *Arabidopsis thaliana*. Plant Cell. Physiol. 39: 247.

Fulda, M., Heinz, E., and Wolter, F.P. (1997) *Brassica napus* cDNAs encoding fatty acyl-CoA synthetase. Plant Mol. Biol. 33: 911.

Gallie, D.R. (1998) Controlling gene expression in transgenics. Curr. opin. Plant Biol. 1: 166.

Gibson, S., Falcone, D.L., Browse, J., and Somerville, C. (1994) Use of transgenic plants and mutants to study the regulation and function of lipid composition. Plant, Cell and Environm. 17: 627.

Gounaris, K., Barber, J., and Harwood, J.L. (1986) The thylakoid membranes of higher plant chloroplasts. Biochem. J. 237: 313.

Grant, S.R. (1999) Dissecting the mechanisms of posttranscriptional gene silencing: divide and conquer. Cell 96: 303.

Gübler, U. and Hoffman, B.J. (1983) A simple and very efficient method for generating cDNA libraries. Gene 30: 195.

Gunstone, F.D., and Herslöf, B.G. (1992) A Lipid Glossary, The oily press ltd., Scotland (ISBN 0 9514171-2-6).

Gunstone, F.D., Harwood, J.L., and Padley, F.B. (1994) The lipid Handbook. Chapman and Hall, London.

Gutiérrez, R.A., Gustavo, M.C., and Green, P.J. (1999) Current perspectives on mRNA stability in plants: multiple levels and mechanisms of control. Trends Plant Sci. 4: 429.

Ha, J., and Kim, K.-H. (1994) Inhibition of fatty acid synthesis by expression of an acetyl-CoA carboxylase-specific ribozyme gene. Proc. Natl. Acad. Sci. USA., 91: 9951.

Hamilton, A.J., and Baulcombe, D.C. (1999) A species of small antisense RNA in posttranscriptional gene silencing in plants. Science 286: 950.

Hanke, C., Wolter, F.P., Coleman, J., Peterek, G., and Frentzen, M. (1995) A plant acyltransferase involved in triacylglycerol biosynthesis complements an *Escherichia coli* *sn*-1-acylglycerol-3-phosphate mutant. Eur. J. Biochem. 232: 806.

Harwood, J.L. (1980) Plant acyl lipids: Structure, distribution and analysis. In: Stumpf, P.K. (ed) The Biochemistry of plants, Academic Press, New York; 2-56.

Harwood, J.L. (1988) Fatty acid metabolism. Ann. Rev. Plant Physiol. Plant mol. Biol. 39: 101.

Harwood, J. (1996) Recent advances in the biosynthesis of plant fatty-acids. Biochim. Biophys. Acta 301: 7.

Haseloff, J., and Gerlach, W.L. (1988) Simple RNA enzymes with new and highly specific endoribonuclease activities. Nature 334: 585.

Hawkins, D.J., and Kridl, J.C. (1998) Characterization of acyl-ACP thioesterases of mangosteen (*Garcinia manostana*) seed and high levels of stearate production in transgenic canola. Plant J. 13: 743.

Heath, R.J., and Rock, C.O. (1998) A conserved histidine is essential for glycerolipid acyltransferase catalysis. J. Bact.:1425.

Hélène, C., and Toulmé, J.J. (1990) Specific regulation of gene expression by antisense, sense and antigene nucleic acids. Biochim. Biophys. Acta 1049: 99.

Hendry, P., McCall, M.J., Santiago, F.S., and Jennings, P.A. (1995) *In vitro* activity of minimised hammerhead ribozymes. NAR. 23: 3922.

Herbers, K., and Sonnewald, U. (1996) Manipulating metabolic partitioning in plants. Trends Biotech. 14: 198.

Herman, E.M. (1994) Cell and molecular biology of seed oil bodies. In Seed Development and Germination, H. Kigel and G. Galili, eds(New York: Marcel Dekker): 195-214.

Herschlag, D. (1991) Implications of ribozyme kinetics for targeting the cleavage of specific RNA molecules *in vivo*: More isn't always better. Proc. Natl. Acad. Sci. USA. 88: 6921.

Hertel, K.J., Pardi, A., Uhlenbeck, O.C., Koizumi, M., Ohtsuka, E., Uesugi, S., Cedergen, R., Eckstein, F., Gerlach, W.L., Hodgson, R., and Symons, R.H. (1992) Numbering system for the hammerhead. NAR. 20: 3252.

Hertel, K.J., Herschlag, D., and Uhlenbeck, O.C. (1994) A kinetic and thermodynamic framework for the hammerhead ribozyme reaction. Biochemistry 33: 3374.

Higgins, D.G., and Sharp, P.M. (1989) Fast and sensitive multiple sequence alignments on a microcomputer. Comput. Appl. Biosci. 5: 151.

Hobs, D.H., Lu, C., and Hills, M.J. (1999) Cloning of a cDNA encoding diacylglycerol acyltransferase from Arabidopsis thaliana and its functional expression. FEBS Lett. 452: 145.

Holtorf, H., Schöb, H., Kunz, C., Waldvogel, R., and Meins Jr., F. (1999) Stochastic and nonstochastic post-transcriptional silencing of chitinase and β-1,3-glucanase genes involves increased RNA turnover – Possible role for ribosome-independent RNA degradation. Plant Cell 11: 471.

Homann, M., Tzortzakaki, S., Rittner, K., Sczakiel, G., and Tabler, M. (1993) Incorporation of the catalytic domain of a hammerhead ribozyme into antisense RNA enhances its inhibitory effect on the replication of human immunodeficiency virus type I. NAR. 21: 2809.

Hormes, R., Homann, M., Oelze, I., Marschall, P., Tabler, M., Eckstein, F., and Sczakiel, G. (1997) The subcellular localization and length of hammerhead ribozymes determine efficacy in human cells. NAR. 25: 769.

Huang, A.H.C. (1992) Oil bodies and oleosins in seeds. Annu. Rev. Plant Physiol. Plant Mol. Biol. 43: 177.

Hugly, S., Kunst, L., Browse, J., and Somerville, C.R. (1989) Enhanced thermal tolerance and altered chloroplast ultrastructure in a mutant of *Arabidopsis* deficient in lipid desaturation. Plant Physiol. 90: 1134.

Hugly, S., and Somerville, C. (1992) A role for membrane lipid polyunsaturation in chloroplast biogenesis at low temperature. Plant Physiol. 99: 197.

Huillier, P.J.L., Davis, S.R., and Bellamy, A.R. (1992) Cytoplasmic delivery of ribozymes leads to efficient reduction in α-lactalbumin mRNA levels in C1271 mouse cells. EMBO J. 11: 4411.

Ichihara, K., Asahi, T., and Fujii, S. (1987) 1-Acyl-*sn*-glycerol-3-phosphate acyltransferase in maturing safflower seeds and its contribution to the non-random fatty acid distribution of triacylglycerol. Eur. J. Biochem. 167: 339.

Ichihara, K., Takahashi, T., and Fujii, S. (1988) Diacylglycerol acyltransferase in maturing safflower seeds: its influence on the fatty acid composition of the triacyl and on the rate of triacylglycerol synthesis. Biochim. Biophys. Acta 958: 125.

Inouye, M., Arnheim, ., and Sternglanz, R. (1973) J. Biol. Chem. 248: 7247.

Ishizaki, O., Nishida, I., Agata, K., Eguchi, G., and Murata, N. (1988) Cloning and nucleotide sequence of cDNA for the plastid glycerol-3-phosphate acyltransferase from squash. FEBS Lett. 238: 424.

Ishizaki-Nishizawa, O., Azuma, M., Ohtani, T., Murata, N., and Toguri, T. (1995) Nucleotide sequence of cDNA from *Spinacia oleracea* encoding plastid glycerol-3-phosphate acyltransferase. Plant Physiol. 108: 1342.

James, Jr., D.W., and Dooner, H.K. (1990) Isolation of EMS-induced mutants in *Arabidopsis* altered in seed fatty acid composition. Theor. Appl. Genet. 80: 241.

Jaworski, J.G., Post-Beittenmiller, D, and Ohlrogge, J.B. (1993) Acetyl- acyl carrier protein is not a major intermediate in fatty acid biosynthesis in spinach. Eur. J. Biochem. 213: 981.

Johnson, T.C., Schneider, J.C., and Somerville, C. (1992) Nucleotide sequence of acyl-acyl carrier protein: glycerol-3-phosphate acyltransferase from cucumber. Plant Physiol. 99: 771.

Jones, A, Davies, H.M., and Voelker, T.A. (1995) Palmitoyl-acyl carrier protein (ACP) thioesterase and evolutionary origin of plant acyl-ACP thioesterases. Plant Cell 7: 359.

Jorgenson, R.A. (1995) Cosuppression, flower color patterns, and metastable gene expression states. Science 268: 686.

Jorgenson, R.A., Cluster, P.D., English, J., Que, Q., and Napoli, C.A. (1996) Chalcone synthase cosuppression phenotypes in petunia flowers: comparison of sense vs antisense constructs and single-copy vs. complex T-DNA sequences. Plant Mol. Biol. 31: 957.

Joshi, C.P. (1987) An inspection of the domain between putative TATA box and translation start site in 79 plant genes. NAR. 15: 6643.

Joyard, D., and Douce, R. (1977) Site of synthesis of phosphatidic acid and diacylglycerol in spinach chloroplasts. Biochim. Biophys. Acta 486: 273.

Joyard, J., and Douce, R. (1987) Galactolipid synthesis. In The Biochemistry of Plants. Vol. 9. Stumpf, P.K., and Conn, E.E., Eds., Academic Press, Orlando, FL: 215.

Joyard, J., Block, M.A., Malherbe, A., Marachal, E., and Douce, R. (1993) Origin and synthesis of galactolipid and sulfolipid headgroups. In Lipid metabolism in Plants, T.S. Moore, Jr., ed(boca Raton, FL:CRC Press): 231-258.

Katavic, V., Reed, D.N., Taylor, D.C., Giblin, E.M., Barton, D.L., Zou, J.-T., McKenzie, S.L., Covello, P.S., and Kunst, L. (1995) Alteration of fatty acid composition by an EMS-induced mutation in *Arabidopsis thaliana* affecting diacylglycerol acyltransferase activity. Plant Physiol. 109: 999.

Kater, M.M. (1994) Structure, function and expression of plant and bacterial enoyl-ACP reductase genes. Ph.D thesis, Free University Amsterdam. The Netherlands.

Kennedy, E. (1961) Biosynthesis of complex lipids. Fed. Proc. 20: 934.

Kerr, R.A. (1998) The next oil crisis looms large-and perhaps close. Science 281: 1128.

Kinney, A.J. (1994) Genetic modification of the storage lipids of plants. Curr. Opin. Biotech. 5: 144.

Kinney, A.J. (1997) Genetic engineering of oilseeds for desired traits. In Genetic Engineering. Ed. By Setlow, J.K. New York: Plenum Press 19: 149-166.

Kinney, A.J., and Knowlton, S. (1997) Designer oils: the high oleic acid soybean. In Genetic Engineering for the food industry. Ed. By Harlander, S., Roller, s. London: Blackie Academic: 193-213.

Kinney, A.J. (1998) Manipulating flux through metabolic pathways. Curr. Opin. In Plant Biol. 1: 173.

Knutzon, D.S., Thompson, G.A., Radke, S.E., Johnson, W.B., and Knauf, V.C. *et al.* (1992) Modification of *Brassica* seed oil by antisense expression of a stearoyl-acyl carrier protein desaturase gene. Proc. Natl. Acad. Sci. USA 89: 2624.

Kroon, J., Souer, E., De Graaff, A., Xue, Y., Mol, J., and Koes, R. (1994) Cloning and structural analysis of the anthocyanin pigmentation locus *Rt* of *Petunia hybrida*: characterization of insertion sequences in two mutant alleles. The Plant J. 5: 69.

Kunst, L., Browse, J., and Somerville, C. (1988) Altered regulation of lipid biosynthesis in a mutant of *Arabidopsis* deficient in chloroplast glycerol-3-phosphate acyltransferase activity. Proc. Natl. Acad. Sci. USA 85: 4143.

Kunst, L., Browse, J., and Somerville, C. (1989a) A mutant of *Arabidopsis* deficient in desaturation of palmitic acid in leaf lipids. Plant Physiol. 90: 943.

Kunst, L., Browse, J., and Somerville, C. (1989b) Altered chloroplast structure and function in a mutant of *Arabidopsis* deficient in plastid glycerol-3-phosphate acyltransferase activity. Plant Physiol. 90: 846.

Lacey, D.J., and Hills, M.J. (1996) Heterogeneity of the endoplasmic reticulum with respect to lipid synthesis in developing seeds of *Brassica napus* L. Planta 199: 545.

Lacey, D.J., Beaudoin, F., Dempsey, C.E., Shewry, P.R., and Napier, J.A. (1999) The accumulation of triacylglycerols within the endoplasmic reticulum of developing seeds of *Helianthus annuus*. Plant J. 7: 397.

Laemmli, U.K. (1970) Cleavage of structural proteins during the assembly of the head bacteriophage T4. Nature 227: 680.

Lamb, J.W., and Hay, R.T. (1990) Ribozymes that cleave potato leafroll virus RNA within the coat protein and polymerase genes. J. Gen. Virol. 71: 2257.

Larsson, S., Hotchkiss, G., Andäng, M., Nyholm, T., Inzunza, J., Jansson, I., and Ährlund-Richter, L. (1994) Reduced β2-microglobulin mRNA levels in transgenic mice expressing a designed hammerhead ribozyme. NAR. 22: 2242.

Lassner, M., Levering, C.K., Davies, M., and Knutzon, D.S. (1995) Lysophosphatidic acid acyltransferase from meadowfoam mediates insertion of erucic acid at the *sn*-2 position of triacylglycerol in transgenic rapeseed oil. Plant Physiol. 109, 1389.

Lee, M., Lenman, M., Banas, A., Bafor, M., Singh, S., Schweizer, M., Nilsson, R., Liljenber, C., Dahlqvist, A., Gummeson, P.O. *et al.* (1998) Identification of non-heme diiron proteins that catalyze triple bond and epoxy group formation. Science 280: 915.

Leonard, J.M., Knapp, S.J., and Slabaugh, M.B. (1998) A *Cuphea* β-ketoacyl-ACP synthase shifts the synthesis of fatty acids towards shorter chains in *Arabidopsis* seeds expressing *Cuphea Fat* B thioesterases. Plant J. 13: 621.

Lewin, T.M., Wang, P., and Coleman, R.A. (1999) Analysis of amino acid motifs diagnostic for the *sn*-glycerol-3-phosphate acyltransferase reaction. Biochem. 38: 5764.

Lightner, V.A., Bell, R.M., and Modrich, P. (1983) The DNA sequences encoding *plsB* and *dgk* loci of *Escherichia coli*. J. Biol. Chem. 255: 9413.

Lightner, J., Wu, J., and Browse, J. (1994a) A mutant of *Arabidopsis* with increased levels of stearic acid. Plant Physiol. 106: 1443.

Lightner, J., James,Jr., D.W., Dooner, H.K., and Browse, J. (1994b) Altered body morphology is caused by increased stearate levels in a mutant of *Arabidopsis*. Plant J. 6: 401.

Lindqvist, Y., Huang, W., Schneider, G., and Shanklin, J. (1996) Crystal structure of Δ^9 stearoyl-acyl carrier protein desaturase from castor seeds and its relationship to other di-iron proteins. EMBO J. 15: 4081.

Lisziewicz, J., Sun, D., Smythe, J., Lusso, P., Lori, F., Louie, A., Markham, P., Rossi, J.J., Reitz, M., and Gallo, R.C. (1993) Inhibition of human immunodeficiency virus type 1 replication by regulated expression of a polymeric *Tat* activation response RNA decoy as a strategy for gene therapy in AIDS. Proc. Natl. Acad. Sci. USA. 90: 8000.

Lockhart, D.J., Dong, H., Byrne, M.C., Follettie, M.T., Gallo, M.V., Chee, M.S., Mittmann, M., Wang, C., Kobayashi, M., Horton, H., and Brown, W.E. (1996) Expression monitoring by hybridization to high-density oligonucleotide arrays. Nat. Biotechnol. 14: 1675.

Los, D.A., and Murata, N. (1998) Structure and expression of fatty acid desaturases. Biochim. et Biophys. Acta : 3.

Lott, W.B., Pontius, B.W., and Von Hippel, P.H. (1998) A two-metal ion mechanism operates in the hammerhead ribozyme-mediated cleavage of an RNA substrate. Proc. Natl. Acad. Sci. USA. 95: 542.

Luzi, E., Eckstein, F., and Barsacchi, G. (1997) The newt ribozyme is part of a riboprotein complex. Proc. Natl. Acad. Sci. USA. 94: 9711.

Majerus, P.W., Alberts, A.W., and Vagelos, P.R. (1969) Acyl carrier protein from *Escherichia coli*. Meth. Enz. 14: 43.

Magnuson, K., Jackowski, S., Rock, C.O., and Cronan., Jr., J.E. (1993) Regulation of fatty acid biosynthesis in Escherichia coli. FEBS Lett. 299: 262.

Mancha, M., and Stymne, S. (1997) Remodelling of triacylglycerols in microsomal preparations from developing castor bean (*Ricinus communis* L.) endosperm. Planta 203: 51.

Manning, K. (1991) Isolation of nucleic acids from plants by differential solvent precipitation. Anal. Biochem. 195: 45.

Marck, C. (1988) DNA Strider – A C-program for the fast analysis of DNA and protein sequences on the Apple Macintosh family of computers. NAR. 16: 1829.

Marglin, A., and Merrifield, R.B. (1970) Chemical synthesis of peptides and proteins. Ann. Rev. Biochem 39: 841.

Marschall, P., Thomson, J.B., and Eckstein, F. (1994) Inhibition of gene expression with ribozymes. Cellul. and Mol. Neurobiol. 14: 523.

Martin, T.F.J. (1998) Phosphoinositide lipids as signalling molecules: Common themes for signal transduction, cytoskeletal regulation, and membrane trafficking. Annu. Rev. Cell Dev. Biol. 14: 231.

Matzke, A.J.M., Neuhuber, F., Park, Y.-D., Ambros, P., and Matzke, M.A. (1994) Homology-dependent gene silencing in transgenic plants: epistatic silencing loci contain multiple copies of methylated transgenes. Mol. Gen. Genet. 244: 219.

Matzke, M.A., and Matzke, A.J.M. (1995a) Homology-dependent gene silencing in transgenic plants-what does it really tell us? Trends Genet. 11: 1.

Matzke, M.A., and Matzke, A.J.M. (1995b) How and why do plants inactivate homologous (trans) genes? Plant. Physiol. 107: 679.

Matzke, M.A., and Matzke, A.J.M. (Eds.) (2000) Special Issue: Plant Gene Silencing. Plant Mol. Biol. 43.

McConn, M., Hughly, S., Somerville, C., and Browse, J. (1994) A mutation at the *fad8* locus of *Arabidopsis* identifies a second chloroplast ω-3 desaturase. Plant Physiol. 106: 1609.

McCourt, P.J., Kunst, L., Browse, J., and Somerville, C.R. (1987) The effects of reduced amounts of lipid unsaturation on chloroplast ultra-structure and photosynthesis in a mutant of *Arabidopsis*. Plant Physiol. 84: 353.

McGarvey, D.J., and Croteau, R. (1995) Terpenoid metabolism. Plant Cell 7: 1015.

McIntyre, C.L., Bettenay, H.M., and Manners, J.M. (1996) Strategies for the suppression of peroxidase gene expression in tobacco. II. *In vivo* suppression of peroxidase activity in transgenic tobacco using ribozyme and antisense constructs. Transgen. Res. 5: 263.

McKeon, T.A., and Stumpf, P.K. (1982) Purification and characterisation of the stearoyl-acyl carrier protein thioesterase from maturing seeds of safflower. J. Biol. Chem. 257: 12141.

Merlo, A.O., Cowen, N., Delate, T., Edington, B., Folkerts, O., Hopkins, N., Lemeiux, C., Skokut, T., Smith, K., Woosley, A., Yang, Y., Young, S., and Zwick, S. (1998) Ribozymes targeted to stearoyl-ACP Δ9 desaturase mRNA produce heritable increases of stearic acid in transgenic maize leaves. Plant Cell 10: 1603.

Metzlaff, M., O'Dell, M., Cluster, P.D., and Flavell, R.B. (1997) RNA-mediated RNA degradation and chalcone synthase A silencing in *Petunia*. Cell 88: 845.

Meyer, P. (1995a) In: Meyer, P. (ed), Gene silencing in higher plants and related phenomena in other eukaryotes. Springer-Verlag, Berlin.

Meyer, P. (1995b) Understanding and controlling transgene expression. Trends Biotechn. 13: 332.

Meyer, P., and Saedler, H. (1996) Homology-dependent gene silencing in plants. Annu. Rev. Plant Physiol. Plant Mol. Biol. 47: 23.

Meyer, P. (2000) Transcriptional transgene silencing and chromatin components. Plant Mol. biol. 43:221.

Millar, A.A., and Kunst, L. (1997) Very-long-chain fatty acid biosynthesis is controlled through the expression and specificity of the condensing enzyme. Plant J. 12: 121.

Miquel, M., and Browse, J. (1992) *Arabidopsis* mutants deficient in polyunsaturated fatty acid synthesis. Biochemical and genetic characterization of a plant oleoyl-phosphatidylcholine desaturase. J. Biol. Chem. 267: 1502.

Miquel, M., James, D., Dooner, H., and Browse, J. (1993) *Arabidopsis* requires polyunsaturated lipids for low temperature survival. Proc. Natl. Acad. Sci. USA 90; 6208.

Mol, J., Van der Krol, A., Van Tunen, A., Van Blokland, R., De Lange, P., and Stuitje, A. (1990) Regulation of plant gene expression by antisense RNA. FEBS Lett. 268: 427.

Mongrand, S., Bessoule, J.-J., Cabantous, F., and Cassagne, C. (1998) The C16:3/C18:3 fatty acid balance in photosynthetic tissues from 468 plant species. Phytochemistry 49: 1049.

Montgomery, R.A., and Dietz, H.C. (1997) Inhibition of fibrillin 1 expression using U1 snRNA as a vehicle for the presentation of antisense targeting sequence. Hum. Mol. Genet. 6: 519.

Moore, T.S., Jr. (1993) Lipid metabolism in plants. Boca raton, FL: CRC Press)

Morand, L.Z., Patil, S., Quasney, M., and German, J.B. (1998) Alteration of the fatty acid substrate specificity of lysophosphatidate acyltransferase by site-directed mutagenesis. Biochem. Biophys. Res. Comm. 244: 79.

Murata, N.,Sato, N., Takahashi, N., and Hamazaky, Y. (1982) Composition and positional distribution of fatty acids in phospholipids from leaves of chilling-sensitive and chilling-resistant plants. Plant Cell Physiol. 23: 1071.

Murata, N. (1983) Molecular species composition of phosphatidylglycerols for chilling-sensitive and chilling-resistant plants. Plant Cell Physiol. 24: 81.

Murata, N. and Yamaya, J. (1984) Temperature-dependent phase behaviour of phosphatidylglycerols from chilling-sensitive and chilling-resistant plants. Plant Physiol. 74: 1016.

Murata, N., and Nishida, I., (1990) In: Chilling injury of horticultural crops; Wang, C.Y. (ed.), CRC Press, FL.: 181-199.

Murata, N., Ishizaki-Nishizawa, O., Higashi, S., Hayashi, H., Tasaka, Y, and Nishida, I. (1992) Genetically engineered alteration in the chilling sensitivity of plants. Nature 356: 313.

Murata, N., and Tasaka, Y. (1997) Glycerol-3-phosphate acyltransferase in plants. Biochim. et Biophys. Acta LIP 55129: 1.

Murphy, D.J. (1992) Modifying oilseed crops for non-edible products. TIBTECH 10: 84.

Murphy, D.J. (1993) Structure, function, and biogenesis of storage lipid bodies and oleosins in plants. Prog. Lipid res. 32: 247.

Murphy, D.J. (1996) Engineering oil production in rapeseed and other oil crops. Trends Biotechn. 14: 206.

Murphy, D.J. (1999) Production of novel oils plants. Curr. Opin. Biotech. 10: 175.

Murray, M.G., and Thompson, W.F. (1980) Rapid isolation of high-molecular weight plant DNA. NAR. 8: 4321.

Muskens, M.W.M., Vissers, A.P.A., Mol, J.N.M., and Kooter, J.M. (2000) Role of inverted DNA repeats in transcriptional and post-transcriptional gene silencing. Plant Mol. Biol. 43: 243.

Nakamaye, K.L., and Eckstein, F. (1994) AUA-Cleaving hammerhead ribozymes: attempted selection for improved cleavage. Biochemistry 33: 1271.

Napier, J.A., Stobart, A.K., and Shewry, P.R. (1996) The structure and biogenesis of plant oil bodies: the role of the ER membrane and the oleosin class of proteins. Plant Mol. Biol. 31: 945.

Napier, J., Michaelson, L.V., and Stobart, A.K. (1999) Plant desaturases: harvesting the fat of the land. Curr. Opin. Plant Biol. 2: 123.

Nellen, W., and Lichtenstein, C. (1993) What makes a mRNA anti-sense-itive? TIBS 18: 419.

Newton, I.S. (1998) Long-chain polyunsaturated fatty acids-the new frontier in nutrition. Lipid Technol. 10: 77.

Nishida, I., Frentzen, M., Ishizaki, O., and Murata, N. (1987) Purification of isomeric forms of acyl-[acyl-carrier-protein]: glycerol-3-phosphate acyltransferase from greening squash cotelydons. Plant Cell Physiol. 28: 1071.

Nishida, I., Tasaka, Y., Shiraishi, H., and Murata, N. (1993) The gene and the RNA for the precursor to the plastid-located glycerol-3-phosphate acyltransferase of *Arabidopsis thaliana.* Plant Mol. Biol. 21: 267.

Nishida, I., and Murata, N. (1996) Chilling sensitivity in plants and cyanobacteria: The crucial contribution of membrane lipids. Annu. Rev. Plant Physiol. Plant Mol. Biol. 47; 541.

Ohlrogge, J.B., Browse, J., and Somerville, C.R. (1991) The genetics of plant lipids. Biochim. Biophys. Acta 1082: 1.

Ohlrogge, J. (1994) Design of new plant products: Engineering of fatty acid metabolism. Plant Physiol. 104: 821.

Ohlrogge, J., and Browse, J. (1995) Lipid biosynthesis. Plant Cell 7: 957.

Ohlrogge, J.B., and Jaworski, J.G. (1997) Regulation of fatty acid synthesis. Annu. Rev. Plant Physiol. Plant Mol. Biol. 48: 109.

Ojwang, J.O., Hampel, A., Looney, D.J., Wong-Staal, F., and Rappaport, J. (1992) Inhibition of human immunodeficiency virus type-I expression by a hairpin ribozyme. Proc. Natl. Acad. Sci. USA. 89: 10802.

Okuley, J., Lightner, J., Feldmann, K., Yadav, N., Lark, E., and Browse, J. (1994) The *Arabidopsis* FAD2 gene encodes the enzyme that is essential for polyunsaturated lipid synthesis. Plant Cell 6: 147.

Ollis, D., and White, S. (1990) Protein crystallisation. In: Protein purification, ed. M.P. Deutscher. Meth. Enzym. 182: 587.

Olsson, G. (1960) Species crosses within the genus *Brassica* II. Artificial *Brassica napus* L. Hereditas 46: 351.

Oo, K.C., Lee, K.B., and Ong, A.S.H. (1986) Changes in fatty acid composition of the lipid classes in developing oil palm mesocarp. Phytochemistry 25: 405.

Pachuk, S.J., Yoon, K., Moelling, K., and Coney, L.R. (1994) Selective cleavage of *bcr-abl* chimeric RNAs by a ribozyme targeted to non-contiguous sequences. NAR. 22: 301.

Patzel, V. and Sczakiel, G. (1998) Theoretical design of antisense RNA structures substantially improves annealing kinetics and efficacy in human cells. Nat. Biotechnol.16: 64.

Perez, P., Tiraby, G., Kallerhoff, J., and Perret, J. (1989) Phleomycin resistance as a dominant selectable marker for plant cell transformation. Plant Mol. Biol. 13: 365.

Perriman, R., Delves, A., and Gerlach, W.L. (1992) Extended target-site specificity for a hammerhead ribozyme. Gene 13: 156.

Perry, H.J., and Harwood, J.L. (1993) Radiolabeling studies of acyl lipids in developing seeds of *Brassica napus* - use of [1-C-14] acetate precursor. Phytochemistry 33: 329.

Persidis, A. (1998) Proteomics; An ambitious drug development platform attempts to link gene sequence to expressed phenotype under various physiological states. Nature Biotechn. 16: 393.

Pley, H.W., Flaherty, K.M., and McKay, D.B. (1994) Model for an RNA tertiary interaction from the structure of an intermolecular complex between a GAAA tetraloop and an RNA helix. Nature 372: 68.

Pollard, M.R., Anderson, L., Fan, C., Hawkins, D.J., and Davies, H.M. (1991) A specific acyl-ACP thioesterase implicated in medium-chain fatty acid production in immature cotelydons of *Umbellularia californica.* Arch. Biochem. Biophys. 284: 306.

Pollard, M., and Ohlrogge, J. (1999) Testing models of fatty acid transfer and lipid synthesis in spinach leaf using *in vivo* oxygen-18 labeling. Plant Physiol. 121: 1217.

Pontius, B.W., Lott, W.B., and Von Hippel, P.H. (1997) Observations on catalysis by hammerhead ribozymes are consistent with a two-divalent-metal-ion mechanism. Proc. Natl. Acad. Sci. USA. 94: 2290.

Post-Beittenmiller, D. (1996) Biochemistry and molecular biology of wax production in plants. Annu. Rev. Plant Physiol. 47: 405.

Promega: Protocols and Applications Guide (1996) Promega Corporation, 3d edition, Cat. #P1610, ISBN 1-882274-57-1.

Pwee, K.H., and Gray, J.C. (1993) The pea plastocyanin promoter directs cell-specific but not full light-regulated expression in transgenic tobacco plants. Plant J. 3: 437.

Pyle, A.M. (1993) Ribozymes: A distinct class of metalloenzymes. Science 261: 709.

Quattrocchio, F.M., Wing, J.F., Leppen, H.T.C., Mol, J.N.M., and Koes, R.E. (1993) Regulatory genes controlling anthocyanin pigmentation are functionally conserved among plant species and have distinct sets of target genes. The Plant Cell 5: 1497.

Rafferty, J.B., Simon, J.W., Stuitje, A.R., Slabas, A.R., Fawcett, T., and Rice, D.W. (1994a) Crystallization of the NADH-specific enoyl acyl carrier protein reductase from *Brassica napus*. J. Mol. Biol. 237: 240.

Rafferty, J.B, Simon, J.W., Baldock, C., Artymiuk, P.J., Baker, P.J., Stuitje, A.R., Slabas, A.R., and Rice, D.W. (1995) Common themes in redox chemistry emerge from the X-ray structure of oilseed rape (*Brassica napus*) enoyl acyl carrier protein reductase. Structure 3: 927.

Rittner, K., Burmester, C., and Sczakiel, G. (1993) *In vitro* selection of fast-hybridizing and effective antisense RNAs directed against the human immunodeficiency virus type 1. NAR. 21: 1381.

Rock, C.O., and Garwin, J.L. (1979) Preparative enzymatic synthesis and hydrophobic chromatography of acyl-acyl carrier protein. J. Biol. Chem. 254: 7123.

Rock, C.O., and Cronan, J.E. (1979) Solubilization, purification, and salt activation of acyl-acyl carrier protein synthetase from *Escherichia coli*. J. Biol. Chem. 254: 7116.

Roughan, P.G., and Slack, C.R. (1982) Cellular organization of glycerolipid metabolism. Anne. Rev. Plant Physiol. 33: 97.

Roughan, G., and Nishida, I. (1990) Concentrations of long-chain acyl- acyl carrier proteins during fatty acid synthesis by chloroplasts isolated from pea (*Pisum sativum*), safflower (*Carthamus tinctoris*), and Amaranthus (*Amaranthus lividus*) leaves. Arch. Biochem. Biophys.276: 38.

Roughan, P.G., and Ohlrogge, J.B. (1994) On the assay of acetyl-CoA synthetase in chloroplasts and leaf extracts. Anal. Biochem. 216: 77.

Roughan, P.G., and Ohlrogge, J.B. (1996) Evidence that isolated chloroplasts contain an integrated lipid-synthesising assembly that channels acetate into long-chain fatty acids. Plant Physiol. 110: 1239.

Ruffner, D.E., Stormo, G.D., and Uhlenbeck, O.C. (1990) Sequence requirements of the hammerhead RNA self-cleavage reaction. Biochemistry 29: 10695.

Saiki, R.K., Gelfand, D.H., Stoffel, S., Scharf, S.J., Higuchi, R., Horn, G.T., Mullis, K.B., and Erlich, H.A. (1988) Primer-directed enzymatic amplification of DNA with a thermostable DNA-polymerase. Science 239: 487.

Sambrook, J., Fritsch, E.F., and Maniatis, T. (1989) Molecular Cloning: A laboratory manual. 2nd Edn. Cold Spring Harbor Laboratory Press, Cold Spring Harbor, New York.

Sarmiento, C., Garces, R., and Mancha, M. (1998) Oleate desaturation and acyl turnover in sunflower (*Helianthus annuus* L.) seed lipids during rapid temperature adaptation. Planta 205: 595.

Sarver, N., Cantin, E.M., Chang, P.S., Zaia, J.A., Ladne, P.A., Stephens, D.A., and Rossi, J.J. (1990) Ribozymes as potential anti-HIV-1 therapeutic agents. Science, 247: 1222.

Sawata, S., Shimayama, T., Komiyama, M., Kumar, P.K.R., Nishikawa, S., and Taira, K. (1993) Enhancement of the cleavage rates of DNA-armed hammerhead ribozymes by various divalent metal ions. NAR. 21: 5656.

Saxena, S.K., and Ackerman, E.J. (1990) Ribozymes correctly cleave a model substrate and endogenous RNA *in vivo*. J. Biol. Chem. 265: 17106.

Scanlon, K.J., Jiao, L., Funato, T., Wang, W., Tone, T., Rossi, J.J., and Kashani-Saber, M. (1991) Ribozyme-mediated cleavage of *c-fos* mRNA reduces gene expression of DNA synthesis enzymes and metalothionein. Proc. Natl. Acad. Sci. USA. 88: 10591.

Schena, M., Shalon, D., Davis, R.W., and Brown, P.O. (1995) Quantitative monitoring of gene expression patterns with complementary DNA microarray. Science 270: 467.

Schmid, R.D. (1988) Unusual fatty acids and their scope in biotechnology. In Proceedings of the world conference on biotechnology for the fats and oils industry. American Oil Chemists Society. Applewhite T.H. (ed): 169-172.

Schneider, G., and Schmidt, H. (1997) Structure-function studies on desaturases and related hydrocarbon hydroxylases. In Physiology, Biochemistry and Molecular Biology of Plant Lipids. Ed. By Williams, J.P., Khan, M.U., Lem, N.W. Kluwer: Dordrecht, The Netherlands.

Schreier, P.H., Seftor, E.A., Schell, J., and Bohnert, H.J. (1985) The use of nuclear-encoded sequences to direct the light-regulated synthesis and transport of a foreign protein into plant chloroplasts. EMBO J. 4: 25.

Schultz, D.J., Cahoon, E.B., Shanklin, J., Craig, R, Cox-Foster, D.L. et al. (1996) Expression of a Δ^9-14:0-acyl carrier protein fatty acid desaturase gene is necessary for the production of omega 5 anacardic acids found in pest-resistant geranium (*Pelargonium xhortorum*). Proc. Natl. Acad. Sci. USA 93: 8771.

Scott, W.G., Finch, J.T., and Klug, A. (1995) The crystal structure of an AII-RNA hammerhead ribozyme: a proposed mechanism for RNA catalytic cleavage. Cell 81: 991.

Sczakiel, G., Homann, M., and Rittner, K. (1993) Computer-aided search for antisense RNA target sequences of the human immunodeficiency virus type I. Antisense Res. Dev. 3: 45.

Settlage, S.B., Wilson, R.F., and Kwanyuen, P. (1996) Localization of diacylglycerol acyltransferase to oil body associated endoplasmic-reticulum. Plant Physiol. Biochem. 33: 399.

Shanklin, J., and Somerville, C. (1991) Stearoyl-acyl-carrier-protein desaturase from higher plants is structurally unrelated to the animal and fungal homologs. Proc. Natl. Acad, Sci. USA 88: 2510.

Shanklin, J., Cahoon, E.B., Whittle, E., Lindqvist, Y., Huang, W., Schneider, G., and Schmidt, H. (1997) Structure-function studies on desaturases and related hydrocarbon hydroxylases. In *Physiology, Biochemistry and Molecular Biology of Plant Lipids*. Edited by Williams, J.P., Khan, M.U., Lem, N.W.: Dordrecht, The Netherlands. Kluwer: 6-10.

Shanklin, J., and Cahoon, E.B. (1998) Desaturation and related modifications of fatty acids. Annu. Rev. Plant Physiol. Plant Mol. Biol. 49: 611.

Shewry, P.A., Napier, J.A., and Davies P.J. (eds), (1998) *Engineering Crop Plants for Industrial End Uses*. Portland Press Ltd.: London.

Singh, S., Green, A., Stoutjesdijk, P., and Liu, Q. (2000) Inverted repeat DNA- A new silencing tool for seed lipid modification. Abstract 14th International Symposium on Plant Lipids. Cardiff, Wales, UK. 23-28 July 2000.

Sioud, M., Natvig, J.B., and Førre, O. (1992) Preformed ribozyme destroys tumour necrosis factor mRNA in human cells J. Mol. Biol. 223: 831.

Slabas, A.R., and Fawcett, T. (1992) The biochemistry and molecular biology of plant lipid biosynthesis. Plant. Mol. Biol. 19: 169.

Slabas, A.R., Simon, J.W., and Elborough, K.E. (1995) Information needed to create new oil crops. Inform 6: 159.

Slabas, A.R., and Brough, C.L. (1997a) Specificity of acyltransferases and their genetic manipulation for environmental adaptation and development of new industrial oils. The Society for Experimental Biology; SEB 1032: 149-156.

Slabas, A.R., Carey, A.T., and White, A.J. (1997b) Manipulation of seed oils for industrial use. Feature: The Biochemist; February/March: 1-5.

Slocombe, S.P., Piffanelli, P., Fairbairn, D., Bowra, S., Hatzopoulos, P. et al. (1994) Temporal and tissue-specific regulation of a *Brassica napus* stearoyl-acyl carrier protein desaturase gene. Plant Physiol.104: 1167.

Soll, J., and Roughan, G. (1982) Acyl- acyl carrier protein pool sizes during steady-state fatty acid synthesis by isolated spinach chloroplasts. FEBS Lett. 146: 189.

Somerville, C., and Browse, J. (1991) Plant Lipids: metabolism, mutants and membranes. Science 252: 80.

Somerville, C.R., and Browse, J. (1996) Dissecting desaturation: Plants prove advantageous. Trends cell. Biol. 6: 148.

Southern, E.M. (1975) Detection of specific sequences among DNA fragments separated by gel electrophoresis. J. Mol. Biol. 98: 503.

Stam, M., Mol., J.N.M., and Kooter, J.M. (1997) The silence of genes in transgenic plants. Ann. Bot. 79: 3.

Steger, G., Hofmann, H., Förtsch, F., Gross, H.J., Randles, J.W., Sänger, H.L., and Riesner, D. (1984) Conformational transitions in viroids and virusoids: comparison of results from energy minimization algorithm and from experimental data. J. Biomol. Struct. Dynamics 2: 543.

Steinecke, P., Herget, T., and Schreier, P.H. (1992) Expression of a chimeric ribozyme gene results in endonucleolytic cleavage of target mRNA and a concomitant reduction of gene expression *in vivo*. EMBO J. 11: 1525.

Steponkus, P.L., Lynch, D.V., and Uemura, M. (1990) The influence of cold acclimation on the lipid composition and cryobehaviour of the plasma membrane of isolated rye protoplasts. Phylosophical Transactions of the Royal Society of London. B 326: 571.

Studier, F.W. (1991) Use of bacteriophage-T7 lysozyme to improve an inducible T7 expression system. J. Mol. Biol. 219: 37.

Stull, R.A. and Szoka, C., Jr. (1995) Antigene, ribozyme and aptamer nucleic acid drugs: progress and prospects. Pharmaceutical Research 12: 465.

Stumpf, P.K. (1981) Plants, fatty acids, compartments. Trends Biochem. Sci. 6: 173.

Stymne, S., and Stobart, A.K. (1987) Triacylglycerol biosynthesis. In The Biochemistry of Plants, Vol. 9 (Stumpf, P.K., ed.), New York: Academic Press: 175-214.

Suh, M.C., Schultz, D.J., and Ohlrogge, J.B. (1999) Isoforms of acyl carrier protein in seed-specific fatty acid synthesis. Plant J. 17: 679.

Sullenger, B.A., Gallardo, H.F., Ungers, G.E., and Gilboa, E. (1990) Overexpression of TAR sequences renders cells resistant to human immunodeficiency virus replication. Cell 63: 601.

Sullenger, B.A., and Cech, T.R. (1993) Tethering ribozymes to a retroviral packaging signal for destruction of viral RNA. Science 262: 1566.

Sun, C., Cao, Y.-Z., and Huang, A.H.C. (1988) Acyl Coenzyme A preference of the glycerol phosphate pathway in the microsomes from the maturing seeds of palm, maize and rapeseed. Plant Physiol. 88: 56.

Symons, R.H. (1991) Ribozymes. Critic. Rev. in Plant Sciences, 10: 189.

Symons, R.H. (1992) Small catalytic RNAs. Annu. Rev. Biochem. 61: 641.

Symons, R.H. (1997) Plant pathogenic RNAs and RNA catalysis. NAR. 25: 2683.

Tabler, M., Tzortzakaki, S., Homann, M., and Sczakiel, G. (1994) A 3-nucleotide helix I is sufficient for full activity of a hammerhead ribozyme – advantages of an asymmetric design. NAR. 22: 3958.

Thompson, G.A., Scherer, D.E., Foxall-Van Aken, S., Kenny, J.W., Young, H.L. et al. (1991) Primary structures of the precursor and mature forms of stearoyl-acyl carrier protein desaturase from safflower embryos and requirement of ferredoxin for enzyme activity. Proc. Natl. acad. Sci. USA 88: 2578.

Todd, J., Post-Beittenmiller, D., and Jaworski, J.G. (1999) *KCS*1 encodes a fatty acid elongase 3-ketoacyl-CoA synthase affecting wax biosynthesis in *Arabidopsis thaliana*. Plant J. 17: 119.

Töpfer, R., and Martini, N. (1994) Molecular cloning of cDNAs or genes encoding proteins involved in *de novo* fatty acid biosynthesis in plants. J. Plant Physiol. 143: 416.

Töpfer, R., Martini, N., and Schell, J. (1995) Modification of plant lipid synthesis. Science 268: 681.

Tsay, J.T., Oh, W., Larson, T.J., Jackowski, S, and Rock, C.O. (1992) Isolation and characterization of the β-ketoacyl-acyl carrier protein synthase-III gene (*fab* H) from *Escherichia coli* K-12. J. Biol. Chem. 267:6807.

Tsuchihashi, Z., Khosla, M., and Herschlag, D. (1993) Protein enhancement of hammerhead ribozyme catalysis. Science 262: 99.

Tuschl, T., and Eckstein, F. (1993) Hammerhead ribozymes:Importance of stem-loop II for activity. Proc. Natl. Acad. Sci. USA. 90: 6991.

Tuschl, T., Gohlke, C., Jovin, T.M., Westhof, E., and Eckstein, F. (1994) 3-Dimensional model for the hammerhead ribozyme based on fluorescence measurements. Science 266: 785.

U, N. (1990) Genome analysis in Brassica with special reference to the experimental formation of *Brassica napus* and peculiar mode of fertilization. Jap. J. Bot. 7: 389.

Uhlenbeck, O.C. (1987) A small catalytic oligoribonucleotide. Nature 328: 596.

Usman, N., and Stinchcomb, D.T. (1996) In: Catalytic RNA, eds. Eckstein, F., and Lilley, D.M.J., Springer, Berlin: 243-264.

Van den Broeck, G., Timko, M.P., Kausch, A.P., Cashmore, A.R., Van Montagu, M., and Herrera-Estrella, L. (1985) Targeting of a foreign protein to chloroplasts by fusion to the transit peptide from the small subunit of ribulose 1,5-biphosphate carboxylase. Nature 313: 358.

Van der Krol, A.R., Lenting, P.E., Veenstra, J., Van der Meer, I.M., Koes, R.E., A.G.M. Gerats, Mol, J.N.M., and Stuitje, A.R. (1988) An antisense chalcone synthase gene in transgenic plants inhibits flower pigmentation. Nature 333: 866.

Vaucheret, H., Béclin, C., Elmayan, T., Feuerbach, F., Godon, C., Morel, J.-B., Mourrain, P., Palauqui, J.-C., and Vernhettes, S. (1998) Transgene-induced gene silencing in plants. Plant J. 16: 651.

Vaux, P., Guerineau, F., Waugh, R., and Brown, J.W.S. (1992) Characterization and expression of U1snRNA genes from potato.

Verwoert, I. (1994) The typeII fatty acid synthetase complex. Ph.D thesis: Free University Amsterdam. The Netherlands.

Vick, B., and Beevers, H. (1977) Phosphatidic acid synthesis in castor bean endosperm. Plant Physiol. 59: 459

Vick, B.A., and Zimmermann, D.C. (1984) Biosynthesis of jasmonic acid by several plant species. Plant Physiol. 96: 130.

Voelker, T.A., Hayes, T.R., Cranmer, A.M., Turner, J.C., and Davies, H.M. (1996) Genetic engineering of a quantitative trait: metabolic and genetic parameters influencing the accumulation of laurate in rapeseed. Plant J. 9: 229.

Vogel, G., and Browse, J. (1996) Cholinephosphotransferase and diacyl glycerol acyltransferase – substrate specificities at a key branchpoint in seed lipid metabolism. Plant Physiol. 110: 923.

Volpe, J.J., and Vagelos, P.R. (1973) Saturated fatty acid biosynthesis and its regulation. Annu. Rev. Biochem. 42: 21.

Von Wettstein-Knowles, P.M. (1993) Waxes, cutin and suberin. In Lipid Metabolism in Plants, T.S. Moore, Jr., ed(Boca Raton, FL: CRC Press): 127-166.

Wan, J.S., Sharp, S.J., Poirier, P., Wagaman, P., Chambers, J., Pyati, J., Hom, Y., Galindo, J., Huvar, A., Peterson, P., Jackson, M., and Erlander, M. (1996) Cloning differentially expressed mRNAs. Nature Biotech. 14: 1685.

Wang, M.-B., and Waterhouse, P.M. (2000) High-efficiency silencing of a β-glucuronidase gene in rice is correlated with repetitive transgene structure but is independent of DNA methylation. Plant Mol. Biol. 43: 67.

Wassenegger, M., and Pélissier, T., (1998) A model for RNA-mediated gene silencing in higher plants. Plant Mol. Biol. 37: 349.

Waterhouse, P.M., Graham, M.W., and Wang, M.-B. (1998) Virus resistance and gene silencing in plants can be induced by simultaneous expression of sense and antisense RNA. Proc. Natl. Acad. USA. 95: 13959.

Waterhouse, P.M., Smith, N.A., and Wang, M.B. (1999) Virus resistance and gene silencing: killing the messenger. Trends Plant Sci. 4: 452.

Weber, S., Wolter, F.-P., Buck, F., Frentzen, M., and Heinz, E. (1991) Purification and cDNA sequencing of an oleate-selective acyl-ACP: *sn*- glycerol-3-phosphate acyltransferase from pea chloroplasts. Plant Mol. Biol. 17: 1067.

Wilkison, W.O., Bell, R.M. (1997) *sn*- Glycerol-3-phosphate acyltransferase from *Escherichia coli*. Biochim. Biophys. Acta 1348: 3.

Wilmer, J.A. (1997) Regulation of erucic acid accumulation in oilseed rape (brassica napus L.): effects of temperature and abscisic acid. Ph.D thesis, Agricultural university Wageningen. The Netherlands.

Willmitzer,L. (1999) Plant biotechnology: output traits – the second generation of plant biotechnology products is gaining momentum. Curr. Opin. In Biotech. 10: 161.

Wolter, F.P., Schmidt, R., and Heinz, E. (1992) Chilling sensitivity of *Arabidopsis thaliana* with genetically engineered membrane lipids. EMBO J. 11: 4685.

Wu, J., James, Jr., D.W., Dooner, H.K., and Browse, J. (1994) A mutant of *Arabidopsis* deficient in the elongation of palmitic acid. Plant Physiol. 106: 143.

Wu, J., and Browse, J. (1995) Elevated levels of High-Melting-Point Phosphatidylglycerols do not induce chilling sensitivity in an *Arabidopsis* mutant. Plant Cell 7: 17.

Wu, J., Lightner, J., Warwick, N., and Browse, J. (1997) Low-temperature damage and subsequent recovery of *fab1* mutant *Arabidopsis* exposed to 2 °C. Plant Physiol. 113: 347.

Yang, X., Yie, Y., Zhu, F., Liu, Y., Kang, L., Wang, X., and Tien, P. (1997) Ribozyme-mediated high resistance against potato spindle tuber viroid in transgenic potatoes. Proc. Natl. Acad. Sci. USA. 94: 4861.

Yokoi, S., Higashi, S.-I., Kishitani, S., Murata, N., and Toriyama, K. (1998) Introduction of the cDNA for *Arabidopsis* glycerol-3-phosphate acyltransferase (GPAT) confers unsaturation of fatty acids and chilling tolerance of photosynthesis of photosynthesis on rice. Mol. Breed. 4: 269.

Yoon, K., Cole-Strauss, A., and Kmiec, E.B. (1996) Targeted gene correction of episomal DNA in mammalian cells mediated by a chimeric RNA/DNA oligonucleotide. Proc. Natl. Acad. Sci. 93: 2071.

Zaug, A.J., Been, M.D., and Cech, T.R. (1986) The *Tetrahymena* ribozyme acts like an RNA restriction enzyme. Nature 324: 429.

Zhu, T., Peterson, D.J., Tagliani, L., St. Clair, G., Baszczynski, C.L., and Bowen, B. (1999) Targeted manipulation of maize genes *in vivo* using chimeric RNA/DNA oligonucleotides. Proc. Natl. Acad. Sci. 96: 8768.

Zhu, T., Mettenburg, K., Peterson, D.J., Tagliani, L., and Baszczynski, C.L. (2000) Engineering herbicide-resistant maize using chimeric RNA/DNA oligonucleotides. Nature Biotec. 18: 555.

Zou, J., Katavic, V., Giblin, E.M., Barton, D.L., MacKenzie, S.L., Keller, W.A., Hu, X., and Taylor, D.C. (1997) Modification of seed oil content and acyl composition in the *Brassicaceae* by expression of a yeast *sn*-2 acyltransferase gene. Plant Cell 9: 909.

Zou, J., Wei, Y., Jako, C., Kumar, A., Selvaraj, G., and Taylor, D.C. (1999) The *Arabidopsis thaliana* TAG 1 mutant has a mutation in a diacylglycerol acyltransferase gene. Plant J. 19: 645.

Zoumadakis, M., and Tabler, M. (1995) Comparative analysis of cleavage rates after systematic permutation of the NUX—consensus target motif for hammerhead ribozymes. NAR. 23: 1192.